THE DEVELOPMENT OF NOVEL ELECTROANALYTICAL INTERFACES FOR POINT OF CARE DIAGNOSTICS

LAURA ANNIE ADA NEWTON

A thesis submitted in partial fulfilment of the requirements of Nottingham Trent University for the degree of Doctor of Philosophy

September 2011

Declaration

Acknowledgements

I would like to take this opportunity to thank all the people who have helped and supported me throughout the duration of my studies at Nottingham Trent University. I would firstly like to express gratitude to my supervisory team for their expertise, guidance and support. I would also like to thank all of the people I have worked with during my studies, Maria Marti Villalba, Duncan Sharp and Jolene Phair, who have made it an enjoyable and truly memorable experience. Finally, I wish to express my deepest thanks to my parents, family and friends for their eternal love, relentless belief and continuous encouragement.

Abstract

Reduced sulphydryl thiols (RSH): cysteine, homocysteine and glutathione are fundamental cellular components having important biological functions, including roles within the pathogenesis of a variety of clinical conditions. Independent analysis of these species is problematic and analytical difficulties relating to instrumental selectivity and sensitivity need to be overcome. This thesis describes the work carried out on the development and characterisation of a range of systems that could be used to facilitate thiol detection, ideally at the point-of-care, focussing largely on electrochemical techniques.

Silver-thiol interactions were studied as a route to assist the sample processing. Here a novel controlled silver release mechanism was assessed. Silver release was found to be dependent upon the thiol structure. This has possible future applications to the development of methods to prevent biofilm formation, although the full mechanism of silver-thiol release requires further understanding.

The development of unique molecular imprinted polymers was attempted. These would facilitate the detection of amino acids and the relevant thiol species via the amine functionality. The polymers proved unstable in the presence of hydroxylamine. However, this property makes the polymers suitable for use as protective or sacrificial polymers which can potentially be exploited in the manufacture of patterned electrodes.

The nucleophilic substitution reaction between thiols and quinones, or quinone type materials, was explored as a possible route to assist selective thiol detection *via* electrochemical or colorimetric methods. Development of such reagentless sensing platforms would be beneficial in clinical analysis. Selectivity of thiol determination was achieved, although sensitivity issues will restrict real-world applications.

A pH sensor utilising uric acid redox sensitivity was developed and was integrated within a disposable electrode assembly to enable wound pH monitoring. This platform was adapted as a prototype generic sensor for thiol analysis.

Contents

Abbreviations

Analtyes/Molecules

2-MCE	2-Mercaptoethanol	**MTBSTFA**	N-(tert-Butyldimethylsilyl)-N-methyltrifluoroamide
2,6-DMBQ	2,6-Dimethylbenzoquinone	**MTHFR**	Methylenetetrahydrofolate reductase
4AP	4-Aminophenol	**NADPH**	Nicotinamide adenine dinucleotide phosphate
4NP	4-Nitrophenol	**NMDA**	N-Methyl-D-asparate
4N1N	4-Nitro-1-Naphthol	**NO**	Nitric oxide
6-IAF	6-Iodoacetamidofluorescein	**NQ-Ada**	Naphthoquione-Adamantane Derivative
8H5NQ	8-Hydroxy-5-Nitroquinoline	**OPA**	o-Phthalaldehyde
AA	Ascorbic acid	**OPA-2-MCE**	o-Phthalaldehyde-2-mercaptoethanol
ABD-F	4-Aminosulfonyl-7-fluoro-2,1,3-benzoxadiazole	**PCA**	Pechloric acid
ADP	Adenosine diphosphate	**PPDMP**	1,1'-p-Phenylenebis(2,5-dimethylpyrrole)
ATP	Adenosine triphosphate	**PPi**	Inorganic diphosphate
BHMT	Betaine homocysteine methyl transferase	**Pi**	Inorganic phosphate
CBS	Cystathionine-β-synthase	**QQ**	Quinoline-5,8-quinone
CMPI	2-Chloro-1-methylpyridinium iodide	**SAH**	S-Adensoylhomocysteine
CQMT	2-Chloro-1-methyl-quinolinium tetrafluoroborate	**SAM**	S-Adenosylmethionine
CSH	Cysteine	**SBD-F**	7-Fluorobenzo-2-oxa-1,3-diazole-4-sulfonate
DNA	Deoxyribonucleic acid	**SSA**	Sulfosalicylic acid
DMG	Dimethyl glycine	**TBAP**	Tetrabutylammonium perchlorate
DMMP	2,5-Dimethyl-1-phenylenebis(2,5-dimethylpyrrole)	**TBP**	Tri-n-butylphosphine
DTNB	5,5'-Dithiobis(2-nitrobenzoic acid)	**TCA**	Trichloroacetic acid
DTT	Dithiothreitol	**TCEP**	Tris(2-carboxylethyl)phosphine
ECF	Ethylchloroformate	**TNB**	5-Thio-2-nitrobenzoic acid
EDMP	1,1'-Ethylenebis(2,5-dimethylpyrrole)	**TPP**	Triphenylphosphine
FAD	Flavin adenine dinucleotide	**Tryp**	Tryptophan
GCL	Glutamate cysteine ligase	**Tyr**	Tyrosine
GSH	Glutathione	**UA**	Uric acid
HCSH	Homocysteine		
mBrB	Monobromobimane		
MCE	Mercaptoethanol		
MS	Methionine Synthase		

Terminology

AE or CE	Auxilary electrode or counter electrode	**ICL**	Chemiluminescence immunoassay
AgNPs	Silver nanoparticles	**ICP-OES**	Inductively coupled plasma optical emission spectroscopy
AIDS	Acquired immune deficiency syndrome	**IPAP**	Intergrated pulsed amperometric detection
C	Chemical	**LC**	Liquid chromatography
CE	Capillary electrophoresis	**LC-ESI-MS/MS**	Liquid chromatography-electrospray ionisation-mass spectroscopy/mass spectroscopy
CE-ED	Capillary electrophoresis-electrochemical detection	**LIF**	Laser induced fluorescence
CE-LIF	Capillary electrophoresis-laser induced fluorescence	**LoD**	Limit of detection
CE-UV	Capillary electrophoresis-ultraviolet-visible	**LSV**	Linear sweep voltammetry
CNT	Carbon nanotubes	**MIP**	Molecular imprinted polymer
CTNS	Cystinosis, nephropathic gene	**MS**	Mass spectrometry
E	Electrochemical	**NG**	Not given
ED	Electrochemical detection	**NMR**	Nuclear magnetic resonace
EIA	Enzyme-linked immunoassay	**Ox**	Oxidation
EQ	Equivalent	**PED**	Pulsed electrochemical detection
EQCM	Electrochemical quartz crystal microbalance	**POCT**	Point of care testing
ESI	Electrospray ionisation	**PSPE**	Plasma treated screen printed electrode
FL	Fluorescence	**RE**	Reference electrode
FPIA	Fluorescence polarisation immunoassay	**Red**	Reduced
FSO-Au	Fluorosurfactant modified gold electrode	**ROS**	Reactive oxygen species
		RSH	Reduced sulphydryl thiols
GC	Gas chromatography	**SPE**	Screen printed electrode
GC-MS	Gas chromatography-mass spectroscopy	**TEM-EDX**	Transmission electron microscope-energy dispersive X-ray spectroscopy
HAI	Hospital acquired infection	**UV**	Ultraviolet
HIV	Human immunodeficiency virus	**VIS**	Visible
HPLC	High performance liquid chromatography	**WE**	Working electrode
HPLC –ED	High performance liquid chromatography-electrochemical detection		
HPLC-FL	High performance liquid chromatography-fluorescence detection		
HPLC-MS	High performance liquid chromatography-mass sprectrometry		
HPLC-MS/MS	High performance liquid chromatography-mass spectrometry/mass spectrometry		
HPLC-PED	High performance liquid chromatography-pulsed electrophoresis detection		
HPLC-UV	High performance liquid chromatography-ultraviolet-visible		

Equation Definitions

a	Acitivity (**Equation 2.2**)	*n*	Number of electrons (**Equation 2.2**)
A	Absorbance (**Equation 2.10**)	**n**	Overtone number (**Equation 2.9**)
A	Area (**Equation 2.9**)	**P**	Transmitted light intensity
C	Concentration	**P0**	Incident lightintensity
C	Concentation (**Equation 2.5**)	ρ	The density of quartz (2.65 g/cm^3)
D	Diffusion coefficient	**R**	Universal Gas Constant (8.314 J K^{-1} mol^{-1})
dΦ/dx	The electric field	**T**	Temperature (K)
E	Electrode Potential	**t**	Time
E0	Standard Electrode Potential	*u*	Ion mobility
E	Molar absorptivity	μ	The shear modulus of quartz
F	The Faraday constant (96500 C/mol)	**V$_x$**	Velocity
I	Current	**V$_{(x,t)}$**	Hydrodynamic Velocity
J	Diffusional flux	**X**	Distance
J	Flux	**z**	Charge on the electroactive species (**Equation 2.5**)
*J*m	Migratory flux	**Δf**	Frequency change
L	Sample path length	**Δm**	Mass change

Chapter 1

The Clinical Significance of Sulphydryl Thiols

Chapter 1

The Clinical Significance of Sulphydryl Thiols

Abstract

Reduced sulphydryl thiols (RSH): Cysteine (CSH), Homocysteine (HCSH) and Glutathione (GSH) are essential cellular components that have a number of vital functions within the body. In recent years, due to their clinical relevance, these molecules have gathered a considerable amount of interest within the research community. Variations in their concentrations, within biological fluids, have been associated with the pathogenesis of a range of medical conditions. The work presented in the subsequent chapters of this thesis, focuses primarily upon the development of novel electroanalytical strategies that can facilitate the specific determination of these compounds within biological samples. The aim of this chapter is to review the existing literature and to summarise the biological and clinical significance of these thiol compounds, whilst giving an overview of the methods that are currently available for their detection, thus putting the work carried out in this thesis into context.

The work presented in this chapter on homocysteine and its analysis has been published within Expert Review of Molecular Diagnostics.

1.1. Introduction

Cysteine, homocysteine and glutathione are indispensable biological components within the body. They are structurally similar molecules, as illustrated in **Figure 1.1**, whose metabolic pathways are strongly interlinked. It is therefore not surprising that they have analogous chemical reactivities and biological properties. When the roles of each of these molecules are considered in the arena of physiological wellbeing they tend to have a Jekyll and Hyde persona, each has a vital part in maintaining normal cellular function, but when their levels deviate from the normal reference ranges they can have a significant role in the development and/or pathogenesis of a variety of clinical conditions [1-8].
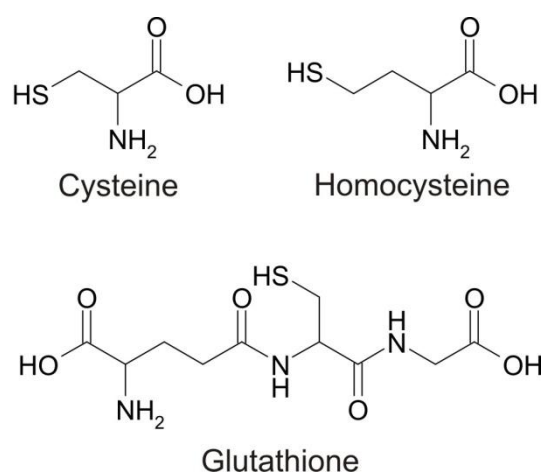
Figure 1.1 The chemical structures of cysteine, homocysteine and glutathione.

Cysteine is by far the more prevalent thiol within human physiology, performing a multitude of important roles [14-16]. It does however have a less beneficial side when its levels are lower than or, more commonly, in excess of the accepted reference range. The most common example is where excessive amounts of cystine, the oxidised disulphide form of cysteine, in urine is a contributory factor in the development of urinary stones, therefore classifying it as a clinical risk factor for renal function [1]. Homocysteine differs from the latter in that there is an additional methylene (CH_2) spacer between the sulphydryl group and the alpha carbon atom. Subtle changes in its metabolism have, in recent years been linked to a number of conditions including cardiovascular [2] and neurochemical [3-5] diseases thus highlighting its potential as a biomarker for preventative screening and treatment options. Glutathione is synthesised from cysteine, glutatamate and glycine and has

some vital antioxidant properties. Research findings have shown that depletions in its levels can be indicative of liver diseases [6], autoimmune diseases [7] and Parkinson's disease [8] which have given it biomarker status.

A substantial amount of literature can been found on the biological significance, pathogenic roles and the methods used for the detection of each of these molecules within biological samples. Detection is normally fraught with a number of analytical difficulties including concerns over sample degradation, speciation problems and sensitivity issues [9]. In the current economic climate there is a need for technological advancements that would enable the rapid, reliable and selective measurement of these compounds, ideally in a point of care type diagnostic platform. The development of these systems would be particularly useful in the case of homocysteine where analytical improvements would allow more detailed epidemiology studies to be performed thus allowing any debates associated with the molecules roles in the pathogenesis of disease to be resolved. New advancements would also allow the true efficacy of these species as early warning and/or preventative biomarkers to be clarified [10].

The central aim of this project was to develop novel electroanalytical approaches that could be used to monitor the levels of these thiol species within biological samples. This chapter sets the scene for the research that follows by highlighting the relevance of cysteine, homocysteine and glutathione within human physiology and disease and summarises the techniques that are currently used for their determination.

1.2. Cysteine

Cysteine (2-Amino-3-mercaptopropionic acid) is a sulphur containing amino acid synthesised in the human body from the essential amino acid methionine and the non essential amino acid serine as illustrated in **Scheme 1.1**. In the first part of this synthesis methionine is converted to S-adenosylmethionine (SAM or AdoMet) in the presence of methionine adensosyltransferase (**Scheme 1.1 a.**). The SAM produced is then converted to homocysteine *via* a transmethylation reaction (**Scheme.1.1 b.**). A

condensation reaction, in the presence of cystathionine synthase, then occurs between the homocysteine produced and serine present within the body to give cystathionine (**Transsulphuration 1, Scheme 1.1 c.**), this is subsequently converted to cysteine and α-ketobutyrate in the presence of cystathionine lyase (**Transsulphuration 2, Scheme.1.1 d.**) [11].
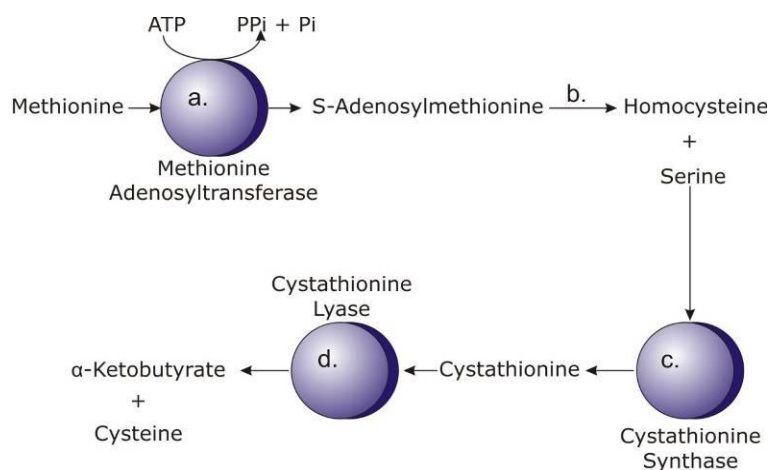
Scheme 1.1 The synthesis of cysteine [11]

Cysteine, like the other sulphydryl thiols, can be present in the body in several forms: the free reduced form (CSH) **(Figure 1.2 (I))** and the oxidised forms, which includes the disulphide cystine (CSSC) **(Figure 1.2 (II))** and the mixed disulphides (CSSR) where cysteine is linked to other sulphydryl thiols, proteins or peptides *via* a disulphide bridge [12].
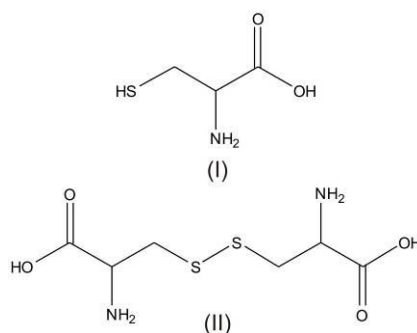
Figure 1.2 The structure of cysteine (I) and cystine (II).

Cysteine is an integral molecule within the human body having a number of vital roles: it is a precursor for many other molecules, it is a key component involved in protein folding and like the other sulphydryl thiol species it is an antioxidant, therefore having an important role in preventing the damage caused by reactive oxygen species during oxidative stress [13]. Cysteine is the most prevalent thiol species within plasma samples [14-16] and its levels are normally assessed by

measuring the total thiol concentration, which includes the concentrations of the reduced and oxidised forms [17]. These levels can vary depending on a number of factors including age, diet and sex but are typically in the micromolar region for both plasma (ca. 300 µM) [12,16] and urine samples (ca. 200 µM) [17]. Numerous studies have demonstrated that when cysteine levels within biological fluids deviate from the typical reference range that normal cellular function is affected, this can have an impact on the pathogenesis of a number of diseases [1,18-20], some of which are discussed briefly over the next few pages.

1.2.1. Cystinuria

Cystinuria is an autosomal recessive disorder in which a mutant allele causes a genetic defect that affects how the kidneys reabsorb cystine, lysine, ornithine and arginine. It is therefore characterised by excessive amounts of these molecules within a sufferer's urine sample. The excessive amounts of lysine, ornithine and arginine appear to have no detrimental effects on kidney function. The presence of excess cystine however can be problematic when its levels exceed its solubility (1.5mM/L) and normal cystine excretion can increase from 0.13mM/day to 1.7mM/day depending on the type and severity of the cystinuria present [18]. This increase can cause the formation and subsequent appearance of cystine crystals and eventually cystine stones within urine [21]. This can cause kidney damage and urinary infections. Cystinuria can be diagnosed by the presence of excessive amounts of cystine within a urine sample by using the cyanide-nitroprusside test [22-23], thin layer chromatography [22-23], ion exchange [24] or liquid chromatographic techniques [24-25], mass spectrometry [26-27] or by a visual examination of the urine sample under a microscope: here yellow-brown hexagonal cystine crystals are observed for a positive result [28-29]. The condition can be treated effectively by a number of routes, all of which work by trying to prevent pathogenic cystine stone formation. Preferred treatment approaches are hydration and alkalinisation methods as treatment with drugs such as D-penicillamin, Captopril [30] or alpha-mercaptoproprionylglycine can have undesirable side effects [18]. The hydration treatment method involves increasing a patient's fluid intake in an effort to reduce cystine saturation within urine and alkalinisation methods involve the patient taking supplements such as bicarbonate

and/or potassium citrate which increases the alkalinity of urine which subsequently increases the solubility of cystine [31-32].

1.2.2. Cystinosis

Cystinosis is another genetic disease that effects cystine concentrations; it has been mapped to chromosome 17p13, the cystinosis, nephropathic (CTNS) gene, which is used to produce cystinosin, an integral membrane protein, which controls the amount of cystine within the lysosomes of cells. There are three types of this disease: nephropathic cystinosis (infantile cystinosis), intermediate nephropathic cystinosis (adolescent cystinosis) and non-nephropathic cystinosis (adult cystinosis) [19] and in each case there is an accumulation of cystine within cell lysosomes, primarily kidney and retinal cells, due to its defective transport over the lysosomal membrane. This build up can eventually result in crystal formation which can cause cell damage and death [33]. Symptoms of the disease will vary depending on the type of cystinosis present but will generally include: kidney problems, acidosis and retinopathy [19]. Diagnosis of the condition may be carried out by determining the cystine levels within blood samples or by looking at the health of the cornea, retina or kidney. Molecular analysis can also be performed as a diagnosis route to confirm the presence of the defect on the CTNS gene. Cystinosis can be treated successfully using cysteamine salts, typically cysteamine bitartrate and phosphocysteamine. These compounds decrease the cystine levels within cells as the cysteamine abduct reacts with the cystine, breaking the disulphide bond to give free reduced cysteine and a cysteine-cysteamine complex [33-34].

1.2.3. Cysteine Deficiencies

Cysteine deficiencies are rare, but levels in the body can decrease if there is a reduction in the amount of any of the components used in its synthesis or if there are any problems with the enzymes involved in its production. This decrease can have a number of detrimental affects: the levels of some other critical cellular components such as taurine, glutathione and homocysteine can be decreased as their precursor

molecule is not present and as cysteine is an antioxidant the bodies ability to fight infections can also be reduced [20].

1.3. Homocysteine

Homocysteine (2-amino-4-sulfanylbutanoic acid) is another sulphur containing amino acid that is chemically and structurally similar to cysteine, the structural difference being the presence of an extra methylene (CH_2) spacer prior to the sulphydryl group. As previously mentioned, homocysteine is produced during the synthesis of cysteine from the essential amino acid methionine which is highlighted, along with how homocysteine is metabolised, in **Scheme 1.2**. During these processes a number of biologically important molecules are synthesised, transsulphuration of homocysteine produces cysteine and taurine [35] and remethylation reconverts homocysteine back into methionine, using the enzyme methionine synthase (MS), vitamin B_{12}, folic acid [36] and methylenetetrahydrofolate [37].
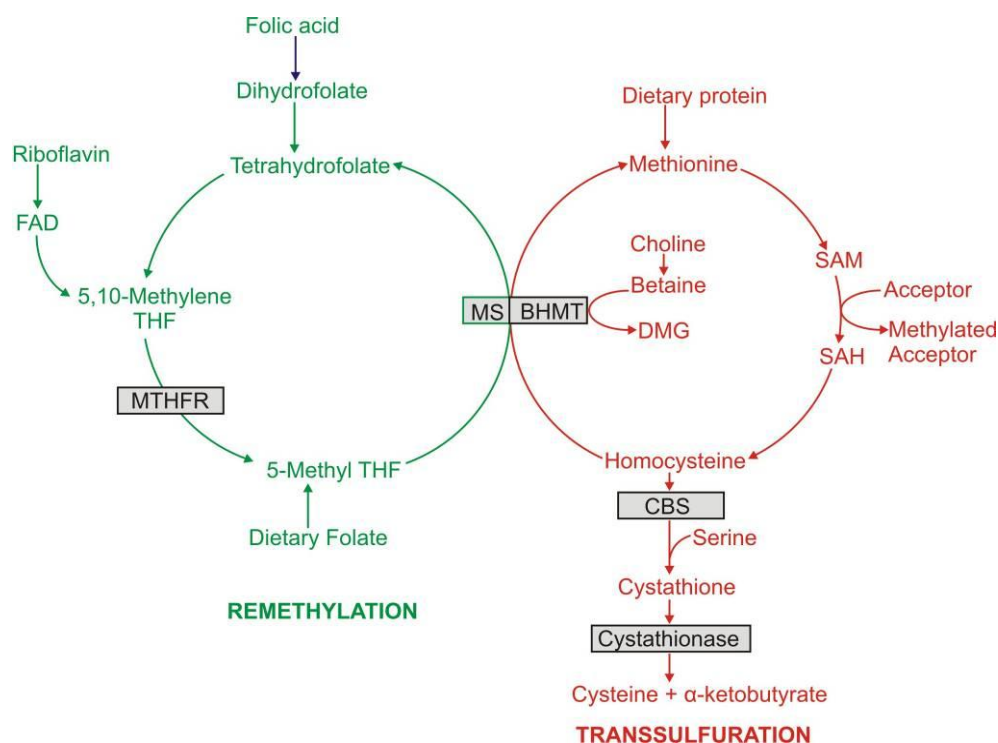
Scheme 1.2 Metabolism of homocysteine and folate
MTHFR, methylenetetrahydrofolate reductase; MS, methionine synthase B_{12}; BHMT, betaine homocysteine methyltransferase; CBS, cystathionine β-synthase; FAD, flavin adenine dinucleotide; DMG, dimethyl glycine; SAM, *S*-adenosylmethionine and SAH, *S*-adenosylhomocysteine [35-37].

Like cysteine, homocysteine is present in the body in several forms (**Figure 1.3**) The reduced form (HCSH) (**I**) and the oxidised forms where homocysteine is

bound to either another homocysteine molecule (**II**) or to another sulphydryl thiol, a protein or a peptide to generate mixed disulfides (**III**) [38-39].
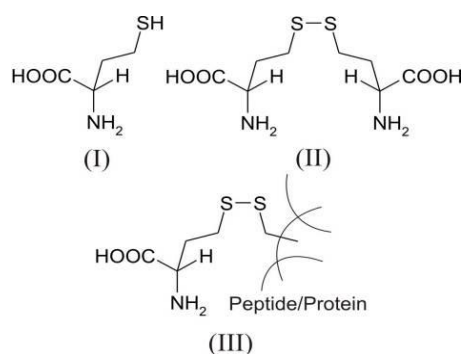
Figure 1.3 The different forms of homocysteine.

Homocysteine levels in the blood are influenced by lifestyle, dietary and genetic factors and vary with gender and age [10]. The overall homocysteine level, which is termed total homocysteine, includes the reduced and oxidised forms and is determined by the rate at which it is metabolised by the body and typically ranges from 5 to 15 μM. Elevations above this reference range are classified as varying levels of hyperhomocysteinemia with 16 to 30 μM being mild; 31 to 100 μM being moderate and levels above 100 μM being categorised as severe [35]. These elevated levels of homocysteine have been implicated in a variety of medical conditions some of which are discussed briefly in the following sections.

1.3.1. Vitamin Deficiency

Measuring homocysteine levels is an established means of assessing patients with possible vitamin deficiencies [40]. There are many causes of folic acid, vitamin B_{12} and vitamin B_6 deficiencies including: inadequate dietary intake, vitamin malabsorption, hereditary conditions and pernicious anaemia [36,41]. Assessment of homocysteine levels for the clinical diagnosis of general B vitamin deficiencies is extremely effective, especially when such measurements are used in conjunction with the direct assessment of vitamin levels as opposed to measuring each analyte individually [42-43]. The majority of cases of hyperhomocysteinemia reported are as a result of these deficiencies [2]. Effective treatment of vitamin deficiencies is important as prolonged suffering can cause irreversible damage to the central nervous system [44] and megaloblastic anaemia [45]. Treatment is simple and can be easily

achieved by vitamin supplementation, which is very effective at returning the homocysteine level back to normal [46].

A link between elevated homocysteine levels and micronutrient deficiency osteoporosis has also been observed [47-48]. It has been proposed that homocysteine interferes with the crosslinking process in collagen, a vital process in bone formation [49]. The exact mechanisms by which these adverse effects are bought about are still unclear but a recent study has suggested that homocysteine disturbs osteoblast function resulting in the damage. Further work is necessary to clarify the pathogenic mechanism along with outcome studies to observe whether homocysteine lowering treatment is of any benefit within this situation [50].

1.3.2. Psychiatric and Neurodegenerative Disorders

A number of studies have highlighted that homocysteine is a neurotoxic substance such that when excessive levels prevail, N-methyl-D-aspartate (NMDA) receptors [51] as well as some non-NMDA receptors become activated [52] resulting in excitotoxicity. It has been proposed that this action promotes neuronal degeneracy and impairs neuronal plasticity [53-54]. This has been supported by research studies that have noted that elevated homocysteine levels contribute to the pathogenesis of numerous psychiatric disorders such as schizophrenia [55], depression [56] and neurodegenerative disorders including Parkinson's disease [3], dementia [4] and Alzheimer's disease [5]. While there is substantial evidence for the association of elevated homocysteine with neurological disorders, treatment with B-vitamin therapy as a means of reducing the homocysteine level has not yet been proven to slow the cognitive decline associated with these conditions [57].

1.3.3. Pregnancy Complications

Homocysteine levels generally decrease during a normal pregnancy [58] and thus the presence of elevated homocysteine levels during pregnancy is a significant warning signal that is associated with a range of pregnancy complications including: an increased risk of early pregnancy loss [37], pre-eclampsia [59] and a number of

birth defects. The latter are the more significant and include the neural tube defects, spina bifida and encephalocele [60]. Folic acid supplementation for women of child bearing age and during pregnancy is well established and recommended by health care practitioners as it is known to reduce the incidence of neural tube defects [61], with literature supporting the fact that this supplementation helps maintain homocysteine levels within the accepted range [62]. In addition to folic acid supplementation, it has been suggested that the administration of the B group vitamins (B_6 and B_{12}) may also help to reduce some of the complications of pregnancy that are associated with hyperhomocysteinaemia [37].

1.3.4. Genetic Disorders

Homocystinuria is an autosomal recessive genetic disorder that affects the metabolism of homocysteine, resulting in an increase in the levels of homocysteine within plasma, serum and urine. Cystathionone- β-synthase (CBS) deficiency is the most common cause of homocystinuria with impairment of the transsulphuration pathway causing the elevation in the levels of homocysteine and a corresponding decrease in the levels of cysteine [63-64]. Those afflicted with the condition have a high risk of experiencing a thrombo-embolic event but the pernicious nature of the disease means that they can generally remain symptom free up until the actual cardiovascular event. There are however other complications, myopia and lens dislocation, which can occur earlier alerting the clinician to the presence of the underlying condition [10]. Children suffering from this condition may also show mental retardation or have a psychiatric disease. If diagnosed sufficiently early, treatment with folic acid and/or pyridoxine can lower the homocysteine levels and prevent the onset of the clinical symptoms, with the possibility that cardiovascular events may also be avoided [65]. In some countries neonates are universally screened for homocystinuria. This isn't currently done in the UK but is done in Ireland where the condition is much commoner. At present this is done by measuring methionine levels because of the analytical issues surrounding homocysteine analysis (these are discussed in detail at the end of this chapter). Not all cases are detected by measuring methionine however as the test has a high false negative rate (>20%) [66]. Homocysteine itself is without a doubt the more relevant analyte and should

ultimately be the analyte measured in screening programmes once the analytical problems associated with its detection are overcome.

Methylene tetrahydrofolate reductase (MTHFR) thermolabile variant is another genetically inherited disorder. In this condition a mutation of the MTHFR gene at the C677T position causes the MTHFR enzyme to be less active causing an impairment of the remethylation of homocysteine to methionine causing elevated homocysteine levels [67-68].

1.3.5. Cardiovascular Disease

Hyperhomocysteinemia is widely recognised as a risk factor for cardiovascular disease and stroke [2,69] but the pathogenic mechanism(s) by which homocysteine causes damage to the cardiovascular system is still unclear. While there have been numerous *in vitro* and animal model studies, there is no single mechanism and it has been postulated that elevated homocysteine levels result in an alteration in the levels of key metabolites which leads to atherosclerosis [70]. It has been suggested that homocysteine causes endothelial damage and dysfunction by affecting the endothelial antiatherogenic agent nitric oxide (NO). It is proposed that NO is affected in two ways: 1. that high levels of homocysteine interfere with the L-arginine synthesis of NO causing a decrease in NO and 2. that the reactivity of NO is reduced due to the presence of more reactive oxygen species due to an increase in oxidative stress [71]. Another hypothesis is that the elevation in homocysteine interferes with NO production causing an increase in the intracellular calcium concentration. This increase has been reported to enhance platelet response to thrombin and adenosine diphosphate (ADP) resulting in enhanced coagulation which is a key contributor in cardiovascular events [72]. It is also thought that the proliferation of vascular smooth muscle cells due to an increase in DNA synthesis in the presence of homocysteine also contributes to the development of the condition [73-74]. The growth of smooth muscle cells has more recently been found to be balanced with cell death [74].

Although the link between homocysteine and cardiovascular disease is apparent, clinical trials have shown conflicting data as to whether the vascular risk

can be manipulated as a consequence of lowering homocysteine levels *via* treatment with folic acid and B vitamins [75-76]. Numerous explanations for these results have been proposed, including insufficient study time scales [77].

1.4. Glutathione

Glutathione (γ-L-glutamyl-L-cysteinyl-glycine) **Figure 1.4**, is a water soluble tripeptide made in the cytosol of virtually all living cells from its constituent amino acids glutamate, cysteine and glycine [78].
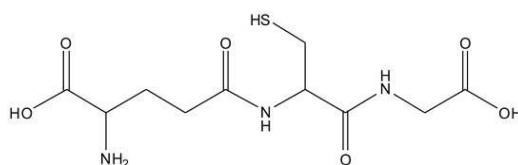
Figure 1.4 The structure of reduced glutathione.

Glutathione synthesis involves 2 enzymatic steps as highlighted in **Scheme 1.3**, the first step is the rate determining step and involves linking glutamate with cysteine using glutamate cysteine ligase (GCL) (formally γ-glutamylcysteine synthetase). The second part of this synthesis involves linking the newly formed γ-L-glutamyl-L-cysteine with L-glycine using glutathione synthase (formally glutathione synthetase). [78-80]
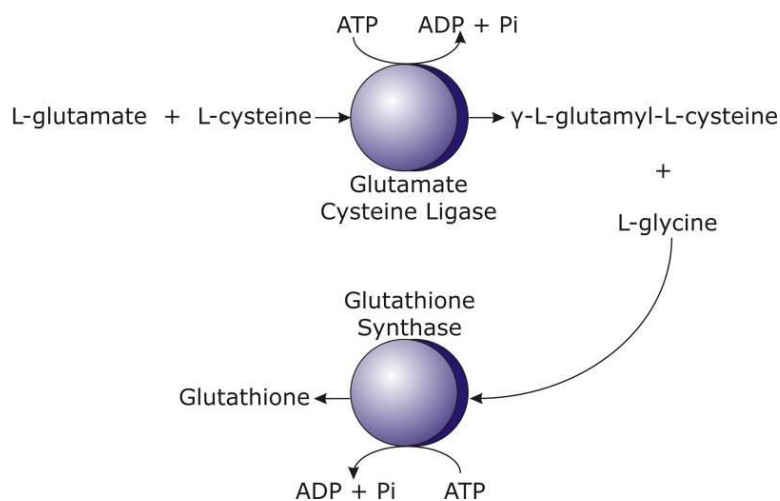
Scheme 1.3 The synthesis of glutathione [78-80].

Glutathione is the most prevalent intracellular sulphydryl thiol species found within the body primarily because the glutamate-cysteine peptide bond is formed

through a linkage of the γ-carboxyl group as opposed to the more conventional α-carboxyl group which makes the structure resistant to most types of hydrolysis and intracellular degradation [78]. Like the other sulphydryl thiols mentioned it can exist in the reduced free form (GSH) (as illustrated in **Figure 1.4**) and the oxidised disulphide and mixed disulphide forms.

The reduced free glutathione from predominates within cells due to the presence of glutathione reductase, a Nicotinamide adenine dinucleotide phosphate (NADPH) dependent enzyme that is constitutively active within the cells [79]. The thiol functionality on the cysteine residue of glutathione enables it to act as both a reducing agent and a nucleophile therefore enabling it to have a multitude of functions including its use in the formation and regulation of certain molecules such as proteins and enzymes, its role as an antioxidant [81] and its role in detoxifying electrophiles [78].

Glutathione levels in the body are affected by a number of factors including sex and age and vary considerably depending on the sample medium. Intracellular levels of glutathione are normally in the range of 1-2mM but can be as high as 10mM in hepatocytes [79]. Levels in plasma and urine are much lower with plasma levels being approximately 10μM (total glutathione concentration) [16,79]. Deviations from these normal reference values can occur due to the dysregulation of glutathione synthesis and lowered glutathione levels have been associated with a number of clinical conditions outlined in brief over the next few pages.

1.4.1. Genetic Disorders

Inborn errors that alter glutathione levels are rare, however, there have been some cases reported where genetic alterations have changed the reactivity of the enzymes used during glutathione synthesis which subsequently causes its levels to be decreased. Deficiencies with the glutathione synthase enzyme appear more frequently than those for the glutamate cysteine ligase enzyme [79]. Two types of glutathione synthase deficiency have been reported. Deficiency one is expressed only in erythrocytes and it has been postulated that it occurs due to a genetic mutation that affects the stability of the enzyme. In deficiency two, which is commonly referred to

as generalised glutathione synthase deficiency it is thought that the deficiency occurs due to a genetic mutation that causes the catalytic activity of the enzyme to be reduced. Both of these deficiencies are characterised by a decrease in glutathione levels and symptoms of the disorders include damage to the central nervous system and haemolytic anaemia [82].

1.4.2. Parkinson's Disease

The link between low glutathione levels and Parkinson's disease has been established for many years. Studies have shown that a decrease in the total glutathione concentration within the substania nigra of patients suffering from Parkinson's disease occurs early on in the diseases progression, before any physical symptoms are presented and as such much work has been focused upon establishing the cause or effect nature of this relationship [83]. The mechanism through which the depletion of glutathione is initiated is unknown, it is however apparent that due to the multifunctional nature of glutathione that this depletion perturbs many cellular processes including the cells oxidative stress defences, DNA synthesis and repair, protein synthesis, amino acid synthesis, toxin removal and neurohormonal signalling all of which may contribute to the pathogenesis of the disease [84-86]. This evidence suggests that restoring glutathione concentrations would be the best approach to prevent disease progression and as such various regimes have been trialled each having varied levels of success [84].

1.4.3. HIV/AIDS

Glutathione has a range of effects on the immune system, it can either stimulate or inhibit an immune response in an attempt to control inflammations. Alterations in the levels of glutathione can therefore have a significant role in those conditions that are caused, promoted or maintained by oxidative stress which includes HIV (human immunodeficiency virus) and AIDS (acquired immune deficiency syndrome) [87]. In patients suffering from these conditions the levels of glutathione can be reduced to depletion in plasma, epithelial lining fluids and peripheral blood and these depletions have been found to correlate with disease mortality [79-80]. The

reduction of glutathione within the lungs of HIV patients has also been correlated with an increased risk of them acquiring an opportunist infection and in these situations levels can be replenished by using aerolised glutathione [87].

1.4.4. Diseases of the Liver

A decrease in the amount of hepatic glutathione is an indicator of many forms of liver disease [83]. This decrease is bought about by a number of factors including impaired glutathione synthesis and transport and/or over-consumption. The decrease causes an increase in oxidative stress and can affect a number of signalling pathways, both of which contribute to the pathogenesis of liver diseases such as acetaminophen-induced liver disease, alcohol induced liver disease and hepatitis c induced liver disease [88].

1.5. Analysis of Sulphydryl Thiols

Cysteine, homocysteine and glutathione levels can be determined using a variety of techniques based on immunoassay [115,135], capillary electrophoresis [133-134], chromatographic [92-93,95,104,111] and enzymatic methods [136-138]. All biological samples are very complex. They contain a multitude of components that can make clinical analysis problematic as they can interfere with the method used making the results obtained inaccurate and unreliable. A further complication when attempting the analysis of the sulphydryl thiols in question is the fact that they can be present in the various forms, the reduced and oxidised forms [15], it may therefore be necessary to carry out sample preparation steps prior to analysis. The extent of this process will vary depending upon the analytical technique being used

Figure 1.5 Outline of the typical thiol analysis protocol after sampling [89,142]

[89]. The majority of literature that discusses thiol analysis is focused upon the analysis of the total thiol concentrations within plasma samples, as this provides the

most stable environment for the thiol species [142]. After the sample has been collected, the analysis will typically follow the general process outlined in **Figure 1.5**, each stage will be discussed in more detail over the next few pages [89,142].

1.5.1. Sample Pre-treatment

After a blood sample has been collected, the thiol levels within the sample will increase. This is because there is a time and temperature dependent release of the thiol species from the erythrocytes present [90,142]. This process can compromise the accuracy of the final analysis, but it can be easily resolved by the immediate separation of erythrocytes from the sample by centrifugation or by storing the samples at low temperatures until centrifugation can take place [90]. As plasma is typically the matrix of choice for the majority of analytical procedures it is then generally processed in three stages [89]:

- Conversion of the oxidised thiol species to the free RSH state,
- Protein precipitation,
- RSH derivatisation.

The conversion of the oxidised thiol species (homo- and hetero disulphides) to the free thiol is necessary to free up the thiol (-SH) functionality. It is this chemical moiety that is normally detected or derivatised subsequently allowing the thiol concentration to be determined. This process can be achieved by the reduction of the -S-S- bound forms by the addition of a reducing agent to the sample. Some of the common reducing agents that have been used for thiol analysis are shown in **Table 1.1**.

Matrix	Reducing Agent	Reference
Plasma	Sodium borohydride (NaBH$_4$)	91-92
Plasma	Dithiothreitol (DTT)	89
Serum Urine	2-Mercaptoethanol (2-MCE)	89
Plasma	2-Mercaptoethanol (MCE)	93
Plasma	Dithiothreitol (DTT)	94
Plasma	Dithiothreitol (DTT)	95-96
Plasma	Tri-n-butylphosphine (TBP)	89
Blood	Triphenylphosphine (TPP)	97
Plasma	Tri-n-butylphosphine (TBP)	98
Cell cultures	Tris(2-carboxylethyl) phosphine (TCEP)	99

Table 1.1 Common thiol reducing agents.

Sodium borohydride was one of the first approaches used for reducing oxidised thiol species. Its handling was found to be problematic (*i.e.* hydrogen evolution) when dealing with biofluids and so alternative agents were investigated [91-92]. The thiol-disulphide exchange method is an alternative reduction route that can used, here the target thiol is released through a nucleophilic substitution reaction with an activated, more easily oxidisable thiol reagent that acts as a sacrificial agent [89,93-96]. These types of reaction are typified by the use of mercaptoethanol (MCE) and dithiothreitol (DTT or Cleland's reagent) and the mechanism through which they act are highlighted in **Scheme 1.4** and **Scheme 1.5,** respectively [93-96].
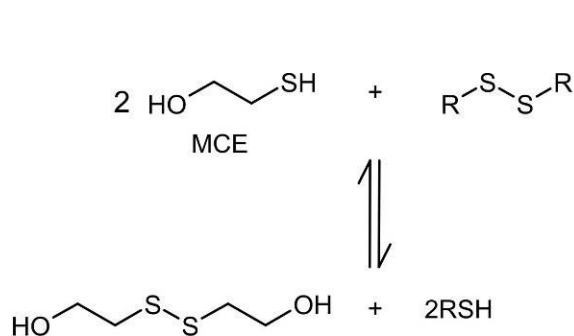
Scheme 1.4 Reduction of RSSR by Mercaptoethanol (MCE) [93-96].
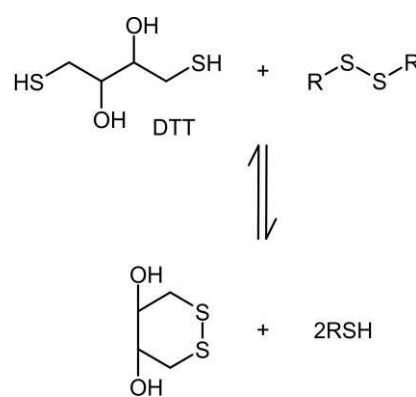
Scheme 1.5 Reduction of RSSR by Dithiothreitol (DTT) [93-96].

The main disadvantage of these types of reagents is that the amount of exchanger thiol used (MCE or DTT) must be in excess of the suspected thiol concentration within the sample. This is necessary to achieve full thiol reduction and, unless the sample is then subjected to a column separation, there is the possibility that the unreacted thiol reducing agent will interfere with the final analysis making the results obtained inaccurate and unreliable. The use of phosphines can counteract this problem, a variety have been assessed including triphenylphosphine (TPP) [97,100], tri-n-butylphosphine (TBP) [98] and tris(2-carboxyethyl) phosphine (TCEP) [99]) with the manipulation of the R substituents reflecting a drive to find a derivative with aqueous solubility. The carboxyethyl derivative TCEP is, at present, reported to be among the more effective given the hydrophilic nature of the acid groups but its mode of action retains the general mechanism outlined in **Scheme 1.6** [13,143].
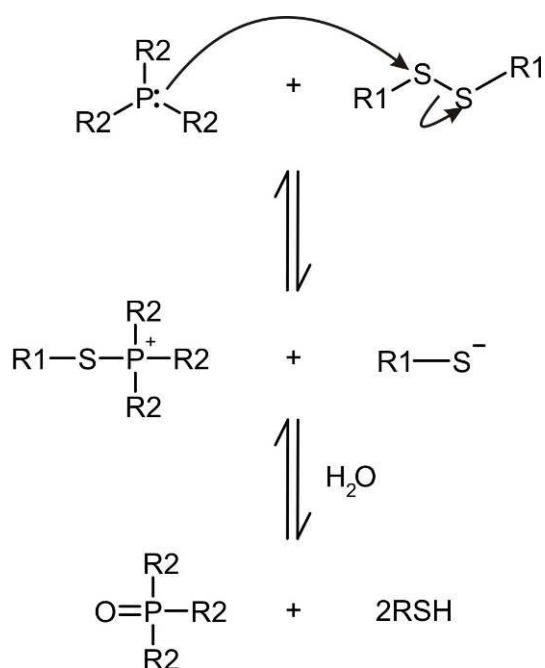
Scheme 1.6 General reaction mechanism for the reduction of disulphides using phosphine reagents [143].

The next part of the sample pre-treatment process is to remove the proteins present within the sample. This is necessary particularly when using chromatographic techniques as it will prevent column fouling and interferences during analysis. Protein removal can be achieved by adding an acid to the sample after the reduction stage of sample pre-treatment is complete. The addition of the acid will cause the proteins to precipitate out of the sample solution whilst the thiol compounds remain soluble thus making separation by centrifugation very simple. Trichloroacetic acid (TCA) [101], perchloric acid (PCA) [102] and sulfosalicylic acid (SSA) [97] are potent protein denaturants and are commonly used as protein precipitating acids. Oxidation of the − SH group has been found to occur in PCA and SSA treated samples and, as such, TCA has been reported to be the most reliable precipitating agent [52].

1.5.2. Derivatisation and Analysis

Table 1.2 highlights the range of methods that can be used for the determination of thiol species within biological samples along with, if necessary, the derivatising agents used.

Method	Sample	LoD/Mm	Derivatising Agent	References
HPLC-UV: 350nm	Plasma	0.4	CQMT	92
HPLC-UV: 312nm	Plasma	0.1	CMPI	101
HPLC-UV	Blood, urine, plasma	0.1	Direct	103
HPLC-FL: 340, 450nm	Plasma	0.08	OPA, MCE	93
HPLC-FL	Plasma	0.12	mBrB	94
HPLC-FL: 300, 470nm	Blood	0.1	mBrB	100
HPLC-FL: 370, 480nm	Cell cultures		OPA	99
HPLC-FL: 385, 515nm	Plasma	NG	SBD-F	101
HPLC-ED	Plasma	Up to 100	Direct	104
HPLC-ED	Blood	0.14	Direct	105
HPLC-ED	Plasma	0.02	Direct	106
ED p- CNT/Nafion/GC	Homocysteine	0.06	Direct	107
ED FSO-Au	Plasma	NG	Direct	108
HPLC-PED	-	0.32	Direct	109
Cation exchange/IPAD	Plasma	0.05	Direct	110
GC-MS	Plasma	0.17	MTBSTFA	95
GC-MS	Plasma	5.0	ECF	96
HPLC- MS	Rat tissues	0.75	Direct	111
HPLC-MS/MS	Serum, plasma	1.0	Direct	112
LC-ESI-MS/MS	Plasma	NG	Direct	113
CE-ED	Plasma	0.5	Direct	89
CE-UV:220nm	Plasma	0.5	ABD-F	89
CE- UV: 234, 250nm	Plasma	NG	mBrB	103
CE-LIF	D, L Homocysteine	0.005	ABD-F	114
ICL	Plasma	0.9	SBD-F	115

Table 1.2 Methodologies used for the detection of RSH.

LoD, limit of detection; NG, not given; HPLC, high performance liquid chromatography; FL, fluorescence detection; UV, ultraviolet detection; EC, electrochemical detection; CNT/nafion/GC, carbon nanotube modified glassy carbon electrode; FSO-Au, fluorosurfactant modified gold electrode; GC, gas chromatography; MS, mass spectroscopy; CE, capillary electrophoresis; LIF, laser induced fluorescence; PED, pulsed electrophoresis detection; IPAD, Integrated Pulsed Amperometric detection; mBrB, monobromobimane; OPA, *o*-phthaladehyde; MCE, 2-mercaptoethanol; SBD-F, 7-flurobenzo-2-oxa-1,3-diazole-4-sulfonate; CQMT, 2-chloro-1-methyl-quinolinium tetrafluroborate; CMPI, 2-chloro-1-methylpyridinium iodide; ABD-F, 4-aminosulfonyl-7-fluoro-2,1,3-benzoxadiazole; MTBSTFA, *N*-(tert-butyldimethylsilyl)-*N*-methyltrifluoroacetamide; ECF, ethylcholoroformate; 6-IAF, 6-iodoacetamindofluorescein; LC-ESI-MS/MS, liquid chromatography-electrospray ionization tandem mass spectroscopy; ICL, Chemiluminescence immunoassay.

A variety of chromatographic techniques have been used for thiol determination, including high-performance liquid chromatography (HPLC) utilising a range of detection methods: ultraviolet-visible (UV-VIS) [92,101,103], fluorescence [93-94,99-100,116] and electrochemical [104-110,117] techniques along with

chromatographic methods coupled to mass spectrometry: gas chromatography-mass spectrometry (GC-MS) [95-96,119] and liquid chromatography-mass spectroscopy (LC-MS) [111-113,119]. Chromatographic techniques are often chosen as the preferential analytical technique as they can be easily automated [89], have a wide analytical range and allow simultaneous detection of multiple analytes present within the sample.

For spectrophotometric analysis (UV-VIS and fluorescence) the thiol species will need to be derivatised as they are not naturally fluorescent and they do not have strong native chromophores in the ultraviolet or visible regions of the electromagnetic spectrum and, as such, are invisible to most spectroscopic detectors [120]. There are a number of fluorescent and UV/VIS derivatising agents available for the detection of thiols. The majority provide a sensitive means of analysis but are unable to differentiate between the various thiol species. *O*-Phthalaldehyde (OPA) is a fluorescent derivatising agent. It reacts readily with the amine functionality on the thiol compound to give a fluorescent OPA derivative. This method can be used over an extensive pH range and also derivatises some amino acids (i.e. aspartate and glutamate) which is useful when carrying out simultaneous chromatographic analysis [93,121]. O-Phthalaldehyde-2-mercaptoethanol (OPA-2-MCE) reagents have also been used and these react in the same way with thiols as OPA but the derivatives produced are only weakly fluorescent. This is thought to be due to the presence of the sulphydryl functionality and so it is necessary to protect these groups prior to the reaction with OPA. A reaction with iodoacetic acid is often used. This is then followed by the derivatisation with OPA in the presence of 2-mercaptoethanol (2-MCE) as indicated in **Scheme 1.7** [93].
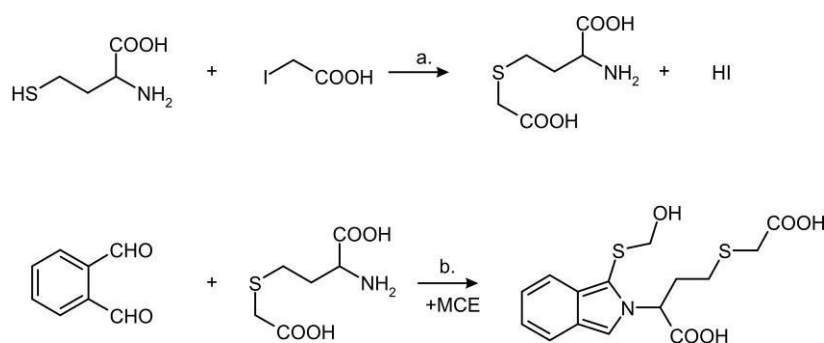
Scheme 1.7 a. The protection of the thiol functionality on homocysteine with iodoacetic acid and b. the derivatisation of the protected homocysteine with OPA (*O*-phthalaldehyde) in the presence of 2-MCE (2-mercaptoethanol)[93].

Another well used non-thiol specific fluorescent reagent is monobromobimane (mBrB). This reacts with the sulphydryl functionality on the thiol species *via* a nucleophilic substituition reaction as indicated in **Scheme 1.8** [94,100].
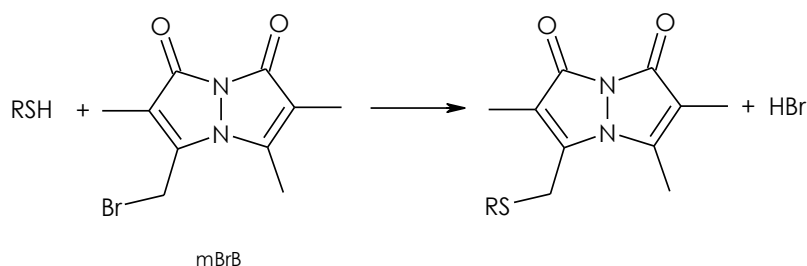
Scheme 1.8 The structure of monobromobimane (mBrB) and its basic thiol (RSH) derivatisation reaction scheme [94,100].

A benefit of mBrB is that when it is used in methanol it can act simultaneously as a protein precipitating and a derivatising agent, thus saving sample pre-treatment time [100]. Another alternative system that has emerged in recent years is based on ammonium 7-fluorobenzo-2-oxa-1,3-diazole-4-sulfonate (SBD-F) or 4-amino-sulphonyl-7-fluoro-2,1-3-benzoxadiazole (ABD-F). The basic reaction pathway with thiol species is detailed in **Scheme 1.9**. This reagent is widely used because there is minimal background fluorescence produced and there are no fluorescent degradation products. Its use is however not ideal as the reaction requires harsh conditions to proceed [89,122].

SBD-F: X = $SO_3^-NH_4^+$
ABD-F: X = SO_2NH_2
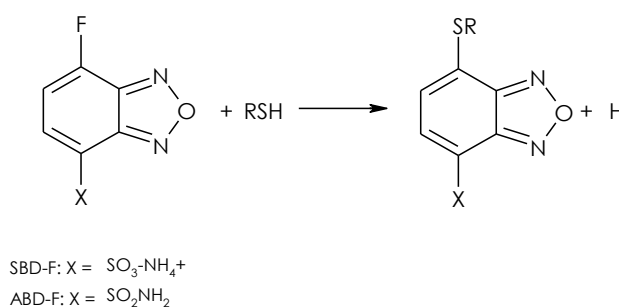
Scheme 1.9 The structures of SBD-F and ABD-F and their general thiol derivatisation reaction [89,122].

The application of UV/VIS derivatising agents has shown good sensitivity towards the determination of thiols. In order to provide effective results, reagents must form a derivative with sufficient UV/VIS absorption to measure the thiol at low concentrations. They must show no background absorption in the absence of the thiol

species and they should also be able to rapidly and specifically react with thiols to generate a stable product [89]. Among these methods of derivatisation, Ellman's reagent (5,5'-dithiobis(2-nitrobenzoic acid) (DTNB)) is predominantly used for the spectrophotometric quantification of thiols [123]. Ellman's reagent reacts with the thiol species leading to the formation of a thiol-TNB adduct and a concomitant release of one equivalent of 5-thio-2-nitrobenzoic acid (TNB). This later absorbs at 412 nm and so the thiol can be quantified (**Scheme 1.10**) [123-124]. This reaction is rapid and a quantitative measurement of the thiol can be achieved when excess DTNB is used at neutral or mildly alkaline pH [123].
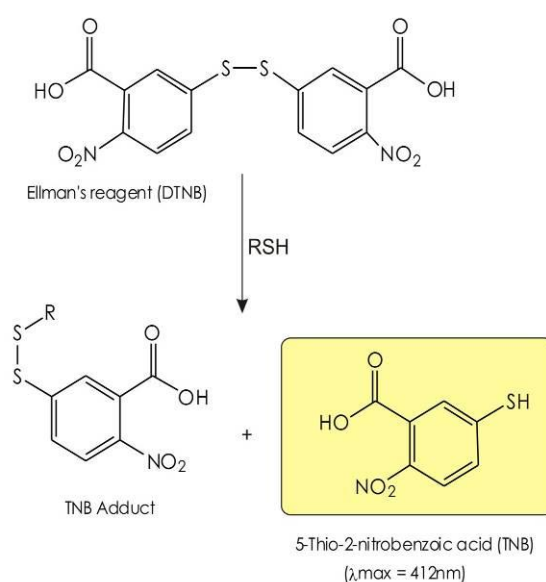
Scheme 1.10 The general reaction scheme for thiol derivatisation with Ellman's reagent [123].

Another common UV/VIS reagent used is 2-chloro-1-methylpyridinium iodide (CMPI). CMPI is able to react rapidly with thiols under slightly alkaline media to produce stable S-pyridinium derivatives, as shown in **Scheme 1.11**, which can be measured spectrophotometrically at 310nm [89,125].
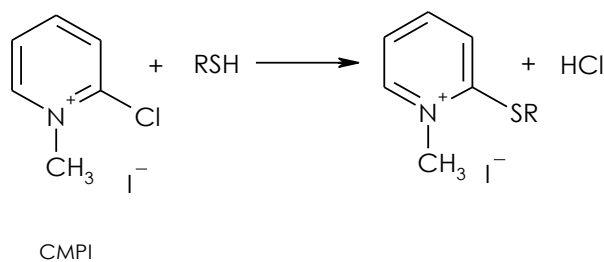
Scheme 1.11 2-chloro-1-methylpyridinium iodide (CMPI) thiol derivatisation reaction scheme [89,125].

Electrochemical thiol detection can be achieved *via* a number of electroanaltyical techniques including cyclic voltammetry [126,127], potentiometry [128], amperometry [129], pulsed techniques [130] and stripping methods [131]. Direct electrochemical analysis of thiol species is achieved *via* their oxidation at the electrode surface [117]. This process can be limited by poor voltammetric behaviour of solid state electrodes, slow electron transfer kinetics and the need to apply a large anodic potential to bring about the electrochemical response which may complicate the analysis as you can get a response from the oxidation of other electroactive components present within the sample. Indirect electrochemical analysis can be achieved by the derivatisation of the thiol species with an electroactive lable. This can result in the signal being enhanced and/or shifted to lower potentials away from interfering signals improving the sensitivity and selectivity of the detection route [14,132].

Capillary electrophoresis can also be used to detect thiol species within biological samples with photometric [89,133-134] and fluorescence [102,114] detection methods being ultilised. Capillary electrophoresis is a simple, fast method for analysis but there are issues related to the sensitivity of the technique especially when UV/VIS detection methods are employed [89].

Immunoassay techniques, including fluorescence polarisation immunoassays (FPIA) [135], chemiluminescence immunoassays (ICL) [115] and enzyme-linked immunoassays (EIA) [136], have all been used for thiol analysis. It is not always necessary for the sample to undergo complex pre-treatment stages when using these techniques [137] which can make them a preferential choice over the other techniques previously described. Immunoassays are however generally more expensive to run than chromatographic methods due to the high cost of reagents even though the labour costs are considerably lower.

Enzymatic assays that allow the selective determination of low molecular weight thiols have also been developed. One example is the Carolina Liquid Chemistries$^{(TM)}$ assay which is used for the selective determination of homocysteine. This method allows homocysteine to be detected without the use of specialised equipment [91] and can therefore offer a number of advantages over the more

traditional analytical approaches used. The colorimetric three enzyme assay (**Scheme 1.12**) is reliant upon an enzyme cascade that offers superior selectivity for homocysteine analysis. In addition, the recycle loop offers an in assay amplification of the response and the end measurement is based on the nicotinamide adenine dinucleotide, NADH/NAD system which has long been a mainstay of clinical biochemistry labs. As such it offers technical and cost advantages when compared to the previously mentioned analytical techniques along with a sufficient level of analytical performance, accuracy and precision, required for routine screening applications [138].
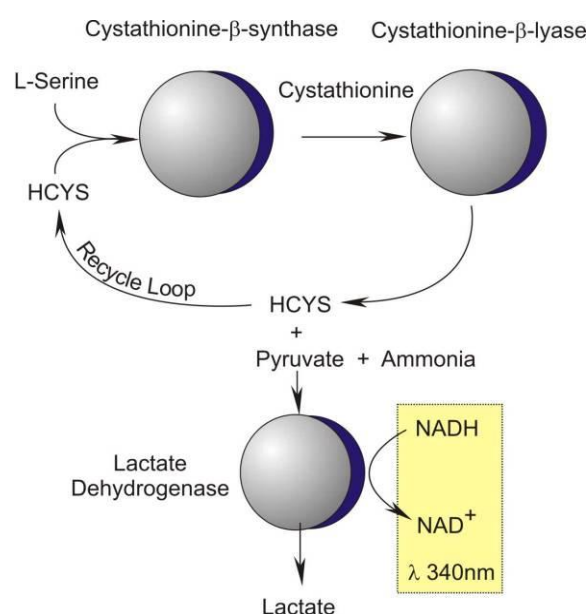
Scheme 1.12 The Carolina Liquid Chemistry^{TM} assay for homocysteine (HCYS) [91,138].

Each method described for the analytical determination of sulphydryl thiols has different levels of accuracy and precision. Studies on the performance of the aforementioned methods used for the analysis of the thiol species in question have shown some significant inconsistencies. Some of these studies have highlighted that the different methods get results that are comparable to one another [139-140], whilst other studies have contradicted this, showing large differences in the accuracy of the measurements, depending on the method used and the testing laboratory [141]. These factors highlight the need for new methods to be developed that can allow for the accurate and standardised analysis of cysteine, homocysteine and glutathione.

1.6. Conclusions

It is clear that the reduced sulphydryl thiols studied have a crucial role to play within the effective running of the human body [14-16] and that they are key players when it comes to the pathogenesis of certain debilitating diseases [1-8]. Current methods used for the determination of these species within biological samples are restricted by a number of factors including speciation and sensitivity issues [9]. This means that analysis, at present, can only be carried out in the specialised central laboratory and even then the results obtained can often be erroneous or ambiguous. A large amount of research is currently focussed upon investigating the cause or effect nature of these molecules within disease [3,7,13,77,83]. Many researchers are also trying to develop new techniques that would facilitate the rapid, reliable and selective determination of thiol species within biological samples [17,90-91,104,106,115,141]. It is hoped that the discoveries made will enable us to gain a better understanding of these diseases and to develop better analyitical methods that can facilitate disease diagnosis, which could ultimately result in the prevention of disease progression.

1.7. Project Aim and Objectives

The aim of the present project is to develop a range of novel electroanalytical approaches that could be used to monitor the sulphydryl thiol compounds: cystiene, homocysteine and glutathione within biological samples. The core objectives were centred upon the development of methods that would:-

- allow interference free thiol analysis,
- enhance the sensitivity of thiol analysis,
- provide a reagentless sensing method for the determination of thiol species,
- allow the selective and unambiguous detection of thiol species, and
- facilitate the detection of biologically relevant molecules, primarily thiol species at the point of care.

Numerous routes to achieve these objectives have been investigated but the majority of the work carried out has focused upon the preparation, examination and

characterisation of a range of quinone materials, in the hope that the chemical properties of these compounds could be exploited to meet the project aim.

1.8. References

[1]   S.N.G. Christopher and B.S. Stevan, Contemporary Management of Cystinuria. Journal of Endourology. 13 (1999) 647-651

[2]   L.H. Humphrey, R. Fu, K. Rogers, M. Freeman and M. Helfard, Homocysteine level and coronary heart disease incidence: a systematic review and meta-analysis. Mayo clinic proceedings. 83 (2008) 1203-1212

[3]   E. Martignoni, C. Tassorelli, G. Nappi, R. Zangaglia, C. Pacchetti and F. Blandini, Homocysteine and Parkinson's disease: A dangerous liaison? Journal of the Neurological Sciences. 257 (2007) 31–37

[4]   R. Obeid and W. Herrmann,. Mechanisms of homocysteine neurotoxicity in neurodegenerative diseases with special reference to dementia. FEBS Letters, 580 (2006) 2994–3005

[5]   C. Babiloni, P. Bosco, R. Ghidoni et al. Homocysteine and electroencephalographic rhythms in alzheimer disease: A multicentric study. Neuroscience, 145 (2007) 942-954

[6]   L. Yuan and N. Kaplowitz, Glutathione in liver diseases and hepatotoxicity, Molecular Aspects of Medicine, 30 (2009) 29–41

[7]   C. Perricone, C. De Carolis and R. Perricone, Glutathione: A key player in autoimmunity. Autoimmunity Reviews, 8 (2009) 697–701

[8]   G.D. Zeevalk, R. Razmpour and L.P. Bernard, Glutathione and Parkinson's disease: Is this the elephant in the room? Biomedicine & Pharmacotherapy, 62 (2008) 236-249

[9]   V. Ducros, K. Demuth, M. Sauvant et al, Methods for homocysteine analysis and biological relevance of the results. Journal of Chromatography B, 781 (2002) 207–226

[10]   H. Refsum, A.D. Smith, P.M. Ueland et al, Facts and Recommendations about Total Homocysteine Determinations: An Expert Opinion. Clinical Chemistry. 50 (2004) 3–32

[11]   J.T. Brosnan, M.E. Brosnan, R.F.P. Bertolo and J.A. Bronton, Methionine: A metabolically unique amino acid. Livestock Science, 112 (2007) 2-7

[12]   P.J. Wlodek, M.B. Iciek, A. Milkowski and O.B. Smolenski, Various forms of plasma cysteine and its metabolites in patients undergoing hemodialysis. Clinica Chimica Acta, 304 (2001) 9–18

[13]   L.E.S. Netto, M.A.D. Oliveira, G. Monteiro et al, Reactive cysteine in proteins: Protein folding, antioxidant defense, redox signaling and more. Comparative Biochemistry and Physiology Part C: Toxicology & Pharmacology, 146 (2007) 180-193

[14]   P.C White, N.S Lawrence, J. Davis and R.G. Compton, Electrochemically initiated 1,4 additions: a versatile route to the determination of thiols. Analytica Chimica Acta, 447 (2001) 1-10

[15]   F. Carlucci and A. Tabucchi, Capillary electrophoresis in the evaluation of aminothiols in body fluids. Journal of Chromatography B, 877 (2009) 3347–3357

[16]   N. Jacob, E. Bruckert, P. Giral, M.J. Foglietti and G. Turpin, Cysteine is a cardiovascular risk factor in hyperlipidemic patients. Atherosclerosis, 146 (1999) 53–59

[17]   M. Rafii, R. Elango, G. Courtney-Martin et al, High-throughput and simultaneous measurement of homocysteine and cysteine in human plasma and urine by liquid chromatography–electrospray tandem mass spectrometry. Analytical Biochemistry. 371 (2007) 71–81

[18]   C.S. Biyani and J.J. Cartledge, Cystinuria—Diagnosis and Management. EAU-EBU Update series. 4 (2006) 175–183

[19]   P. DeVilliers, R. Gutta and V.F. Szymela, Cystinosis, Fanconi syndrome, and odontogenic cysts. Oral Surgery, Oral Medicine, Oral Pathology, Oral Radiology & Endodontics, 106 (2008) 866-871

[20]   A.K. Majors and R.E. Pyeritz, A Deficiency of Cysteine Impairs Fibrillin-1 Deposition: Implications for the Pathogenesis of Cystathionine b-Synthase Deficiency. Molecular Genetics and Metabolism, 70 (2000) 252–260

[21]   C.A. Burtis, E.R. Ashwood and D.E. Burns, 2006. Tietz textbook of clinical chemistry and molecular diagnostics. 4th edition. Missouri:Elsevier Saunders

[22]   R. Giugliani, I. Ferrari and L.J. Greene, An evaluation of four methods for the detection of heterozygous cystinuria. Clinical Chimica Acta, 164 (1987) 227-233

[23]   M. Guillen, D. Corella, M.L. Cabello, A.M. Garcia and J. Hernandez-Yago, Reference Values of Urinary Excretion of Cystine and Dibasic Aminoacids: Classification of Patients with Cystinuria in the Valencian Community Spain. Clinical Biochemistry, 32 (1999) 25-30

[24]   J. Csapol, C. Albert, K. Loki and Z. Csapo-Kiss, Separation and determination of the amino acids by ion exchange column chromatography applying post column derivatisation. Acta Universitatis Sapientia, 1 (2008) 5-29

[25]   R.A. Sherwood, A.C. Titheradge and D.A. Richards, Measurement of plasma and urine amino acids by high-performance liquid chromatography with electrochemical detection using phenylisothiocyanate derivatisation. Journal of Chromatography, 528 (1990) 293-303

[26]   T. Kuhara, Diagnosis of inborn errors of metabolism using filter paper urine, urease treatment, isotope dilution and gas chromatography–mass spectrometry. Journal of Chromatography B, 758 (2001) 3–25

[27]   H. Watanabe, K. Sugahara, K. Inoue, Y. Fujita and H. Kodama, Liquid chromatographic-mass spectrometric analysis for screening of patients with cystinuria, and identification of cystine stone. Journal of Chromatography, 568 (1991) 445-450

[28]   F.S. Patch, Cystinuria and Cystine Lithiasis. The Canadian Medical Association Journal, (1934) 250-255

[29]   P. Goodyer, The Molecular Basis of Cystinuria. Nephron Experimental Nephrology, 98 (2004) e45-e49

[30]   M.G. Coulthard, J. Richardson and A. Fleetwood, The treatment of cystinuria with captopril. American Journal of Kidney Diseases, 25 (1995) 661-662

[31]   R.S. Purohit and M.L. Stoller, Stone clustering ofpatients with cystine urinary stone formation. Urology. 63 (2004) 630-634

[32]   S.P. Sterrett, K.L. Penniston, J.S. Wolf Jr. and S.Y. Nakada, Acetazolamide is an effective adjunct for urinary alkalization in patients with uric acid and cystine stone formation recalcitrant to potassium citrate. Urology, 72 (2008) 278-281

[33]   H. Schierbeek, K. Bijsterveld, T.E. Chapman et al, Stable isotope dilution analysis of cystine in granulocyte suspensions as cysteine: a powerful method for the diagnosis, the follow-up, and treatment of patients with cystinosis. Clinica Chimica Acta, 191 (1990) 39-48

[34]   N.A. Hall and E.P. Young, A high performance liquid chromatography method for the analysis of 35S-cystine: application to the diagnosis of cystinosis. Clinica Chimica Acta, 184 (1989) 1-6

[35]   S. Kaul, A.A. Zadeh and P.K Shah, Homocysteine Hypothesis for Atherothrombotic Cardiovascular Disease. Journal of the American College of Cardiology, 48 (2006) 914-923

[36]   W.M. Hague, Homocysteine and pregnancy. Best Practice & Research Clinical Obstetrics & Gynaecology, 17 (2003) 459-469

[37]   M. De la Calle, R. Usandizaga, M. Sancha et al, Homocysteine, folic acid and B-group vitamins in obstetrics and gynaecology. European Journal of Obstetrics & Gynecology and Reproductive Biology. 107 (2003) 125–134

[38]   D.W. Jacobsen, Homocysteine and vitamins in cardiovascular disease. Clinical Chemistry. 44 (1998) 1833-184

[39]   Y. Kuan, A.E. Dear and M.J. Grigg, Homocysteine: An aetiological contributor to peripheral vascular arterial disease. ANZ Journal of Surgery, 72 (2002) 688-671

[40]   G.J. Cuskelly, P.W Stacpoole, J. Williamson, T.G. Baumgartner and J.F. Gregory, Deficiencies of folate and vitamin B_6 exert distinct effects on homocysteine, serine, and methionine kinetics. American Journal of Physiology- Endocrinology and Metabolism, 281 (2001) E1182-E1190

[41]   S.N. Wickramasighe, Diagnosis in megaloblastic anaemias. Blood Reviews, 20 (2006) 299-318

[42]   S.P. Stabler, J. Lindenbaum and R.H. Allen, The Use of Homocysteine and Other Metabolites in the Specific Diagnosis of Vitamin B-12 Deficiency. Journal of Nutrition, 126 (1996) 1266S-1272S

[43]   R. Clarke, H. Refsum, J. Birks et al, Screening for vitamin B12 and folate deficiency in older persons. The American Journal of Clinical Nutrition, 77 (2003) 1241-1247

[44]   H.M. Williams, H. Lippok and G.H Doherty, Nitric oxide and peroxynitrite signalling triggers homocysteine mediated apoptosis in trigeminal sensory neurons in vitro. Neuroscience research, 60 (2008) 380-388

[45]   P. Ventura, R. Panini, S. Tremosini and G. Salvioli, A role for homocysteine increase in haemolysis of megaloblastic anaemias due to vitamin B_{12} and folate deficiency: results from an in vitro experience. Biochimica et Biophysica Acta (BBA) - Molecular Basis of Disease, 1739 (2004) 33-42

[46]   G.J. Schorah, H. Devitt, M. Lucock and A.C. Dowell, The responsiveness of plasma homocysteine to small increases in dietary folic acid: a primary care study. European Journal of Clinical Nutrition, 52 (1998) 407-411

[47]   N. Yazdanpanah, M.C. Zillikens, F. Rivadeneira et al, Effect of dietary B vitamins on BMD and risk of fracture in elderly men and women: The Rotterdam Study. Bone, 41 (2007) 987-994

[48]   R.A. Alley, E.L. Chen, T.D. Beyer and R.A. Prinz, Does homocysteine contribute to bone disease in hyperparathyroidism? The American Journal of Surgery, 195 (2008) 374–378

[49]   B. Lubec, S. Fang-Kircher, T. Lubec, H.J Blom and G.H.J Boers, Evidence for McKusick's hypothesis of deficient collagen cross-linking in patients with homocystinuria. Biochimica et Biophysica Acta (BBA) - Molecular Basis of Disease, 1315 (1996) 159-162

[50]   W. Sakamoto, H. Isomura, K. Fujie et al, Homocysteine attenuates the expression of osteocalcin but enhances osteopontin in MC3T3-E1 preosteoblastic cells. Biochimica et Biophysica Acta (BBA) - Molecular Basis of Disease, 1740 (2005) 12-16

[51]   S.A. Lipton, W. Kim, Y. Choi et al, Neurotoxicity associated with dual actions of homocysteine at the *N*-methyl-d-aspartate receptor. Proceedings of the National Academy of Sciences of the United States of America, 94 (1997) 5923-592

[52]   E. Zieminska, A. Stafiej and J.W. Łazarewicz, Role of group I metabotropic glutamate receptors and NMDA receptors in homocysteine-evoked acute neurodegeneration of cultured cerebellar granule neurones. Neurochemistry International, 43 (2003) 481–492

[53]   S.A. Algaidi, L.A. Christie, A. McE et al, Long-term homocysteine exposure induces alterations in spatial learning, hippocampal signalling and synaptic plasticity. Experimental Neurology, 197 (2006) 8-21

[54]   M.P. Mattson and T.B. Shea, Folate and homocysteine metabolism in neural plasticity and neurodegenerative disorders. Trends in Neuroscience, 26 (2003) 137-146

[55]   A. Haidemenos, Kontis D, A. Gazi et al, Plasma homocysteine, folate and B12 in chronic schizophrenia. Progress in Neuro-Psychopharmacology & Biological Psychiatry, 31 (2007) 1289–1296

[56]   J. Assies, A. Lok, C.L. Bocking et al, Fatty acids and homocysteine levels in patients with recurrent depression: an explorative pilot study. Prostaglandins, Leukotrienes and Essential Fatty Acids, 70 (2004) 349-356

[57]   R. Diaz, Update on the relationship between homocysteine, B-vitamins, and one-carbon metabolism in aging and neurodegenerative disease. Alzheimers and Dementia, 4 (2008) T200-T201

[58]   V.A. Holmes, Changes in haemostasis during normal pregnancy: does homocysteine play a role in maintaining homeostasis? Proceedings of the Nutrition Society, 62 (2003) 479-793

[59]   A. Gurbuz, A. Karateke and M. Mengulluoglu, Elevated plasma homocysteine levels in preeclampsia and eclampsia. International Journal of Gynecology and Obstetrics, 87 (2004) 165-166

[60]   H. Zhang, G. Luo, Q. Liang et al, Neural tube defects and disturbed maternal folate- and homocysteine-mediated one-carbon metabolism. Experiment Neurology, 212 (2008) 515 -521

[61]   P. Oakley, Elimination of Folic Acid–Preventable Neural Tube Defects. American Journal of Preventive Medicine, 35 (2008) 606-607

[62]   J. Ellison, P. Clark, I.D. Walker and I.A. Greer, Effect of supplementation with folic acid throughout pregnancy on plasma homocysteine concentration. Thrombosis Research, 114 (2004) 25-27

[63]   S. Hutchinson, R.T. Aplinn, H. Webb et al, Molecular effects of homocysteine on cdEGF domain structure: Insights into the pathogenesis of homocysteinuria. Journal of Molecular Biology, 346 (2005) 833-844

[64]   A. Lawson-Yuen and H.L. Levy, The use of betaine in the treatment of elevated homocysteine, Molecular Genetics and Metabolism, 88 (2006) 201-207

[65]   S. Yap, G.H.J. Boers, B. Wilcken et al, Vascular Outcome in Patients With Homocystinuria due to Cystathionine ß-Synthase Deficiency Treated Chronically: A Multicenter Observational Study. Arteriosclerosis, Thrombosis and Vascular Biology, 21(2001) 2080-208

[66]   E.R Naughten, S. Yap and P.D. Mayne, Newborn screening for homocystinuria: Irish and world experience. European Journal of Paediatrics, 157 (1998) S84-87

[67]   M. Buysschaert, J.L. Gala, A, Bessomo and M.P. Hermans, C677T methylene-tetrahydrofolate reductase mutation in type 2 diabetic patients with and without hyperhomocysteinaemia. Diabetes & Metabolism, 30 (2004) 349-354

[68]   Z. Todorović, E. Džoljić, I. Novaković et al, Homocysteine serum levels and MTHFR C677T genotype in patients with Parkinson's disease, with and without levodopa therapy. Journal of the Neurological Sciences, 248 (2006) 56-61

[69]   The Homocysteine Studies Collaboration, Homocysteine studies collaboration, Homocysteine and risk of ischemic heart disease and stroke: a meta analysis. The Journal of the American Medical Association, 288 (2002) 2015-2022

[70]   G. Cacciapuoti, C. Manna, D. Napoli, V. Zappia and M. Porcelli, Homocysteine-induced endothelial cell adhesion is related to adenosine lowering and is not mediated by S-adenosylhomocysteine. FEBS Letters, 581 (2007) 4567-4570

[71]   M.C. Stühlinger, R.K. Oka, E.E. Graf et al, Endothelial Dysfunction Induced by Hyperhomocyst(e)inemia: Role of Asymmetric Dimethylarginine. Circulation, 107 (2003) 933-938

[72]   F. Luo, X. Liu, S. Wang and H. Chen, Effect of homocysteine on platelet activation induced by collagen. Nutrition, 22 (2006) 69-75

[73]   J. Tsai, M.A. Perrella, M. Yoshimizumi et al, Promotion of vascular smooth muscle cell growth by homocysteine: a link to atherosclerosis. Proceedings of the National Academy of Sciences of the United States of America, 91 (1994) 6369-6373

[74]   M. Buemi, D. Marino, G. Di Pasquale et al, Effects of Homocysteine on Proliferation, Necrosis, and Apoptosis of Vascular Smooth Muscle Cells in Culture and Influence of Folic Acid. Thrombosis Research, 104 (2001) 207-213

[75]   R. Marcucci, M. Zanazzi, E. Bertoni et al, Homocysteine-Lowering Therapy and Carotid Intima-Media Thickness in Renal Transplant Recipients. Transplantation Proceedings, 37 (2005) 2491-2492

[76]   H. Lim, Y. Cha and R. Chove, Dietary intervention with emphasis on folate intake reduces serum lipids but not plasma homocysteine levels in hyperlipidemic patients. Nutrition research, 28 (2008) 767-774

[77]   F. Martin-Herrero, Jiménez-Candil, J. Martín-Moreiras et al, Homocysteine, Cause or Consequence? International Journal of Cardiology, 129 (2008) 276-277

[78]   S.C. Lu, Regulation of glutathione synthesis. Molecular Aspects of Medicine, 30 (2009) 42–59

[79]   H.J. Forman, H. Zhang and A. Rinna, Glutathione: Overview of its protective roles, measurement, and biosynthesis. Molecular Aspects of Medicine, 30 (2009) 1–12

[80]   D.M. Townsend, K.D. Tew and H. Tapiero. The importance of glutathione in human disease. Biomedicine & Pharmacotherapy, 57 (2003) 145–155

[81]   A.C. White, V.J. Thannickal and B.L. Fanburg, Glutathione deficiency in human disease. The Journal of Nutritional Biochemistry, 5 (1994) 218-226

[82]   E. Ristoff and A. Larsson, Patients with genetic defects in the g-glutamyl cycle. Chemico-Biological Interactions, 111 (1998) 113–121

[83]   G.D. Zeevalk, R. Razmpour and L.P. Bernard, Glutathione and Parkinson's disease: Is this the elephant in the room? Biomedicine & Pharmacotherapy, 62 (2008) 236-249

[84]   K. Marshall, M. Reist, P. Jenner and B. Halliwell, The neuronal toxicity of sulfite plus peroxynitrite is enhanced by glutathione depletion: Implications for Parkinson's Disease. Free Radical Biology & Medicine, 27 (1999) 515–520

[85]   G.F. Weber, Final common pathways in neurodegenerative diseases: regulatory role of the glutathione cycle. Neuroscience and Biobehavioral Reviews, 23 (1999) 1079–1086

[86]   C.B. Pocernich, A.L. Cardin, C.L. Racine, C.M. Lauderback and D.A. Butterfield, Glutathione elevation and its protective role in acrolein-induced protein damage in synaptosomal membranes: relevance to brain lipid peroxidation in neurodegenerative disease. Neurochemistry International, 39 (2001) 141–149

[87]   C. Perricone, C. De Carolis and R. Perricone, Glutathione: A key player in autoimmunity. Autoimmunity Reviews, 8 (2009) 697–701

[88]   L. Yuan and Neil Kaplowitz, Glutathione in liver diseases and hepatotoxicity. Molecular Aspects of Medicine, 30 (2009) 29–41

[89]   O. Nekrassova, N.S. Lawrence and R.G. Compton, Analytical determination of homocysteine: a review. Talanta, 60 (2003) 1085-1095

[90]   K. Rasmussen and L. Moller, Total homocysteine measurement in clinical practice. Annals of Clinical Biochemistry, 37 (2000) 627-648

[91]   R.E. Hansen and J.R. Winther, An introduction to methods for analyzing thiols and disulfides: Reactions, reagents, and practical considerations. Analytical Biochemistry, 394 (2009) 147-158

[92]   G. Chwatko and E. Bald, Determination of different species of homocysteine in human plasma by high-performance liquid chromatography with ultraviolet detection. Journal of Chromatography A, 949 (2002) 141-151

[93]   Y.V. Tcherkas and A.D. Denisenko, Simultaneous determination of several amino acids, including homocysteine, cysteine and glutamic acid, in human plasma by isocratic reversed-phase high-performance liquid chromatography with fluorimetric detection. Journal of Chromatography A, 913 (2001) 309-313

[94]   S. Chou, L. Ko and C. Yang, High performance liquid chromatography with fluorimetric detection for the determination of total homocysteine in human plasma: method and clinical applications. Analytica Chimica Acta, 429 (2001) 331-336

[95]   V. Ducros, D. Schmitt, G. Pernod et al, Gas chromatographic–mass spectrometric determination of total homocysteine in human plasma by stable isotope dilution: method and clinical applications. Journal of Chromatography B: Biomedical Sciences and Applications, 729 (1999) 333-339

[96]   S. Myung, M. Kim, H. Min, E. Yoo and K. Kim, Determination of homocysteine and its related compounds by solid-phase microextraction–gas chromatography–mass spectrometry. Journal of Chromatography B: Biomedical Sciences and Applications, 727 (1999) 1-8

[97]   E. Caussé, C. Issac, P. Malatray et al, F. Assays for total homocysteine and other thiols by capillary electrophoresis–laser-induced fluorescence detection: I. Preanalytical condition studies. Journal of Chromatography A, 895 (2000) 173-178

[98]   E. Bald, E. Kaniowska, G. Chwatko and R. Glowacki, Liquid chromatographic assessment of total and protein-bound homocysteine in human plasma. Talanta, 50 (2000) 1233-1243

[99]   Y. Mukai, T. Togawa, T. Suzuki, K. Ohata and S. Tanabe, Determination of homocysteine thiolactone and homocysteine in cell cultures using high-performance liquid chromatography with fluorescence detection. Journal of Chromatography B: Analytical Technologies in the Biomedical and Life Sciences, 767 (2002) 263-268

[100]   A.R. Ivanov, I.V. Nazimov and L. Baratova, Determination of biologically active low-molecular-mass thiols in human blood: I. Fast qualitative and quantitative, gradient and isocratic

reversed-phase high-performance liquid chromatography with photometric and fluorescence detection. Journal of Chromatography A, 895 (2000) 157-166

[101] G. Minniti, A. Piana, U. Armani and R. Cerone, Determination of plasma and serum homocysteine by high-performance liquid chromatography with fluorescence detection. Journal of Chromatography A, 828 (1998) 401-405

[102] C. Chassaing, J. Gonin, C.S. Wilcox and I.W. Wainer, Determination of reduced and oxidized homocysteine and related thiols in plasma by thiol-specific pre-column derivatisation and capillary electrophoresis with laser-induced fluorescence detection. Journal of Chromatography B: Biomedical Sciences and Applications, 735 (1999) 219-227

[103] K. Amarnath, H.L. Valentine and W.M. Valentine, A specific HPLC-UV method for the determination of cysteine and related aminothiols in biological samples. Talanta, 60 (2003) 1229-1238

[104] G. Zhang, D. Liu, S. Shuang and M.M.F. Choi, A homocysteine biosensor with eggshell membrane as an enzyme immobilization platform. Sensors and Actuators B: Chemical, 114 (2006) 936-942

[105] R. Accinni, S. Bartesaghi, G. De Leo et al, Screening of homocysteine from newborn blood spots by high-performance liquid chromatography with coulometric array detection. Journal of Chromatography A, 896 (2000) 183-189

[106] L. Agüí, C. Peña-Farfal, P. Yáñez-Sedeño and J.M. Pingarrón. Electrochemical determination of homocysteine at a gold nanoparticle-modified electrode. Talanta, 74 (2007) 412-420

[107] K. Gong, Y. Dong, S. Xiong, Y. Chen and L. Mao, Novel electrochemical method for sensitive determination of homocysteine with carbon nanotube-based electrodes. Biosensors and Bioelectronics, 20 (2004) 253-259

[108] Z. Chen and Y. Zu, Electrochemical recognition of single-methylene difference between cysteine and homocysteine. Journal of Electroanalytical Chemistry, 624 (2008) 9-13

[109] T.R.I. Cataldi and D. Nardiello, A pulsed potential waveform displaying enhanced detection capabilities towards sulfur-containing compounds at a gold working electrode. Journal of Chromatography A, 1066 (2005) 133-142

[110] P. Jandik, J. Cheng, J. Evrovski and N. Avdalovic, Simultaneous analysis of homocysteine and methionine in plasma. Journal of Chromatography B: Biomedical Sciences and Applications, 759 (2001) 145-151

[111] X. Guan, B. Hoffman, C. Dwivedi and D.P. Matthees, A simultaneous liquid chromatography/mass spectrometric assay of glutathione, cysteine, homocysteine and their disulfides in biological samples. Journal of Pharmaceutical and Biomedical Analysis, 31 (2003) 251-261

[112] J. Kuhn, C. Götting and K. Kleesiek, Rapid micro-scale assay for homocysteine by liquid chromatography-tandem mass spectrometry. Clinical Biochemistry, 39 (2006) 164-166

[113] S. Li, J. Jia, G. Liu et al, Improved and simplified LC–ESI-MS/MS method for homocysteine determination in human plasma: Application to the study of cardiovascular diseases. Journal of Chromatography B, 870 (2008) 63-67

[114] S.H. Kang, W. Wei and E.S. Yeung, On-column derivatisation for the analysis of homocysteine and other thiols by capillary electrophoresis with laser-induced fluorescence detection. Journal of Chromatography B: Biomedical Sciences and Applications, 744 (2000) 149-156

[115] K. Demuth, V. Ducros, S. Michelsohn and J. Paul, Evaluation of Advia Centaur® automated chemiluminescence immunoassay for determining total homocysteine in plasma. Clinica Chimica Acta, 349 (2004) 113-120

[116] T.D. Nolin, M.E. McMenamin and J. Himmelfarb, Simultaneous determination of total homocysteine, cysteine, cysteinylglycine, and glutathione in human plasma by high-performance liquid chromatography: Application to studies of oxidative stress. Journal of Chromatography B, 852 (2007) 554-56

[117] N.S. Lawrence, R.P. Deo and J. Wang, Detection of homocysteine at carbon nanotube paste electrodes. Talanta, 63 (2004) 443-449

[118] A. Windelberg, O. Arseth, G. Kvalheim and P.M. Uelandclin, Automated Assay for the Determination of Methylmalonic Acid, Total Homocysteine, and Related Amino Acids in Human Serum or Plasma by Means of Methylchloroformate Derivatisation and Gas Chromatography–Mass Spectrometry. Clinical Chemistry, 51 (2005) 2103-2109

[119] K. Gempel, K. Gerbitz, B. Casetta and M.F. Bauer, Rapid Determination of Total Homocysteine in Blood Spots by Liquid Chromatography-Electrospray Ionization-Tandem Mass Spectrometry. Clinical Chemistry, 46 (2000) 122-123

[120] R. Głowacki and E. Bald, Fully automated method for simultaneous determination of total cysteine, cysteinylglycine, glutathione and homocysteinein plasma by HPLC with UV absorbance detection. Journal of Chromatography B, 877 (2009) 3400-3404

[121] I. Molnar-Perl, Derivatisation and chromatographic behavior of the o-phthaldialdehyde amino acid derivatives obtained with various SH-group-containing additives. Journal of Chromatography A, 913 (2001) 283–302

[122] P. Monostori, G. Wittmann, E. Karg and S. Turi, Determination of glutathione and glutathione disulfide in biological samples: An in-depth review. Journal of Chromatography B, 877 (2009) 3331–3346

[123] W. Chen, Y. Zhao, T. Seefeldt and X. Guan, Determination of thiols and disulfides via HPLC quantification of 5-thio-2-nitrobenzoic acid. Journal of Pharmaceutical and Biomedical Analysis, 48 (2008) 1375-1380

[124] F. Ricci, F. Arduini, A. Amine, D. Moscone and G. Palleschi, Characterisation of Prussian blue modified screen-printed electrodes for thiol detection. Journal of Electroanalytical Chemistry, 563 (2004) 229-237

[125] G. Chwatko and E. Bald, Determination of cysteine in human plasma by high-performance liquid chromatography and ultraviolet detection after pre-column derivatisation with 2-chloro-1-methylpyridinium iodide. Talanta, 52 (2000) 509–515

[126] A.A. Ensafi and S. Behyan, Sensing of L-Cysteine at glassy carbon electrodes using Nile Blue A as a mediator. Sensors and Actuators B: Chemical, 122 (2007) 282-288

[127] L. Yao-Tong, A. Ganguly, C. Li-Chyong and K. Chen, Direct voltammetric sensing ood L-cysteine at pristine GAN nanowires electrode. Biosensors and Bioelectronics, 26 (2010) 1688-1691

[128] M.K. Amini, J.H. Khorasani, S.K. Shokooh and S. Tange, Cobalt (II) salophen-modified carbon paste electrodes for potentiometric and voltammetric determination of cysteine. Analytical Biochemistry, 320 (2003) 32-38

[129] A. Salimi and S. Pourbeyran, Renewable sol-gel carbon ceramic electrodes modified with a Ru-complex for the amperometric detection of L-cysteine and glutathione. Talanta, 60 (2003) 205-214

[130] P.J. Vanderberg and D.C. Johnson, Pulsed electrochemical detection of cysteine, cystine, methionine and glutathione at gold electrodes following their separation by liquid chromatography. Analytical Chemistry, 65 (1993) 2713-2718

[131] G. Jin, L. Chen, G. Hang, S. Yang and X. Wu, Stripping chronopotentiometric analysis of cysteine on nano-silver coat polyquercetin-MWCNT modified platinum electrode. Journal of solid state electrochemistry, 14 (2010) 1163-1169

[132] O. Nekrassova, N.S. Lawrence and R.G. Compton, Selective electrochemical assay for cysteine at a boron doped diamond electrode. Electroanalysis, 16 (2004) 1285-1291

[133] V. Ducros, K. Demuth, M. Sauvant et al, Methods for homocysteine analysis and biological relevance of the results. Journal of Chromatography B, 781 (2002) 207-226

[134] E. Caussé, N. Siri, H. Bellet et al, Plasma Homocysteine Determined by Capillary Electrophoresis with Laser-induced Fluorescence Detection. Clinical Chemistry, 45 (1999) 412-414

[135] N.L. Duarte, X.L. Wang and D.E.L. Wilcken, Effects of Anticoagulant and Time of Plasma Separation on Measurement of Homocysteine. Clinical Chemistry, 48 (2002) 665-668

[136] H.H. Yu, R. Joubran, M. Asmi et al, Agreement among four homocysteine assays and results in patients with coronary atherosclerosis and controls. Clinical Chemistry, 46 (2000) 258–264

[137] M.T. Shipchandler and E.G. Moore, Rapid, Fully Automated Measurement of Plasma Homocyst(e)ine with the Abbott lMx Analyzer. Clinical Chemistry, 41 (1995) 991-994

[138] B. Zappacosta, S. Persichilli, A. Minucci et al, Evaluation of a new enzymatic method for homocysteine measurement. Clinical Biochemistry, 39 (2006) 62-66

[139] R.F. Roberts and W.L. Roberts, Performance characteristics of a recombinant enzymatic cycling assay for quantification of total homocysteine in serum or plasma. Clinica Chimica Acta, 344 (2004) 95-99

[140] P. Pernet, G. Cuzon, S.K. Lim et al, Plasma homocysteine measurement with ion exchange chromatography (Jeol Aminotac 500): A comparison with the Abbott IMx assay. Medical Principles and Practice, 15 (2006) 149- 152

[141] M. Haltmayer, T. Mueller, A. Gegenhuber and W. Poelz, Comparison of the automated AxSYM and ADVIA centaur immunoassays for homocysteine determination. Clinical Laboratory, 50 (2004) 175-180

[142] I.Fermo, E. DeVocchi, C. Arcelloni, A.D'Angelo and R. Paroni, Methodological aspects of total plasma homocysteine measurements. Haematologia, 82 (1997) 246-250

[143] J.A. Burns, J.C. Butler, J. Moran and G.M. Whitesides, Selective reduction of disulphides by tris(2-carboxyethyl)phosphine. Journal of Organic Chemistry, 56 (1991) 2648-2650

Chapter 2

Core Methodologies

Chapter 2

Core Methodologies

Abstract

Electroanalytical techniques have a number of advantages including their high sensitivity, low cost and versatility. This, along with the compact nature of the sensing area, makes them ideal for use within clinical analysis, particularly the point of care diagnostic sector. For this reason these techniques, primarily cyclic voltammetry and square-wave voltammetry, have been used extensively throughout this project in an attempt to develop new routes for the analysis of reduced sulphydryl thiols. This chapter therefore provides an overview of these procedures. Supplementary techniques, electrochemical quartz crystal microbalance and spectrophotometry, used to a lesser extent throughout the project are also discussed.

2.1. Introduction to Electrochemistry

Electrochemistry is the study of chemical species by looking at the electron transfer reactions that can occur at an electrode-solution interface. The low cost, availability of numerous operational set ups and the wide variety of electrode materials available means that electrochemical methods are a popular choice for a range of different applications, including qualitative and quantitative clinical analysis [1-2]. Electrochemical techniques can be used directly or can be integrated into other analytical systems, such as chromatographic methods [3-4]. This can provide the selective and sensitive analysis of a range of analytes within a variety of different biological samples, including therapeutic drugs [3,5], neurotransmitters [4,6], amino acids [7], electrolytes (e.g. sodium, potassium and calcium ions) [2] and the thiol compounds (cysteine, homocysteine and glutathione) [8-9] associated with this project.

2.2. The Electrochemical Cell

In order to study electrochemical processes successfully it is necessary to have a certain operational set up. This is defined as the electrochemical cell which consists of 2 or 3 electrodes (electron conductors) and an electrolyte / test solution (ionic conductor). The electrodes are linked to a potentiostat. This controls the potential of the system whilst measuring any changes in current that occur at the electrode-solution interface. The electrode configuration used will vary depending on the electrochemical technique being implemented. A reference electrode (RE) and a working electrode (WE) will be present in a 2 electrode configuration and an additional auxillary or counter electrode (AE or CE) will be present in a 3 electrode set up.

2.2.1. Reference Electrodes

Reference electrodes are a crucial component of the electrochemical cell as they provide a stable and reproducible potential against which the potential of the working electrode can be measured. A range of different reference electrodes are

available. Each has a number of advantages and disadvantages which will determine if and when they are used. The silver/silver chloride half cell reference electrode was used primarily throughout this work because these electrodes are cheap, easily constructed and can be conveniently incorporated within the electrochemical cell.

The set up of the silver/silver chloride electrode is illustrated in **Figure 2.1**. It consists of a silver wire coated with a layer of silver chloride immersed in a solution of potassium chloride, typically 3M, contained within a glass sheath. This set up is separated from the test solution *via* a porous frit which acts as a salt bridge allowing a slow outflow of KCl enabling electrical contact with the test solution.
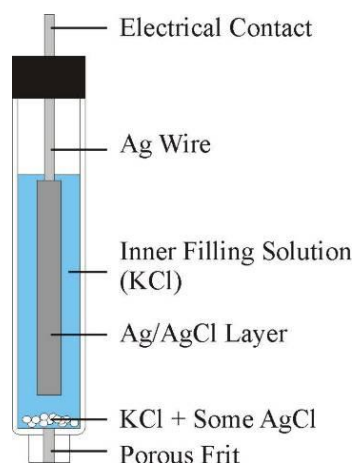
Figure 2.1 Schematic illustrating the set up of the silver/silver chloride reference electrode [1].

$$AgCl_{(s)} \quad + \quad e^- \quad \leftrightarrow \quad Ag_{(s)} \quad + \quad Cl^-_{(aq)} \qquad \textbf{Equation 2.1}$$

The electrode reaction occurring within the silver/silver chloride half cell is given in **Equation 2.1** and the electrochemical processes taking place can be described using the Nernst equation (**Equation 2.2**).

$$aOx \; + \; ne\text{-} \; \rightarrow bRed$$

$$E \; = \; E^o \; - \; \frac{2.303RT}{nF} \log \frac{aRed^b}{aOx^a}$$

Where; E, is the electrode potential; E^0, is the standard electrode potential; R, is the universal gas constant ($8.314 \; J \; K^{-1} \; mol^{-1}$); T, is the temperature (K); n is the number of electrons involved in the reaction; F, is the Faraday constant ($96485 \; C \; mol^{-1}$); a is the activities of the oxidised and reduced species and ^{b} and ^{a} is the stoichiometry of the reduced and oxidised species.

Equation 2.2 The Nernst Equation [1].

If the Nernst equation is examined for the silver/silver chloride reference electrode it can be concluded that the potential of the electrode will be controlled solely by the activity of the chloride ions present as the activities of the silver metal and the silver chloride solid are both unity. As such, with a saturated and therefore invariable concentration of chloride ions, assuming that the chloride activity is unity and that the system is under standard conditions, then the reduction potential of the AgCl/Ag couple (**Equation 2.1**) is +0.222V. For the set up in **Figure 2.1** the activity of the chloride ions is not unity and so the potential of the couple at 25ºC is +0.197V [1].

2.2.2. Working Electrodes

The working electrode is the conductor at which the reaction of interest will occur. A variety of different working electrodes are available and so the one selected for an experiment will vary depending upon the redox properties of the species under study and the background current that is generated from that electrode. These electrodes can be made from a range of different materials including carbon, mercury and noble metals, such as platinum or gold [2].

Carbon electrodes make excellent working electrodes as they can be used over wide operating potentials, have low background currents and are chemically inert [2,10]. A variety of different carbon electrodes are available including the glassy carbon electrode, printed carbon electrodes and carbon fibre electrodes. Glassy or vitreous carbon electrodes are a very popular choice for use as a working electrode as they have excellent mechanical and electrical properties. They are easy to use and have a simple pre-treatment process which involves polishing the electrode surface with alumina particles followed by ultrasonic cleaning in deionised water which can enhance the electrodes response and ensure that the data obtained is reproducible [2]. Printed carbon electrodes have had much success for research and industrial applications [11-13]. These electrodes are cheap and are easily fabricated by printing conductive inks, containing graphite, binders and solvents onto the desired electrode substrate [11]. They are ideal for sensing purposes because the conductive ink can be tailored by the addition of certain modifiers, such as inorganic compounds [12-13],

organic compounds [14] and enzymes [13,15] which will impart functionality onto the electrode surface which can subsequently enhance the electrodes selectivity, sensitivity and overall all round performance [16].

2.2.3. Auxiliary or Counter Electrode

The auxiliary or counter electrode is added to the electrochemical cell when the electrochemical method being used is a controlled potential technique. The counter electrode is the current carrying electrode that allows the electrons to flow through the system without the potential of the reference electrode being affected. This is important as it ensures that the potential measured at the working electrode is measured against a stable potential therefore guaranteeing the accuracy of the results. These electrodes are made from chemically inert materials, such as carbon or platinum [2,10].
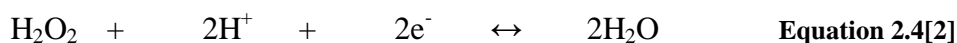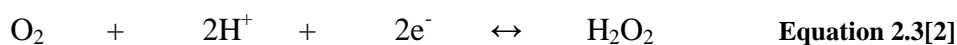
2.2.4. The Test Solution

Electrochemical measurements are typically carried out in a test solution. This is a solvent medium that contains the electroactive species under study and a supporting electrolyte. The choice of solvent will depend on a number of factors including the solubility and activity of the electroactive species and the physical properties of the solvent (i.e. the electrical conductivity, the electrochemical activity and the chemical reactivity). Commonly used solvents include water, acetonitrile, dimethyformamide, dimethylsulfoxide and methanol. It is important the solvent used does not react with the electroactive species and/or undergo any electrochemical reactions over the potential range being examined. The supporting electrolyte is present to decrease the resistance of the solution therefore removing any electromigration effects. It also ensures that the ionic strength of the solution remains constant. The electrolyte must be inert to the system under study and is commonly an inorganic salt, an acid or a buffer, with the latter being particularly useful when the pH of the cell needs to be maintained [2-10].

2.2.4.1. Brittion-Robinson Buffer

Britton-Robinson buffer was used primarily as the test solution throughout this thesis. It consists of a mixture of acetic, boric and phosphoric acids, all at 0.04M and it is adjusted to the required pH *via* the addition of sodium hydroxide. It can be used over the pH range from 2 to 12 which makes it ideal for electrochemical analysis.

2.3. Oxygen Removal

In many experiments it is necessary to remove any dissolved oxygen from the cell before making any measurements. This is essential as oxygen is easily reduced *via* two 2e- transfer steps, **Equation 2.3** and **2.4 [2]**.

$$O_2 \quad + \quad 2H^+ \quad + \quad 2e^- \quad \leftrightarrow \quad H_2O_2 \qquad \textbf{Equation 2.3[2]}$$

$$H_2O_2 \quad + \quad 2H^+ \quad + \quad 2e^- \quad \leftrightarrow \quad 2H_2O \qquad \textbf{Equation 2.4[2]}$$

Both of these steps produce large background currents which may interfere with the results obtained. Oxygen can be removed from the system using a variety of different methods including the use of nitrogen-activated nebuisers, electrochemical or chemical zinc scrubbers and chemical reduction. The easiest route used is to purge the system with an inert gas, typically nitrogen prior to the experiment, followed by blanketing the solution with the gas whilst making any measurements. This route of oxygen removal was used when necessary during this project [2].

2.4. Mass-Transport

Since electrochemical measurements are performed at an electrode-solution interface in order for a redox reaction to occur the electroactive species must be transported from the bulk solution to the electrode surface, this process is called mass transport. As the overall rate of a reaction is determined by the slowest reaction step mass transport effects can have a significant effect on the rate of the reaction and therefore may need to be considered when interpreting the data produced. Three modes of mass transport are significant: diffusion, convection and migration [2, 10].

The *flux* (*J*), is used to measure the rate of mass transport at a fixed point and is defined as the number of molecules moving into a unit area of an imaginary plane in a unit of time. It is described, for movement in one dimension, using the *Nernst-Planck equation* (**Equation 2.5**) [2].

$$J(x,t) = -D \frac{dC(x,t)}{dx} - \frac{zFDC}{RT} \frac{d\Phi(x,t)}{dx} + C(x,t)V(x,t)$$
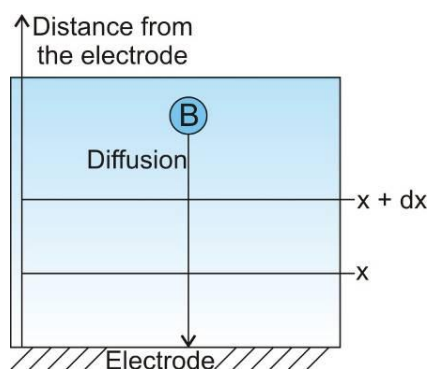
Where; *J, flux* ($cm^{-2}s^{-1}$); x, distance (cm); t, time (s); D, diffusion coefficient (cm^2s^{-1}); dC(x,t)/dx, concentraton gradient; z, charge of the species involed; F, the Faraday constant (96485 C mol^{-1}); C, concentration ($mol^{-1}dm^{-3}$); R, the universal gas constant (8.314 J K^{-1} mol^{-1}); T, temperature (K); dΦ(x,t)/dx, potential gradient and V(x,t), hydrodynamic velocity in the x direction.

Equation 2.5 The *Nernst-Planck equation* [2]

Equation 2.5 is quite complex but the situation can be made easier as the effects caused by convection and migration can be removed by using a quiescent solution and by adding an excess of inert electrolyte respectively.

2.4.1. Diffusion

Diffusion is the movement of components from a region of high concentration to a region of low concentration down a concentration gradient as highlighted in **Figure 2.2**. This movement occurs in an attempt to try and minimize concentration differences within the cell. According to Fick's first law of diffusion (**Equation 2.6**) the rate of diffusion or diffusional flux (*j*, mol cm^{-2} s^{-1}) for a species B at

Figure 2.2 The process of diffusion [2]

a distance x from the electrode surface is proportional to the concentration gradient of the species at that point [2].

$$j = -D \frac{d[B]}{dx}$$

Where; *j*, diffusional flux (mol cm^{-2} s^{-1}); [B], is the concentration of species B ($mol^{-1}dm^{-3}$); D is the diffusion coefficient for B (cm^2 s^{-1}) and dx, distance (cm).

Equation 2.6 Fick's first law of diffusion [2].

To study diffusion changes over time, for example the diffusion of B from x plus dx to x during the time interval dt (s), Fick's second law of diffusion (**Equation 2.7**) must be used [2].

$$\frac{d[B]}{dt} = D\frac{d^2[B]}{dx^2}$$

Equation 2.7 Fick's second law of diffusion [2].

2.4.2. Convection

Convection is the movement of components to the electrode surface as a result of the application of a mechanical force to the solution. This can be natural convection which arises due to thermal and/or density differences within the solution or it can be forced convection which can be achieved by bubbling gas through the solution, by mechanical stirring of the solution or by pumping the solution over the electrode surface [2]. Forced convention usually has well-defined hydrodynamic behaviour and as a result the concentration changes over time can be defined using **Equation 2.8**.

$$\frac{d[B]}{dt} = -v_x\frac{d[B]}{dx}$$

Where: v_x is the velocity of the solution.

Equation 2.8 The equation for convection [2].

2.4.3. Migration

Migration is the movement of charged particles due to the electric field produced at the interface as a result of the differences in the electrical potentials of the 2 phases (the electrode and the solution), i.e. cations are attracted by a negatively charged field and repelled by a positively charged field, the reverse is true for anions. The migratory flux (j_m) of an ion is proportional to the concentration of the ionic species [B], the electric field ($d\Phi/dx$) and the mobility of the ion (u) as indicated in **Figure 2.3** [2].

$$j_m \propto -u[B]\frac{d[\Phi]}{dx}$$

Figure 2.3 Representation of migration [2].

2.5. Voltammetry

Voltammetry is the term given to the collection of electrochemical techniques that measure the changes in current (amps) at the working electrode when a potential (volatge) is applied to the system. There are a range of different methods including staircase voltammetry, stripping voltammetry, polarography, cyclic voltammetry and square-wave voltammetry. The last two techniques have been used extensively throughout this work due to their usefulness in quantitative analysis [1,2,10].

2.5.1. Cyclic Voltammetry

Cyclic voltammetry is a popular electrochemical technique used for obtaining qualitative information on the electrochemical processes taking place within a cell and was the main electrochemical method used during this project. It enables the redox processes of the electroactive species to be located easily and the operational set up can be altered to give vital information on the reactions occurring. Cyclic voltammetry is carried out by scanning the potential of the working electrode using a triangular waveform; here the potential is swept linearly from a potential E_1 to a potential E_2 and then back again to E_1, as illustrated in **Figure 2.4**. During this, the redox processes of the electroactive species should occur altering the current observed for the system. It should be noted that if no backward sweep is applied to the system then the technique is called linear sweep voltammetry (LSV) [1,2,10].
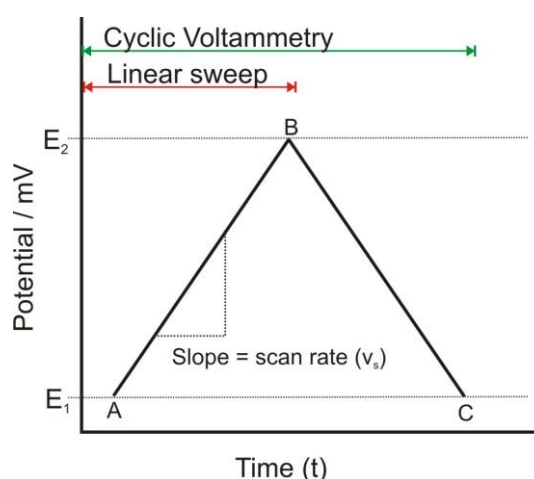
Figure 2.4 Potential vs. time signal during a cyclic/linear sweep voltammetric experiment [1,2,10].

In cyclic voltammetry the potential cycling can be carried out once or several times so that a large amount of information can be collected on the system under study. As the potential of the system is changed the potentiostat will measure the current formed by the system producing a plot of current (I/µA) vs. potential (E/mV) which is called a cyclic voltammogram. The cyclic voltammogram produced can be

very complex and will vary depending on the species under examination. A typical cyclic voltammogram for a reversible redox couple is highlighted in **Figure 2.5**.

Figure 2.5 shows the cyclic voltammogram for the oxidation followed by the reduction of a typical reversible redox couple (Fe^{2+} + e- $\leftrightarrow$ Fe^{3+}). The starting point of the voltammogram (**Figur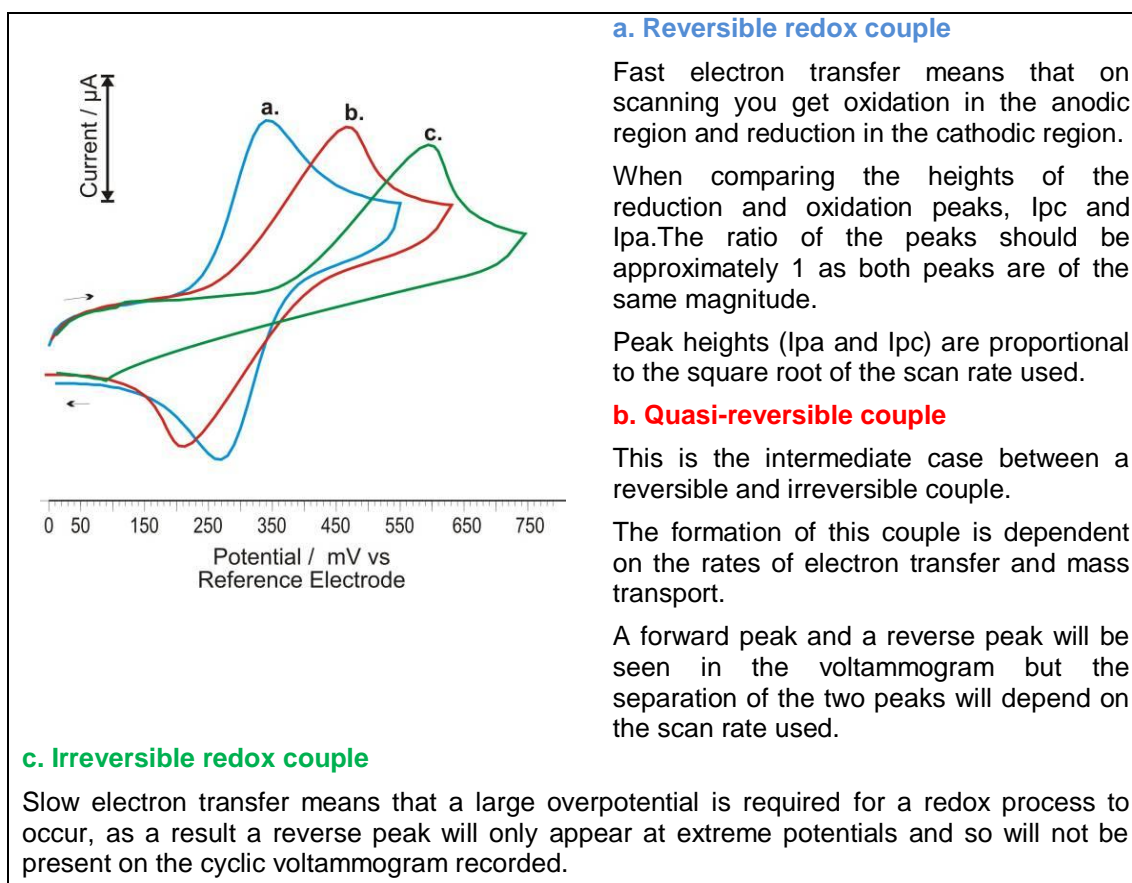e 2.5 A**), is such that at this potential (E_1) no reactions are occurring at the electrode surface. This results in the observation of a steady residual current as the potential is not sufficient to induce any electron transfer reactions. As the potential increases, from E_1 to E_2, during a forward scan (**Figure 2.5 A→B**), the potential will eventually reach a point at which the oxidation of the species in the solution is favourable and therefore starts to occur (Fe^{3+}→Fe^{2+} + e-).

Figure 2.5 A typical cyclic voltammogram for a reversible redox couple (Fe^{2+} + e- $\leftrightarrow$ Fe^{3+}).

This oxidation is accompanied by an increase in current, an anodic current, which will continue to increase until the concentration of the electroactive species at the electrode surface reaches zero. At this point the current will then decrease as there is a balance between the rate constant of the oxidation and the rate of diffusion of the fresh starting material to the electrode surface. This whole process has generated an anodic peak at the potential E_{pa} with a height of I_{pa}. During the backward scan, from E_2 to E_1 (**Figure 2.5 B→C**), for a reversible redox couple, the analogous process is observed. Upon scanning the potential will reach a point at which the reduction of the generated oxidised species (Fe^{2+} + e-→ Fe^{3+}) is favourable and will therefore occur. Again the electrochemical processes cause an alteration in the current response observed. This time a cathodic current, which will create a peak that has the same shape as the anodic peak due to the system again being under diffusion control. This peak is a cathodic peak, it is formed at the potential E_{pc} and has the height I_{pc}.

2.5.1.1. Types of Redox Couple

The shape of the cyclic voltammogram produced and how the peaks formed are affected by altering the scan rate can provide useful information on the type of redox couple occurring. The general volammetric profile for the different types of redox couple and how the voltammogram varies when the scan rate is changed are discussed in **Figure 2.6**.

a. Reversible redox couple

Fast electron transfer means that on scanning you get oxidation in the anodic region and reduction in the cathodic region.

When comparing the heights of the reduction and oxidation peaks, Ipc and Ipa.The ratio of the peaks should be approximately 1 as both peaks are of the same magnitude.

Peak heights (Ipa and Ipc) are proportional to the square root of the scan rate used.

b. Quasi-reversible couple

This is the intermediate case between a reversible and irreversible couple.

The formation of this couple is dependent on the rates of electron transfer and mass transport.

A forward peak and a reverse peak will be seen in the voltammogram but the separation of the two peaks will depend on the scan rate used.

c. Irreversible redox couple

Slow electron transfer means that a large overpotential is required for a redox process to occur, as a result a reverse peak will only appear at extreme potentials and so will not be present on the cyclic voltammogram recorded.

Figure 2.6 Types of redox couples along with a description of their characteristic properties.

2.5.1.2. Reaction Mechanisms

Another important application of cyclic voltammetry is that it can be used to identify the mechanism by which the reactions under study proceed [2,10]. These reactions can be classified by using E to represent the electrochemical or redox processes and C to represent the chemical processes taking place, the letter notation series follows the order in which the process first appears in the reaction sequence, some simple examples are highlighted in **Table 2.1**.

Classification	Reaction Sequence
CE (preceding reaction)	The electroactive species are produced in a reaction that precedes the electron transfer reaction. C ...... Y ↔ O E ...... O + ne- ↔ R
EC (following reaction)	The electron transfer reaction generates species that are chemically reactive. The products of this chemical reaction will not be electroactive. E ...... O + ne- ↔ R C ...... R ↔ X
EC' (catalytic reaction)	This is a special type of EC reaction, here the chemical reaction that follows the electrochemical process results in the initial electroactive species being regenerated. E ...... O + ne- ↔ R C ...... R ↔ O
EE	The product of the first electrochemical process is electroactive and so is able to under go an additional electrochemical process. E ...... A + ne- ↔ B E ...... B + ne- ↔ C
ECE	This mechanism is similar to the EC mechanism but the product of the chemical reaction is electroactive and so can undergo an additional electrochemical process. E ...... O + ne- ↔ R C ...... R ↔ A E ...... A + ne- ↔ B

Table 2.1 Different electrochemical reaction mechanisms [2,10].

2.5.2. Square-Wave Voltammetry

Square-wave voltammetry is a voltammetric technique that applies a potential waveform at the working electrode as illustrated in **Figure 2.7**. This waveform consists of a square-wave (**Figure 2.7 blue**) superimposed on a voltage staircase (**Figure 2.7 red**). During an experiment the current generated at the electrode is measured at two points (**Figure 2.7 Point a and point b**), the difference in the current, Im (Im = Ia − Ib) is then

Figure 2.7 Square-wave wave form (square-wave - blue and voltage staircase - red) [1,2,10].

plotted against the staircase potential at that point (**Figure 2.7 E1**) to give a square-wave voltammogram (**Figure 2.8**). The reduction or oxidation of chemical species is
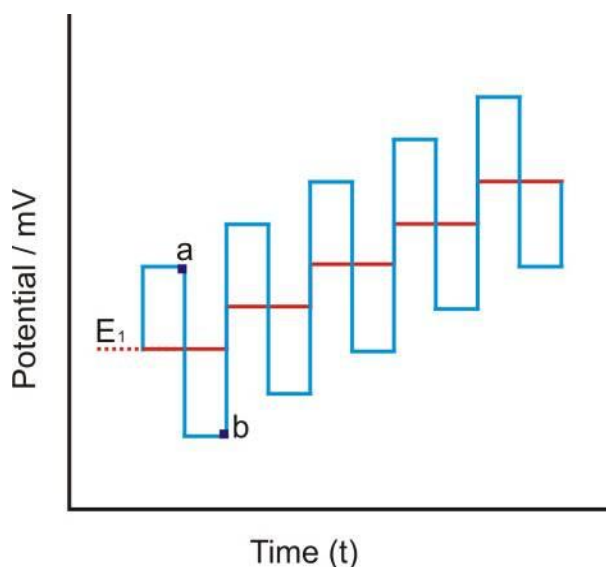
presented as a trough or a peak on the voltammogram and the peak height recorded will be proportional to the concentration of the electroactive species responsible for the peak making the technique ideal for quantitative analysis. Square-wave voltammetry is regarded as being more sensitive than the other voltammetric methods because the current is measured at the end of each potential change (**Figure 2.7; a and b**). This creates a pause which allows the capacitive current to dissipate before the measurement is made leaving only the Faradaic component from the electrode process of interest. The removal of the capacitive current essentially means that there is less background noise and hence the improved sensitivity of the analysis. Square-wave voltammetry also has the added advantage in that it is a fast analytical technique when compared to other methods, because once the sample has been prepared the measurement can be made within a matter of seconds depending on the operational parameters [2].
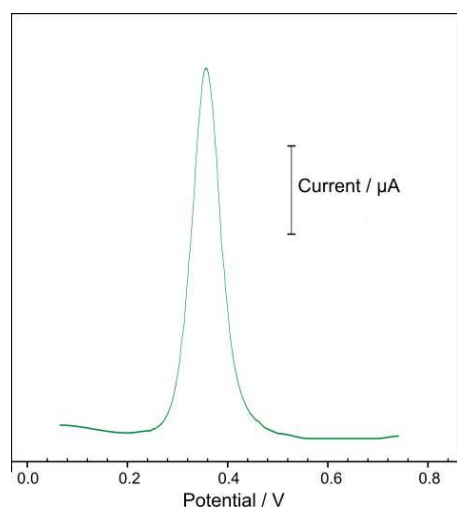

Figure 2.8 A typical square-wave voltammogram.

2.6. Electrochemical Quartz Crystal Microbalance

The electrochemical quartz crystal microbalance (EQCM) is an important instrument that is based upon the electrochemical methods previously described. It is a useful technique as it can measure the electrochemical parameters as well as any mass changes that occur at the electrode surface. An EQCM works by utilising the piezoelectric qualities of a quartz crystal to measure changes in the attached surface mass. A quartz crystal, illustrated in **Figure 2.9**, is coated on both sides with a metal, typically platinum or gold. One side of the crystal is exposed to the electrochemical

solution and is used as the working electrode whilst the other side is exposed to the air within the sensor completing the electrochemical circuit [2,17].
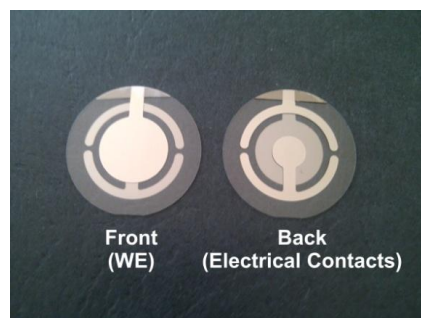
Figure 2.9 Photograph of a platinum coated quartz crystal (a) the front (working electrode) and (b) the back (electrical contacts).

The sandwiched construction of the crystal is such that during use an electric field is produced. This causes a mechanical oscillation within the bulk of the crystal which will resonate at a certain frequency. Any reactions that result in changing the mass of the electrode/crystal surface exposed to the cell solution will also alter the resonant oscillating frequency of the crystal. The frequency change (Δf) can be related to the mass change (Δm) according to the Sauerbrey equation (**Equation 2.9**) [2].

$$\Delta f = -2\Delta m n f_0^2 / A \sqrt{\mu\rho}$$

Where:
Δf is the frequency change (Hz)
Δm is the mass change (g))
n is the overtone number
f_0 is the resonant frequency of the crystal
A is the area (cm^2)
μ is the shear modulus of quartz (2.95×10^{11} g cm^{-1} s^{-1})
ρ is the density of quartz (2.65 g/cm^3)

Equation 2.9 The Sauerbrey equation [2].

The set up of the EQCM can be adjusted so that a range of parameters can be recorded during an experiment. Such parameters include frequency changes (Hz), mass changes (g), differences in time (s), potential (V) and current (A). An example of how such data can be presented is illustrated in **Figure 2.10**. This shows a plot of Δfreqeuncy vs. potential for a solution of silver nitrate (1mM, 0.1M nitric acid).
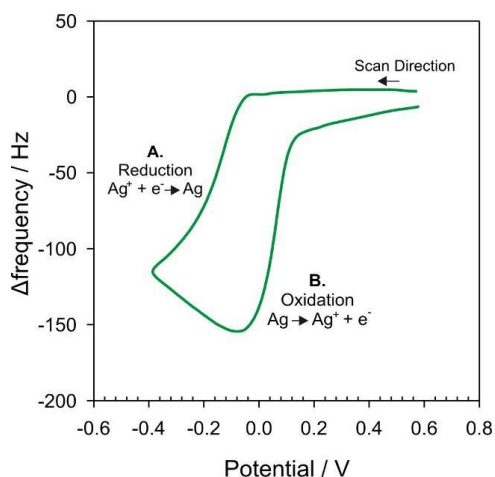
Figure 2.10 A typical EQCM profile for the electrochemistry of silver (silver nitrate, 1mM, 0.1M nitric acid).

According to the Sauerbrey Equation an increase in mass at the electrode surface during an experiment/reaction is defined by a decrease in the oscillating frequency of the crystal, as indicated in **Figure 2.10 A** for the reduction of silver ions to silver metal which is subsequently deposited onto the electrode surface. Likewise a decrease in mass is defined by an increase in frequency, as illustrated in **Figure 2.10 B.** for the oxidation of the silver metal to its ions and the subsequent loss of silver from the electrode surface.

The EQCM is a very sensitive device as it is able to monitor extremely small mass changes down to $1ng/cm^2$ [2]. It has a number of applications including monitoring deposition [10-11], dissolution [12] and uptake processes during electrochemical experiments and it is also useful for studying the formation and properties of polymer films [13-14].

2.7. Spectrophotometry

Spectrophotometry is any technique that exploits light to measure the concentration of certain species within a sample. There are a range of spectrophotometric methods available that vary depending on the type of light used including: Infrared Spectroscopy and Ultraviolet-Visible Spectroscopy, the latter has been used during this project and therefore will be discussed over the next few pages.

2.7.1. Ultraviolet-Visible Spectroscopy

Ultraviolet-Visible (UV-VIS) spectroscopy is an analytical technique that uses radiation from the ultraviolet and visible regions of the electromagnetic spectrum to gain quantitative information on the system under study. The absorption of ultraviolet or visible radiation by the sample causes an electronic transition within the molecule. An electron in one molecular orbital is excited to another molecular orbital that has a higher energy state and this corresponds to a transition from the ground state, the lowest energy state of the molecule, to an excited state (*). The transitions that are possible are illustrated in **Figure 2.11** [1]. The energy of visible radiation is only strong enough to cause n → π* or π→ π* transitions and it is these transitions that result in a compound being coloured. The bonds present within these compounds responsible for the transition are called chromophores.
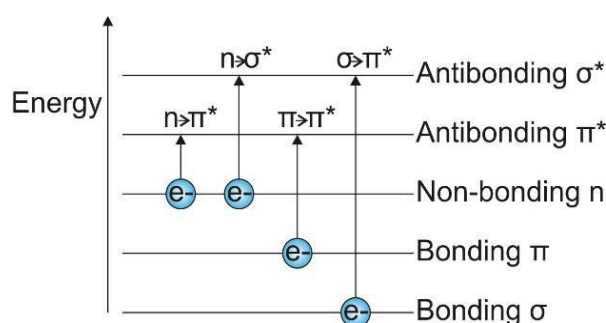
Figure 2.11 The possible electronic transitions available when irradiating with ultraviolet-visible radiation [1].

The light being absorbed by the sample can be measured using a spectrophotometer as the intensity of the emitting beam of light will decrease as it passes through the sample. If P is the intensity of transmitted light (the intensity of the light coming out of the sample) and P_0 is the intensity of the emitted light (the intensity of the light going into the sample) then the percentage of the light transmitted through the sample, the absorbance (A) can be defined by **Equation 2.10**, a version of the Beer-Lambert law.

$$A = \log [P_0/P]$$

Equation 2.10 [1]

The absorbance is the parameter that is measured in the majority of ultraviolet-visible procedures and it is normally measured as a function of the wavelength to

produce a spectrum. The spectrum produced will vary depending on the species present. A typical spectrum will look like the one illustrated in **Figure 2.12** for a solution of naphthazarin (5,8-Dihydroxy-1,4-naphthoquinone, 522µM, pH 7).
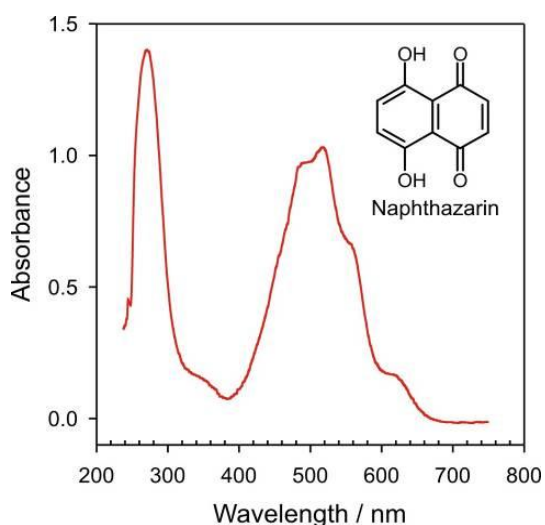
Figure 2.12 A typical UV-VIS spectra for naphthazarin.

The absorbance peak is typically broad, spread out over a number of different wavelengths because vibrational and rotational transitions are often superimposed on top of the electronic transitions. As a result the wavelength that corresponds to the maximum absorbance is typically used to provide quantitative information on the system. According to the Beer-Lambert law, **Equation 2.11** form, the concentration of an absorbing compound in the sample is directly proportional to the absorbance measured.

$$A = \varepsilon c l$$

Where:

ε is the molar absorptivity ($M^{-1} cm^{-1}$)

l is the sample path length (cm)

c is the concentration of the chromophore in the sample (M)

Equation 2.11 Beer-Lambert law [1].

The molar absorptivity calculated will be characteristic of the compound under study and tells us how much light is absorbed by that compound at a particular wavelength. It therefore gives an indication of the strength of the chromophore present. Beer's law holds true for dilute solutions, typically those having a concentration of less than or equal to 0.01M and when the instrument is using monochromatic radiation (light of one colour or one wavelength).

For UV-VIS spectroscopy to be used for accurate and precise quantitative analysis an analyte must be able to absorb light from a portion of the ultraviolet or visible spectrum that is distinguishable from the other components within the sample. The technique is normally very accurate but can be limited as not all compounds have strong native chromophores which can affect the selectivity and sensitivity of the procedure. This problem can be resolved by reacting the target analyte with a UV-VIS label so that upon reacting a coloured conjugate is formed that can be quantified more effectively. The labels chosen should be selective to the analyte and should ideally produce conjugates that are strong chromophores [1].

2.8. References

[1]   D.C. Harris, 2007. Quantitative Chemical Analysis. 7th Edition, USA: W.H. Freeman and Company.

[2]   J. Wang, 2006. Analytical Electrochemistry. 3rd Edition, New Jersey: John Wiley and Sons.

[3]   T.A. Ivandini, B.V. Sarada, C. Terashima et al, Electrochmical detection of tricyclic antidepressant drugs by HPLC using highly boron-doped diamond electrodes. Journal of Electroanalytical Chemistry, 521 (2002) 117-126

[4]   H. Weicker, M. Feravai, H. Hagele and R. Pluto, Electrochemical detection of catecholamines in urine and plasma after separation with HPLC. Clinica Chimica Acta, 15 (1984) 17-25

[5]   E.M.P.J Garrido, J.M.P.J Garrido, N. Milhazes, F. Borges and A.M Oliveira-Brett, Electrochemical oxidation of amphetamine-like drugs and application to electroanalysis of ectasy in human serum. Bioelectrochemistry, 79 (2010) 77-83

[6]   A. Zapata, V.I. Chefer, T.S. Sieppenberg and L. Denoroy, Detection and quantification of neurotransmitters in dialysates. Current Protocols in neuroscience, 7 (2007) 430

[7]   G. Herzog and D.M.W. Arrigah, Electrochemical strategies for the label-free detection of amino acids, pepides and proteins. Analyst, 132 (2007) 615-632

[8]   A.A. Ensafi and S. Behyan, Sensing of L-Cysteine at glassy carbon electrodes using Nile Blue A as a mediator. Sensors and Actuators B: Chemical, 122 (2007) 282-288

[9]   L. Yao-Tong, A. Ganguly, C. Li-Chyong and K. Chen, Direct voltammetric sensing ood L-cysteine at pristine GAN nanowires electrode. Biosensors and Bioelectronics, 26 (2010) 1688-1691

[10]   P.T. Kissinger and W.R. Heineman, 1996. Laboratory Techniques in Electroanalytical Chemistry. 2nd Edition, New York: Marcel Dekker, Inc

[11]   M. Alvarez-lcaza and U. Bilitewski, Mass production of biosensors. Analytical Chemistry, 65 (1993) 525A-533A

[12]   F. Ricci, F. Arduini, A. Amine, D. Moscone and G. Palleschi, Characterisation of Prussian blue modified screen-printed electrodes for thiol detection. Journal of Electroanalytical Chemistry, 563 (2004) 229–237

[13]   S.H. Lee, H.Y. Fang and W.C Chen, Amperometric glucose biosensor based on screen-printed carbon electrodes mediated with hexacyanoferrate–chitosan oligomers mixture. Sensors and Actuators B, 117 (2006) 236–243

[14]   A, Vasilescu, S. Andreescu, C. Bala et al, Screen-printed electrodes with electropolymerized Meldola Blue as versatile detectors in biosensors. Biosensors and Bioelectronics, 18 (2003) 781-790

[15]   S. Ledru, N. Ruille and M. Boujtita, One-step screen-printed electrode modified in its bulk with HRP based on direct electron transfer for hydrogen peroxide detection in flow injection mode. Biosensors and Bioelectronics, 21 (2006) 1591–1598

[16]   M.M. Villalba and J. Davis, New directions for carbon-based detectors: exploiting the versatility of carbon substrates in electroanalysis. Journal of Solid State Electrochemistry, 12 (2008) 1245-1254

[17]   A.J. Bard and L. Faulkner, 2002. Electrochemical Methods Fundamentals and Applications. 2nd Edition, USA; John Wiley ans Sons, Inc.

[18] P. Krtil, S. Nishimura and M. Yoshimura, Electrochemical formation of ternary oxide films – an EQCM approach to galvanostatic deposition of alkali earth metal tungstates and molybdates. Electrochemica Acta, 44 (1999) 3911-3920

[19] C. Lin and K. Ho. A study on the deposition efficiency, porosity and redox behaviour of Prussian blue thin films using an EQCM, Journal of Electroanalytical Chemistry, 524-525 (2002) 286-293

[20] I.A. Rutkowska, J. Stroka, P.K. Wrona and Z. Galus, Electrochemical and EQCM studies of growth and dissolution processes of deposits on gold electrodes: uranyl-hexacyanoferrate films. Journal of Electroanalytical Chemistry, 564 (2004) 199-208

[21] J. Widera, M. Skompska and K. Jackowska, The influence of anions on formation, electroactivity, stability and morphology of poly(o-methoxyaniline) films - EQCM studies. Electrochemica Acta, 46 (2001) 4125-4131

[22] A. Mahmoud, B. Keita and L. Nadjo, EQCM study of the process of silicomolybdic anion doping in polyaniline films electrosynthesized in the presence of various anions. Journal of Electroanalytical Chemistry, 446 (1998) 211-225

Chapter 3

Exploiting Silver-Thiol Interactions for Thiol Analysis

Chapter 3

Exploiting Silver-Thiol Interactions for Thiol Analysis

Abstract

This chapter describes the work, primarily electrochemical quartz crystal microbalance (EQCM) studies, that has been carried out to investigate silver-thiol (Ag-SH) interactions. The explotation of these interactions, as a potential sample preparation route, to enhance the analysis of thiol compounds is evaluated. The reaction procedure developed during this chapter relies initially upon the deposition of a silver layer onto an electrode substrate followed by its electrochemical manipulation to bring about thiol binding and then release. It was envisaged that this process would be able to facilitate the removal of any possible sample interferants, whilst concentrating the thiol species the electrode assembly, improving the performance of the assay that follows. The results displayed in this chapter are contrary to what was expected. It was found that the electrochemical silver-thiol release mechanism varied considerably depending on the chemical structure of thiol compound used. In some cases, the expected reaction mechanism was observed when the electrode substrate was subjected to a reducing potential. Here the thiol compound was released from the substrate surface whilst the silver layer was retained. However, when the carboxylic acid functionality was present on the thiol compound both the thiol species and the pre-deposited silver layer were removed from the substrate surface. The mechanism behind this removal has been studied and tentatively assessed.

3.1. Introduction

The ultimate goal of any analytical technique, regardless of the testing environment, is the production of results that are accurate and reliable. The successful achievement of this goal can be complicated by many factors including: pre-analytical errors (e.g. sample collection, sample storage and sample labelling), analytical errors (e.g. sample preparation and insufficient analytical performance of the chosen technique) and post-analytical errors (e.g. result misinterpretation and report writing faults) [1-3].

The analysis of biologically relevant molecules within clinical samples can be particularly complex because the samples used for analysis contain a plethora of different components. Some of these components can interfere with the analytical procedure, influencing the results obtained, which can affect how the data produced is interpreted. If erroneous conclusions are drawn it can have potentially severe detrimental effects on the overall clinical outcome for the patient [1,4]. Clinical analysis can also be complicated because in some cases the analyte may only be present in the sample at trace concentrations. This can make sensitive and selective analysis increasingly more difficult [5-6]. Both of these factors pose a significant hurdle when trying to develop new analytical strategies that can be used for the fast, reliable and selective determination of reduced sulphydryl thiol species within biological fluids [7-8]. The level of complexity being increased further as technology is driven from conventional laboratory type diagnostics to those which can be used at the point of care [6].

Point of care testing (POCT) can be defined as any type of diagnostic test that is performed outside of the laboratory [9]. This type of testing has become increasingly popular in recent years given the current economic climate and the increased pressures being put on healthcare providers by the government and by patients to provide a better quality service. The simplicity, speed and the low cost of point of care testing makes it an ideal solution [10-11]. A multitude of various tests are currently available for use within the point of care environment and these utilize a range of different analytical techniques as the detection strategy with the more

successful devices utilizing either optical or electrochemical methods [12-13]. When using electrochemical methods as the sensing solution precautions may need to be taken to ensure that the accuracy of the underlying methodology is maintained.

One of the main areas for concern is the sample composition, a number of electroactive substances (e.g. tryptophan, tyrosine, ascorbic acid and uric acid) are present. These can cause a considerable amount of interference during the final analysis because they can be easily oxidised within the potential windows typically used which can result in the current response observed for the analyte being obscured. Incorporating chromatographic separations into the analytical procedure can effectively remove these sample interferants, this gives results that are based solely on the the signal generated from the analyte present making the results more accurate and reliable [14-16]. However, the instrumentation size and complexity, along with the cost constraints associated with these methods means that they are not ideal for implementation within a point of care type diagnostic system and as such alternative routes must be developed that will allow interference free analysis. A route that could simultaneously concentrate the analyte at the sensing area would also be advantageous.

The work presented in this chapter has sought to study silver-thiol interactions, examining the possibility that these processes could be exploited to form the basis of a sample processing step, to aid thiol pre-concentration and interference removal during analysis. It is well known that thiol compounds interact with a range of metal substrates, including gold, silver, and copper to form very stable metal-sulphur bonds or metal-thiolate complexes [1,17-18]. Although the nature of these types of interactions are not fully understood some theories have been hypothesised:-

- The bond is formed by the cleavage of the sulphur-hydrogen bond on the thiol compound (homolysis) followed by the spontaneous formation of the covalent metal-sulphur bond with the metal substrate [19].
- The bond is formed as a result of the sulphydryl group on the thiol molecule donating some of its electron density to the metal substrate which

subsequently results in the thiol species being chemisorbed onto the metal surface [19].

Even though the metal-sulphur bonds formed are as a result of a very strong and stable interaction they can be easily broken *via* a number of routes including heat treatment [20] and electrochemical methods [21], this will result in the thiol compound being released from the metal surface.

The study of these metal-thiol systems is appealing as they are easily prepared and can be used to study fundamental and applied surface interactions. These systems have been useful in a number of applications, including thiol analysis. Here the binding or release of the thiol compound onto or from the substrate allows the thiol species to be selectively determined. It has been reported that the thiol molecules in a test solution will accumulate at a metal surface, due to the interaction between the sulphydyl group and the metal, which results in the electrochemical response being observed during the analyte stripping step being enhanced as the thiol has essentially been pre-concentrated at the electrode surface. The use of these types of systems can however be limited as it can take a long time for the thiol compounds to accumulate at the electrode surface [22].

The work presented in this chapter has sought to exploit the metal-thiol interactions previously described to provide a possible route for the analysis of cysteine, homocysteine and glutathione. The basis of the approach lies firstly in the functionalisation of an electrode surface with silver *via* conventional electrodeposition methods [23-24] and the subsequent modification of the surface with the thiol species. It was envisaged that the silver layer could be electrochemically manipulated to overcome the slow thiol accumulation problems currently experienced by researchers. It was hoped that upon oxidation of the modified silver electrode, in the presence of the thiol species, that the silver ions generated would bind directly with the sulphur functionality on the thiol compounds resulting in the instantaneous formation of a silver-thiol complex. This should be insoluble and thus deposited at the electrode surface as illustrated in **Figure 3.1 (2)**.
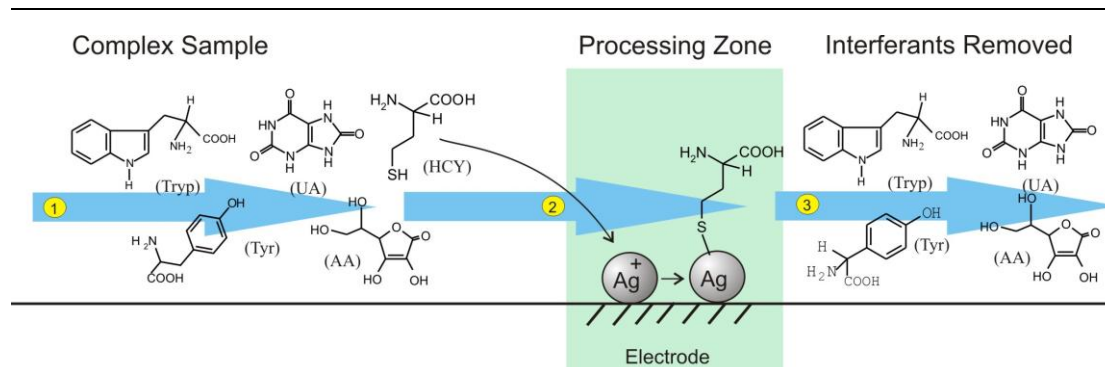
Figure 3.1 Schematic illustrating 1. some common sample components 2. the thiol accumulation route at the electrode surface and 3. the removal strategy for some common sample components (Tryp- tryptophan, UA- uric acid, HCYS- homocysteine, Tyr – tyrosine and AA- ascorbic acid).

The schematic in **Figure 3.1** also shows some of the other electroactive sample components that can act as interferants (**Figure 3.1 (1)**) and how they would be removed from the sensing platform during the processing step (**Figure 3.1 (3)**).

The electrochemical reduction of the silver-sulphur bond should follow conventional routes whereby the thiol is released, allowing it to be detected, and the silver is re-deposited onto the electrode substrate [22]. A variety of thiol compounds (**Table 3.1**) have been investigated in an effort to elucidate the underlying dynamics of the interfacial processes involved.

Table 3.1 Thiol compounds examined.

These studies were facilitated through a combination of electroanalytical investigations, electrochemical quartz crystal microbalance (EQCM) studies, Inductively Coupled Plasma-Optical Emission Spectroscopy (ICP-OES) and Transmission Electron Microscopy- Energy-Dispersive-X-ray spectroscopy (TEM-EDX).

3.2. Experimental Details

All reagents were of the highest grade available, were used without further purification and unless stated otherwise were purchased from Sigma Aldrich (UK) or Alfa Aesar (UK). The silver nitrate solution (typically 1mM) was prepared in a 0.1M solution of sodium nitrate. Stock thiol solutions: cysteine, homocysteine, glutathione, N-acetyl-D-cysteine, 3-mercaptopropionic acid, propanethiol and 3-mercaptopropanol along with the methionine solutions (typically 10mM) were also prepared in 0.1M sodium nitrate. Electrochemical measurements were conducted using a µAutolab computer controlled potentiostat (Eco-Chemie, Utrecht, The Netherlands) coupled to a electrochemical quartz crystal microbalance (EQCM) (Maxtek INC, USA) using a three electrode configuration consisting of a 5 MHz Titanium / Platinum crystal (Maxtek INC, USA) as the working electrode, a platinum wire counter electrode and a 3M NaCl Ag | AgCl half cell reference electrode (BAS Technicol, UK). The scan rate in all cases was 50 mV/s and unless specified otherwise all measurements were conducted at $22^{o}C \pm 2^{o}C$.

Inductively coupled plasma-optical emission spectroscopy (ICP-OES) experiments were conducted on an ICP-OES 2100 DV instrument (Perkin Elmer, UK) and a solution of 0.1M nitric acid was used to prepare the calibration standards and the sample solutions. Full ICP-OES experimental details and results can be found in appendix 1. Transmission electron microscopy-energy dispersive X-ray spectroscopy (TEM-EDX) studies were carried out using a JOEL JEM-2100 TEM (Oxford elemental analysis, UK) using a copper mess sample support grid.

3.3. Results and Discussion

The electrochemical properties of a solution of silver nirate (1mM, 0.1M NaNO$_3$) were investigated at a platinum coated quartz crystal working electrode. Conventional silver electrochemistry was observed with the reduction and oxidation process being seen at -0.11V and 0.09V respectively. **Figure 3.1** shows the corresponding EQCM results which confirms that these redox processes are occuring. The electrodeposition of the silver can be seen upon the application of a reducing potential, represented by a decrease in frequency (Δf), which corresponds to the increase in mass at the electrode surface as the silver ions are reduced and deposited onto the electrode (**Figure 3.1 A.**). Silver stripping can also be seen as the oxidative potential is applied and is represnted by an increase in the frequency, which corresponds to the decrease in mass at the electrode surface as the silver layer is lost (**Figure 3.1 B.**).
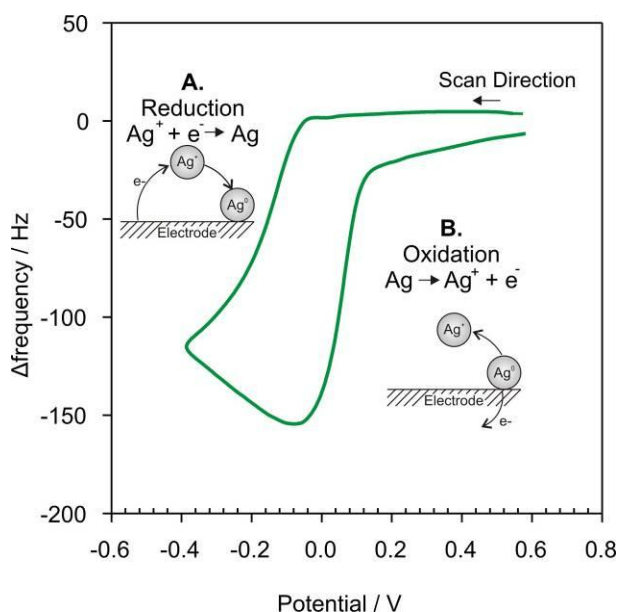
Figure 3.1 EQCM results for the electrochemistry of silver nitrate (1mM, 0.1M sodium nitrate).

The silver-thiol binding and release processes were then investigated. The EQCM profile for the experiment in the presence of homocysteine is highlighted in **Figure 3.2 (A)** with the schematic **Figure 3.2 (B)** illustrating the interactions occuring at the electrode-solution interface during the different stages (**1** to **7**) of the experiment (as annotated within **Figure 3.2 (A)** and **(B)**), for clarity a larger version of this figure is provided in appendix 1.
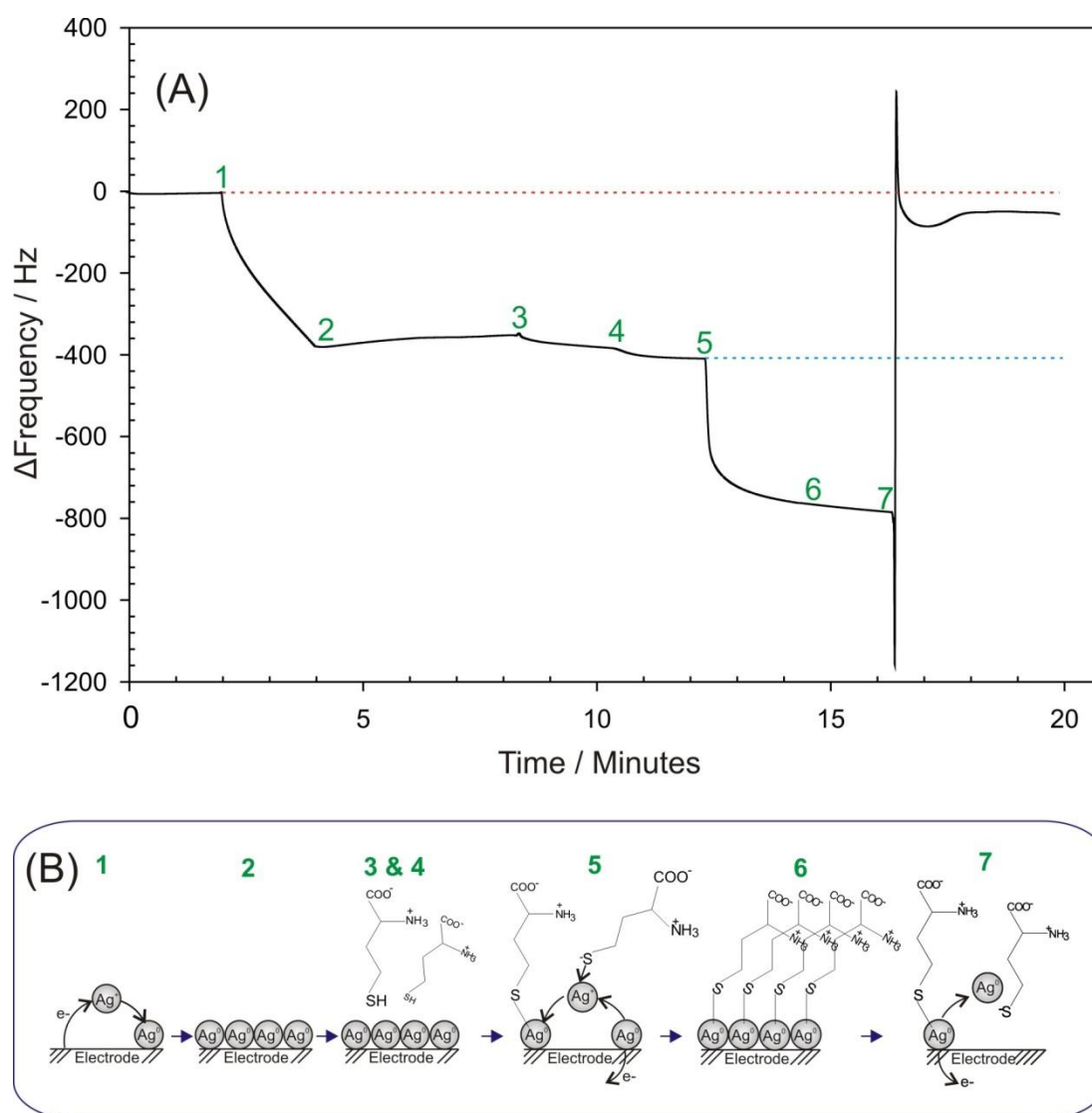
Figure 3.2 (A) EQCM profile and (B) corresponding explanatory schematic for the interaction of silver with homocysteine during the stages (1 to 7) of the experiment.

Silver was electrodeposited, at a reductive potential of -0.4V, onto the platinum coated quartz crystal (working electrode) from a solution of silver nitrate (1mM, 0.1M NaNO$_3$). A decrease in the frequency is observed (**Figure 3.2 Stage 1**) and corresponds to the increase in mass at the electrode surface as the silver layer is deposited. The potential of the electrode was then returned to 0V. This was to ensure that the deposition step had produced a stable silver layer and is confirmed by the constant frequency observed during this process (**Figure 3.2 Stage 2**). The modified crystal was removed, rinsed and placed into a solution of 0.1M NaNO$_3$. The electrode, no potential applied, was allowed to equilibriate (**Figure 3.2 Stage 3**) and a solution of homocysteine (10mM, 0.1M NaNO$_3$) was then added to the cell (**Figure 3.2 Stage 4**). Upon this addition no changes in the frequency of the crystal were observed. This

indicates that there are no interactions between the thiol compound and the silver layer. On the imposition of an oxidising potential, +0.5V (**Figure 3.2 Stage 5**) a decrease in the crystal frequency is observed. This can be attributed to the stripping of Ag^0 to Ag^+, the formation of the silver-thiolate complex and its deposition at the electrode surface as expected. This newly formed complex was stable under the oxidative potential and at 0V (**Figure 3.2 Stage 6**). It was anticipated that upon the imposition of a large reducing potential, -1.0V (**Figure 3.2 Stage 7**) that the silver-sulphur bond would be reduced and broken causing the thiol compound to be released and the retention of the silver, as Ag^0, at the electrode surface. This process would cause the frequency of the crystal to return to the same point that it was at prior to thiol addtion (**Figure 3.2 (A) blue dashed line**). However, in this instance this was not the case and the application of the reducing potential caused the frequency of the crystal to return to almost the same value that was observed for the clean platinum crystal. This suggests that the thiol and the electrodeposited silver layer had been lost (**Figure 3.2 (A) red dashed line**).

Visual examination of the crystal surface confirmed that the entire electrodeposited silver layer had been removed. This removal was reinforced by the apperance of colloidal silver aggregates within the interfacial solution and by the presence of metallic silver, determined by ICP-OES, within the interfacial and bulk solutions, at a concentration of 125.125µg/ml and 0.308µg/ml respectively (ICP-OES experimental details and results can be found in appendix 1). TEM-EDX analysis was carried out on dried deposits of the cell solutions so that the silver aggregates could be visualised. **Figure 3.3** shows the TEM image of the particles (**Figure 3.3 a.**), the corresponding EDX analysis results (**Figure 3.3 b.**), which shows the presence of metallic silver reinforcing the ICP-OES results and a particle size measurement (**Figure 3.3 c.**). The last image illustrates that the silver particles released were in the nm size range having an approximate diameter of 33nm. The removal of the silver in this experiment is clearly contrary to what was expected and suggests that the properties of the thiol must in some way be facilitating its removal.
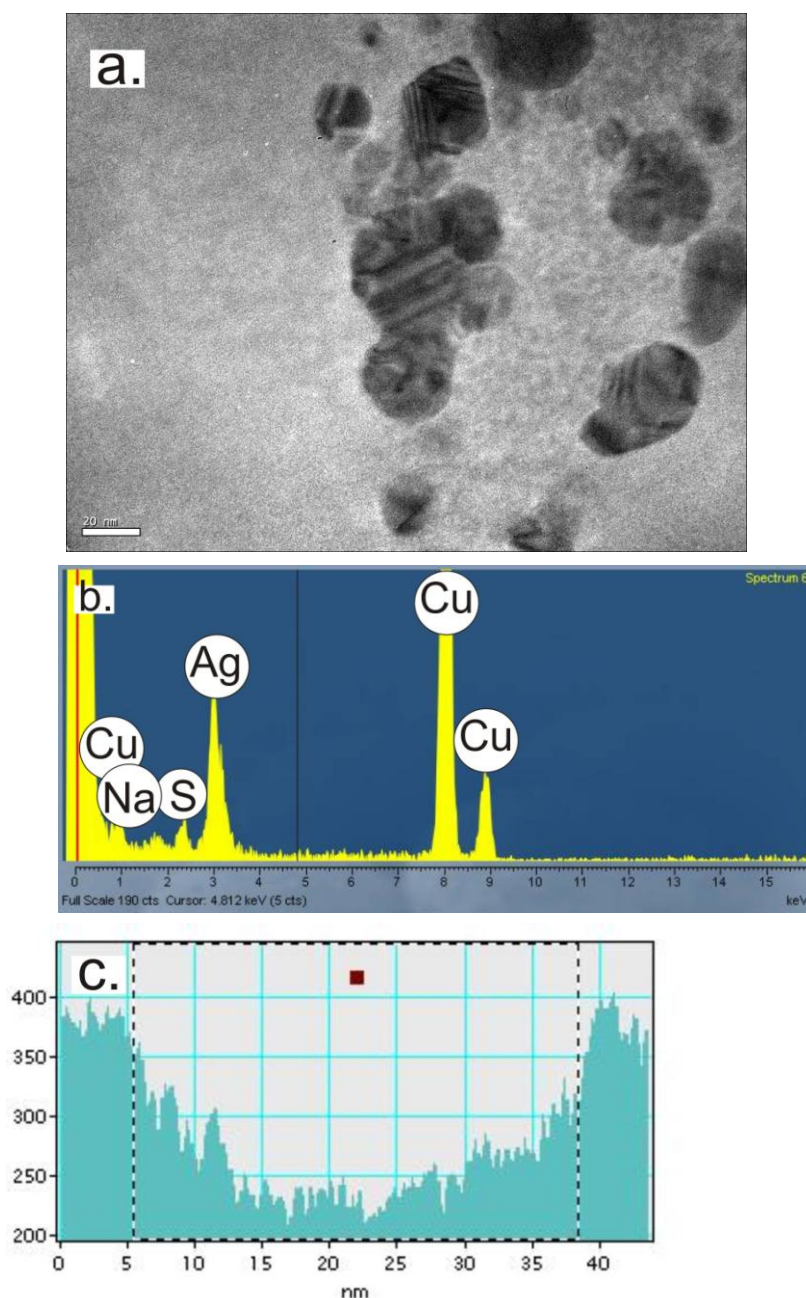
Figure 3.3 a.TEM image, b. EDX analysis and c. particle size measurement for the silver particles present within the interfacial solution.

Before investigating the mechanism causing the removal of the silver particles it was necessary to confirm that the weight change in **Figure 3.2 Stage 5** is caused by the interaction of the silver layer with the thiol functionaly as previously described, opposed to any of the other functionalities present on the homocysteine. The same procedure described previously was carried out but this time methionine was added to the electrolyte solution opposed to homocysteine. Methionine is similar in structure to the homocysteine but the thiol functionality is not present as the sulphur atom is bonded to a methyl group. It was therefore expected that upon the application of the oxidsing potential of +0.5V, to the silver modified electrode assembly, in the presence of the methionine, that no interaction would occur between the methionine and the

silver. The silver would therefore be lost from the substrate surface following the conventionial silver oxidation route seen in **Figure 3.1**. The resultant EQCM results for this system are highlighted in **Figure 3.4 (A)**, the shape of the profile is as expected and **Figure 3.4 (B)** illustrates the interactions occuring at the electrode-solution interface. For clarity a larger version of this figure is provided in appendix 1.
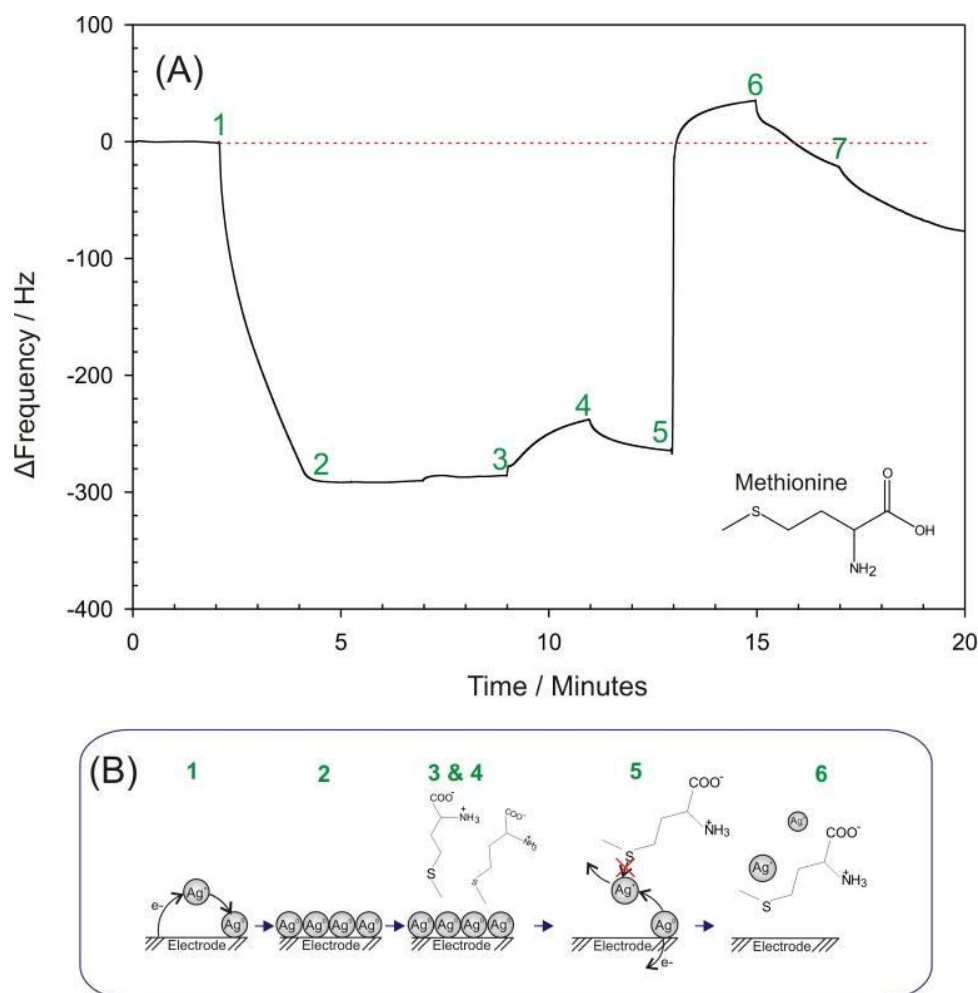
Figure 3.4 (A)The EQCM profile and (B) the corresponding explanatory schematic for the interaction of silver with methionine during the stages (1 to 7) of the experiment.

To investigate the mechanism causing silver removal the same procedure was repeated for the thiol species listed in **Table 3.1**. The same EQCM profile observed for homocysteine, as illustrated in **Figire 3.2 (A)** was also seen for cysteine, glutathione, N-acetyl-D-cysteine and 3-mercaptopropionic acid. A different profile shape was observed, as indicated in (**Figure 3.5 (A)**), for 3-mercaptopropane and 3-mercaptopropanol (for clarity a larger version of this figure is provided in appendix 1). This EQCM profile is initially similar to those previously described. Silver plating occurs when a reducing potential is applied to the system (**Figure 3.5 Stage 1**), giving

a stable silver layer (**Figure 3.5 Stage 2**). No weight changes are seen whilst the system equilibriates and when the thiol species is added to the solution (**Figure 3.5 Stage 3** and **Stage 4**). An increase in the crystal weight, as an oxidising potential (+0.5V) is applied to the system, is observed indicating that the stable silver-thiol complex has be formed (**Figure 3.5 Stage 5** and **Stage 6**). The difference in this instance occurs at stage 7, on the application of the reducing potential (-1.0V), the expected/conventional reaction route is observed. The electrochemical reduction of the silver-sulphur bond occurs, this causes the release of the thiol compound and the retention of the silver at the electrode surface. This is indicated by the increase in frequency (weight lost) to the value observed prior to the addition of the thiol (**Figure 3.5 Stage 7**) indicated by the **blue dashed line**. The retention of the silver was confirmed by the visual examination of the electrode surface. It was clearly apparent that the silver layer was intact, and ICP-OES analyis showed that no silver was detected in the interfacial or bulk solutions.
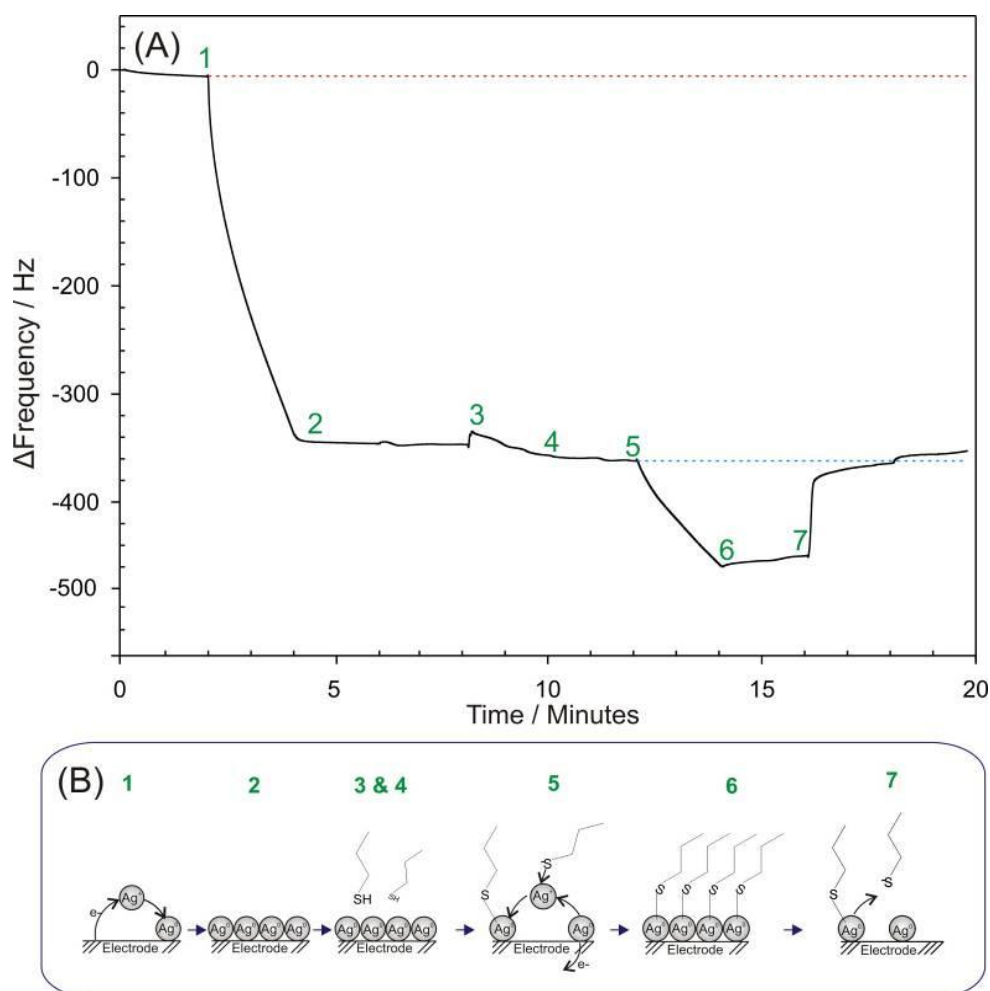
Figure 3.5 (A) The EQCM profile and (B) the corresponding explanatory schematic for the interaction of silver with 3-Mercaptopropane during the stages (1 to 7) of the experiment.

This series of experiments illustrates that two different electrochemical responses are possible when applying the reductive potential of -1.0V (Stage 7) were either thiol release, silver release or thiol release, silver retention will occur. The process occuring appears to be dependent on the nature of the thiol compound present. Looking at the functional groups present or absent on the thiol compounds studied, it can be noted that, where both the thiol and the silver were lost from the electrode surface, that the common functionality appears to be the presence of the carboxylic acid group.

The presence of the carboxylic acid group appears to be pivotal to the silver/thiol release mechanism and although the mode of action for this hasn't been fully elucidated one explanation could be that the carboxylic acid groups serve as a conduit allowing the transfer of electro-reducible protons to the electrode surface. The underlying platinum on the electrode is an excellent catalytic substrate for the electroreduction of protons and given the application of the reducing potential (-1V) it could well be that the adherence of the metallic silver (or aggregate layer) is weakened as a consequence of the formation of an adsorbed hydrogen adlayer on the platinum electrode thus causing the ejection of the silver.

3.4. Conclusions

The results in this chapter highlight the different types of silver-thiol interactions that can occur depending on the functionalities present on the thiol compound. It is clear that it is possible to accelerate the accumulation of the thiol species at the substrate and also control its ejection thus providing a means of sample pre-concentration prior to any subsequent analysis. It has also been shown that depending on the nature of the thiol species used that the ejection of silver from the substrate can also be controlled by the application of an appropriate electrochemical potential. This offers a secondary application of the system as the controlled release of these silver nanoparticles (AgNPs), which are known to possess antibacterial properties [25-26], could be exploited as a route to prevent biofilm formation/electrode fouling within electronic medical implants.

3.5. References

[1]   H. McCormick, R, McMillan, K. Merrett, F. Bensebaa, Y. Deslandes, M.A. Dube and H. Sheardown, XPS study of the effect of the conditions of peptide chemisorption to gold and silver coated polymer surfaces. Colloids and Surfaces B: Biointerfaces, 26 (2002) 351-363

[2]   M. Plebani, Errors in clinical laboratories or errors in laboratory medicine? Clinical Chemical Laboratory Medicine, 44 (2006) 750-759

[3]   M. Plebani and P. Carraro, Mistakes in stat laboratory: types and frequency. Clinical Chemistry, 43 (1997) 1348-1351

[4]   I. Talapatra, D.J. Tymms and D. Lloyd, Assay interference of hormones leading to erroneous results: two case reports. Journal, Indian Academy of Clinical Medicine, 8 (2007) 97-98

[5]   E. Prichard, G.M. Mackay and J. Points, Trace analysis: A structured approach to obtaining reliable results, 1996 Royal Society of Chemistry, Cambridge

[6]   M.S. Belluzo, M.E. Ribone and C.M. Lagier, Assembling amperometric biosensors for clinical diagnostics. Sensors, 8 (2008) 1366-1399

[7]   V. Ducros, K. Demuth, M. Sauvant et al, Methods for homocysteine analysis and biological relevance of the results. Journal of Chromatography B, 781 (2002) 207–226

[8]   F. Carlucci and A. Tabucchi, Capillary electrophoresis in the evaluation of aminothiols in body fluids. Journal of Chromatography B, 877 (2009) 3347–3357

[9]   C.P Price, Point of care testing, British Medical Journal, 322 (2001) 1285-1288

[10]   R.L. Sautter and E.H. Lipford, Point-of-Care Testing: Guidelines and Challenges, North Carolina Medical Journal, 68 (2007) 132-135

[11]   F.D.R. Hobbs, G.M.T. Thorpe, B.C. Delaney, A.S.M. Earl-Slater, D.A. Fitzmaurice, S. Jowett, S. Wilson, R.S. Tobias and C.J. Hyde, A review of near patient testing in primary care, Health Technology Assesment, 1 (1997) 1-229

[12]   M. Mehrvar and M. Abdi, Recent Developments, Characteristics, and Potential Applications of Electrochemical Biosensors, Analytical Sciences, 20 (2004) 1113-1126

[13]   M. Gerard, A. Chaubey and B.D. Malhotra, Application of conducting polymers to biosensors, Biosensors and Bioelectronics, 17 (2002) 345-359

[14]   G. Zhang, D. Liu, S. Shuang and M.M.F. Choi, A homocysteine biosensor with eggshell membrane as an enzyme immobilization platform. Sensors and Actuators B: Chemical, 114 (2006) 936-942

[15]   R. Accinni, S. Bartesaghi, G. De Leo et al, Screening of homocysteine from newborn blood spots by high-performance liquid chromatography with coulometric array detection. Journal of Chromatography A, 896 (2000) 183-189

[16]   L. Agüí, C. Peña-Farfal, P. Yáñez-Sedeño and J.M. Pingarrón. Electrochemical determination of homocysteine at a gold nanoparticle-modified electrode. Talanta, 74 (2007) 412-420

[17]   T. Laiho, J.A. Leiro, M.H. Heinonen, S.S. Mattila and J. Lukkari, Photonelectron spectroscopy study of irradiation damage and metal-sulfur bonds of thiols on silver and copper surfaces. Journal of Electron Spectroscopy and Related Phenomena, 142 (2005) 105-112

[18]   A. Kudelski, Characterization of thiolate-based mono- and bilayers by vibrational spectroscopy: A review. Vibrational Spectoscopy, 39 (2005) 200-213

[19] A. Henglein and D. Meisel, Spectrophotometric Observations of the Absorption of Orgaosulfur Compunds on Colloidal Silver Nanoparticles. The Journal of Physical Chemistry B, 102 (1998) 8364-8366

[20] J. Noh, E. Ito and M. Hara, Self-assembled monolayers of benzenethiol and benzenemethanethiol on Au(111): Influence of an alkyl spacer on the structure and thermal desoprtion behaviour. Journal of Colloid and Interface Science, 342 (2010) 513-517

[21] M.B. Buchmann, T.M. Fyles and T. Sutherland, Electrochemical release from gold-thiolate electrodes for controlled insertion of ion channels into bilayer membranes. Bioorganic and Medicinal Chemistry, 12 (2004) 1315-1324

[22] H. Matsuura, Y. Sato, T. Sawaguchi and F. Mizutani, Rapid and highly-sensitive determination of acetylcholinesterase activity based on the potential-dependent adsorption of thiocholine on silver electrodes. Sensors and Actuators B: Chemical, 91 (2003) 148-151

[23] W. Zhang, X. Qiao and J. Chen, Synthesis of silver nanoparticles – effects of concerned parameters in water/oil microemulsion. Materials Science and Engineering B, 142 (2007) 1-15

[24] M. Muzur, Electrochemically prepared silver nanoflakes and nanowires. Electrochemistry Communications, 6, (2004) 400-403

[25] M. Rai, A. Yadav and A. Gade, Silver nanoparticles as a new generation of antimicrobials. Biotechnology Advances, 27 (2009) 76-83

[26] J. Kim, E. Kuk, K.N. Yu, J. Kim, S.J. Park, H.J. Lee, S.H. Kim, Y.K. Park. Y.H. Park, C. Hwang, Y. Kim, Y. Lee, D.H. Jeong and M. Cho, Antimicrobial effects of silver nanoparticles. Nanomedicine: Nanotechnology, Biology, and Medicine, 3 (2007) 95– 101

Chapter 4

Molecularly Imprinted Polymers: Templated Amino Acid Films?

Chapter 4

# Molecularly Imprinted Polymers: Templated Amino Acid Films?

Abstract

The development of polymer films incorporating amines, based on dimethylpyrrole analogues, and the assessment of these films to act as molecular imprinted polymers (MIPs) for the detection of the former is described. It was anticipated that a generic synthetic strategy could be developed, initially by using some simple amines as the template species, and that this could be easily adapted to develop MIPs for some more complex amines and amino acids, including cysteine, homocysteine and glutathione, thus facilitating their detection. The design considerations required to ensure the successful incorporation of the template, *via* the amine functionality, within the monomer, along with its subsequent electropolymerisation is described. It was envisaged that the substrate would be removed from the polymer, by the addition of hydroxylamine, which would leave behind a MIP with a size specific cavity that would allow substrate rebinding and therefore its subsequent detection when it was reintroduced into the system. It was however found that the addition of this reagent caused the complete dissolution of the polymer films and instead of creating MIPs, unique sacrificial or protective type polymers had been developed. These could be beneficial in the development of micro-engineered devices were electrode patterning is problematic. Film formation and removal have been studied using cyclic voltammetry and electrochemical quartz crystal microbalance studies.

4.1. Introduction

Molecular imprinted polymers (MIPs) have received a considerable amount of interest within the scientific community over the past few years. They are able to facilitate the selective separation and recognition of a range of molecules including drugs [1-3], peptides [4], proteins [5], nucleic acids [6], hormones [7-8] and toxins [9]. Molecular imprinting can be achieved *via* a number of routes. The typical route is illustrated in **Scheme 4.1** and involves allowing the functional monomers to interact, either non-covalently or covalently, with the template molecules to give a complex that can subsequently undergo polymerization to give the polymeric material. The template molecule is then extracted to give an imprinted polymer that has complimentary cavities for the template (same size, shape and reactive chemical functionalities) which allows it to rebind onto the polymer [9-10].
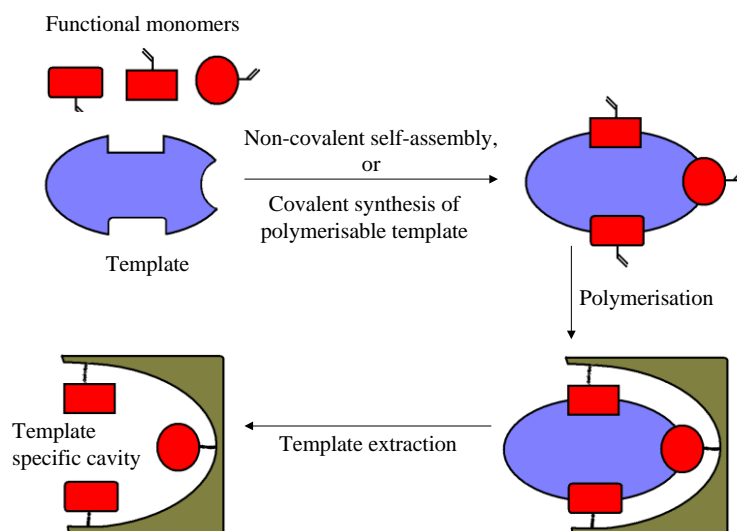

Scheme 4.1 Schematic showing the typical route for the preparation of a MIP [9-10].

As the template is able to rebind to the polymeric material MIPs can be used for a range of applications that rely upon specific binding events, such as, catalysis [11-12], separation and purification techniques [7,13] and controlled drug delivery [10,14]. MIPs have some unique physical properties which include excellent template specificity, high durability, low production costs and the applicability of the technique to mass manufacture which makes them an ideal candidate for use within sensors. Here they can be an advantageous alternative to antibodies and/or enzymes that are conventionally used [3,5,15]. A range of MIPs have been developed for use within

sensors using different polymerization and transduction methods, which includes the template rebinding being detected by fluorescence spectroscopy [3-4], colorimetric methods [16-17], quartz crystal microbalance studies [18], chromatography [19-20] and various electrochemical methods, including voltammetry [21], potentiometry [22-23] and amperometry [1]. The work presented in this chapter has investigated the development of a range of electrochemically prepared MIPs that could be used for the detection of a variety of compounds that possess the primary amine functionality.

The approach advocated here was to produce a range of pyrrole monomers that had the amine functionality of the desired substrate incorporated within a pyrrole ring. This could be achieved by using acetonylacetone, a reagent used for protecting primary amine functionalities which upon use results in the formation of a substituted pyrrole ring *via* a Paal-Knorr type synthesis, as indicated in **Scheme 4.2 A** [24]. This method provides a chemically robust group that, in conventional organic
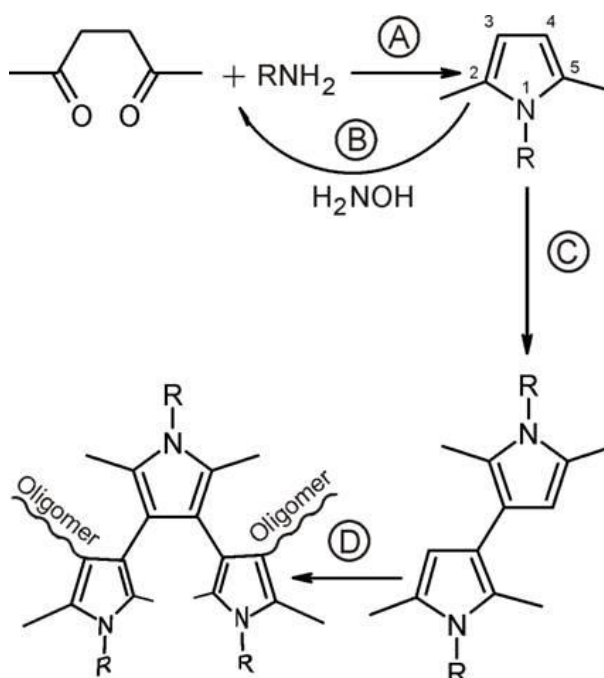

Scheme 4.2 Conventional amine protection route and electro-oxidation method for monopyrrolic monomers.

synthesis, allows other parts of the molecule to be modified with the amine being recovered in later stages through exposure to hydroxylamine (**Scheme 4.2 B**) [25].

Pyrrole polymerisation invariably relies upon chain growth through radical cation coupling at the 2 and 5 positions [26-27]. However, the reaction of acetonylacetone, with amines yields a pyrrole monomer where both these positions are blocked by methyl groups and thereby, for film formation to occur, coupling must proceed through the more sterically congested 3 and 4 positions (**Scheme 4.2 C**). It could be envisaged that this would impede the development of a coherent MIP and, at best, lead to oligomer formation as highlighted in **Scheme 4.2 D**. In order to counteract this issue a range of dipyrrolic derivatives, using some simple diamines as

the substrate, were prepared, similar to the one illustrated in **Scheme 4.3** (1,1'-p-phenylenebis[2,5-dimethylpyrrole). It was anticipated that, upon oxidation, that these derivatives would couple through the 3 and 3' positions on opposite pyrrole moieties to form a coherent film (**Scheme 4.3**). It was expected that this film would be susceptible to the reaction with hydroxylamine, thus allowing the release of the substrate and the formation of our MIP.
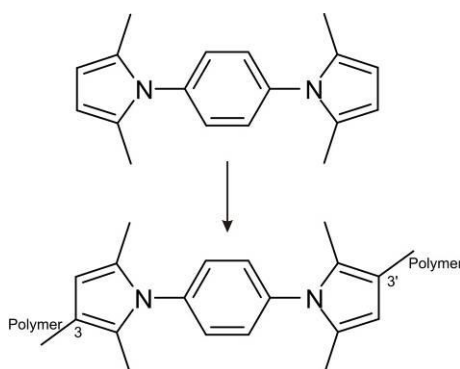
Scheme 4.3 Schematic illustrating the proposed polymerisation route for the dipyrrolic monomer 1,1'-p-phenylenebis-2,5-dimethylpyrrole.

The aim of the initial investigation was therefore to determine if this route could be exploited to form molecularly imprinted polymers for the detection of some simple diamine compounds. It was envisaged that the developed route would be generic and applicable to the development of MIPs capable of sensing a variety of other compounds containing the amine functionality, including cysteine, homocysteine and glutathione. In the case of the thiol species, the oxidised forms of the substrate (containing two amine groups) could be incorporated within the pyrrole monomer. The main questions that needed to be addressed within this investigation were:-

- Could the monomers be synthesised?
- Were they polymerisable?
- Were the films produced stable?
- Could the substrate be removed from the film through the addition of hydroxylamine?
- Could the template be reincorporated into the film?
- Could template rebinding be detected through amperometric or voltammetric oxidation of the reformed polymer?

4.2. Experimental Details

4.2.1. Materials and Methods

All reagents were of the highest grade available, were used without further purification and unless stated otherwise were purchased from Sigma Aldrich (UK) or Alfa Aesar (UK). For the electrochemical investigations, the synthesised monomers were dissolved in a solution of acetonitrile containing 0.05M tetrabutylammonium perchlorate (TBAP) as the electrolyte. Electrochemical measurements were conducted using a μAutolab computer controlled potentiostat (Eco-Chemie, Utrecht, The Netherlands) using a three electrode configuration consisting of a glassy carbon working electrode (3mm diameter, BAS Technicol, UK), a platinum wire served as the counter electrode and a 3 M NaCl Ag | AgCl half cell reference electrode (BAS Technicol, UK) completed the cell assembly. Electrochemical Quartz Crystal Microbalance (EQCM) measurements were obtained using a computer controlled Quartz Crystal Microbalance (Maxtek INC, USA) and a polished 5MHz Titanium/Gold crystal (Maxtek INC, USA). Unless otherwise specified a scan rate of 0.1V/s was used and all measurements were carried out at $22^{o}C \pm 2^{o}C$. Nuclear magnetic resonance (NMR) spectra were measured on a JEOL (Welwyn Garden City, UK) ECX 400 MHz spectrometer. Chemical shifts are reported in parts per million (ppm) downfield from tetramethylsilane (TMS).

4.2.2. Preparation of Monomers

2,5-Dimethyl-1-phenylenepyrrole (DMMP)

Aniline (1.86g, 0.02mol), hexane-2,5-dione (2.28g, 0.02mol), 5ml of methanol and 2 drops of concentrated hydrochloric acid were placed into a 100ml round bottom flask fitted with a reflux condenser. The reaction mixture was heated under reflux for 15 minutes, poured into 10ml of 0.5M hydrochloric acid and then cooled on ice. The product was collected by suction filtration, washed with water and was then recrystalised using a 9:1 methanol:water to give 2,5-Dimethyl-1-phenylenepyrrole (3.30g, 96%) as pale yellow crystals.

NMR data

^{1}H NMR (CDCl$_3$) δ 7.47-7.20 (m, Ar-H), 5.90 (s, Ar-H), 2.03 (s, R-H)

^{13}C NMR (CDCl$_3$) δ 12.9977, 76.6987, 77.0134, 105.6025, 127.6118, 128.2412, 129.0327

1,1'-p-phenylenebis[2,5-dimethylpyrrole] (PPDMP)

Phenylenediamine (1.08g, 0.01mol), hexane-2,5-dione (2.28g, 0.02mol), 15ml of methanol and 2 drops of concentrated hydrochloric acid were placed into a 100ml round bottom flask fitted with a reflux condenser. The reaction mixture was heated under reflux for 15 minutes, poured into 10ml of 0.5M hydrochloric acid and then cooled on ice. The product was collected by suction filtration, washed with water and the product was then recrystalised using acetonitrile to give 1,1'-p-phenylenebis[2,5-dimethylpyrrole] (1.48g, 56%) as pale yellow crystals.

NMR data

^{1}H NMR (CDCl$_3$) δ7.30-7.25 (m, Ar-H), 5.93-5.93 (m, Ar-H), 2.08-2.08 (m, R-H)

^{13}C NMR (CDCl$_3$) δ 13.0549, 76.6987, 77.0229, 77.3376, 106.0412, 128.8229, 138.3208

1,1'-Ethylenebis[2,5-dimethylpyrrole] (EDMP)

Ehtylenediamine (0.60g, 0.01mol), hexane-2,5-dione (2.28g, 0.02mol), 15ml of methanol and 2 drops of concentrated hydrochloric acid were placed into a 100ml round bottom flask fitted with a reflux condenser. The reaction mixture was heated under reflux for 15 minutes, poured into 10ml of 0.5M hydrochloric acid and then cooled on ice. The product was collected by suction filtration, washed with water and was then recrystalised using acetonitrile to give 1,1'-Ethylenebis[2,5-dimethylpyrrole] (1.56g, 69%) as pale brown crystals.

NMR data

^{1}H NMR (CDCl$_3$) δ 5.75 (s, Ar-H), 3.93 (s, Ar-H), 2.01 (s, R-H)

^{13}C NMR (CDCl$_3$) δ 11.8820, 43.8660, 76.6987, 77.0229, 77.3376, 105.7074, 127.6022

4.3. Results and Discussion

Cyclic voltammograms detailing the response of a glassy carbon electrode to 2,5-dimethyl-1-phenylenepyrrole (DMPP) and 1,1'-p-phenylenebis[2,5-dimethylpyrrole] (PPDMP) in acetonitrile (2mM, 0.05M TBAP) containing ferrocene (2mM), as an internal reference to act as a marker to prove that film formation is occurring, are shown in **Figure 4.1 A** and **Figure 4.1 B** respectively. Looking at **Figure 4.1 A** for the DMPP monomer, three electrode processes are observable, one reversible couple and two irreversible oxidation processes. The first corresponds to the oxidation and reduction of the internal ferrocene reference. The remaining two peaks correspond to the initial oxidation of the DMPP ring leading to the formation of the dimer and the oxidation of the electrogenerated product. Repetitive scans showed little change in the magnitude of all of the peaks observed. Restricting the scan range to encompass only the first oxidation (dimer formation or low unit oligomers) and employing multiple scans did not yield any appreciable film and confirms the earlier assumption that steric congestion associated with 3,4 coupling prevents the formation of a coherent film.
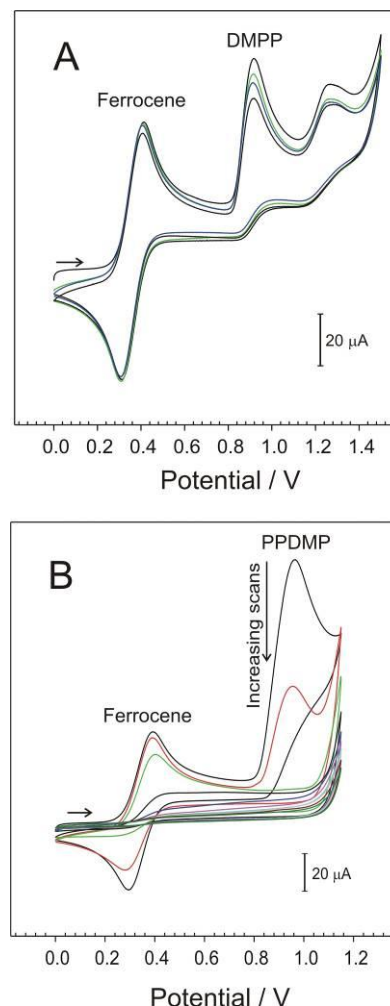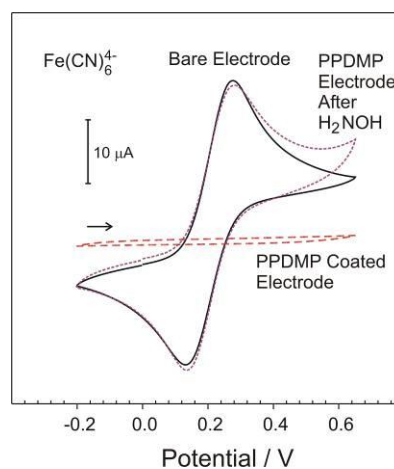

Figure 4.1 Cyclic voltammograms detailing the response of a glassy carbon electrode towards A) DMPP monomer and B) PPDMP monomer.

Looking at **Figure 4.1 B** for the electrochemistry of the PPDMP monomer a reversible redox couple for ferrocene oxidation and reduction and an irreversible oxidation for the oxidation of the PPDMP can be seen. On repetitive scans a decrease in the magnitude of the peaks can be observed with the eventual loss of both peaks being seen. This indicates that a coherent PPDMP polymer film has been formed and the original electrode response could be recovered through the mechanical polishing
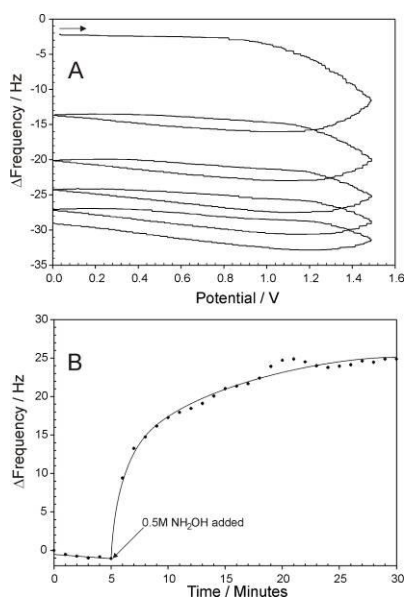
of the electrode. The difference in the electrode profile for the DMPP and PPDMP can be attributed to the bifunctionality of the latter and its ability to couple at opposing ends of the molecule thereby leading to the linear chain growth and film formation.

The integrity of the resulting PPDMP film was probed by examining the voltammetric response to ferrocyanide (2mM, pH 7) at the electrode before and after PPDMP film formation. The resulting scans are compared in **Figure 4.2**. The film modified electrode (**Figure 4.2 red dashed**) was found to effectively exclude the redox probe thus indicating that a dense film that passivates the electrode surface had been formed. The addition of hydroxylamine (0.5M, H_2O) to the PPDMP was found to degrade the film such that the electrode response to the ferrocyanide redox probe could be seen (**Figure 4.2 purple dotted**). This response was almost identical

Figure 4.2 Cyclic voltammograms detailing the response of a glassy carbon electrode towards 2mM ferrocyanide (pH 7) before (black) and after (red dashed) film formation and after exposure to hydroxylamine (purple dotted).

to the profile observed for the redox probe at a bare glassy carbon electrode (**Figure 4.2 black**) and suggests that the addition of the hydroxylamine removes the whole of the PPDMP film opposed to just releasing the phenylenediamine template as desired.

The formation and removal of the film were examined further using electrochemical quartz crystal microbalance experiments. **Figure 4.3 A** shows the EQCM profile observed when the electrochemical properties of the PPDMP were observed at a gold coated quartz crystal working electrode under the same conditions previously used. The frequency can be seen to decrease as the potential reaches the

Figure 4.3 EQCM responses showing A) polymerisation of PPDMP (2mM) and B) the removal of the film after the addition of 0.5M hydroxylamine (pH 7).

anodic region corresponding to the oxidation of the PPDMP monomer and the deposition of the film at the crystal surface. Repetitive scans show a cumulative decrease in the frequency but the magnitude of the change between each scan becomes correspondingly smaller as the film begins to slowly passivate the electrode and pin holes are progressively plugged. The solution was then replaced with free electrolyte and the frequency response recorded **Figure 4.3 B**. A stable resonance was observed up until the addition of an aliquot of hydroxylamine. After the addition the frequency was found to increase before a constant value characteristic of the clean crystal was seen as shown in **Figure 4.3 A**. This therefore corroborates the fact that the whole film was lost from the electrode solution rather than just the loss of the phenylenediamine from the polymer.

Although the synthesied monomer can produce a coherent polymer film, the fact that the whole film degrades in the presence of hydroxylamine makes it inadequate for use as a MIP. The full dissolution of the film does however offer an alternative use of the monomer/polymer as it displays characteristics that can be exploited as the basis of sacrificial or protective film. The development of these types of films has long been of interest within sensor communities where fine control over the sequential patterning of molecular receptors (chemical or biological) within micro-engineered devices is a considerable challenge [28-30]. Degradation and dissolution of the protective films is typically modulated by a change in the prevailing chemical environment – pH, redox conditions or through interaction with a particular chemical moiety [28,31-33]. The possible advantage of the new route discovered here is that it can overcome the difficulties associated with current film processing methods used within conventional microfabrication techniques where site specific spatial positioning on discrete electrode systems needs to be controlled [34-35].

To confirm the applicability of the dipyrrole type monomers as sacrificial or protective polymers the polymerisation process was repeated with an ethylene diamine pyrrole derivative (1,1'-Ethylenebis[2,5-dimethylpyrrole], (EDMP)). Similar protection followed by removal characteristics were observed thus confirming the efficacy of the polymer. From this work it appears that the formation of these types of films is dependent on the possession of two pyrrole moieties on each monomer and that its formation and stability is unaffected by the nature of the bridging group

present, be it alkyl or acyl. It could be envisaged that through the manipulation of the bridge chain length or the addition of other substituents, that a template action could be achieved whereby the latter alters the porosity of the film allowing partial functionalisation of the underlying substrate and that the addition of hydroxylamine could then remove the protective template to reveal the patterned surface.

4.4. Conclusions

Although the aim set out at the start of this chapter, to develop MIPs that could detect compounds containing the amine functionality including cysteine, homocysteine and glutathione haven't been realised a novel approach for the generation of sacrificial electropolymerised polymers has been discovered, demonstrated and the versatility of the preparation, removal and potential applications outlined. The core strength of this approach lies in the selectivity of the removal process – achievable under neutral conditions at room temperature using a relatively benign chemical key that is unlikely to induce any significant perturbations of other chemical functionality.

4.5. References

[1]   K. Ho, W. Yeh, T. Tung and J. Liao, Amperometric detection of morphine based onpoly(3,4-ethylenedioxythiophene) immobilized molecular imprinted polymer particles prepared by precipitation polymerization. Analytica Chimica Acta, 542 (2005) 90-96

[2]   G. Theodoridis, G. Konsta and S. Bagia, Synthesis and evaluation of molecularly imprinted polymers for enalaprl and lisinopril, two synthetic peptide anti-hypertensive drugs. Journal of Chromatography B, 804 (2004) 43-51

[3]   L. Wang and Z. Zhang, The study of oxidization fluorescence sensor with molecular imprinting polymer and its application for 6-mercaptopurine (6-MP) detection. Talanta, 76 (2008) 768-771

[4]   A. Rachkov and N. Minoura, Recognition of oxytocin and oxytocin-related peptides in aqueous media using a molecularly imprinted polymer synthesized by the epitope approach. Journal of Chromatography A, 889 (2000) 111-118

[5]   C. Hu and T. Chou, Albumin molecularly imprinted polymer with high template affinity – Prepared by systematic optimization in mixed organic/aqueous media. Microchemical Journal, 91 (2009) 53-58

[6]   K. Sreenivasan, Synthesis and evaluation of molecularly imprinted polymers for nucleic acid bases using aniline as a monomer. Reactive and Functional Polymers, 67 (2007) 859-864

[7]   I. Gavrilovic, K. Mitchell, A.D. Brailsford, D.A. Cowan, A.T. Kicman and R.J.Ansell, A molecularly imprinted receptor for separation of testosterone and epitestosterone, based on a steroidal crosslinker. Steroids, 76 (2011) 478-483

[8]   A. Rachkov, S. McNiven, A. El'skaya, K. Yano and I. Karube, Fluorescence detectin of β-estradiol using a molecularly imprinted polymer. Analytica Chimica Acta, 405 (2000) 23-29

[9]   I. Sanchez-Barragan, K. Karim, J.M. Costa-Fernandez, S.A. Piletsky and A. Sanz-Medel, A molecularly imprinted polymer for carbaryl determination in water. Sensors and Actuators B, 123 (2007) 798-804

[10]   B. Singh and N. Chauhan, Preliminary evaluation of molecular imprinting of 5-fluorouracil within hydrogels for use as drug delivery systems. Acta Biomaterialia, 4 (2008) 1244–1254

[11]   A. Volkmann and O. Bruggemann, Catalysis of an ester hydrolysis applying molecularly imprinted polymer shells based on an immobilised chiral template. Reactive and Functional Polymers, 66 (2006) 1725-1733

[12]   A. Sisnjevski, R. Schomacker, E. Yilmaz and O. Bruggemann, Catalysis of a Diels-Alder cycloaddition   with differently fabricated molecularly imprinted polymers. Catalysis Communications, 6 (2005) 601-606

[13]   H. Byun, Y. Youn, Y. Yun and S. Yoon, Selective separation of aspirin using molecularly imprinted polymers. Separation and Purification Technology, 74 (2010) 144–153

[14]   V.S. Sumi, R. Kala, R.S. Praveen and T.P. Rao, Imprinted polymers as drug delivery vehicles for metal-based anti-inflammatory drug. International Journal of Pharmaceutics, 349 (2008) 30–37

[15]   A. Merkoc and S. Alegret, New materials for electrochemical sensing IV. Molecular imprinted polymers. Trends in analytical chemistry, 21 (2002) 717-725

[16]   M. Petcu, P.N. Schaare and C.J. Cook, Propofol-imprinted membranes with potential applications in biosensors. Analytica Chimica Acta, 504 (2004) 73–79

[17]   H. Hsu, L. Chen and K. Ho, Colorimetric detection of morphine in a molecularly imprinted polymer using an aqueous mixture of Fe3+ and [Fe(CN)6]3−. Analytica Chimica Acta, 504 (2004) 141–147

[18]   L. Feng, Y. Liu, Y. Tan and J. Hu, Biosensor for the determination of sorbitol based on molecularly imprinted electrosynthesized polymers. Biosensors and Bioelectronics, 19 (2004) 1513–1519

[19]   Y. Liu, K. Hoshina and J. Haginaka, Monodispersed molecularly imprinted polymers for cinchonidine by precipitation polymerization. Talanta, 80 (2010) 1713-1718

[20]   Y. Lu, C. Li, X. Wang, P. Sun and A. Xing, Influence on polymerization temperature on the molecular recognition of imprinted polymers. Journal of Chromatography B, 804 (2004) 53-59

[21]   M.C. Blanco-Lopez, M.J. Lobo-Castanon, A.J. Miranda-Ordieres and P. Tunon-Blanco, Voltammetric sensor for vanillylmandelic acid based on molecularly imprinted polymer-modified electrodes. Biosensors and Bioelectronics, 18 (2003) 353-362

[22]   R. Liang, R. Zhang and W. Qin, Potentiometric sensor based on molecularly imprinted polymer for determination of melamine in milk. Sensors and Actuators B, 141 (2009) 544–550

[23]   M. Javanbakht, S.E. Fard, A. Mohammadi, M. Abdoussa, M.R. Ganjali, P. Norouzi and L. Safaraliee, Molecularly imprinted polymer based potentiometric sensor for the determination of hydroxyzine in tablets and biological fluids. Analytica Chimica Acta, 612 (2008) 65-74

[24]   B. Mothana and R.J. Boyd, A density functional theory study of the mechanism of the Paal–Knorr pyrrole synthesis. Journal of Molecular Structure, 811 (2007) 97-107

[25]   I.T. Kim and R.L. Elsenbaumer, Convenient synthesis of 1-alkyl-2, 5-bis(thiophenylmethylene)pyrroles using the Mannich reaction. Tetrahedron Letters, 39 (1998) 1087-1090

[26]   P.G. Pickup and R.A. Osteryoung, Electrochemical polymerization of pyrrole and electrochemistry of polypyrrole films in ambient temperature molten salts. Journal of the American Chemical Society 106 (1984) 2294-2299

[27]   A.F. Diaz, K.K. Kanazawa and G.P. Gardini, Electrochemical polymerization of pyrrole. Journal of the Chemical Society, Chemical Communications,14 (1979) 635-636

[28]   R. Knake and P.C. Hauser, Sensitive electrochemical detection of ozone. Analytica Chimica Acta, 459 (2002) 199-207

[29]   C.-H. Weng, W.-M. Yeh, K.-C. Ho and G.-B. Lee, A microfluidic system utilizing molecularly imprinted polymer films for amperometric detection of morphine. Sensors and Actuators B: Chemical, 121 (2007) 576-582

[30]   S. Cosnier and C.H. Gondran, Fabrication of biosensors by attachment of biological macromolecules to electropolymerized conducting films. Analysis, 27 (1999) 558-563

[31]   R. Mažeikienė, G. Niaura and A. Malinauskas, Raman spectroelectrochemical study on the kinetics of electrochemical degradation of polyaniline. Polymer Degradation and Staility, 93 (2008) 1742-1746

[32]   B.M. Kennedy and V.J. Cunnane, The degradation of pinhole free poly (1,3-dihydroxybenzene) films in sodium hydroxide for the production of microelectrode ensembles. Journal of Electroanalytical Chemistry, 615 (2008) 197-204

[33]   R. Tucceri, The change of the electron scattering at the gold film–poly-(o-aminophenol) film interface after partial degradation of the polymer film: its relation with the electron transport process within the polymer film. Journal of Electroanalytical Chemistry, 562 (2004) 173-186

[34]   C. Huang, G. Jiang and R. Advincula, Electrochemical Cross-Linking and Patterning of Nanostructured Polyelectrolyte−Carbazole Precursor Ultrathin Films. Macromolecules, 41 (2008) 4661-4670

[35]   T.D. Chung, R.-A. Jeong, S.K. Kang and H.C. Kim, Electrochemical Cross-Linking and Patterning of Nanostructured Polyelectrolyte−Carbazole Precursor Ultrathin Films. Biosensors and Bioelectronics, 16 (2001) 1079-1087

Chapter 5

Plumbagin: A New Route to the Electroanalytical Determination of Cystine

Chapter 5

Plumbagin: A New Route to the Electroanalytical Determination of Cystine

Abstract

The interaction between the natural product plumbagin (5-hydroxy-2-methyl-1,4-naphthoquinone) and a variety of thiol derivatives has been assessed and the subsequent results are presented within this chapter. A clearly resolved voltammetric signature was observed for plumbagin in the presence of cysteine that could potentially be used as the basis of an electrochemical assay for the determination of the thiol. A structure-function study was carried out to assess the nature of the resulting voltammetric profile and to evaluate the highly selective response of the system to cysteine. The translation of the system as the basis of an assay for the indirect determination of cystine was investigated using mercaptopropanol as an *in-situ* reducing agent. The lack of response of plumbagin to the latter and the high recovery performance of the label opens up a new direction for the one pot, mercury free analysis of cystine.
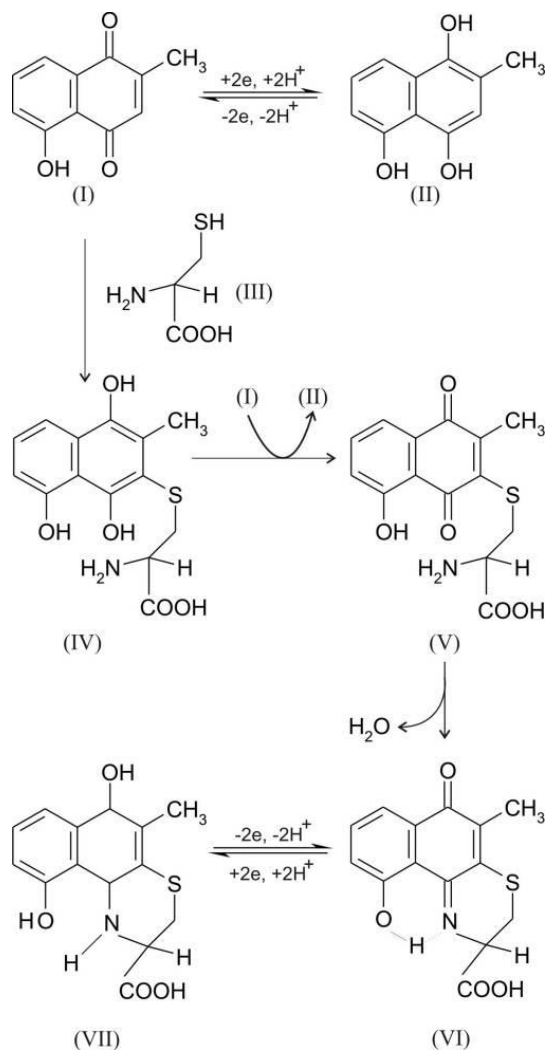
The work presented in this chapter has been published within Electroanalysis

5.1. Introduction

The cytotoxic properties of naphthoquinones derivatives derived from plant sources have long been recognised and many have been investigated as potential candidates for use as antimicrobial [1-4] and chemotherapeutic agents [5-7]. Plumbagin (5-hydroxy-2-methyl-1,4-naphthoquinone) **Scheme 5.1 (I)** has gathered particular interest in recent years as it was identified as one of the core active ingredients within numerous Siddha and Ayurveda remedies [7-9]. The pharmacological action of the latter has been attributed largely to its ability to redox cycle with the local generation of reactive oxygen species within the cytoplasm inducing apoptosis [5,7]. It can however undergo a variety of other inter and intra cellular reactions, particularly through nucleophilic addition at the unsubstituted 3 position. As such, it has

Scheme 5.1 Plumbagin reaction pathways.

been postulated that it can initiate a secondary attack on the cell machinery through depleting the endogenous sulphydryl thiol anti-oxidant defences that would otherwise scavenge the reactive oxygen species present. The reaction between sulphydryl thiols and naphthoquinones is well established within the literature and it is likely that cysteine, homocysteine and glutathione would follow an analogous reaction pathway with plumbagin [10-12]. The aim of the work presented in this chapter were to assess the propensity for plumbagin to undergo such reactions with these thiol species and to determine whether the substituent configuration influences the electrochemical properties of the resulting conjugates formed.

The reaction scheme highlighting the basic nucleophilic addition of the thiol functionality, in this case cysteine (**III**), onto plumbagin (**I**) is detailed in **Scheme 5.1** (**I → IV**). Whilst the reduced form of the conjugate **(IV)** is the initial reaction product, molecular oxygen or the naphthoquinone starting material itself can re-oxidise the conjugate **(IV→V)** [13]. The presence of the oxidised conjugate now creates the possibility of a secondary transformation, if the structure of the thiol compound is such that an intra molecular cyclisation can occur. This will be between the quinone and the amine functionality, if present, through the formation of a Schiff base (C=N). For cysteine a six membered ring will form, conferring a degree of stability to the final conjugate (**V→VI**). It was expected that the formation of a cyclised conguate for homocysteine would be slow to form, due to steric and kinetic limitations. For glutathione, the cysteine amino group is tied up within the peptide linkage and, as such, no ring closure can occur. Due to the possibility of having a range of different plumbagin-thiol conjugates present, it was anticipated that there would be a significant difference in the electrochemical behaviour observed for the plumbagin in the presence of the various thiol species. One possibility was that the voltammetric profile for the plumbagin and the resulting cyclised conjugated would be fully resolvable for the interaction with cysteine therefore allowing the naphthoquinone to be harnessed as a versatile redox indicator for the speciation of cysteine. The electrochemical responses of plumbagin in the presence of various thiol compounds has been investigated in an effort to elucidate the nature of the reaction mechanism and to probe the potential use of this method as a bioanalytical assay for cyteine detection.

5.2. Experimental Details

All reagents were of the highest grade available, were used without further purification and unless stated otherwise were purchased from Sigma Aldrich (UK) or Alfa Aesar (UK). Solutions of plumbagin, 2-methyl-1,4-naphthoquinone and 5-hydroxy-1,4-naphthoquinone (typically 5mM) were prepared in methanol and stock thiol (cysteine, homocysteine, glutathione, mercaptopropionic acid, N-acetylcysteine, mercaptoethylamine and penicillamine) and ascorbic acid solutions (typically 10mM) were prepared in pH 8 Britton-Robinson buffer, this was also used as the supporting

electrolyte throughout the electrochemical investigations. Electrochemical measurements were conducted using a µAutolab computer controlled potentiostat (Eco-Chemie, Utrecht, The Netherlands) using a three electrode configuration consisting of a glassy carbon working electrode (3 mm diameter, BAS Technicol, UK), a platinum wire counter electrode and a 3M NaCl Ag | AgCl half cell reference electrode (BAS Technicol, UK). Unless specified otherwise the scan rate in all cases was 0.1V/s and all measurements were conducted under nitrogen and at $22^{\circ}C \pm 2^{\circ}C$.

5.3. Results and Discussion

Cyclic voltammograms detailing the response of plumbagin (0.454mM, pH 8) at a glassy carbon electrode in the absence and presence of increasing amounts of cysteine (0 – 0.45mM) are detailed in **Figure 5.1 A**. The reduction and re-oxidation processes of the native quinone component can be observed at -0.32V and -0.06V respectively and follows the process outlined in **Scheme 5.1 (I→II)**. The peak separation (260mV) is significantly larger than that expected for a conventional two electron system and follows an irreversible profile similar to that previously found with naphthoquinone systems [12]. The introduction of cysteine to the solution (0.045mM additions) causes a decrease in both the reduction and oxidation peaks (**Figure 5.1 A**). This can be attributed to the formation of the conjugate outlined in **Scheme 5.1 (I→IV)** and again is typical of the response found in previous naphthoquinone systems [10-13].
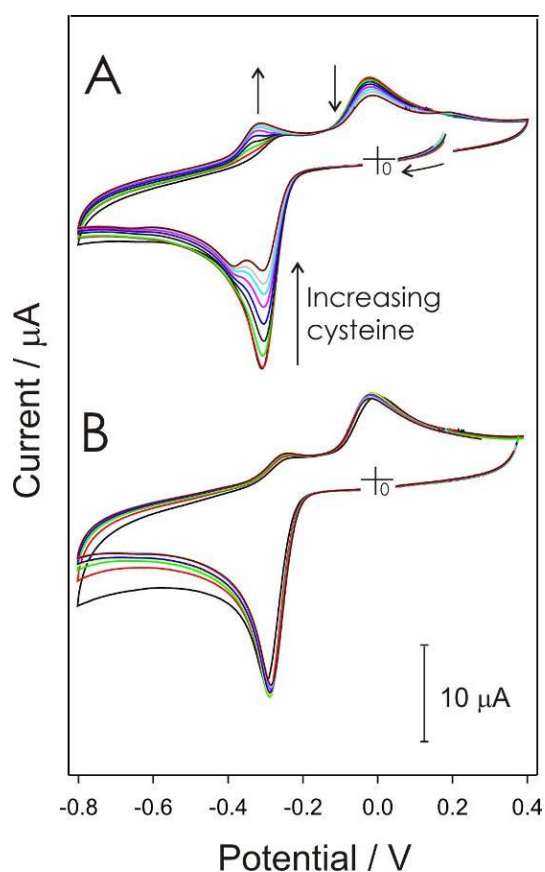

Figure 5.1 Cyclic voltammograms detailing the response of plumbagin (0.45mM, pH 8) towards increasing concentrations (45µM) of cysteine (A) and glutathione (B).

In contrast to many of the previous studies, a new redox couple (-0.44V and -0.33V) was found to emerge as the concentration of cysteine was increased and this can be attributed to the reduction of the quinone-imine cyclisation product (**VI→VII**). The reduction process appears initially as a shoulder on the native plumbagin reduction peak but is wholly resolvable as the latter is depleted. The oxidation process however occurs in a position distinct from any competing processes (-0.33V). The peak separation for the conjugate redox couple is markedly smaller (120mV) than for the native naphthoquinone. This could be due to the disruption in the planarity of the system as a consequence of the extended Schiff base (imine) ring system being saturated and hence buckled which may alter the interaction with the underlying carbon electrode.

The electrode response to the reaction of plumbagin with glutathione (0-0.45mM) is highlighted in **Figure 5.1 B**. Very little difference in the native plumbagin voltammetric profile is observed when increasing the concentration of glutathione (0.045mM additions). The lack of any appreciable interaction stands in marked contrast to that observed with cysteine and indicates that it may indeed be possible to use the naphthoquinone as a means of speciation between the two thiols.

A range of thiol derivatives possessing a carbon skeleton analogous to cysteine were investigated (**Figure 5.2**). It was hoped that through the subtle manipulation of the α-carbon functional groups that the shapes of the resulting voltammetric profiles could help elucidate the nature of the interactions
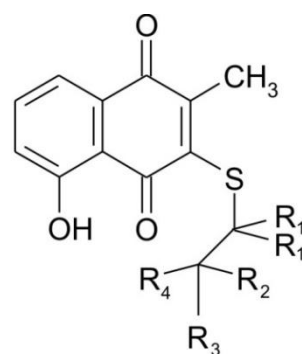

	R_1	R_2	R_3	R_4
Mercaptopropionic Acid	H	H	H	COOH
N-Acetylcysteine	H	H	COOH	CH_3CONH
Mercaptoethylamine	H	H	H	NH_2
Penicillamine	CH_3	H	COOH	NH_2

Figure 5.2 Composition of the conjugates used.

occurring.

Cyclic voltammograms detailing the response of a glassy carbon electrode to N-acetylcysteine under the same conditions employed for the cysteine investigations are detailed in **Figure 5.3 A**. The response obtained was similar to the one observed for cysteine but in this instance there were no new redox peaks seen as in this case, the amino group is protected and thus prevented from reacting to form the cyclic conjugate indicated in **Scheme 5.1** (**VI**). Mercaptopropionic acid exhibited similar behaviour to glutathione and reinforces the need for the available primary amino group for the secondary transformation to take place. This was confirmed by the positive response obtained with mercaptoethylamine (**Figure 5.3 B**) and penicillamine. These have a free primary amino group and followed the path originally observed with cysteine with the emergence of a resolved set of peak processes corresponding to the formation of the cyclic conjugate.
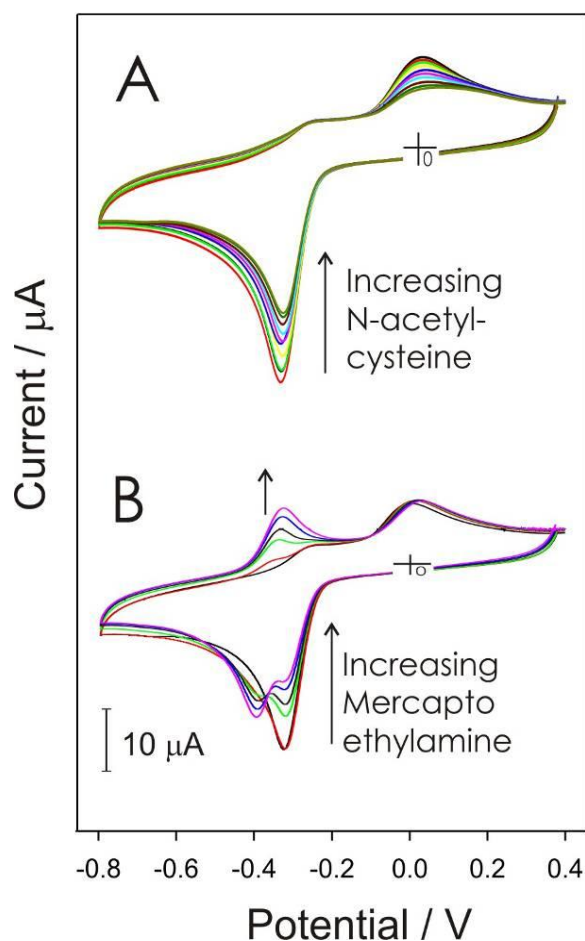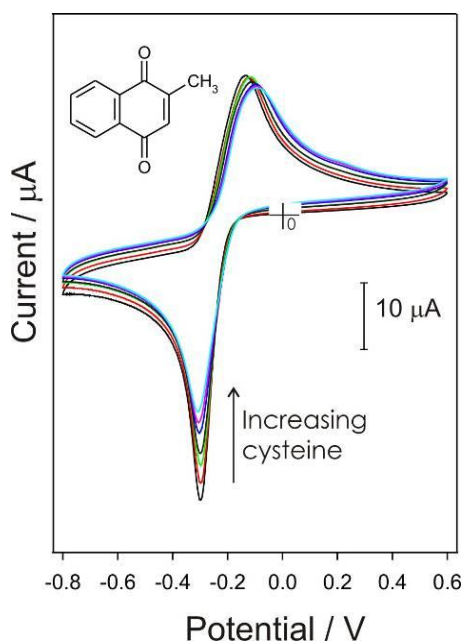

Figure 5.3 Cyclic voltammograms detailing the response of plumbagin (0.45mM, pH 8) towards increasing concentrations (0.045mM additions) of N-acetylcysteine (A) and mercaptoethylamine (B).

The assumption that formation of a six member ring is a prerequisite for intra-molecular cyclisation was corroborated by the negative response of plumbagin to homocysteine (no new redox peaks were seen). In this instance, the amino group is available but the additional methylene (CH_2) group between the amino and thiol would result in the formation of a seven member ring which is sterically (and kinetically) less favourable.

The availability of the 5-hydroxyl group on the plumbagin appears to be significant in obtaining the resolvable peaks as while the response of 5-hydroxy-1,4-naphthoquinone to cysteine was found to be analogous to that observed with plumbagin, no distinct/resolvable peaks were observed with 2-methyl-1,4-naphthoquinone (**Figure 5.4**). While it is still plausible that intra-molecular cyclisation occurs, the possibility of hydrogen bonding between the imine amino group and the neighbouring 5-hydroxy group, as indicated in **Scheme 5.1.** (**VI**), could facilitate stabilisation of the intermediate and hence the more negative potential required to induce reduction of the conjugate.


Figure 5.4 Cyclic voltammograms detailing the response of 2-methylnaphthoquinone (0.45mM, pH 8) towards increasing concentrations (0.045mM additions) of cysteine.

The relative failure of the other thiols to elicit any appreciable response with the plumbagin indicator results in the label having a high degree of selectivity towards

cysteine. This creates a unique opportunity where the interaction could be exploited as the basis of an electrochemical assay for the detection of cystine (the homologous disulphide of cysteine). Cystine has long been recognised as an important biomarker for renal function but it has proven to be an extremely difficult target for determination using electroanalytical techniques [14]. While it has been investigated at mercury electrodes, the safety and practical limitations of these electrodes has significantly restricted their application [15,16]. The unreactive nature of cystine invariably requires the introduction of pre-treatment steps to reduce the disulphide bond, releasing the two cysteine constituents which are subsequently derivatised and normally analysed using chromatographic techniques [14].

The issue that has hindered the development of direct electroanalytical techniques relates to the fact that the disulphide reduction process is usually achieved through the introduction of an excess quantity of another, activated thiol, typically possessing an electron-releasing alcohol functionality (e.g. dithiothreitol, mercaptoethanol or mercaptopropanol). The mercaptopropanol used in this instance effectively substitutes for the cysteine as indicated in **Scheme 5.2** [14,17]. The reaction mixture will therefore contain the unreacted mercaptopropanol and the cysteine released through the reaction of the mercaptopropanol with the cystine. As such there are two red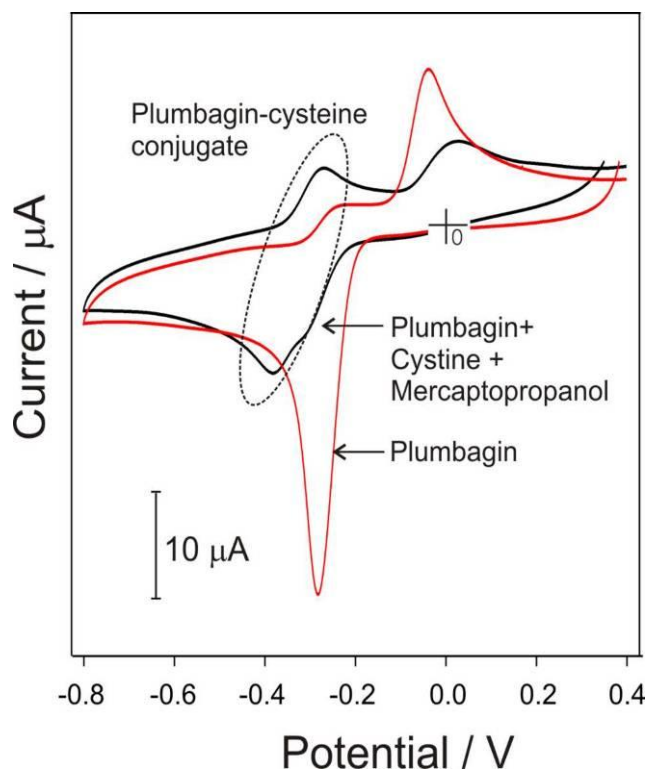uced thiol moieties present that can undergo the derivatisation process and thus the main challenge has been to differentiate
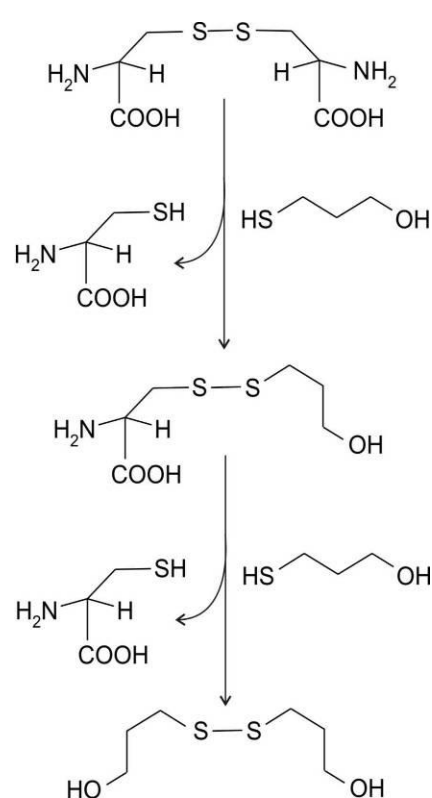
Scheme 5.2 Reduction of cystine with mercaptopropanol.

between the released cysteine and the introduced thiol reducing agent which, in the absence of chromatographic resolution, have traditionally interfered with one another. Unfortunately, most labels designed to enhance the electrochemical signal often fail to provide any significant difference in the redox positions and hence the continued search for new labelling agents.

The acquisition of a distinct signal in the presence of cysteine would clearly offer a new approach to the determination of cystine. The response of the plumbagin label to mercaptopropanol (both 1 and 2 substituted isomers) was found to exhibit behaviour consistent with that observed for the glutathione responses detailed in **Figure 5.1 B** and hence would give little interference when trying to detect the cysteine released.

A preliminary evaluation of the utility of using 2-mercaptopropanol in the context of detecting cystine was conducted by constructing a calibration graph looking at the decrease in the plumbagin reduction peak at -0.32 V as the concentration of cysteine in the sample increases, (Peak height / µA = -1.052 [cysteine / mM] + 1.117). A solution containing 16mM cystine and 32mM mercaptopropanol was then prepared, allowed to react for 5 minutes (which was the optimal time to allow full cystine reduction) and was then added to a

Figure 5.5 Cyclic voltammograms detailing the response of plumbagin (0.45mM, pH 8) to an aliquot of cystine (16mM) and mercaptopropanol (32mM).

fresh solution of plumbagin (5mM, pH 8). The reaction mixture was mixed for 2-3 minutes, left to attain quiescence and the cyclic voltammogram recorded. The cyclic voltammograms detailing a typical reaction run are highlighted in **Figure 5.5**. In the absence of mercaptopropanol there is no change in the plumbagin profile. Similarly, there is also no change when only mercaptopropanol is added. It is only when both reagents are present that a change in the voltammetric profile is observed. A substantial decrease in the magnitude of the reduction peak and the appearance of the redox processes characteristic of the plumbagin-cysteine conjugate. The magnitude of the plumbagin peak was then evaluated and the concentration of the cysteine released

determined from the calibration data obtained previously. The recovery of cystine (based on the cysteine calibration) was found to be 100.69% (%RSD = 5.14, N = 3) and confirms the potential viability of the procedure.

5.4. Conclusions

The reaction of plumbagin with various thiol derivatives has been assessed using cyclic voltammetry with a view to understanding the nature of the interactions between the thiol substituent and the core quinone. A distinct, clearly resolvable peak signature for the conjugate resulting from the reaction with cysteine has been observed and structure- function relationship data collated and critically assessed. The peak process attributed to the cysteine conjugate has been found to be highly selective and could be used as the basis of a new assay for the direct electrochemical analysis of cystine, which has, hitherto, proven to be a challenge for all but mercury based electrodes.

5.5. References

[1]   B.S. Park, H.K. Lee, S.E. Lee, X.L. Piao, G.R. Takeoka, R.Y. Wong, RY; Y.J. Ahn, Antibacterial activity of *Tabebuia impetiginosa* Martius ex DC (Taheebo) against *Helicobacter pylori*. Journal of Ethnopharmacology, 105 (2005) 255-262

[2]   J.W. Chen, C.M. Sun,W.L. Sheng, Y.C. Wang and W.J.Syu, Expression Analysis of Up-Regulated Genes Responding to Plumbagin in *Escherichia coli*. Journal of Bacteriology, 188 (2006) 456-463

[3]   J.S. Mossa, F.S. El-Feraly and I Muhammad, Antimycobacterial constituents from Juniperus procera, Ferula communis and Plumbago zeylanica and their in vitro synergistic activity with isonicotinic acid hydrazide. Phytotherapy Research, 18 (2004) 934-937

[4]   Y.C. Wang and T.L. Huang, High-performance liquid chromatography for quantification of plumbagin, an anti-Helicobacter pylori compound of Plumbago zeylanica L. Journal of Chromatography A, 1094 (2005) 99-104

[5]   V. SivaKumar, R. Prakash, M.R. Murali, H. Devaraj and S.N. Devaraj, In Vivo Micronucleus Assay and GST Activity in Assessing Genotoxicity of Plumbagin in Swiss Albino Mice. Drug and Chemical Toxicology, 28 (2005) 499-507

[6]   Y.L. Hsu, C.Y. Cho, P.L. Kuo, Y.T. Huang and C.C. Lin, Plumbagin (5-Hydroxy-2-methyl-1,4-naphthoquinone) Induces Apoptosis and Cell Cycle Arrest in A549 Cells through p53 Accumulation via c-Jun NH_2-Terminal Kinase-Mediated Phosphorylation at Serine 15 in Vitro and in Vivo. Journal of Pharmacology and Experimental Therapeutics, 318 (2006) 484-494

[7]   L.C. Lin, L.L. Yang and C.J. Chou, Cytotoxic naphthoquinones and plumbagic acid glucosides from Plumbago zeylanic. Phytochemistry, 62 (2003) 619-622

[8]   J.C. Tilak, S. Adhikari and T.P.A. Devasagayam, Antioxidant properties of *Plumbago zeylanica*, an Indian medicinal plant and its active ingredient, plumbagin Redox Report, 9 (2004) 219-227

[9]   S. Sowmyalakshmi, M. Nur-e-Alam, M.A.Akbarsha, S.Thirugnanam, J. Rohr, D. Chendil, Investigation on *Semecarpus Lehyam*—a *Siddha* medicine for breast cancer. Planta, 220, (2005) 910-918

[10]   P.C. White, N.S. Lawrence, J. Davis and R.G. Compton, Electrochemical Determination of Thiols: A Perspective. Electroanalysis, 14 (2002) 89-98

[11]   P.C. White, N.S. Lawrence, J. Davis and R.G. Compton, Electrochemically initiated 1,4 additions: a versatile route to the determination of thiols, Analytica Chimica Acta, 447 (2001) 1-10

[12]   R.B. Smith, C. Canton, N.S. Lawrence, C. Livingstone and J. Davis, Molecular anchors—mimicking metabolic processes in thiol analysis. New Journal of Chemistry, 30 (2006) 1718-1724

[13]   A. Digga, S. Gracheva, C. Livingstone and J. Davis, Potentiometric detection of thiols: a mechanistic evaluation of quinone–thiol interactions Electrochemistry Communications, 5 (2003) 732-736

[14]   J. Lock and J. Davis. The determination of disulphide species within physiological fluids. TrAC Trends in Analytical Chemistry, 21 (2002) 807-815

[15] T.R. Ralph, M.L. Hitchman, J.P. Millington and F.C. Walsh, The reduction of L-cystine in hydrochloric acid at mercury drop electrodes. Journal of Electroanaytical Chemistry, 587 (2006) 31-41

[16] B. Marco-Monterroso and R.B. Lopez-Ruiz, pH effect on cysteine and cystine behaviour at hanging mercury drop electrode. Talanta, 61 (2003) 733-741

[17] L.A.A. Newton, K. Sandhu, C. Livingstone, R. Leslie and J. Davis, Clinical diagnostics for homocysteine: a rogue amino acid? Expert Reviews in Molecular Diagnostics, 10 (2010) 489-500

Chapter 6

Plumbagin: A Natural Product for Smart Electrode Materials?

Chapter 6

Plumbagin: A Natural Product for Smart Electrode Materials?

Abstract

The exploitation of the natural product plumbagin (5-hydroxy-2-methyl-1,4-naphthoquinone) as a monomer to produce polymer films is discussed within this chapter. It was envisaged that the film produced would be able to react with reduced sulphydryl thiols (RSH) at an electrode interface, with the possibility of this providing a reagentless sensing platform for the latter. The generation of the polymer film and the efficacy of its response to RSH has been evaluated using cyclic voltammetry and electrochemical quartz crystal microbalance studies. The polymeric film was found to have inadequate stability in the presence of RSH and therefore has limited potential for facilitating thiol detection *via* this route. During these studies, it was however found that the quinone redox centre on the plumbagin was able to catalyse the reduction of oxygen to produce reactive oxygen species (ROS). The ability of the plumbagin polymer and monomer to produce ROS has therefore been evaluated. The application of this material to prevent electrode fouling has also been critically assessed.

The work presented in this chapter has been published within New Journal of Chemistry

6.1. Introduction

The development of reagentless sensing platforms has generated a large amount of interest in recent years due to the growth of point of care diagnostics. These types of systems have been developed for a variety of biologically relevant molecules and are advantageous as they allow analyte determination quickly and easily without the need for large amounts of user intervention which can be a major contributor to erroneous results [1]. The development of these types of platforms can however be very problematic as the reagents need to be incorporated within the sensor so that they have good long term stability, are sensitive and selective whilst being easy to use and cheap to fabricate [2].

The work in the previous chapter described how plumbagin (5-hydroxy-2-methyl-1,4-naphthoquinone) could be used for the determination of cystine (after its *in-situ* reduction to cystiene) *via* a nucleophilic addition at the unsubstituted 3 position. Plumbagin has another important functionality, a 5-hydroxyl group and it is envisaged that the availability of this phenolic group could allow the molecule to undergo electropolymerisation therefore facilitating the production of thin film that is capable of reacting with and therefore detecting the thiol species as illustrated in **Scheme 6.1**. The work presented in this chapter has therefore sought to examine the possibility of exploiting plumbagin as the basis of a smart polymeric material that is able to facilitate reagetless thiol detection. Electrochemical oxidation of the phenol moiety on the plumbagin should, in line with conventional phenol based electropolymerisation, result in the production of a radical
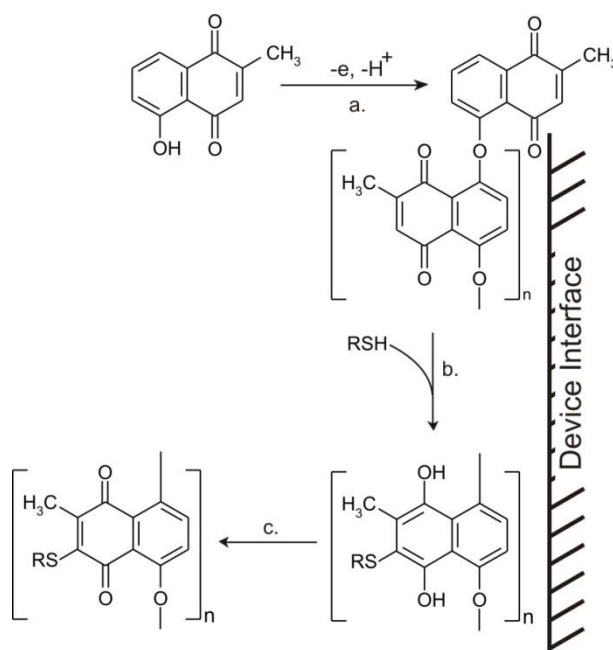
Scheme 6.1 Reaction scheme showing a. the electroplymerisation of plumbagin, b. the reaction of poly-plumbagin with sulphydryl thiols (RSH) and c. the redox processes that will facilitate thiol detection.

cation whose head to tail coupling should lead to the deposition of a thin plumbagin polymer film directly at the electrode surface [3-4] (**Scheme 6.1 a.**). It was envisaged that the quinone component on the compound would be retained and remain accessible to the sulphydryl group on the thiol compounds allowing the nucleophilic addition to occur and any accompanying change in the redox state of the polymer that occurs as a result of this to be detected and thus the thiol can be determined (**Scheme 6.1 b.** and **c.**) [5-6].

6.2. Experimental Details

All reagents were of the highest grade available, were used without further purification and unless stated otherwise were purchased from Sigma Aldrich (UK) or Alfa Aesar (UK). Solutions of plumbagin (5mM) were prepared in acetone. Stock glutathione and ascorbic acid solutions (typically 10mM) were prepared in pH 7 Britton-Robinson buffer and solutions of Ellmans reagent (1mM) were prepared in pH 8 Britton-Robinson buffer. Electrochemical measurements were conducted using a µAutolab computer controlled potentiostat (Eco-Chemie, Utrecht, The Netherlands) using a three electrode configuration consisting of a glassy carbon working electrode (3mm diameter, BAS Technicol, UK), a platinum wire counter electrode and a 3M NaCl Ag | AgCl half cell reference electrode (BAS Technicol, UK) completing the cell assembly. Unless specified otherwise the scan rate for all experiments was 50mV/s and all measurements were conducted at $22^{o}C \pm 2^{o}C$. Electrochemical Quartz Crystal Microbalance (EQCM) measurements were obtained using a computer controlled Quartz Crystal Microbalance (Maxtek INC, USA) and polished 5 MHz Titanium / Gold crystals (Maxtek INC, USA).

6.3. Results and Discussion

6.3.1. Poly-plumbagin for the Detection of Sulphydryl Thiols

Plumbagin film formation was attempted through the direct electro-oxidation of the 5-hydroxy functionality. It was anticipated that this would lead to polyphenylene oxide film formation consistent with conventional phenolic electro-
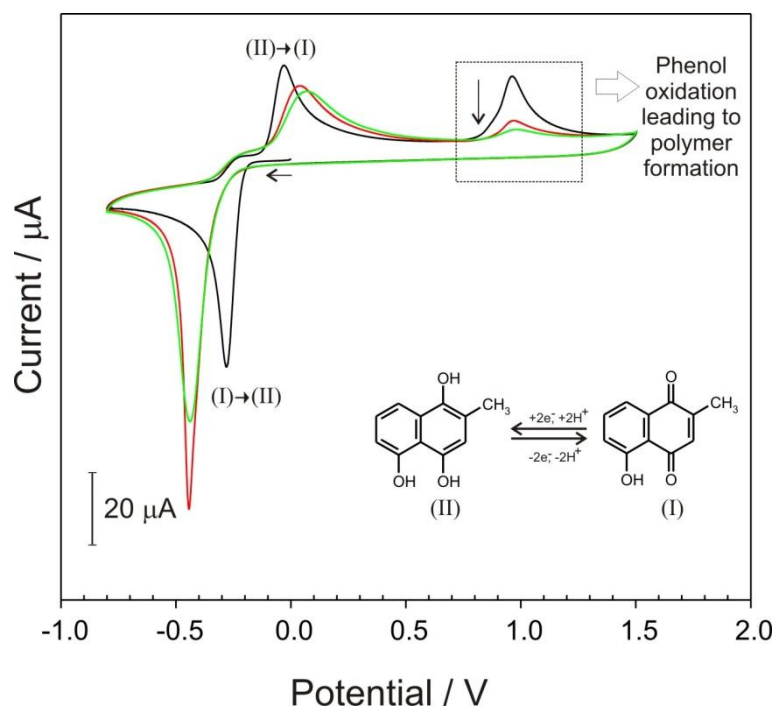
oxidation [3-4]. Repetitive scan cyclic voltammograms detailing the response of plumbagin (0.8mM, pH 7) at a glassy carbon electrode are shown in **Figure 6.1**. The irreversible oxidation of the phenol was observed at +0.95 V and this peak was found to decrease on successive scanning which is consistent with the formation of a phenol type film. The profile of

Figure 6.1 Repetitive scan cyclic voltammograms detailing the electropolymerisation of Plumbagin (0.8mM, pH 7) at a glassy carbon electrode.

the quinone component changed markedly with increasing scan number. On the first scan, prior to oxidation of the phenol, the reduction and oxidation processes are consistent with those experienced for a monomer based solution (**Chapter 5-Figure 5.1**). The subsequent scans, after oxidation of the phenol has occurred, show a shift in the quinone reduction peak to more negative potentials, along with an increase in the magnitude and the sharpness of this peak. This can be rationalised on the basis of formation of a surface immobilised redox centre and confirms the formation of the plumbagin polymer.

Removal of the modified glassy carbon electrode and placement within fresh buffer, devoid of plumbagin monomer, revealed that the activity of the quinone component was retained at the electrode surface as highlighted in the cyclic voltammogram in **Figure 6.2** (**black line**). The shape of the redox processes are broad and stand in contrast to the sharp processes observed in the initial polymerisation stages, seen in **Figure 6.1**, and this may reflect the fact that a more heterogeneous population of different redox species at the electrode surface. The magnitude of these peak processes were found to be markedly smaller than expected. This can be ascribed to the formation and subsequent loss of oligomeric material during the

polymerisation, electrode washing and transfer processes. The shape of this cyclic voltammogram suggests the presence of particulate/oligomeric structures which are only loosely adhered to the electrode surface rather than the conventional coherent polymer film.
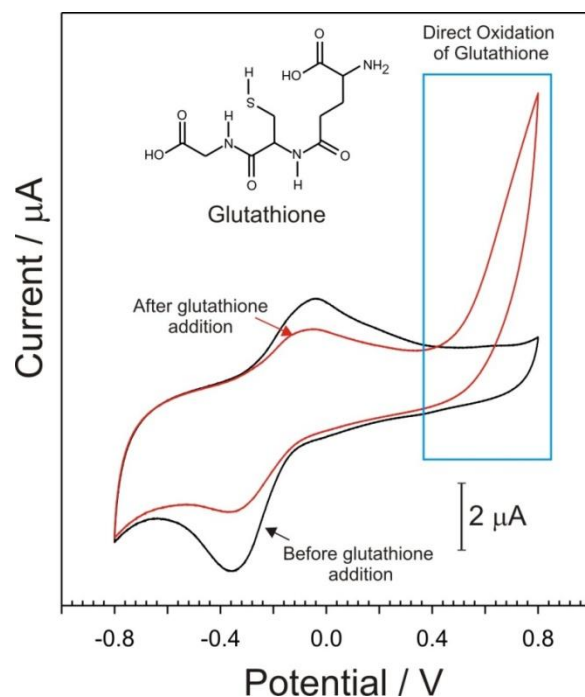
Figure 6.2 Cyclic voltammograms detailing the response of a plumbagin modified glassy carbon electrode in the absence (black line) and presence (red line) of glutathione (0.3mM, pH 7).

When the electrochemistry of the film was studied in the presence of glutathione (**Figure 6.2 red line**) the redox processes ascribed to the polymer are seen to decrease and the direct oxidation of glutathione can be seen. This appears to suggest that the polymer degrades in the presence glutathione. EQCM studies were used to study the stability/reactivity of the poly-plumbagin film in the presence of glutathione (**Figure 6.3**).
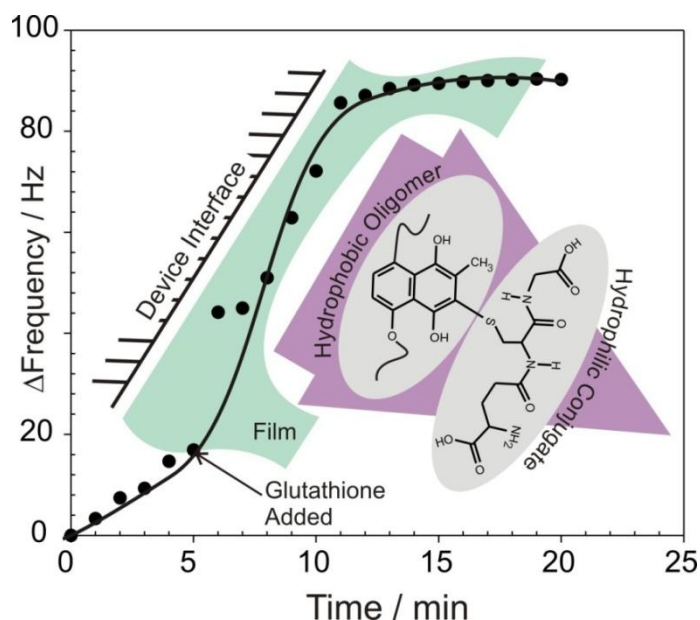
Figure 6.3 EQCM response of an Au-plumbagin modified electrode before and after the addition of glutathione (0.385mM, pH 7).

The polymerisation process was repeated using a gold quartz crystal (deposited from 10mM plumbagin dissolved in ethylacetate containing 0.05M tetrabutylammonium perchlorate as the supporting electrolyte, 50 scans). Upon removing the crystal and placing in fresh pH 7 buffer, devoid of the monomer, it can be seen that there is a gradual loss of material from the electrode surface (expressed as ΔFreq, 0-5minutes) this can be ascribed to the oligomers slowly diffusing from the electrode surface into the solution confirming that the film is only loosely adhered to the electrode surface. Glutathione (0.385mM) was added to the buffer solution and a dramatic increase in the frequency was observed this corresponds to the decrease in mass at the electrode surface as the polymer is removed, after this a stable plateau was reached (**Figure 6.3**).   In some cases thiols have been known to react with napthoquinone derivatives to produce water soluble conjugates, this must be the case here as indicated in the inset schematic within **Figure 6.3** [7-8]. There must however be an underlying layer of insoluble polymer left at the electrode surface, as the redox process attributed to the quinone component of the poly-plumbagin are not removed completely. The fact that the poly-plumbagin film degrades in the presence of thiol however compromises its use as a reagentless sensing material.

During these studies it was noted that the glutathione concentration of the electrochemical solutions had been significantly depleted to an amount that could not just be attributed to the addition of the thiol onto the polymeric/oligomeric plumbagin.   The
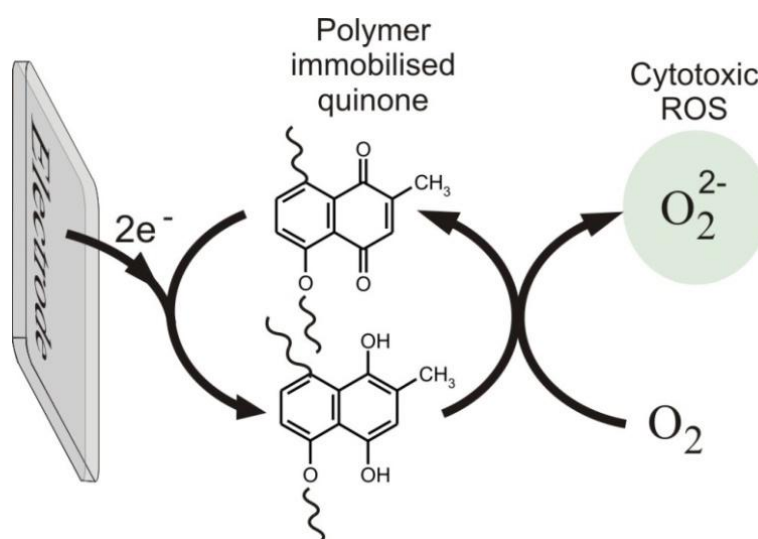

Scheme 6.2 The production of ROS from plumbagin.

substantial loss of RSH from the cell solution can be attributed to the plumbagins ability to act as a redox cycler, catalysing the reduction of the oxygen present in the solution to yield reactive oxygen species (ROS) as outlined in **Scheme 6.2**, which subsequently reacts with the glutathione present causing its depletion [9-11].

6.3.2. Plumbagin as an ROS Generator

The ability of the poly-plumbagin film to produce ROS was examined using a spectrophotometric technique that relied upon using Ellman's reagent to monitor the glutathione concentrations as the film was redox cycled to produce ROS. The poly-plumbagin modified glassy carbon electrodes were placed into a solution containing glutathione (167μM) and were held at a reduction potential of -1.2V for 5 and 10 minutes to produce ROS. An aliquot of the electrolysis solution was then reacted with a solution of the Ellmans reagent allowing the glutathione concentration to be determined spectrophotometrically *via* pre constructed calibration graph as discussed in chapter 1. The glutathione concentration was seen to decrease by 56.9% and 88.9% respectively for the 5 and 10 minute time intervals compared to the no change in glutathione concentration that was seen for the control solution (modified electrode placed in a glutathione solution for 10 minutes with no potential applied). This confirms that the glutathione concentration is decreasing as a result of the poly-plumbagin film being able to catalyse the production of ROS rather than its nucleophilic addition onto the film.

Further work was done to assess the ability of the poly-plumbagin film to produce ROS, cyclic voltammograms detailing the response of the plumbagin modified glassy carbon electrode in buffer solution in the presence and absence of oxygen are detailed in **Figure 6.4.**. The magnitude of the quinone reduction peak is significantly larger in the scan carried out in oxygen than what it is in the absence of oxygen and can be attributed to the catalytic reduction of oxygen by the electro-reduced quinone. The polymer film is
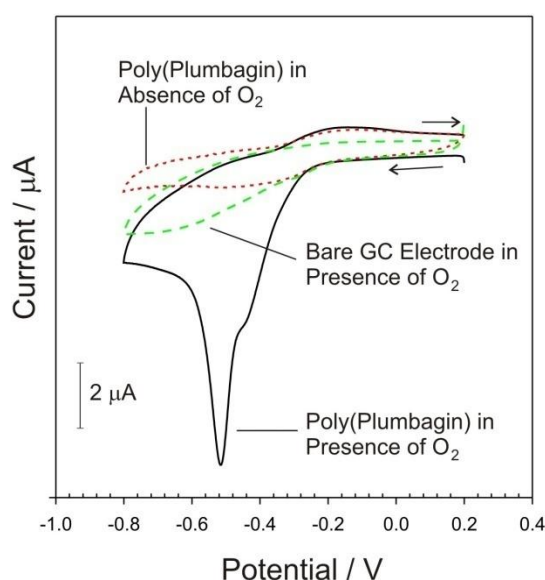
Figure 6.4. Cyclic voltammograms detailing the response of a glassy carbon electrode in the presence of oxygen (green dashed line) and a plumbagin modified glassy carbon electrode in the presence (black solid line) and absence (red dashed line) of oxygen.

clearly able to catalyse the reduction of oxygen. This has many possible uses, primarily the prevention of electrode fouling, but the films instability, particularly in the presence of glutathione inevitably compromise the effectiveness the films ability to generate ROS and would therefore limits its use within biological sensors.

The ability of plumbagin to act as a ROS generator was assessed further by looking at the performance of the monomer. Cyclic voltammograms detailing the response of plumbagin (0.8mM, pH 7) at a glassy carbon electrode in the presence and absence of oxygen are detailed in **Figure 6.5** Upon scanning towards negative potentials, the quinone is reduced (-0.28V) with the corresponding oxidation process being observed at -0.03V. In the presence of oxygen, the magnitude of the reduction peak is significantly increased compared to the peaks obtained in a solution degassed with nitrogen. This confirms that, like the polymer, the monomer is capable of catalysing the reduction of oxygen.
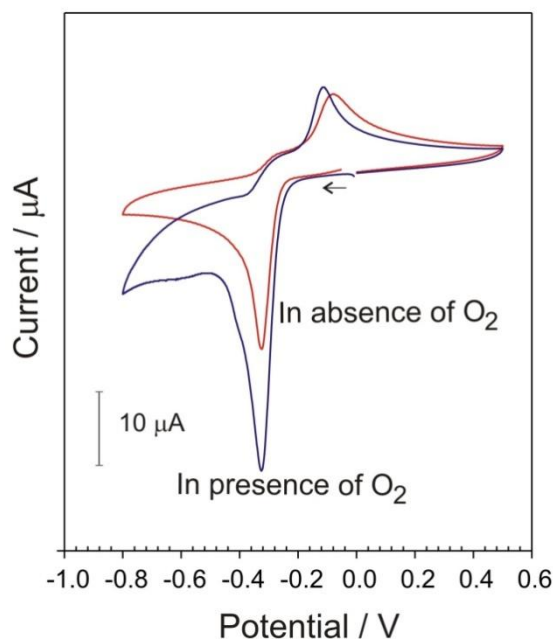
Figure 6.5 Cyclic voltammograms detailing the responseof a glassy carbon electrode to plumbagin (0.8mM pH 7) in the presence and absence of oxygen.

To test the effectiveness of plumbagin as an interfacial ROS generator a novel evaluation strategy was designed in which the interfacial concentration of an anti-oxidant probe would be used to estimate the production of ROS. Ascorbic acid served as a model probe as its free-radical scavenging properties are well established [12]. It also possesses the key advantage of having a well defined redox signature which is sufficiently distinct from that of plumbagin allowing its unambiguous quantification [13-14]. It was hypothesised that the ROS generated as a consequence of the electrochemically induced plumbagin redox cycling would react with the ascorbic acid (converting it to the electrochemically invisible de-hydroascorbic acid) and thereby leading to a visible decrease in the ascorbic acid within the solution. The

advantage of this approach was that the decrease in concentration would directly reflect the production of ROS at the electrode interface. Five repetitive scan cyclic voltammograms detailing the response observed at a glassy carbon electrode to plumbagin (0.8mM) and ascorbic acid (0.4mM) in pH7 buffer under nitrogen flow are highlighted in **Figure 6.6 A**. Three distinct processes can be observed, the redox cycling of the quinone component of plumbagin (at -0.28V and -0.03V respectively) and the irreversible oxidation of the ascorbic acid at +0.37V. The scans can be seen to be effectively stable but there is a gradual decrease in the magnitude of the ascorbate peak which can be attributed to the irreversible oxidation causing a small but cumulative depletion of ascorbic acid at the electrode surface with the scan rate being too fast to allow complete diffusional replenishment of the interfacial concentration between cycles. The same experiment was then repeated in the presence of oxygen and the corresponding voltammograms are detailed in **Figure 6.6 B**. It can be seen that the magnitude of the quinone reduction peak process increases markedly and the ascorbic acid peak diminishes much more rapidly than that observed under the degassed conditions. Given the near identical conditions, bar the presence of oxygen, it is possible to draw the conclusion that the electro-generation of ROS species at the interface results in the marked depletion of the ascorbic acid probe.
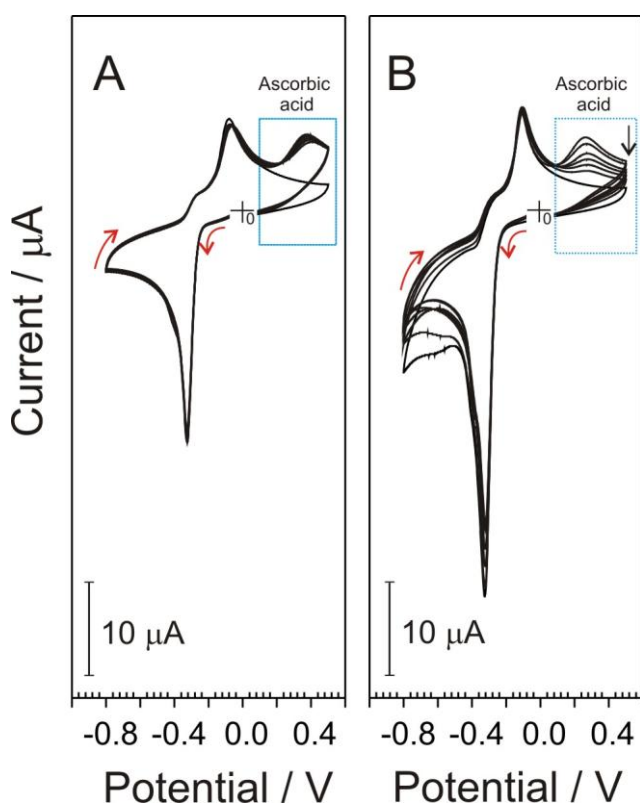
Figure 6.6 Cyclic voltammograms detailing the response of repetitive scanning of plumbagin and ascorbic acid (0.8 and 0.4 mM respectively) in the absence (A) and presence (B) of oxygen.

A more quantitative appraisal of the effect of repetitive cycle number on the removal of ascorbic acid is shown in **Figure 6.7**.
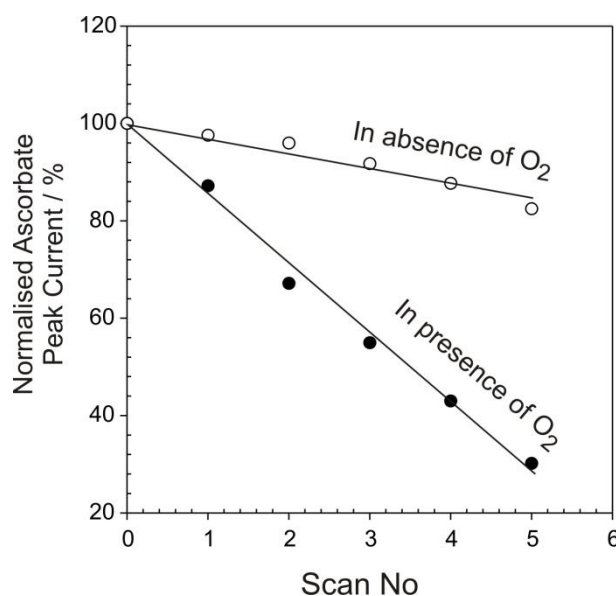
Figure 6.7 Graph illustrating the removal of ascorbic acid with increasing scan number in the absence and presence of oxygen.

There is a depletion of ascorbic acid under degassed conditions but this can be ascribed to the diffusional artefact noted earlier and results in a 10% decrease over the experiment lifetime. In contrast, in the presence of oxygen the interfacial ascorbic acid is reduced by 70% and indicates clearly the efficacy of plumbagin redox cycling as a means of generating ROS.

6.4. Conclusions

The ability of poly-plumbagin film to facilitate the reagentless sensing of sulphydryl thiols has been assessed. The polymer has limited stability in the presence of RSH so its use for sensing purposes is invalid. It was however found that the plumbagin was capable of acting as a redox cycler catalysing the reduction of oxygen to produce ROS. Both the plumbagin monomer and polymer are able to generate ROS at the electrode interface and although the polymer is limited in terms of film thickness it has the potential to be used as a smart material to prevent electrode fouling within devices opening up a new avenue for exploration and adaptation.

6.5. References

[1]   G. Geersing, D.B. Toll, K.J.M. Janssen, R. Oudega, M.J.C. Blikman, R. Wijland, K.M.K. de Vooght, A.W. Hoes and K.G.M. Moons, Diagnostic Accuracy and User-Friendliness of 5 Point-of-Care D-Dimer Tests for the Exclusion of Deep Vein Thrombosis. Clinical Chemistry, 56 (2010) 1758-1566

[2]   P. St-Louis, Status of point-of-care testing: promise, realities, and possibilities. Clinical Biochemistry, 33 (2000) 427-440

[3]   K.A. Marx, T.A. Zhou, D. McIntosh and S.J. Braunhut, Electropolymerized tyrosine-based thin films: Selective cell binding via peptide recognition to novel electropolymerized biomimetic tyrosine RGDY films. Analytical Biochemistry, 384 (2009) 86-95

[4]   M. Ferreira, H. Varela, R.M. Torresi and G. Tremiliosi, Electrode passivation caused by polymerization of different phenolic compounds. Electrochimica Acta, 52 (2006) 434-442

[5]   M. Marti Villalba, V.J. Litchfield, R.B. Smith, A.M. Franklin, N.S. Lawrence and J. Davis, Rapid assesment of the latent hazard posed by dissolved mercaptans within aqueous effluent. Journal of Hazardous Materials, 154 (2008), 444-450

[6]   A. Digga, S. Gracheva, C. Livingstone and J. Davis, Potentiometric detection of thiols: a mechanistic evaluation of quinone-thiol interactions. Electrochemistry Comunications, 5 (2003) 732-736

[7]   I.A. Solsona, R.B. Smith, C. Livingstone and J. Davis, Metabolic mimics: Thiol responsive drug release. Journal of Colloid and Interface Science, 302 (2006) 698-701

[8]   R.B. Smith, C. Canton, N.S. Lawrence, C. Livingstone, J. Davis, Molecular anchors— mimicking metabolic processes in thiol analysis. New Journal of Chemistry, 30 (2006) 1718-1724

[9]   P. Babula, V. Adam, R. Kizek, Z. Sladky and L. Havel, Naphthoquinones as allelochemical triggers of programmed cell death. Environmental and Experimental Botany, 65 (2009) 330-337

[10]   R.J. McKallip, C. Lombard, J. Sun and R. Ramakrishnan, Plumbagin-induced apoptosis in lymphocytes is mediated through increased reactive oxygen species production, upregulation of Fas and activation of the caspase cascade. Toxicology and Applied Pharmacology, 247 (2010) 41-52

[11]   C. Ortiz, L. Caja, P. Sancho, E. Bertran and I. Fabregat, Inhibition of the EGF receptor blocks autocrine growth and increases the cytotoxic effects of doxorubicin in rat hepatoma cells: Role of reactive oxygen species production and glutathione depletion. Biochemical Pharmacology, 75 (2008) 1935-1945

[12]   D. Bagchi, A. Gard, R.L. Krohn et al, Oxygen free radical scavenging abilities of vitamin C and E, and a grape seed proanthocyanidin extract in vitro. Research Communications in Molecular Pathology and Pharmacology, 95 (1997) 179-189

[13]   J. Wu, J.Suls and W. Sansen, Amperometric determination of ascorbic acid on screen-printing ruthenium dioxide electrode. Electrochemistry Communications, 2 (2000) 90-33

[14]   N.S. Lawrence, E.L. Beckett, J. Davis and R.G. Compton, Advances in the voltammetric analysis of small biologically relevant compounds. Analytical Biochemistry, 303 (2002) 1-16

Chapter 7

Electrochemically Initiated Thiol Detection

Chapter 7

Electrochemically Initiated Thiol Detection

Abstract

The ability to use electrochemically generated quinone intermediates to facilitate the detection of sulphydryl thiols is discussed. The electrochemical properties of a range of suitable derivatives were examined and their ability to react with sulphydryl thiols assessed. It was found that the chemical structure of the derivative could be selected such that the signal responsible for the detection of the thiol would occur at a potential where there would be no interferences seen from the direct oxidation of the thiol or the other electroactive components present within the sample. The structures of the derivatives used were also chosen so that they would be able to undergo electrochemical polymerisation. It was envisaged that the films produced would create modified electrodes that would facilitate reagentless thiol sensing. The electrochemical properties and reactivities of the monomers and polymers were studied in an attempt to prove the applicability of using this approach for the reagentless and interference-free analysis of sulphydryl thiols.

7.1. Introduction

The significance of techniques that can enable interference-free and reagentless sensing of sulphydryl thiols has been discussed previously within this thesis and numerous strategies have been presented and critically assessed in an attempt to overcome the issues associated with the development of these methods. The work described in this chapter looks at an alternative route that could possibly overcome these analytical challenges. The use of electrochemically generated quinone type intermediates to facilitate thiol detection is discussed, with the performance of the monomer and the polymer modified electrode being assessed.

The route exploited here looks at utilising derivatives that can be electrochemically manipulated to produce quinone type intermediates. These intermediates can act as labels to assist thiol analysis as they are able to undergo a nucleophilic addition with the thiol moiety *via* the same reaction route previously described elsewhere in this thesis [1-3].
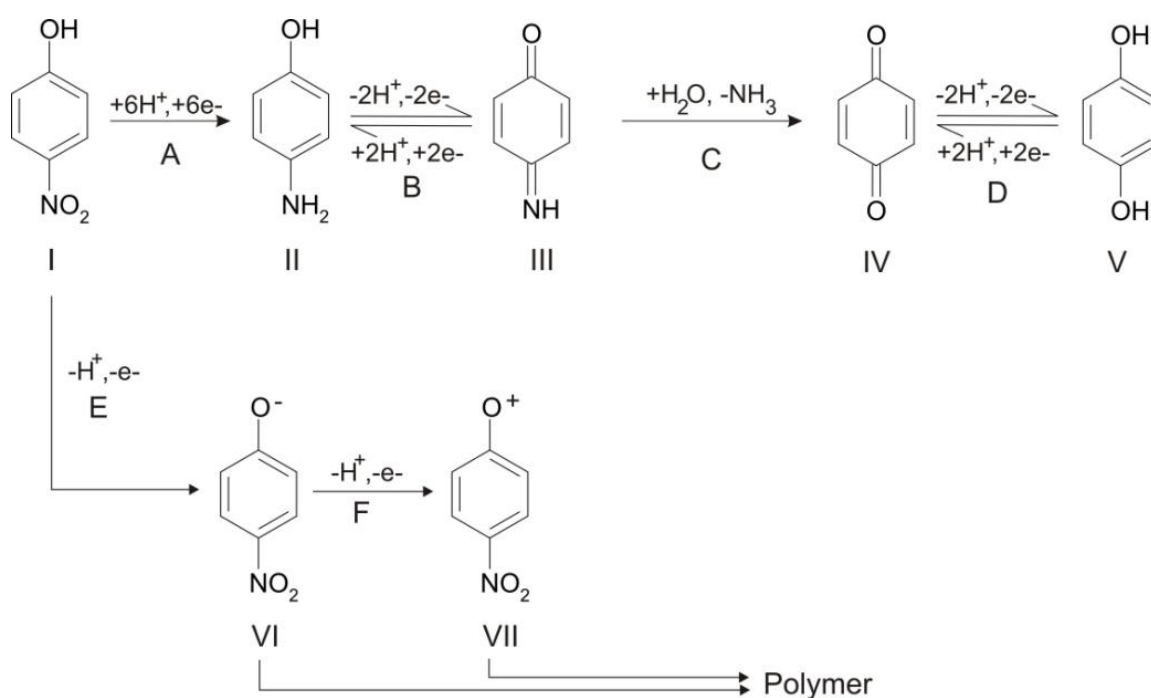
Scheme 7.1. Proposed electrochemistry of 4-Nitrophenol.

The approach advocated in this instance is highlighted in **Scheme 7.1**, where 4-nitrophenol (4NP) (**Scheme 7.1 I**) is used as the derivative. The structure of the derivatives selected is such that a hydroxyl group (OH) and either a nitro-group (NO_2)

or an amine (NH_2) is present in a 1,4 configuration (**Scheme 7.1** structures **I** and **II** respectively). These derivatives are, in this state, unreactive to the thiol species and so electrochemical and/or chemical manipulation of the compounds must take place in order to generate the quinone type intermediates that can label the thiol. This will either be the quinone/imine type intermediate (**Scheme 7.1 III**), formed during the electrochemical oxidation of the derivative (**Scheme 7.1 B**), or it will be the conventional quinone type intermediate (**Scheme 7.1 IV**), which is formed when quinone/imine intermediate (**Scheme 7.1 III**) is hydrolysised (**Scheme 7.1 C**). In the case of 4NP, a reduction (**Scheme 7.1 A**) followed by an oxidation (**Scheme 7.1 B**) is necessary to yield the responsive labels [4], but for all of the derivatives selected it is possible to control the production of the thiol label at the electrode surface [5-7]. Both of the quinone type intermediates produced, (**Scheme 7.1 III**) and (**Scheme 7.1 IV**) are able to redox cyclise and react with sulphydryl thiols *via* the pre-described nucleophilic addition route as illustrated in **Scheme 7.2** for the quinone/imine type intermediate (**III**). This reaction should result in the intermediate being chemically reduced (**Scheme 7.2 II-SR**) and subsequently re-oxidised at the electrode amplifying the oxidative current recorded (**Scheme 7.2 III-SR**). This enhanced response can then be used to determine the concentration of the sulphydryl thiol present.
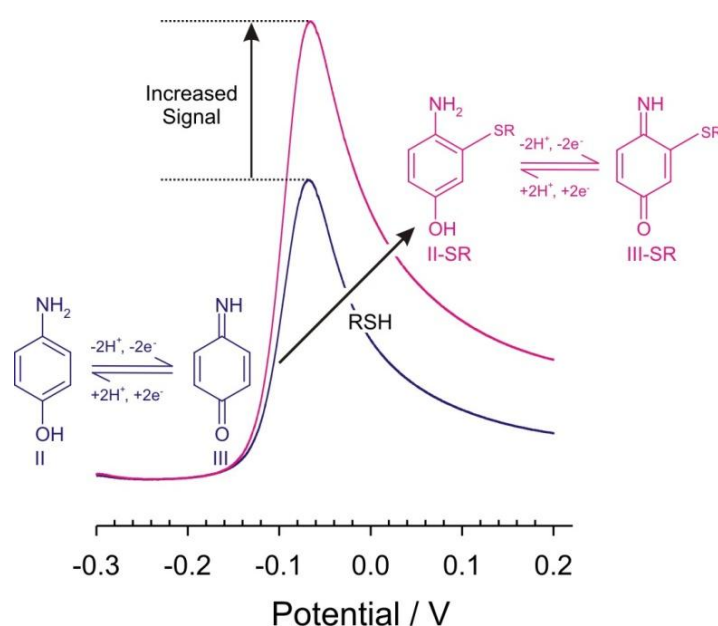
Scheme 7.2 Proposed reaction pathway leading to thiol (RSH) analysis.

It was envisaged that by varying the chemical structure of the derivatives used that the potential of the quinone/imine type redox couple would shift to more negative

values thus allowing the analysis of the thiol species without any interferences being seen from the direct oxidation of the thiol and the oxidation of the other electroactive components present within the sample medium. Other studies have shown the applicability of this kind of approach for the detection of sulphide and sulphydryl thiols within complex sample matrices [1-3]. The difference in this study is that the polymerisation of the most suitable derivative is examined and its ability to detect thiol species is investigated. All of the derivatives studied are able to undergo electrochemical polymerisation upon the imposition of an oxidative potential [4-5,9], as is highlighted in **Scheme 7.1** for the 4NP derivative. In this instance the imposition of the oxidative potential causes the oxidation of the phenolic group resulting in the formation of the nitrophenoxy radical (**Scheme 7.1 VI**), this can undergo a secondary oxidation the give the nitrophenoxy cation (**Scheme 7.1. VII**), both species are very reactive and can couple to give polymer films [4,8,10]. It was anticipated that the polymers formed would be stable at the electrode surface and although the structures of these polymers have not been fully elucidated it was envisaged that they would retain some of the same electrochemical characteristics and reactivities seen for the monomers, providing a route for the interference-free and reagentless analysis of sulphydryl thiols.
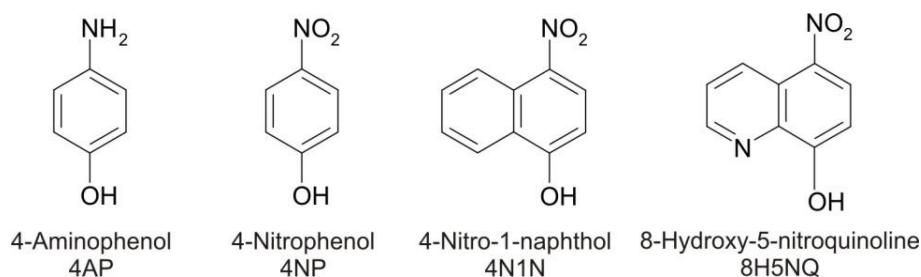
Figure 7.1 The structures of the derivatives studied

The electrochemical properties of a range of structurally suitable derivatives, highlighted in **Figure 7.1**, were assessed and the ability of the monomers and polymers to react with sulphydryl thiols, uric acid and ascorbic acid (primary sample interferants) [11-12] was investigated to assess the overall viability of the approach proposed.
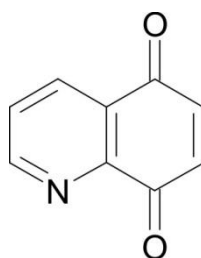
7.2. Experimental Details

7.2.1. Materials and Methods

All reagents were of the highest grade available, were used without further purification and unless stated otherwise were purchased from Sigma Aldrich (UK) or Alfa Aesar (UK). Solutions of 4-aminophenol, 4-nitrophenol, 4-nitro-1-naphthol, 8-hydroxy-5-nitroquinoline and quinoline-5,8-quinone (5mM) were prepared in methanol, protected from light prior to use and were diluted accordingly when required. Stock solutions of cysteine, homocysteine, glutathione and ascorbic acid (typically 10mM) were prepared in pH 7 Britton-Robinson buffer, the latter was also used throughout as the supporting electrolyte. Solutions of uric acid (typically 10mM) were prepared in 0.1M sodium hydroxide. Electrochemical measurements were conducted using a µAutolab computer controlled potentiostat (Eco-Chemie, Utrecht, The Netherlands) using a three electrode configuration consisting of a glassy carbon working electrode (3 mm diameter, BAS Technicol, UK), a platinum wire counter electrode and a 3M NaCl Ag | AgCl half cell reference electrode (BAS Technicol, UK). All solutions were degassed with nitrogen prior to use and unless specified otherwise – the scan rate for all experiments was 50mV/s and all measurements were conducted at $22^{o}C \pm 2^{o}C$. NMR spectra were measured on a JEOL (Welwyn Garden City, UK) ECX 400 MHz spectrometer. Chemical shifts are reported in parts per million (ppm) downfield from tetramethylsilane (TMS).

7.2.2. Preparation of Quinoline-5,8-quinone

Quinoline-5,8-quinone (**Figure 7.2**) was prepared following the methods, with modifications, previously described [13-14]. A solution of 8-hydroxyquinoline (0.91g, 6.3mM, 1EQ) in 15mls of

Figure 7.2
Quinoline-5,8-Quinone

acetonitrile:water (2:1) was added dropwise to a cooled solution of bis(trifluoroacetoxy)iodobenzene (4.964g, 11.5 mM, 1.8EQ) in 15mls of acetonitrile:water (2:1). The reaction mixture was stirred at 4 °C for 3 hours. Water

(30ml) was then added to the reaction mixture and the aqueous layer was extracted with dichloromethane (3x100mls). The combined organic fractions were washed with water (3x100mls), brine (2x50mls) and water (100ml), it was then dried over sodium sulphate and was concentrated *in vacuo* to give an orange solid. The crude product was washed with petroleum ether 40-60, filtered and dried to give quinoline-5,8-quinone as a golden brown powder (0.56g, 56.1%).
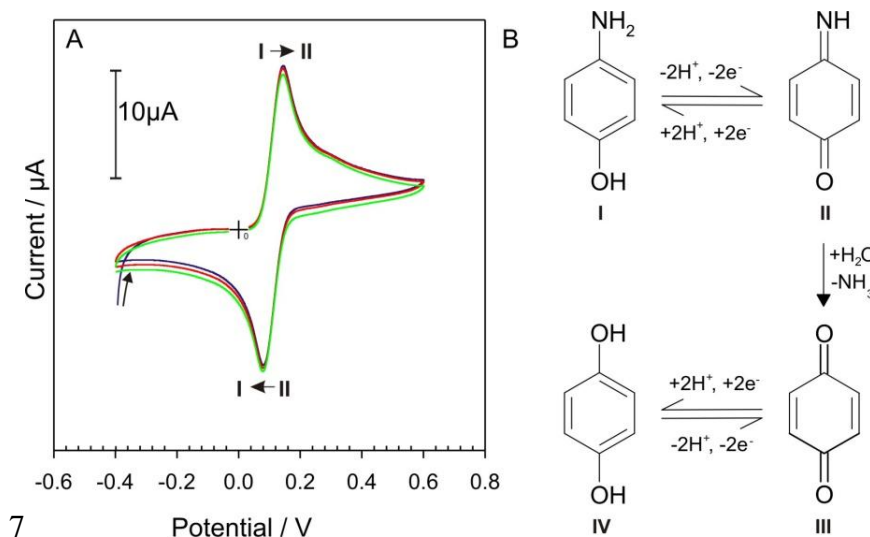
NMR data

^{1}H in CDCl$_3$: 9.05 (1H, dd), 8.42 (1H, dd), 7.70 (1H, dd), 7.24 (residual solvent peak), 7.16 (1H, d), 7.07 (1H, d)

7.3. Results and Discussion

7.3.1. Monomer Studies

Figure 7.3 shows the cyclic voltammogram (**A**) for the response of a glassy carbon electrode to 4-Aminophenol (4AP) (0.455mM, pH 7) along with a schematic (**B**) of the proposed reaction pathway.


Figure 7.3 Cyclic voltammogram (A) and schematic (B) for the electrochemistry of -Aminophenol (0.455mM, pH7).

The oxidation of the 4AP (**Figure 7.3 I**) and the corresponding reduction of the quinoine/imine intermediate (**Figure 7.3 II**) can be observed at +0.152V and

+0.079V respectively and is in line with the electrochemistry observed by other authors [5-6]. These peaks have been attributed to this redox couple (**Figure 7.3 I→II**) opposed to the quinone intermediate redox couple (**Figure 7.3 III→IV**) because the duration of the experiment was deemed as being insufficient to allow the hydrolysis of the quinone/imine intermediate and so no quinone intermediate (**Figure 7.3 III**) has been produced. Repetitive cycling of the solution does not alter the voltammetric profile obtained thus confirming the stability of the derivative studied.

Figure 7.4 shows the cyclic voltammogram for the response of a glassy carbon electrode to 4-nitrophenol (4NP) (0.455mM, pH 7). The profile shape observed is consistent with the pathway proposed in **Scheme 7.1**. On initiating the scan, in the anodic direction, no redox processes are observed as the quinone/imine intermediate has not yet been generated. During the reverse scan, going towards negative potentials, an irreversible reduction process can be observed at -0.781V. This can be attributed to the six proton, six electron reduction of the nitro group to an amine (**Scheme 7.1 I→II**). *In-situ* generated 4-aminophenol is now present at the electrode/solution interface, this is confirmed by the emergence of the quinone/imine redox couple (**Scheme 7.1 II→III**), with the oxidation and corresponding reduction being observed at +0.123V and +0.076V respectively.
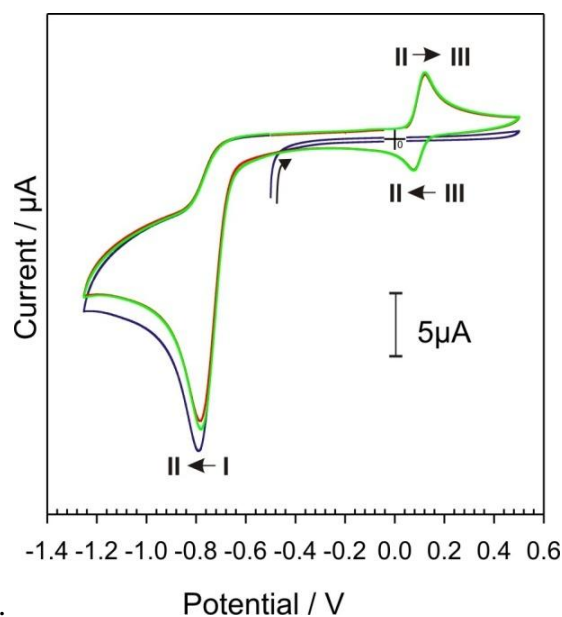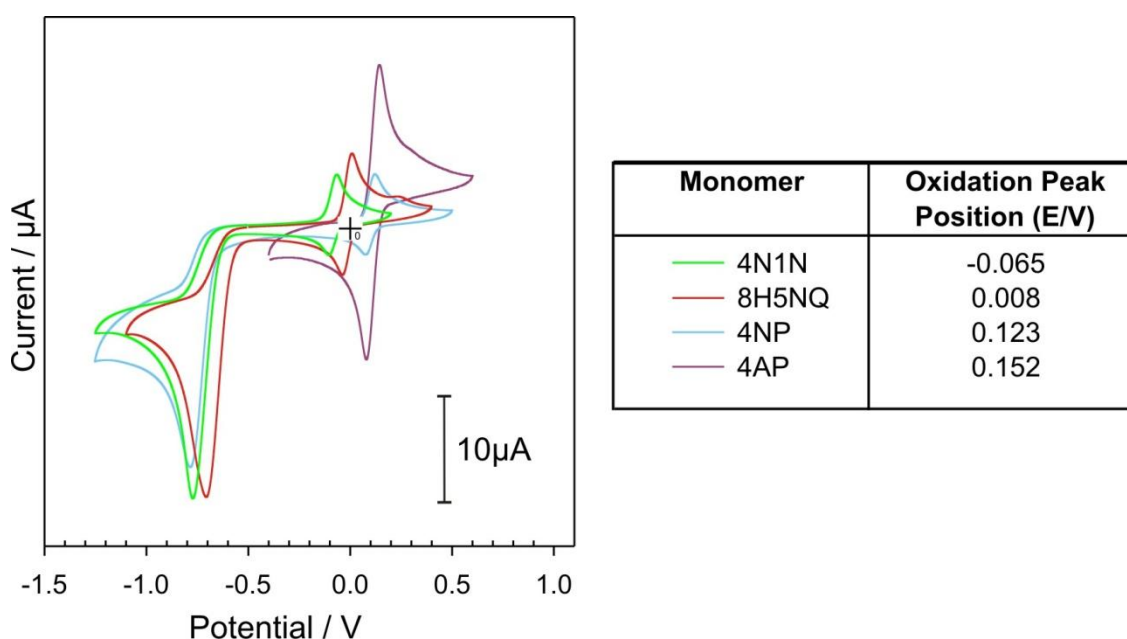

Figure 7.4 Cyclic voltammogram for the electrochemistry of 4-Nitrophenol (0.455mM, pH7).

The cyclic voltammograms detailing the response of a glassy carbon electrode to 4-nitro-1-naphthol (4N1N) and 8-hydroxy-5-nitroquinoline (8H5NQ) (0.455mM,

pH 7) are analogous to the one observed for 4NP (**Figure 7.4**) in that no quinone/imine redox chemistry is observed until the reduction of the nitro group takes place to generate the derivative with the amine functionality present. Once the amine form of the intermediate is present redox cycling can occur to give the quinone/imine derivative which should be able to react with sulphydryl thiols to facilitate their detection. Although the electrochemical profiles observed for the derivatives are essentially the same, apart from the fact that no reduction step needed for the 4AP derivative, the changes in the chemical structure of the monomer alters the potential at which the electrochemical processes occur.

Figure 7.5 shows the cyclic voltammograms for all of the derivatives studied (0.455 mM, pH 7).


Monomer	Oxidation Peak Position (E/V)
4N1N	-0.065
8H5NQ	0.008
4NP	0.123
4AP	0.152

Figure 7.5 Cyclic voltammogram showing the overlapping electrochemistry of 4N1N (green), 8H5N (red), 4NP (blue) and 4AP (purple) (0.455mM, pH7). The table insert shows the position of the quinone/imine oxidation peak.

The differences in the profiles, which are the changes in the potentials observed for the reduction of the nitro group and the redox cycling of the quinone/imine type intermediate, are clearly visible. The difference in the position of the redox couple, with varying the chemical structure of the derivative, is of particular interest as it is this couple that will be responsible for allowing the thiol species to be detected and so if the potential window is moved to more negative values, away from the potentials that can cause the direct oxidation of the thiols and the oxidation of the

other electroactive components present within the sample, it can be used as a route to provide interference-free analysis. The table insert in **Figure 7.5** summarises the differences in the potentials observed for the oxidation of the quinone/imine intermediate with the ease of oxidation of the derivative or *in-situ* generated intermediate being summarised as 4N1N < 8H5N < 4NP < 4AP. This reactivity series can be ascribed to the addition of the pyridine and benzene rings which increases the reactivity of the derivative, decreasing its stability and allowing the two electron, two proton oxidation to be brought about more easily. The lowest potential required to oxidise the quinone/imine intermediate was observed for 4N1N, with the lowest potential window for thiol detection, this derivative has the greatest capacity to provide interference-free analysis and so all of the further investigations were focussed primarily on this molecule. It should be noted that when investigating the quinone/imine redox couple it was found that the peak separations, for all of the derivatives, are larger than expected for a conventional two electron, two hydrogen redox couple, this indicates that these couples have some degree of irreversibility which is consistent with the results found by other authors studying these types of systems [15].

Figure 7.6 shows the voltammetric profiles for the oxidation of: the quinone/imine intermediate of the 4N1N derivative (0.455mM, pH7) (after nitro group reduction has been achieved by the application of a reducing potential of -0.8V for 5 seconds), uric acid (0.476mM, pH7), ascorbic acid (0.476mM, pH7) and a solution containing an equal mix of the latter two substances (uric acid, 0.455mM, pH7 and ascorbic acid 0.455mM, pH7). The oxidation of the
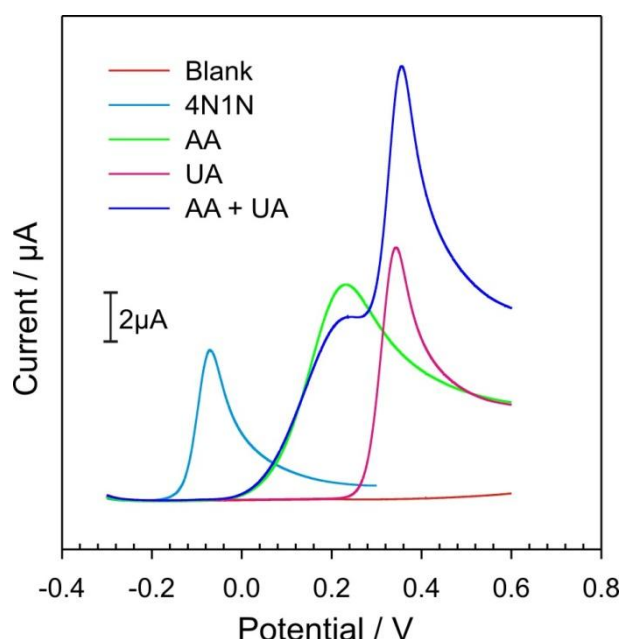
Figure 7.6 Voltammograms comparing electrochemistry of the 4N1N derivative (0.455mM, pH7) with a blank, ascorbic acid (0.476mM, pH7), uric acid (0.476mM, pH7) and a mixture of the latter two (both at 0.455mM, pH7).

quinone/imine type intermediate is observed at -0.074V and the oxidation of the ascorbic acid to dehydroascorbic acid and uric acid to 5-ureidohydantoin can be seen at +0.231V and +0.343V respectively. The position of these oxidation potentials mean that there will be no overlap in the signal generated for the label if the sample contains ascorbic acid and uric acid. The previously described experiment was repeated for 4N1N (0.435mM, pH7) in the presence of ascorbic acid (0.435mM, pH7), uric acid (0.435mM) and 4N1N (0.417mM, pH7) in the presence of a solution containing an equal mix of ascorbic acid and uric acid (both 0.417mM, pH7) and no changes in the oxidation peak (peak height or position) for the quinone/imine intermediate was observed confirming that no interference will be observed from these species when using 4N1N as the thiol label.

The possibility of using the 4N1N derivative as a substance that can be electrochemically manipulated to generate a label for the analysis of sulphydryl thiols was subsequently examined. **Figure 7.7** shows the voltammograms obtained for the oxidation of the electrochemically generated reduced form of the derivative (0.455mM, pH7), generated by the application of a reducing potential of -0.8V for a period of 5 seconds, in the presence of increasing amounts of cysteine (45μM aliquots, 0-450μM, pH7). The calibration data for all of the thiols: cysteine, homocysteine and glutathione are displayed in the insert within **Figure 7.7**.
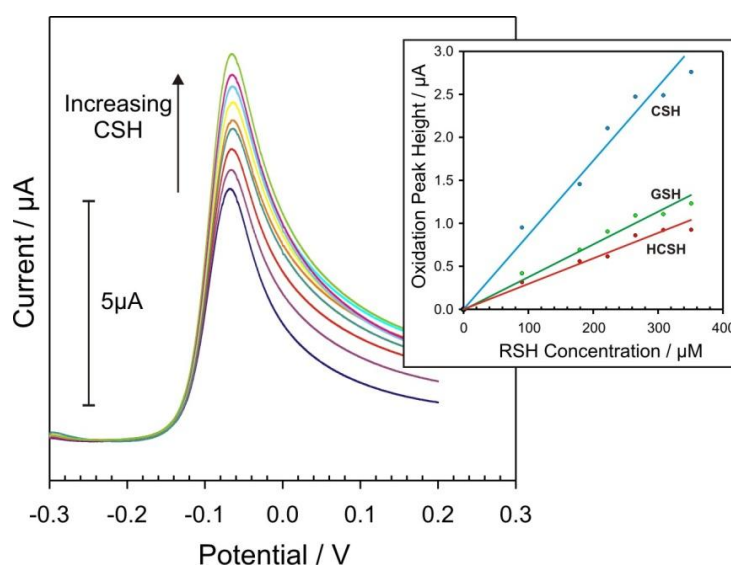
Figure 7.7 The voltammograms for the oxidation of the electrochemically generated reduced form of the 4N1N derivative (0.455mM, pH7), generated by the application of a reducing potential of -0.8V for a period of 5 seconds prior to scanning, in the presence of increasing amounts of cysteine (45μM aliquots, 0-450μM, pH7). Insert: The calibration data for all of the thiols under study: cysteine, homocysteine and glutathione.

The height of the oxidation peak for the quinone/imine intermediate, as expected, was found to increase on increasing the amount of thiol present (**Figure 7.7**). This can be attributed to the electrochemically generated quinone/imine intermediate undergoing a nucleophilic addition with the thiol species, this chemically reduces the intermediate which is then re-oxidised at the electrode surface causing an increase in the oxidative current recorded, therefore increasing the height of the peak observed, which was found to be the case for all of the thiols studied (**Figure 7.1 Insert**). This behaviour was found to be linear and characteristic for all of the derivatives studied, illustrating the generic nature of the approach, with the voltammetric trace observed in the presence of RSH being similar to that shown in **Figure 7.7** for the 4N1N derivative, with the only variation being the position of the oxidation peak due to the previously described structural differences of the molecules. The fact that only one oxidation peak is observed on the voltammogram confirms our initial assumption that only the quinone/imine type intermediate is being formed and that the quinone intermediate is not present. If the quinone intermediate was formed, then in the presence of cysteine we would expect to see a new oxidation peak emerging for the redox chemistry of the cyclised quinone-thiol conjugate as was observed for the quinone analogues of the derivatives studied: benzoquinone, naphthoquinone and quinonline-5,8-quinone. The fact that these new redox processes aren't emerging upon the addition of the thiol moiety also indicates that the nucleophilic addition between the electrochemically generated quinone/imine intermediate and the sulphydryl thiol species is occuring at the 3 position on the intermediate opposed to the 2 position as indicated in **Figure 7.8**.
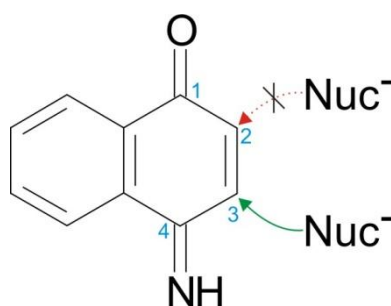
Figure 7.8 The favoured site of nucleophilic (Nuc-) attack on the quinone/imine intermediate form of the 4N1N derivative.

If the attack was occurring at the 2 position then cyclisation of the newly formed conjugate would be possible and so the extra oxidation peak would be recorded on the voltammogram. This favoured reaction pathway may be due to the

fact that the formation of the quinone enolate on the quinone/imine intermediate is more stable than the formation of the imine enolate. This is because the oxygen atom is more electronegative than the nitrogen atom and so stabilises the negative charge on the enolate more effectively, thus making thiol addition more favourable at the 3 position.

The applicability of this approach for the interference-free analysis of sulphydryl thiols was then assessed. The reaction of the electrochemically generated quinone/imine intermediate of the 4N1N derivative (0.444mM, pH7) to sulphydryl thiols (0.222mM, pH7) was carried out in the presence of increasing amounts of ascorbic acid (88μM aliquots, 0-0.816mM, pH7) or uric acid (88μM aliquots, 0-0.816mM, pH7). The characteristic increase in the peak height for the oxidation of the quinone/imine intermediate in the presence of cysteine was still observed in the presence of ascorbic acid and uric acid and the position of this peak was unaffected by the presence of these compounds. These factors indicate that the nucleophilic addition of the thiol species onto the derivative is unaffected by the presence of the other compounds within the sample, this confirms that a route that allows for the interference-free analysis of sulphydryl thiol species has been developed.

7.3.2. Polymer Studies

The derivatives used have the ability to undergo electrochemical polymerisation [4-5,8-10]. It was envisaged that the polymers formed during this process would be stable and that they could be manipulated in the same way as the monomers such that they could be used to determine sulphydryl thiols in a reagentless manor. As the 4N1N monomer provides the best route for interference-free thiol analysis its polymer was studied. **Figure 7.9**
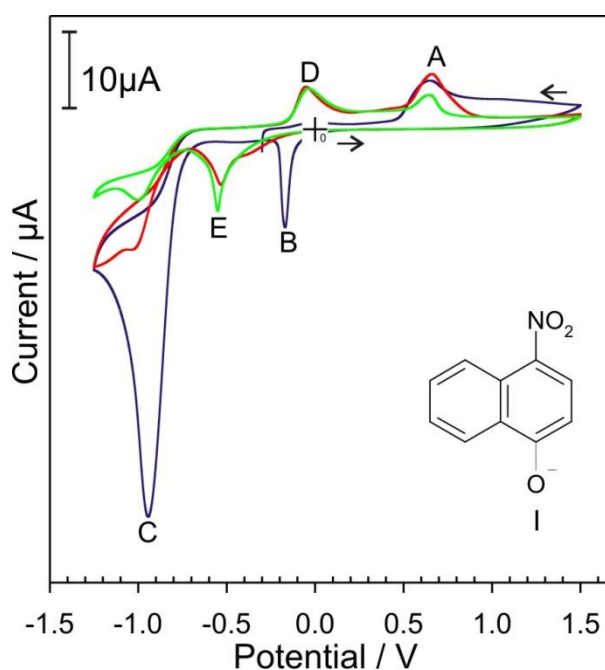
Figure 7.9 Repetitive scan cyclic voltammogram for 4N1N (0.455mM, pH7).
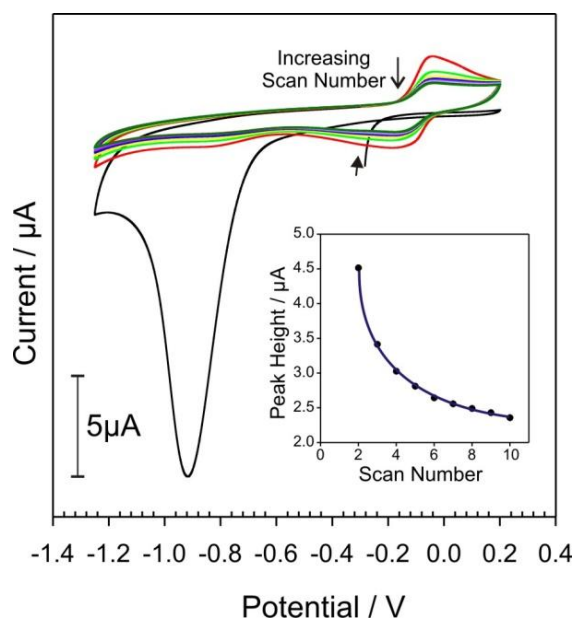
shows the repetitive scan cyclic voltammograms detailing the response of a glassy carbon electrode to 4N1N (0.455mM, pH7).

On initiating the scan, in the anodic direction, an irreversible oxidation peak can be seen at +0.603V (**Figure 7.9 A**), this corresponds to the oxidation of the phenol group on the 4N1N monomer to give the nitrophenoxy type radical (**Figure 7.9 I**) and the subsequent formation of the 4N1N polymer. This peak was found to decrease upon successive scanning which is consistent with the formation of a coherent polyphenol type film. Upon reversing the scan, in the cathodic direction, two irreversible reduction peaks can be seen at -0.197V and -0.883V (**Figure 7.9 B** and **C** respectively). The peak at -0.197V, is only present on the first scan and may therefore be attributed to the reduction of dimeric, oligomeric or polymeric material that is only loosely adhered to the electrode surface, with the successive scans leading to the development of a more coherent film that is resistant to reductive degradation. The peak at -0.883V can be attributed to the reduction of the nitro group to an amine on the 4N1N polymer. It should be noted that this reduction is now at a more negative potential than when the analogous process was observed for the monomer solution (reduction seen at -0.772V) which can be ascribed to the fact that the functional group is now surface immobilised within a polymer film, which along with the slowed electron transfer due to the presence of the polymer, means that a more negative potential is needed to cause the reduction. Upon successive scanning this peak was found to decrease, this is consistent with the formation of a 4N1N, phenol type polymer film, which is grown and passivates the electrode surface. The quinone/imine redox couple is, as expected, only present after the polymerisation of the monomer and the subsequent reduction of the nitro group within the film and in this instance the oxidation can be seen at -0.064V (**Figure 7.9 D**) with the corresponding reduction being seen as a shoulder on the reduction peak at -0.544V (**Figure 7.9 E**). The large peak separation seen for this redox couple can be attributed to the slowed electron transfer due to the presence of the 4N1N polymer film. The difference in the shape and potentials observed for the redox couple seen here, compared to that observed for the monomer solution, may be attributed to the fact that there may be a number of different types of redox centres present within the film depending on how the nitrophenoxy type radical coupling has occurred, and although the structure of the polymer may be complex and hasn't been fully elucidated, the fact that we see a redox

couple is encouraging as this may allow the thiol species to be detected. The peak heights for the quinon/imine type redox couple remain the same on successive cycling indicating the formation of a stable polymer film which is switching between the active (oxidised) and inactive (reduced) thiol label forms.

The 4N1N polymer was then investigated to see, firstly if it was stable and secondly if it could be electrochemically manipulated and subsequently reacted with sulphydryl thiols to facilitate their detection. A clean glassy carbon electrode was placed into a fresh solution of 4N1N (0.455mM, pH7) and was subjected to a single voltammetric cycle from 0V to +0.8V which was sufficient to allow the formation of the polymer at the electrode surface. The polymer modified electrode was then removed from the monomer solution, rinsed, to remove any loosely adhered material and placed within a


Figure 7.10 Repetitive scan cyclic voltammogram showing the electrochemical manipulation of the 4N1N polymer modified electrode (pH 7). Insert: Shows a plot of the quinone/imine oxidation peak height vs. scan number.

buffer solution devoid of monomer. This electrode was then cycled repetitively to give the voltammetric profiles observed in **Figure 7.10**.

The first scan, in the anodic direction, shows that no quinone/imine redox couple is seen until the nitro group on the polymer is reduced to the amine. This reduction is observed at -0.910V, which again is characteristic of a surface adsorbed species and slowed electron transfer. This reduction is only present on the first scan indicating that all of the nitro groups present on the polymer are reduced during this initial scan. The quinone/imine redox couple is now observed at – 0.039V and -0.187V, for the oxidation and reduction respectively, with the broad peaks being indicating the presence of the surface adsorbed redox couple. The peak heights for these redox processes were found to decrease on successive scanning until a stable plateau was reached, this is highlighted on the graph insert in **Figure 7.10** which

shows the quinone/imine oxidation peak height vs. scan number and is such because there is an initial loss of loosely adhered, oligomeric material from the electrode surface before a stable equilibrium is attained.

The 4N1N modified electrode was left with the quinone/imine intermediate in its oxidized form and was tested to see if it would react with sulphydryl thiols. **Figure 7.11** displays the cyclic voltammograms for the 4N1N polymer in the absence and presence of cysteine (**Figure 7.11 A**) and glutathione (**Figure 7.11 B**) (both at 88μM).
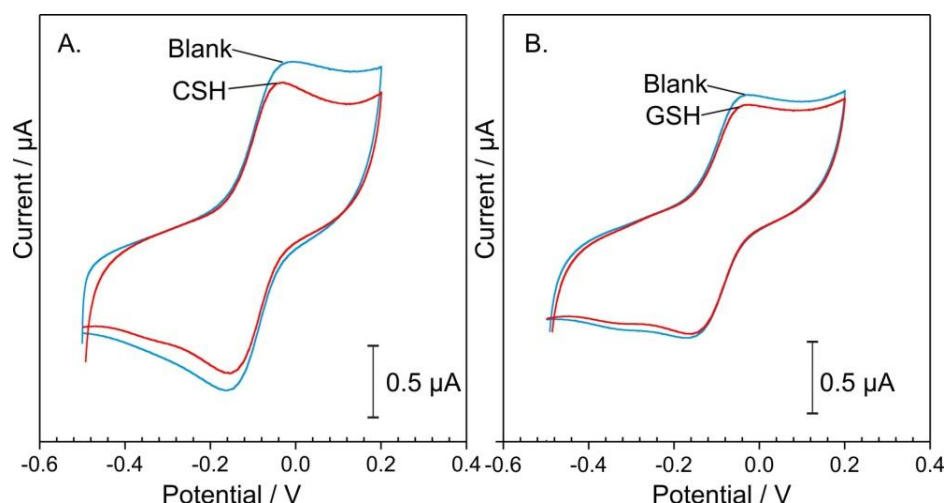
Figure 7.10 Cyclic voltammograms detailing the response of the 4N1N polymer in the presence and absence of cysteine (A) and Glutathione (B) (88μM).

A decrease in the oxidation peak for the quinone/imine intermediate can be seen which stands in contrast to the response observed by the monomer and suggests that the polymer degrades in the presence of the sulphydryl thiols resulting in a gradual loss of the redox group from the polymer surface. After the initial decrease in the redox processes, upon the further addition of thiol, the redox processes then remain the same height suggesting that the reactive portion of the polymer has been removed and although some of the polymer remains intact at the electrode surface its reactive site must be inaccessible to the thiol. The decrease in peak height is more pronounced for cysteine than glutathione and can be attributed to the size of the tripeptide limiting its ability to infiltrate and react with the film. These results suggest the applicability of this approach for reagentless sensing is flawed.

7.4. Conclusions

The routes presented here show that the electrochemically produced quinone/imine type derivatives provide a selective method for the interference-free analysis of sulphydryl thiols. The derivatives were electrochemically polymerised to give stable films, however the ability of these films to provide reagentless sensing of sulphydryl thiols was severely compromised as the films were seen to degrade in the presence of these species.

7.5. References

[1] P.C. White, N.S. Lawrence, J. Davis and R.G. Compton, Electrochemically initiated 1,4 addition: A versatile route to the determination of thiols. Analytica Chimica Acta, 447 (2001) 1-10

[2] N.S, Lawrence, J. Davis, L. Tiang et al, Selective determination of thiols: a novel electrochemical approach. Analyst, 125 (2000) 661-663

[3] N.S, Lawrence, J. Davis, L. Tiang et al, The electrochemical analog of the methylene blue reaction: A novel amperometric approach to the detection of hydrogen sulfide. Electroanalysis, 12 (2000) 1453-1460

[4] T. Alizaden, M.R. Ganjali, P. Norouzi et al, A novel high selective and sensitive para-nitrophenol voltammetric sensor, based on molecularly imprinted polymer-carbon paste based electrode. Talanta, 79 (2009) 1197-1203

[5] Y. Song. Theoretical studies on electrochemistry of p-aminophenol. Spectrochimica Acta Part A: Molecular and Biomolecular Spectroscopy, 67 (2007) 611-618

[6] B.N. Chandrashekar, B.E. Kumara Swamy, M. Pandurangachar et al, Electrochemical Investigations of 4-Aminohenol at CTAB Modified Carbon Paste Electrode: A Cyclic Voltammetric Technique. Analytical and Bioanalytical Electrochemistry, 3 (2011) 227-232

[7] M.M. Ghoneim, H.S. El-Desoky and M.M. Abdel-Galeil, Electrochemistry of the antibacterial and antifungal drug nitroxoline and its determination in bulk form, pharmaceutical formulation and human blood. Bioelectrochemistry, 80 (2011) 162-168

[8] P.C. Canizares, C. Saez, J. Lobato and M.A. Rodrigo, Electrochemical treatment of 4-nitrophenol containing aqueous wastes using boron doped diamond anodes. Industrial and Engineering Chemical Research, 43 (2003) 1944-1952

[9] D.L Franco, A.S. Afonso, L.F. Ferreira et al, Electrodes modified with polyaminophenols: Immobilzation of purines and pyrimidines. Polymer Engineering and Science, 48 (2008) 2043-2050

[10] X. Zhu, S. Shi, J. Wei et al, Electrochemical oxidation of p-substituted phenols using a boron doped diamond electrode. Environmental Science and Technology, 41 (2007) 6541-6546

[11] T.H. Huang, T. Kuwana and A. Warsinke, Analysis of thiols with tyrosinase modified carbon paste electrodes based on blocking of the substrate. Biosensors and Bioelectronics, 17 (2002) 1107-1113

[12] T. Inoue and J.R. Kirchoff, Electrochemical detection of thiols with coenzyme pyrroloquinoline quinone modified electrode. Analytical Chemistry, 72 (2000) 5755-5760

[13] C. Morin, T. Besset, J. Moutet, M. Fayolle, M. Brückner, D. Limosin, K. Becker and E. Davioud-Charvet, The aza-analogues of 1,4-naphthoquinones are potent substrates and inhibitors of plasmodial thioredoxin and glutathione reductases and of human erythrocyte glutathione reductase. Organic and Biomolecular Chemistry, 6 (2008) 2731-2742

[14] R. Barret and M. Daudon, Oxidation of phenols to quinones using bis(trifluoroacetosy)iodobenzene. Tetrahedron letters, 31 (1990) 4871-4872

[15] R.B. Smith, C. Canton, N.S. Lawrence, C. Livingstone and J. Davis, Molecular anchors—mimicking metabolic processes in thiol analysis. New Journal of Chemistry, 30 (2006) 1718-1724

Chapter 8

Quinones as Colorimetric Labels for Thiol Analysis

Chapter 8

Quinones as Colorimetric Labels for Thiol Analysis

Abstract

This chapter highlights the possibilty of exploiting the previously described nucleophilic addition reaction between thiol species and quinone derivatives as a route to provide the specific colorimetric detection of cysteine, homocysteine and glutathione. The interaction of a range of benzoquinone and naphthoquinone derivatives with the reduced sulphydryl thiols has been studied. It was hoped, in this instance, that different spectral properties would be observed for the starting material and the quinone-thiol conjugate and that this would allow the analysis of the thiol species involved in the reaction. It was found that 2,6-dimethylbenzoquione and the naphthoquinone-adamantane derivative (2-(adamantyl-1-carboxylic acid)-1,4-naphthoquinone ester) reacted in the proposed way with the sulphydryl thiol species, and that superior selectively was observed for cysteine and homocysteine respectively. The spectral properties of each of these labels were examined and the possibility of using these systems as specific colorimetric determinants of the appropriate sulphydryl thiol assessed. The possibility of using electrochemical methods to quantify the conjugates produced was also examined in an attempt to see if the sensitivity of the colorimetric approach could be enhanced.

8.1. Introduction

A range of techniques have been used for the qualitative and quantitative analysis of sulphydryl thiols including: high performance liquid chromatography (HPLC) [1-2], capillary electrophoresis (CE) [3], electrochemical detection [4-5], ultraviolet-visible detection [1-2] and fluorescent detection [6]. Colorimetric techniques based on visible spectrophotometry are becoming popular routes for analysis because they allow the analyte to be detected by the naked eye or by carrying out a simple spectrophotometric measurement. This method allows the analysis to be carried out quickly and without the need for expensive instrumentation, making it an even more attractive route for analysis. As cysteine, homocysteine and glutathione do not possess a native chromophore current colorimetric analysis relies on sample derivatisation with a colorimetric label [1-2].

Ellmans reagent (5,5'dithio-(2-nitrobenzoic acid)) is one of the most commonly used labels for the colorimetric detection of sulphydryl thiols, turning yellow in the presence of the thiol species due the release of 5-thio-2-nitrobenzoic acid. This reagent is very sensitive but its use is limited as discrimination between the different thiol species in not possible [7]. Indeed differentiation of these thiol species is extremely difficult given the structural similarities and analogous chemical reactivities of the thiol species [8], but it would clearly be beneficial due to the implications that changes in the levels of these individual molecules have in a number of clinical conditions. As such many research groups are trying to develop new methods that can facilitate their individual unambiguous detection. Although the current issue surrounding discrimination is difficult, methods that can differentiate between the individual thiol species have been developed, their use is however still limited due to the problems associated with their analytical set ups [9-11].

The work detailed within this chapter exploits the nucleophilic addition reaction between benzo/naphthoquinone derivatives and the sulphydryl thiol species in an attempt to find selective labels for each of the thiols under study. The basic reaction scheme should follow the same steps as indicated for the nucleophilic addition of the thiol species onto plumbagin as outlined in chapter 5.

Scheme 8.1 highlights the same reaction for 1,4-benzoquinone (**I**) with cysteine, homocysteine and glutathione. As described previously, the initial reaction product is the reduced form of the quinone-thiol conjugate (**II**), this is readily oxidized by either molecular oxygen or by the quinone starting material to give the oxidized quinone-thiol conjugate (**III**). It was hoped that the spectral properties of this newly formed conjugate would be different when compared to the starting quinone such that it would allow the thiol concentration to be determined. In the case of cysteine (**Scheme 8.1 a**) and homocysteine (**Scheme 8.1 b**) intramolecular cyclisation can occur to give secondary conjugates, (**IV**) and (**V**) respectively and it was envisaged that the altered conjugation of these secondary adducts would result in a further spectral change thus allowing cysteine and/or homocysteine to be determined and providing a route for the unambiguous determination of the thiol constituents within the sample *via* a multi-parametric approach. Based on this hypothesis a range of benzoquinone and naphthoquinone derivatives were examined. The derivatives that displayed the desired reaction characteristics were assessed further to see if there was any possibility of using this approach for the analysis of sulphydryl thiols.
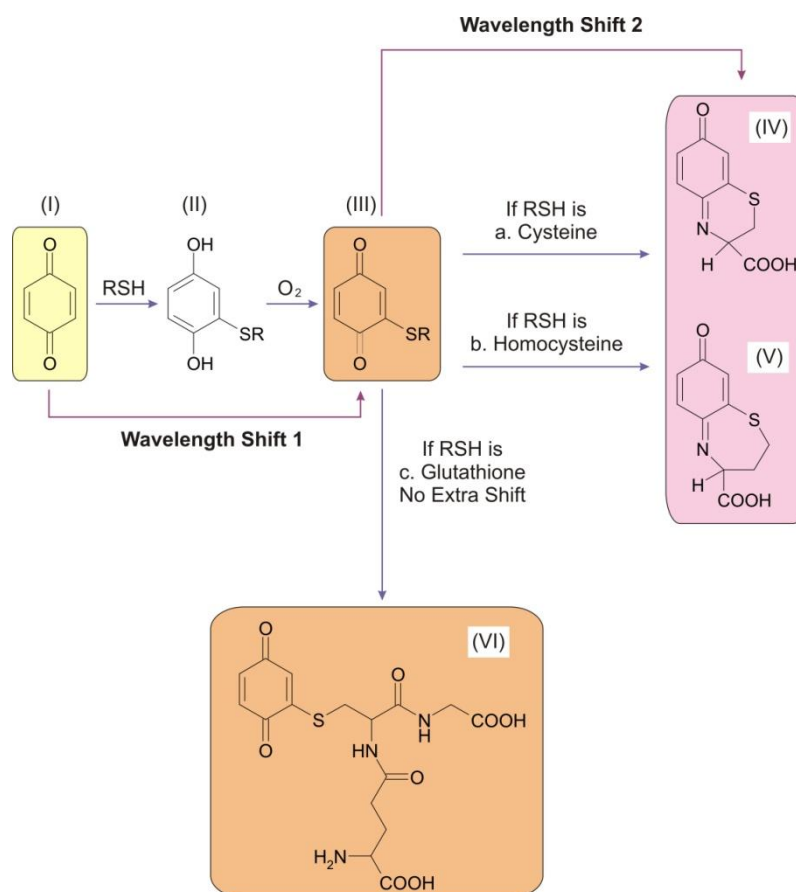
Scheme 8.1 Reaction pathway of quinones, in this case benzoquonone, with sulphydryl thiol species (RSH).

8.2. Experimental Details

8.2.1. Materials and Methods

All reagents were of the highest grade available, were used without further purification and unless stated otherwise were purchased from Sigma Aldrich (UK) or Alfa Aesar (UK). Benzo/naphthoquinone derivative solutions (typically 10mM) were prepared in methanol, protected from light and were diluted accordingly prior to use. Stock solutions of cysteine, homocystene and glutathione (typically 10mM) were prepared daily in pH 7 Britton-Robinson buffer. Creatinine, L-histidine, L-ascorbic acid, L-lysine, glycine (typically 1mM) and albumin (50mg/L) were prepared in pH 7 Britton-Robinson buffer and stock solutions of uric acid (1mM), dithiothreitol (5mM) and cystine (25mM) were prepared in 0.1M sodium hydroxide.

Spectral measurements were made on a Perkin Elmer Lambda 25 UV/VIS Spectrometer (Perkin Elmer Inc, USA) using a UV quartz cuvette with a sample volume of 0.7ml and a PTFE stopper (sigma Aldrich, UK). Electrochemical measurements were conducted using a μAutolab computer controlled potentiostat (Eco-Chemie, Utrecht, The Netherlands) using a three electrode configuration consisting of a glassy carbon working electrode (3 mm diameter, BAS Technicol, UK), a platinum wire counter electrode and a 3M NaCl Ag | AgCl half cell reference electrode (BAS Technicol, UK). In the case of the latter work for this chapter (centrifugal filter electrochemistry) an electrode assembly consisting of a plasma treated screen printed carbon working and counter electrode and a silver/silver chloride paste reference electrode (Lifescan, UK) was used. Unless specified otherwise all measurements were conducted at $22^{\circ}C \pm 2^{\circ}C$.

8.2.2. Preparation of the Naphtoquinone-adamantane Derivative

The naphthoquinone-adamantane derivative [2-(adamantyl-1-carboxylic acid)-1,4-naphthoquinone ester], illustrated in **Figure 8.1**, was prepared from 2-
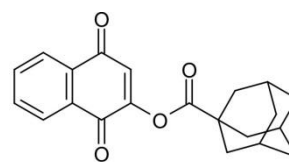
Naphthoquinone-adamantane derivative

Figure 8.1 Structure of naphthoquinone-adamantane derivative.

hydroxy-1,4-naphthoquinone and adamantane-1-carboxyl chloride using the procedure previously developed by the research group [12].

8.3. Results and Discussion

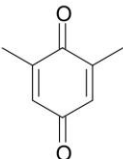### 8.3.1. Benzoquinone Labelling Strategies

A range of benzoquinone derivatives were assessed to see if they had any aqueous solubility. The ones that were soluble were subsequently examined to see if their spectrophotometric profile was stable over a prolonged time period and if there was any alteration in this profile in the presence of the sulphydryl thiols. **Figure 8.2** shows the spectral response for the most stable and reactive label, 2,6-dimethylbenzoquinone (2,6-DMBQ) (1mM, pH7 Britton-Robinson
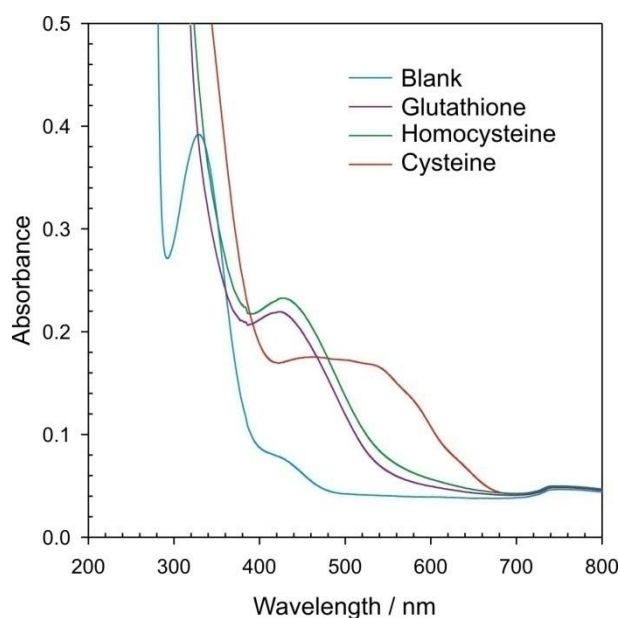
Figure 8.2 Spectral response of 2,6-DMBQ (1mM, pH7) in the absence (blank) and presence of glutathione, homocysteine and cysteine (0.25mM) ten minutes after thiol addition.

buffer) in the absence (**Figure 8.2 blue**) and presence of the sulphydryl thiol species (0.25 mM): cysteine (**Figure 8.2 red**), homocysteine (**Figure 8.2 green**) and glutathione (**Figure 8.2 purple**) ten minutes after thiol addition. Upon the introduction of thiol species a bathochromic shift from 330nm to 424nm, 426nm and 440nm was observed for glutathione, homocysteine and cysteine respectively. This can be attributed to the loss of the initial quinone and the formation of the corresponding quinone-thiol conjugates (**Scheme 8.1 III**). An additional bathochromic shift to 460nm, along with peak broadening, is observed for cysteine ten minutes after the thiol addition which can be attributed to the formation of the cyclised quione-thiol conjugate as outlined in **Scheme 8.1 IV**. No additional changes in the spectral profiles were seen for glutathione and homocysteine which can be attributed to the fact that cyclisation is not possible with glutathione and whilst

cyclisation may occur with homocysteine it will probably be at a much slower rate when compared to cysteine. **Table 8.1** shows the structure of 2,6-DMBQ and the corresponding molar absorptivities for the quinone-thiol conjugates formed after ten minutes. Although the sensitivity of the 2,6-DMBQ label is weak, especially in comparison to the commercially available labels such as Ellman's reagent (~13,000 L mol^{-1} cm^{-1}) [14], the system still has some potential for the speciation of cysteine due to the second spectral shift and the fact that the physical appearance of the resultant solution is notably different for cysteine when compared to the other thiol species (pink compared to yellow).


| Solution	λmax / nm	Absorbance	ε / L mol^{-1}cm^{-1}
Blank	330	0.39183	391.83
Cysteine(Initial)	440	0.22504	900.16
Cysteine(10minutes)	460	0.1754	701.6
Homocysteine	426	0.22067	882.68
Glutathione	424	0.2179	871.6

2,6-Dimethylbenzoquinone

Table 8.1 Chemical structure of 2,6-DMBQ, λmax shift, absorbance and molar absoptivities for the quinone-thiol conjugates formed.

The variations in the spectral profiles of 2,6-DMBQ in the presence of the different thiol species therefore offers a potential route for the colorimetric determination of cysteine and the performance of this label to facilitate the determination of cysteine/cystine was therefore assessed. In terms of the latter, as previously discussed within this thesis, it is necessary to reduce the disulphide to release the thiol moiety which is used within the analysis. A range of different reducing agents were studied in an attempt to find one that would be suitable for use within this assay including mercaptopropanol, mercaptoethanol, tris(2-Carboxyethyl)phosphine hydrochloride, sodium borohydride and dithiothreitol (DTT), and although all were successful at cleaving the disulphide bond, only DTT did not significantly interfere with the spectrophotometric determination of the cysteine released.
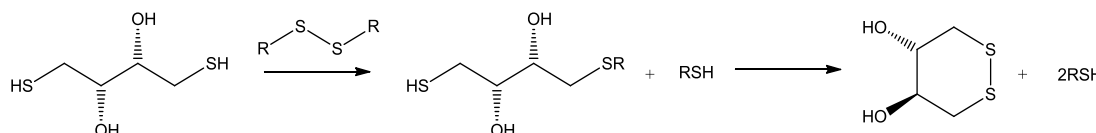

Scheme 8.2 Reduction of disulphides (R-S-S-R) with DTT.

The DTT reduction route is detailed in **Scheme 8.2** and for DTT to be used successfully as a reducing agent it must be prepared in a basic solution, typically pH8. This ensures that the nucleophilic nature of the thiol function is maintained, thus allowing the reduction and subsequent cyclisation of the DTT to occur. When the spectral profile of 2,6-DMBQ (1mM, pH7) in the presence of cysteine (0.5mM) and DTT (5mM, 0.1M NaOH) was evaluated, the extent of the spectral shift initially seen after a 10 minute period (**Figure 8.2**) for the cysteine-quinone conjugate was reduced. This can be attributed to the fact the increased basicity reduces the rate at which the conjugate cyclises (**Scheme 8.1 III→IV**) therefore decreasing the concentration of the conjugate responsible for the characteristic shift. This now limits the system for the speciation of cysteine due to the spectral overlap of this species with the glutathione and homocysteine conjugates. This issue can be resolved by making the 2,6-DMBQ solution slightly acidic before it is mixed with the reduced sample, this will adjust the pH of the solution counteracting the aforementioned effect allowing the selective colorimetric determination of the cysteine produced in the presence of homocysteine and glutathione either by eye or by measuring the absorbance at 600nm, as highlighted in **Figure 8.3**.
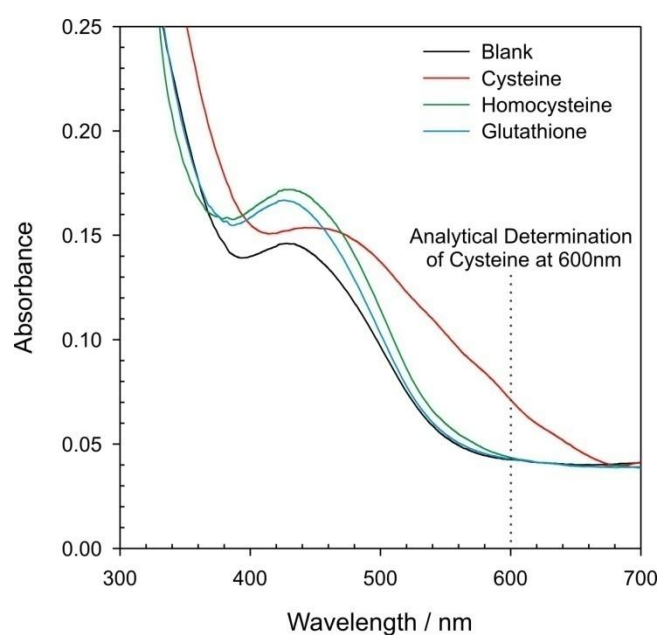

Figure 8.3 Spectral response of acidified 2,6-DMBQ in the absence and presence of glutathione:DTT, homocysteine:DTT and cysteine:DTT (0.5mM:5mM) after ten minutes.

To assess whether this assay could be applied in the context of quantitative cystine analysis, a calibration series was carried out for cysteine in the presence of DTT. The corresponding spectral responses, photographic image and calibration curve are shown in **Figure 8.4**. The calibration data was linear over a sample concentration range of 0-700µM with the equation of the line being: Absorbance = 0.00006[Concentration of Cysteine in the sample (µM)] + 0.0442, having a correlation coefficient R^2 = 0.9943.
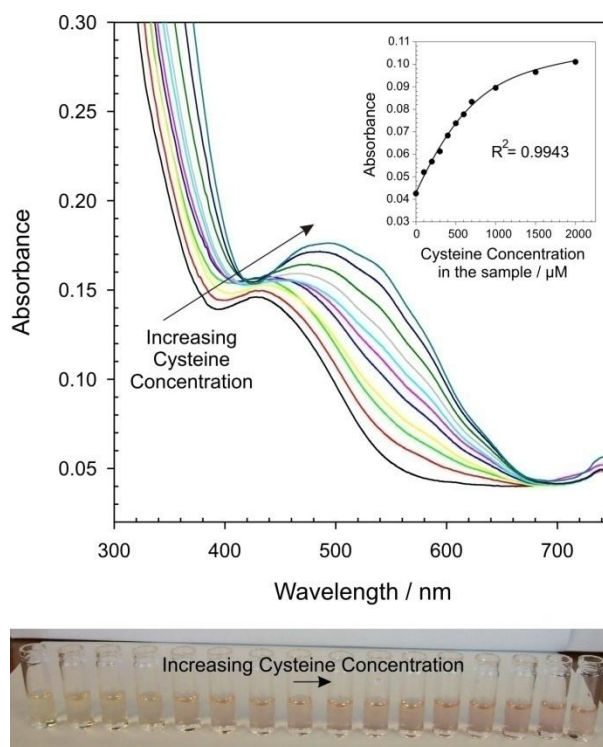
Figure 8.4 The spectral responses, photographic image and calibration curve for the cysteine calibration in the presence of DTT.

A solution containing cystine (250µM) and DTT (5mM) was prepared and allowed to stand for 10 minutes so that all the cystine would be reduced to cysteine. This solution was then added to an acidified solution of 2,6-DMBQ (1mM) and the reaction mixture was left for an additional ten minutes before the spectral profile was recorded. The spectral response observed for this cystine/DTT mix was almost identical to that seen when the same process was repeated for a solution containing a cysteine (500µM) and DTT (5mM) mix as illustrated in **Figure 8.5**. The absorbance for the
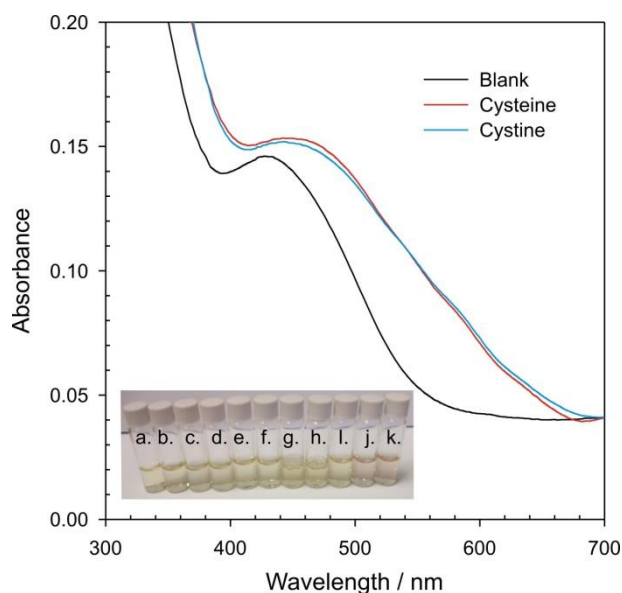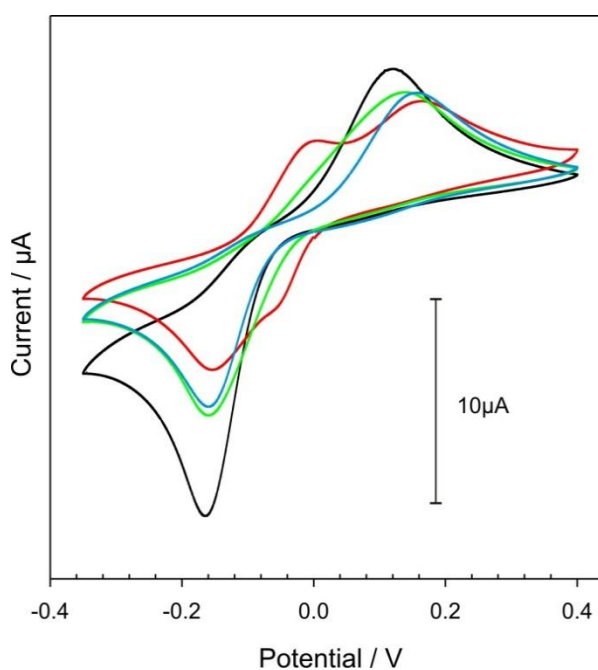

Figure 8.5 The spectral response for 2,6-DMBQ in the absence (blank) and presence of cysteine:DTT and cystine:DTT. Insert: Photograph showing the resultant solutions in the preference of a range of sample interferents.

cystine/DTT solution was measured at 600nm and the concentration of cysteine released determined from the calibration graph previously obtained. The concentration of cysteine was found to be 482.77µM, with the experiment having a 96.55% average recovery (%RSD = 2.46, N = 3) thus proving the tentative applicability of the procedure. The spectral response of 2,6-DMBQ in the prescene of DTT (5mM) to a range of components that are typically present within biological samples: a. creatinine, b. L-histidine, c. ascorbic acid, d. L-lysine, e. glycine, f. uric acid, g. albumin (from bovine serum), h. homocysteine, i. glutathione, j. cysteine and k. cystine, (1mM solutions, except albumin where a 50mg/L solution was used) were assessed and the photograph (**Figure 8.5 insert**) shows the resultant solutions after ten minutes. The failure of these other species to elicit the same change in spectral profile seen for cysteine along with the data described previously clearly demonstrates the selectivity of 2,6-DMBQ as a colorimetric label for the detection of the latter, even though the overall sensitivity of the system is compromised by the low molar absorptivity of chromophores present.

Electrochemical methods are known to have superior performance characteristics when compared to spectrophotometric methods and it was it therefore envisaged that the presence of the quinone moiety on the 2,6-DMBQ would allow the sulphydryl thiols to be determined due to the differences in the redox properties of the initial quionone and the quinone-thiol conjugates formed, much like the route employed within Chapter 5. Cyclic voltammograms detailing the electrochemical behaviour of 2,6-DMBQ (454µM, pH7) in the absence and presence of
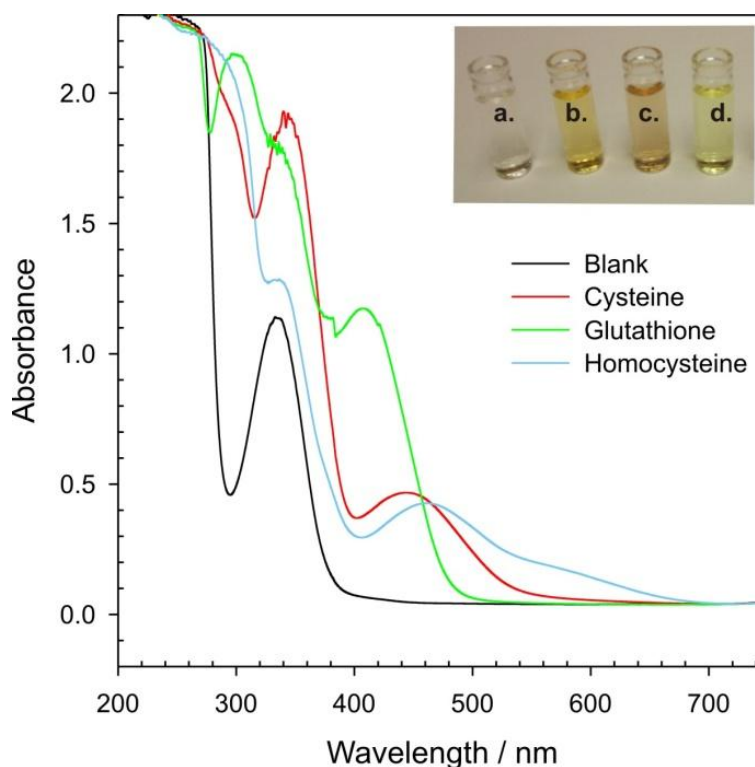

Figure 8.6 Cyclic voltammograms detailing the response of 2,6-DMBQ (454µM,pH7) in the absence (black line) and presence of cysteine (red line), homocysteine (green line) and glutathione (blue line) (111µM, pH7).

cysteine (**red**), homocysteine (**green**) and glutathione (**blue**) (111µM, pH7) are detailed in **Figure 8.6**.

The 2 electron, 2 proton reduction and re-oxidation of the quinone component can be seen at -0.16V and 0.12V respectively and follows the process typically expected for quinone species as discussed elsewhere within this thesis. As expected, in the presence of the reduced sulphydryl thiol species, a change in the 2,6-DMBQ redox couple can be seen, with a decrease in the reduction and re-oxidation peaks observed and although there is the emergence of a new redox couple in the presence of cysteine the new peaks are not fully resolvable and so 2,6-DMBQ has limited use as an electrochemical label showing inferior selectivity compared to the plumbagin previously studies and so was not examined further.

8.3.2. Naphthoquione Labelling Strategies

The same route applied previously for the study of the benzoquinone derivatives was used to evaluate the applicability of using a range of naphthoquinone derivatives as labels for the selective determination of sulphydryl thiol species. Although a range of derivatives were studied, the naphthoquinone-adamantane (NQ-Ada) derivative, 2-(adamantyl-1-carboxylic acid)-1,4-naphthoquinone ester,

Figure 8.7 Spectral response of NQ-Ada (500μM) in the absence (blank) and presence of glutathione, homocysteine and cysteine (238μM) 5 minutes after thiol addition.
Insert: Photograph showing the appearance of the spectral solutions (blue line) (111μM, pH7).

previously synthesized by the research group [12] was found to have the most useful spectral profile. **Figure 8.7** shows the spectral profile for the NQ-Ada derivative

(500μM, methanol) in the absence (**Figure 8.7 black**) and presence of the thiol species (238μM) 5 minutes after thiol addition**.** A bathochromic shift from 333nm to 407nm, 443nm and 460nm can be seen for glutathione (**Figure 8.7 green**), cysteine (**Figure 8.7 red**) and homocysteine (**Figure 8.7 blue**) respectively. These differences can be attributed to the formation of the different quinone-thiol conjugates. The spectra for the mocysteine NQ-Ada conjugate is notably different to that observed for the other conjugates, here the λmax is at a higher wavelength, the peak is broader in comparison to the others shown and a new peak appears to be emerging at approximately 580nm. The photo insert in **Figure 8.7** shows the characteristic differences in the appearance of these solutions.

The spectral differences open up a possible route for the detection of homocysteine, if the absorbance is recorded in the tail of the conjugate peak were no interference from the cysteine and glutathione NQ-Ada conjugates or the NQ-Ada monomer can be seen. The molar absorptivities of the quinone-thiol conjugates are illustrated in **Table 8.2**, the latter, like those calculated for the benzoquione derivatives are low and this, along with the low concentration range experienced for homocysteine within biological samples and the poor aqueous solubility of the NQ-Ada label will seriously impede the application of this derivative for the colorimetric speciation of homocysteine within a sample so alternative routes must be explored.

Solution	λmax / nm	Absorbance	ε / L mol^{-1}cm^{-1}
NQ-Ada	333	1.1414	2282.8
Cysteine	443	0.467	1962.2
Homocysteine	460	0.4264	1791.6
Glutathione	407	1.1734	4930.3

Table 8.2 λmax, absorbance and molar absorptivities for the naphthoquinone-adamantane derivative and the corresponding thiol conjugates formed.

The approach advocated in this case exploits the different hydrophobic and hydrophilic properties of the NQ-Ada label and its thiol conjugates to facilitate thiol detection. Electrochemical quartz crystal microbalance studies were carried out to prove the viability of this concept and the results are highlighted in **Figure 8.8**.

Figure 8.8. EQCM data for a solvent cast NQ-Ada film in the absence and presence of cysteine, homocysteine and glutathione (1mM, pH7).

The approach advocated in this case exploits the different hydrophobic and hydrophilic properties of the NQ-Ada label and its thiol conjugates to facilitate thiol detection. Electrochemical quartz crystal microbalance studies were carried out to prove the viability of this concept and the results are highlighted in **Figure 8.8**.
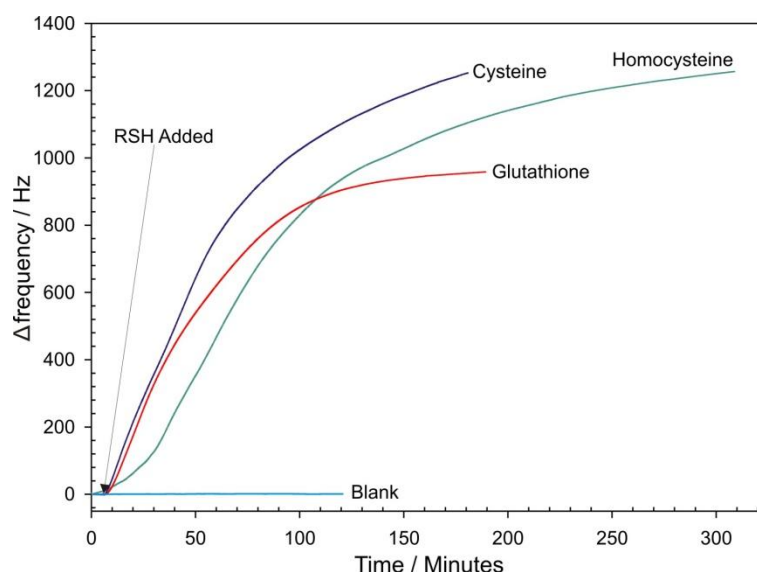
A platinum coated quartz crystal was coated in a layer of the NQ-Ada (solvent cast) and was placed into a solution of deionised water, the deposited layer was stable for well over an hour (**Figure 8.8. blank**) and confirms that the NQ-Ada derivative is hydrophobic. When the thiol species were added (1mM) to the solution (cysteine, homocysteine and glutathione **Figure 8.8 blue, green** and **black** lines respectively), after a 5 minute period, the frequency of the crystal was found to increase corresponding to a decrease in weight and therefore indicating that the NQ-Ada becomes hydrophilic as it reacts with the thiol species to give the conjugate, thus confirming the earlier hypothesis.

Figure 8.9 illustrates how the method can be applied for the colorimetric detection of the thiol species. The NQ-Ada label is loaded onto precut filter paper circles which are then placed within a centrifugal filter assembly. This construct is hydrophobic and thus immobilised within the system and will remain so until it comes into contact with a reduced sulphydryl thiol species. The quinone-thiol conjugate formed is hydrophilic and is therefore rendered mobile within the system and so upon

centrifugation the conjugate is able to pass through the filter assembly and will be present within the filtrate.
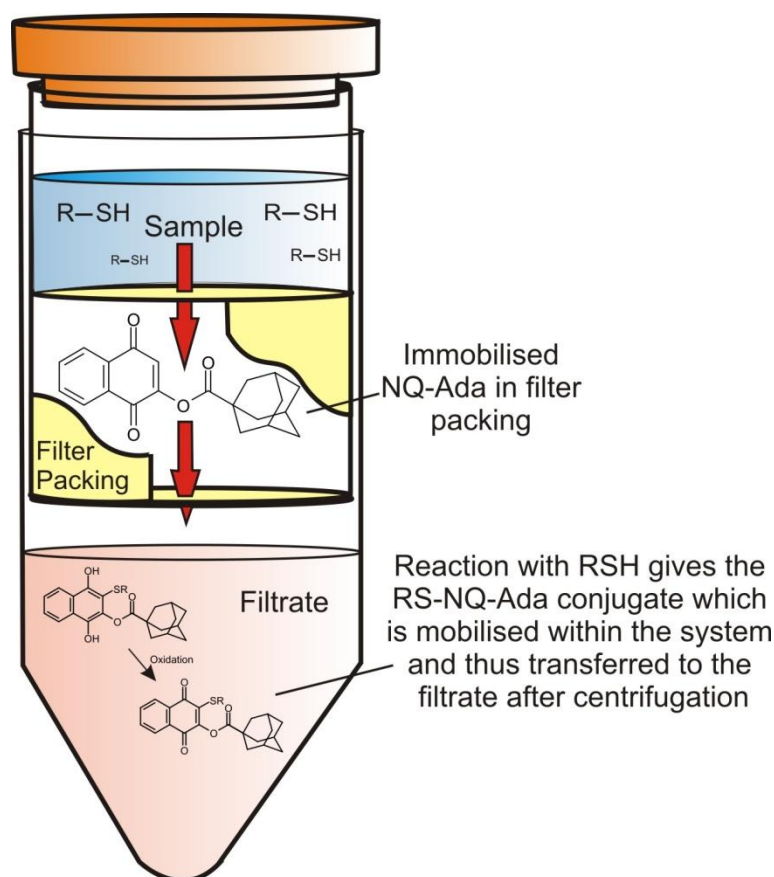
Figure 8.9 Schematic illustrating the centrifugal approach for the analysis of sulphydryl thiols using the NQ-Ada label.

The presence of the thiol-NQ-Ada conjugate in the filtrate should be detectable *via* colorimetric means, however the concentration of the quinone-thiol conjugate passing though the filter is very low (μM concentration range) and as the concentration of the reduced thiol species in the sample will also be low, and although the differences in colour can be seen by eye, the selective determination by spectrophotometric techniques cannot be achieved due to the low molar absorptivity of the label. Due to the enhanced sensitivity of electrochemical techniques we do however have a potential route that can be used to evaluate the concentration of the quinone-thiol conjugate and, as such, the electrochemical performance characteristics of the system were assessed.

Initially solutions containing large amounts of thiols (500µM) were examined to see if the filter-electrochemical approach could be used to facilitate thiol analysis. The thiol solutions and blank solution (no thiol present) contained 100µM KCl to provide the electrolyte for the reference electrode. These solutions were added to the centrifugal filter set up (**Figure 8.9**), left to react for ten minutes and then centrifuged at 4000rpm for ten minutes. The electrochemistry of the filtrate was assessed
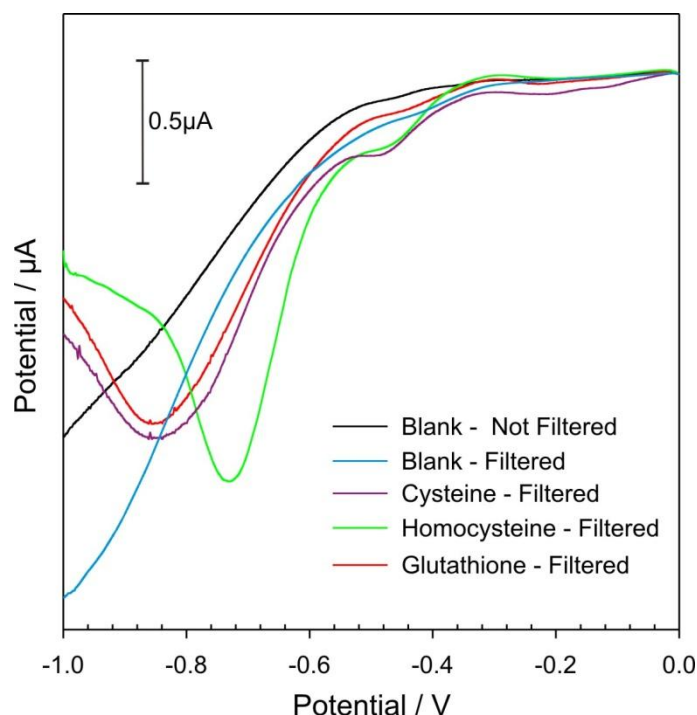
Figure 8.10 Square-wave voltammograms detailing the response of a screen printed electrode assemble to a blank solution (prior to and after centrifugation) and thiol solutions (500uM) after centrifugation through an NQ-Ada saturated system in the presence of KCl (100uM).

immediately after centrifugation and the square-wave voltammogramms detailing the response of a plasma treated screen printed electrode assembly (lifescan uk) to the resultant sample solutions after centrifugation are detailed in **Figure 8.10**.

A pre-treatment step, where an oxidising potential of +0.5V was applied to the electrode for 5 seconds, was used to ensure that the all of the conjugate in the filtrate was present in the oxidised form prior to analysis. In **Figure 8.10** reduction peaks at -0.73V and -0.85V for the filtered homocysteine (**green**), cysteine (**purple**) and glutathione (**red**) solutions respectively, which can be attributed to the reduction of the quinone component on the NQ-Ada-thiol conjugate. The lack of any appreciable signal for the blank solutions (**Figure 8.10 black** and **blue**) confirms that the NQ-Ada derivative is immobilised within the filter assembly and will only pass through to the filtrate if the thiol species is present. The above procedure was repeated for samples containing molecules such as albumin and glycine that could interfere with the analysis and the responses observed were identical to the trace observed for the blank filtered solution thus highlighting the efficacy of the approach for the

determination of thiol species, however, the low currents recorded for such high concentrations of thiol species present, show that the selectivity of the approach is extremely limited.

8.4. Conclusions

Benzoquinone and naphthoquinone derivatives have been shown to be selective labels for the analysis of reduced thiol functionalities. The reaction pathway that causes the changes in the spectral profiles have been elucidated and the selectivity of the assays along with their adaptability to be used with electrochemical detection routes have been assessed. Although the assays have limited sensitivity, they do highlight a possible route for the determination of thiol species if these issues can be resolved.

8.5. References

[1]   G. Chwatko and E. Bald, Determination of different species of homocysteine in human plasma by high-performance liquid chromatography with ultraviolet detection. Journal of Chromatography A, 949 (2002) 141-151

[2]   G. Minniti, A. Piana, U. Armani and R. Cerone, Determination of plasma and serum homocysteine by high-performance liquid chromatography with fluorescence detection. Journal of Chromatography A, 828 (1998) 401-405

[3]   O. Nekrassva, N.S. Lawrence and R.G. Compton, Analytical determination of homocysteine: A review. Talanta, 60 (2003) 1085-1095

[4]   G. Zhang, D. Liu, S. Shuang and M. Choi, A homocysteine biosensor with eggshell membrane as an enzyme immobilisation platform. Sensors and Actuators B: Chemical, 114 (2006) 936-942

[5]   R. Accinni, S. Bartesaghi, G. DeLeo et al, Screening of homocysteine from newborn bloodspots by high-performance liquid chromatography with coulometric array detection. Journal of Chromatography A, 896 (2000) 183-189

[6]   Y.V. Tcherkas and A.D. Denisenko, Simultaneous determination of several amino acids, including homocysteine, cysteine and glutamic acid, in human plasma by isocratic reversed-phase high-performance liquid chromatography with fluorimetric detection. Jounal of Chromatography B: Biomedical Sciences and Applications, 913 (2001) 309-313

[7]   W. Chen, Y. Zhao, T. Seefeldt and X. Guan, Determination of thiols and disulfides via HPLC quantification of 5-thio-2-nitrobenzoic acid. Journal of Pharmaceutical and Biomedical Analysis, 48 (2008) 1375-1380

[8]   D. Zhang, M. Zhang, Z. Liu et al, Highly selective colorimetric sensor for cysteine and homocysteine based on azo derivatives. Tetrahedron Letters, 47 (2006) 7093–7096

[9]   W. Wang, J.O. Escobedo, C.M. Lawrence and R.M. Strongin, Direct Detection of Homocysteine. Journal of the American Chemical Society, 126 (2004) 3400-3401

[10]   O. Rusin, N.N. St.Luce, R.A. Agbaria et al, Visual Detection of Cysteine and Homocysteine. Journal of the American Chemical Society, 126 (2004) 438-439

[11]   F. Huo, Y. Sun, J. Su et al, Colorimetric Detection of Thiols Using a Chromene Molecule. Organic Letters, 11 (2009) 4918-4921

[12]   I.A. Solsona, R.B. Smith, C. Livingstone and J. Davis, Metaboloc mimics: Thiol responsive drug release. Journal of Colloid and Interface Science, 302 (2006) 698-701

[13]   S. Gracheva, C. Livingstone and J. Davis, Development of a Disposable Potentiometric Sensor for the Near Patient Testing of Plasma Thiol Concentrations. Analytical Chemistry, 76 (2004) 3833-3836

[14]   G.L. Ellman, Tissue sulfhydryl groups. Archives of Biochemistry and Biophysics, 82 (1959) 70-77

Chapter 9

The Development of a Uric Acid Sensor for Wound Management

Chapter 9

The Development of a Uric Acid Sensor for Wound Management

Abstract

pH plays a significant role in the wound healing process and as such wound status can be assessed through monitoring the pH of wound exudates. The electrochemical oxidation of uric acid is pH dependent and so, due to the prevalence of this species within biological fluids, the possibility of exploiting the shift in the potential observed for the electrochemical oxidation of uric acid, upon variation of pH, as a possible method to evaluate wound status was investigated. Disposable screen printed electrode assemblies have been characterised and their response to uric acid assessed. The electrode response to uric acid was found to change linearly with pH and it was observed that when the working electrode had been subjected to an anodic pre-treatment that the performance criteria of the electrode could be enhanced to an acceptable level that would allow the pH of the sample to be determined. A preliminary investigation to assess the efficacy of using this pH dependent uric acid response to determine the pH of whole blood is presented.

9.1. Introduction

Wound healing is a fragile and complex process consisting of a series of stages: hemostasis, inflammation, proliferation and tissue remodelling [1-3]. Each stage is well regulated to bring about effective healing but the process can be affected by a number of factors, endogenous and exogenous, and will be severely compromised if an infection develops within the wound [4-5]. A number of factors may be responsible for a wound becoming infected, the most common being the invasion and colonisation of the wound by opportunistic bacteria such as *Staphylococcus aureus, Escherichia coli* and *Enterococci* [6-7]. The threat of infection is a constant problem and is complicated further within a healthcare environment given the prevalence of hospital acquired infections (HAIs) [8-9] and the ongoing issues surrounding antibiotic resistance [10-11]. There is therefore an urgent need for the development of new technologies that can reduce the incidence of infection and/or detect the onset of an infection within the wound which would alert clinicians to the change in wound status and therefore allow earlier and potentially more effective treatment to be carried out.

The pH of a wound contributes significantly to all of the biochemical processes that bring about successful wound healing [12]. One example being that it is principally involved in regulating the activity and conformation of enzymes (proteinases) responsible for tissue generation during the remodelling stage [1]. The pH of a normal healing wound will fluctuate during the healing process, from a neutral pH to an acidic pH with a lower pH limit of approximately 4.8, thus regulating the individual processes. The acidic environment is important as it increases the amount of oxygen present within the healing tissue, stimulating wound healing, whilst inhibiting bacterial growth and reducing the histotoxicity of any bacterial end products [13-14]. Deviations from the expected pH sequence or normal pH range can therefore indicate that certain problems are occurring during the healing process. Of particular significance is a rise in the pH of a wound; the increased alkalinity will promote the colonisation and survival of bacterial species within the wound and so the rise can be an indicator that infection is present [12-14]. Given these factors, it is clear to see why the measurement of surface wound pH is regarded as a simple and

effective approach for wound monitoring/management strategies [14]. A number of non-invasive methods can be used to determine the pH of a wound including a conventional glass pH probe [14], wound dressings that contain indicator species that change colour with pH [15] and more advanced biosensor type systems [16], all of which have the primary aim of detecting when the pH of the wound deviates into the alkaline region [14-16]. These systems can be very effective, however, due to their size, complexity and the ambiguity associated with some of the results obtained, the development of a smaller, more reliable system that could be cheaply manufactured and easily integrated within a wound dressing to provide a numerical pH measurement would be a clear advantage.

Uric acid is the end product of purine metabolism and is therefore present within a range of biological fluids including wound exudates. It is a strong reducing agent and an important antioxidant that has a number of vital roles within the body. Uric acid has long been recognised as a biomarker for assessing conditions such as hypertension [17], renal disfunction [17-18] and cardiovascular diseases [19] that are associated with oxidative stress, whereby the severity of the underlying condition is directly related to the uric acid concentration. The electrochemistry of uric acid is dominated by the two electron, two proton oxidation as illustrated in **Scheme 9.1**. The oxidation of uric acid (**I**) gives the corresponding di-imine (**II**) which is unstable and readily reacts with water to give the final oxidation product allantoin (**III**) [20].
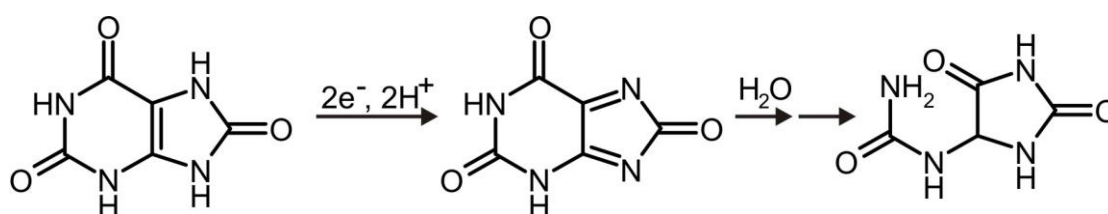
Scheme 9.1 The oxidation of uric acid.

The current produced and measured during this oxidation is derived solely from the initial oxidation process (**Scheme 9.1 I→II**) and the current response will be proportional to the concentration of uric acid within the sample. The position of this oxidation peak has been found to be pH dependent, with the ease of oxidation increasing linearly with pH [21-22]. It was therefore envisaged that the uric acid present within a wound and its pH dependent electrochemistry could be exploited to

form a detection strategy within a smart sensor that would provide a quantitative assessment of wound pH and give an indication of wound status. Although uric acid concentrations within a wound will vary within the reference range 190–420 µM [23-24], depending on the individual, wound status and the presence of bacterial species [25], the diagnostic remit of the proposed sensors lies not in the extraction of an absolute uric acid concentration but rather with the relative position of the oxidation peak and so this variability in uric acid concentration is unimportant within this work.

The work detailed within this chapter looks at utilising standard screen printed, disposable electrode assemblies as the sensing platform. The screen printed electrode assemblies currently available often have poor electrode characteristics when trying to assess biological components within complex sample matrices. It was therefore envisaged that carrying out an anodic pre-treatment, which is known to improve the performance criteria of carbon based electrodes, would enhance the sensitivity of the sensing platform [26-27].

9.2. Experimental Details

All reagents were of the highest grade available, were used without further purification and unless stated otherwise were purchased from Sigma Aldrich (UK) or Alfa Aesar (UK). Stock solutions of uric acid (typically 10 mM) were prepared in 0.1 M sodium hydroxide. Britton–Robinson buffer was used throughout as the supporting electrolyte and was adjusted to the appropriate pH through the addition of sodium hydroxide.

Electrochemical measurements were conducted using a µAutolab computer controlled potentiostat (Eco-Chemie, Utrecht, The Netherlands) using a three electrode configuration. A plasma treated screen printed carbon electrode or a standard screen printed carbon electrode (Lifescan, UK) was used as the working electrode (either left untreated or treated using an anodic oxidation), platinum wire served as the counter electrode and a 3 M NaCl Ag | AgCl half cell reference electrode (BAS Technicol, UK) completed the cell assembly. Anodic pre-treatment was achieved by applying a potential of +0.2V to the electrode for 5 minutes in a solution of 0.1M sodium hydroxide. All measurements were conducted at $22^{o}C \pm 2^{o}C$.

9.3. Results and Discussion

Figure 9.1 shows the square-wave voltammogramms detailing the response of the unmodified and electrochemically anodised screen printed electrodes (SPE) (**Figure 9.1 a**) and plasma treated screen printed electrodes (PSPE) (**Figure 9.1 b**) towards uric acid (244μM, pH 7.2). The two electron, two proton oxidation of the uric acid (**Scheme 9.1**) is visible, albeit slightly different, on all of the voltammetric profiles displayed. The response of the unmodified PSPE to uric acid (**Figure 9.1 b-blue**) is more apparent than the response observed for the
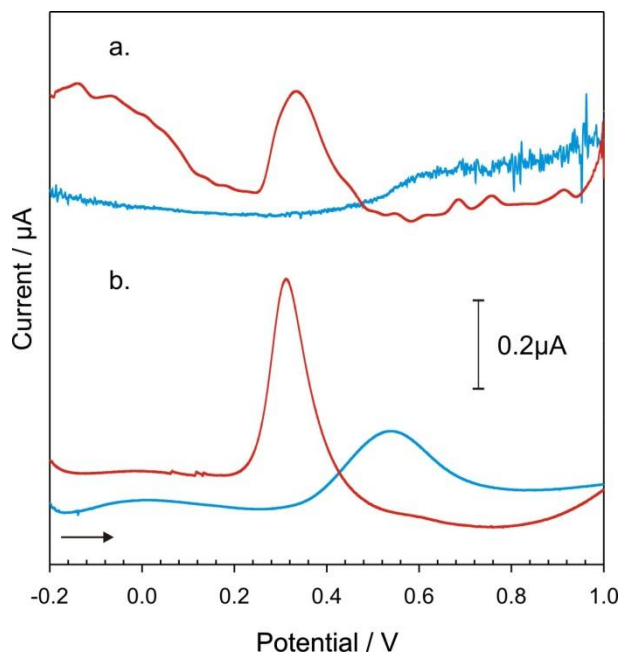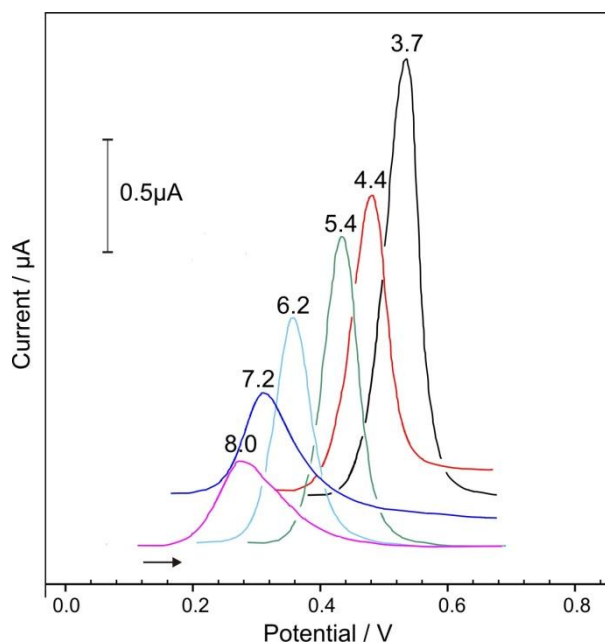

Figure 9.1 Squarewave voltammograms highlighting the response of a. SPE and b. PSPE, with (red profiles) and without (blue profiles) anodisation, to uric acid (244μM, pH 7.2).

unmodified SPE (**Figure 9.2 a-blue**) and can be attributed to the fact that plasma treatment of screen printed carbon electrodes can enhance their electrochemical properties therefore improving the signal response [28-29]. The response observed for the electrodes to uric acid was, in both cases, improved upon the application of an anodic pre-treatment step (**Figure 9.1 a and b red**), as predicted, and is in keeping with work previously published [26-27]. The anodised PSPE gave the best profile for the oxidation of uric acid (**Figure 9.1 b-red**). A sharp, fully resolvable oxidation peak can be seen at +0.312V, which stands in marked contrast to the broader, less pronounced peaks observed for the other electrode assemblies tested. This can be ascribed to the combinational effects that the plasma treatment and anodisation steps have had on modifying the electrode surface (i.e. improved wettability, surface reactivity, porosity and conductivity). The anodised PSPE electrode was therefore used for all of the subsequent investigations as the sensing platform.

The intended application of the electrode assembly is to determine the sample pH by monitoring the variation in the oxidation peak observed for uric acid upon altering the pH. A calibration type series was therefore examined to see if a pH dependent peak shift could be established at the anodised PSPE for uric acid, laying down the foundations for this measurement. **Figure 9.2** shows the voltammteric responses of the anodised PSPE to uric acid (244μM) when the pH of the test solution was varied over a


Figure 9.2 Squarewave voltammograms detailing the response of the APSPE to uric acid (244μM) at various pH.

pH range of 3.66 to 9.79. In each case, regardless of the pH, a well defined peak for the oxidation of uric acid can be observed, and it is clearly apparent that the position of this peak shifts to more negative potentials as the pH increases. This shifts follows a linear response with the equation: E(V)= -0.0599[pH] + 0.747 and the correlation coefficient R^2=0.992. The establishment of this linear response highlights the potential applicability of using the proposed methodology for making pH measurements. Although not directly relevant to this study it should be noted that the current response observed for the oxidation decreases as the pH increases. This shows that the electrodes have a better response to uric acid in acidic solutions.

The viability of the anodised PSPE for use within biofluids was assessed by determining the pH of a whole blood sample *via* measuring the position of the uric acid oxidation. Whole blood was chosen as the principle test medium as it would represent a strong challenge to the sensor whilst enabling a valid pH measurement to be made as the sample from a healthy volunteer would be subject to stringent homestatic regulation, with the expected pH being in the range of 7.32-7.43 [28]. The whole blood sample, approximately 50μl, was extracted from the subject *via* the fingerprick method and was analysed directly without any sample pre-treatment. **Figure 9.3** shows the voltammetric response of the electrode assembly to a whole

blood sample, with the repetitive scans showing the reproducibility of the approach. The uric acid oxidation peak is clearly visible as a sharp fully resolvable peak at +0.304V providing an unambiguous signal from which the pH can be deduced. Other oxidation processes can be seen on the voltammogram– a broad peak at +0.689V is observed and can be attributed to the direct oxidation of other amino acids present within the sample. The position of this oxidation peak is important as it demonstrates that there will be no interference seen for the uric acid response and so the measureable signal is solely due to uric acid and the position can therefore be directly related to the pH of the sample.
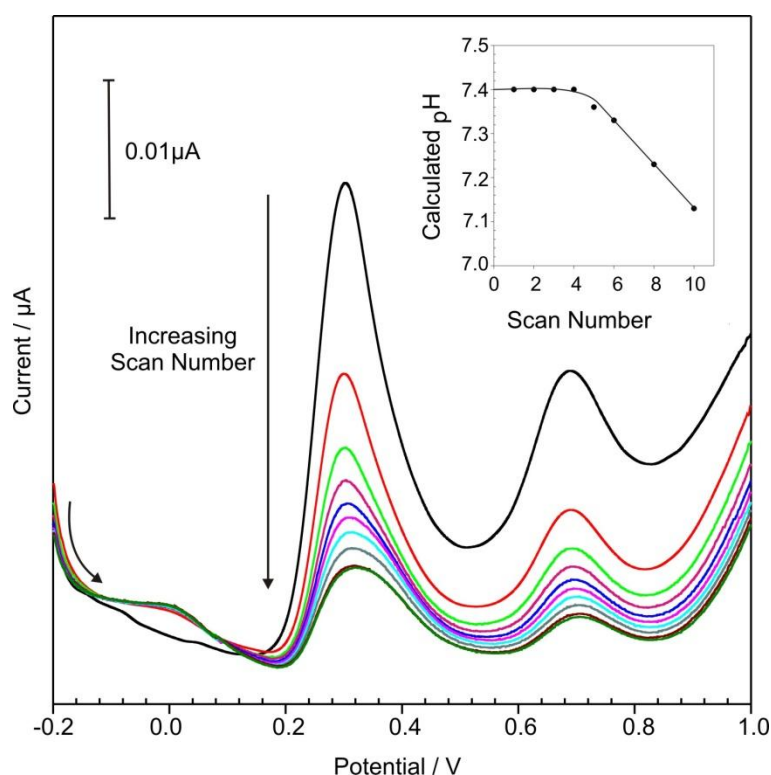
Figure 9.3 The successive scan voltammetric response of the anodised PSPE to whole blood.

Upon successive scanning the peak position for uric acid is stable for four scans, after which it begins to deviate from its initial value which can be attributed to the electrode being fouled by the coagulation of the sample at the electrode surface and from the oxidation of the sample components. The height of the uric acid peak also diminishes on successive scanning and, although irrelevant to this study, it is indicative of the depletion of the uric acid species at the electrode surface due to its irreversible oxidation. Signal broadening is also apparent and can be ascribed to the aforementioned electrode fouling. Evidence of electrode contamination is also

apparent due to the emergence of the new oxidation peak on the second scan at approximately +0.024V.

The position of the uric acid oxidation peak (+0.304V) and the previously determined calibration data were used to determine the pH of the blood sample and ensure the accuracy of the sensing approach investigated. The results obtained for a range of electrode assemblies; different electrodes (APSPE - Inter), the same electrode (APSPE - Intra) and a electrode after it had been stored for two week (APSPE Storage), are displayed in **Table 9.1** and proves the effectiveness of using this approach on real biological samples as the resultant pH in all cases falls well within the accepted pH range for venous blood (from 7.32 to 7.43) [28].

	Average pH	N	% RSD
APSPE - Inter	7.397	3	0.278
APSPE - Intra	7.392	5	0.241
APSPE Storage	7.404	5	0.588

Table 9.1 Sensor results.

The intra and inter reproducibility (same strip and multiple strips respectively) has been calculated and the low RSD values in both instances show that little variation in the measurement has occurred when comparing the responses observed. Although the previous square-wave voltammogram (**Figure 9.3**) shows that the intra reproducibility is limited due to the inherent electrode fouling, which makes the sensing assemblies only suitable for measurements on one sample, the fact that the variability between different sensing assemblies is extremely low means that comparative measurements of the wound environment can still be made by periodic monitoring using fresh electrode assemblies.

A number of electrode assemblies were fabricated and stored in a closed container at ambient room temperate for two weeks before the test on whole blood was carried out (**Table 9.1** APSPE Storage). High levels of accuracy and reproducibility were seen between these different electrodes, indicating that the modified electrode assemblies are stable after storage reinforcing the fact that the approach is applicable for pH sensing.

9.4. Conclusions

The modified PSPE assemblies have been shown capable of providing a robust and versatile sensing system for determining pH. When comparing the screen printed electrode assemblies currently available, the plasma treated surfaces give an enhanced electrochemical response over standard screen printed systems and the further modification of these electrodes *via* anodic oxidation pre-treatment methods can enhance the resolution further. A sensitive route for the detection of uric acid across a range of different pH's has been demonstrated and assessment of the uric acid peak shift with changing pH has been shown to be linear over the applicable pH range, thus highlighting the feasibility of the approach as an indirect route to determine the pH in whole blood.

9.5. References

[1] S. Schreml, R. Szeimies, L. Prantl, M. Landthaler and P. Babilas, Wound healing in the 21st century. Journal of the American Academy of Dermatology, 63 (2010) 866-881

[2] T. Kondo and Y. Ishida, Molecular pathology of wound healing. Forensic Science International, 203 (2010) 93–98

[3] F. Strodtbeck, Physiology of Wound Healing. Newborn and Infant Nursing Reviews, 1 (2001) 43–52

[4] M.C. Robson, Wound Infection: A failure of wound healing caused by a imbalance of bacteria. Surgical Clinics of North America, 77 (1997) 637-650

[5] P.G. Bowler, Wound pathophysiology, infection and therapeutic options. Annals of Medicine, 6 (2002) 419-427

[6] J. Weber and A. McManus, Infection control in burn patients. Burns, 30 (2004) A16–A24

[7] W. Song, K.M. Lee, H.J. Kang, D.H. Shin and D.K. Kim, Microbiologic aspects of predominant bacteria isolated from the burn patients in Korea. Burns, 27 (2001) 136–139

[8] H. Sax, D. Pittet and the Swiss-NOSO Network, Interhospital Differences in Nosocomial Infection Rates. Archives of Internal Medicine, 162(2002) 2437-2442

[9] R. Plowman, N. Graves, M.A.S. Griffin et al, The rate and cost of hospital-acquired infections occurring in patients admitted to selected specialties of a district general hospital in England and the national burden imposed. Journal of Hospital Infection. 47 (2001) 198–209

[10] M. Sisirak, A. Zvizdic and M. Hukic, Methicillin-Resistant Staphylococcus Aureus (MRSA) as a cause of nosocomial wound infections. Bosnian Journal of Basic Medical Sciences, 10 (2010) 32-37

[11] G. A. Noskin, Vancomycin-resistant enterococci: clinical, microbiologic, and epidemiologic features. Journal of Laboratory and Clinical Medicine, 130 (1997) 14–20

[12] L.A. Schneider, A. Korber, S. Grabbe and J. Dissemond, Influence of pH on wound-healing a new perspective for wound therapy. Archives of dermatological research, 298 (2007) 413-420

[13] M.H. Pipelzadeh and I.L. Naylor,The in vitro enhancement of rat myofibroblast contractility by alterations to the pH of the physiological solution. European Journal of Pharmacology, 357 (1998) 257–259

[14] G. Gethin, The significance of surface pH in chronic wounds. Wounds UK, 3 (2007) 52-56

[15] G. Mohr, Dressings indicate infection. Fraunhofer Research News, 11 (2010) 5-6

[16] S. Pasche, S. Angeloni, R. Ischer, M. Liley, J. Luprano and G.Voirin, Wearable Biosensors for Monitoring Wound Healing. Advances in Science and Technology, 57 (2008) 80-87

[17] M. Heinig and R.J. Johnson, Role of uric acid in hypertension, renal diseae, and metabolic syndrome. Cleveland Clinic Journal of Medicine, 73 (2006) 1059-1064

[18] D. Kang, T. Nakagawa, L. Feng et al, A role for uric acid in the progression of renal disease. Journal of the American Society of Nephrology, 13 (2002) 2888–2897

[19] S.D. Anker, W. Doehner, M. Rauchhaus et al, Uric Acid and Survival in Chronic Heart Failure: Validation and Application in Metabolic, Functional, and Hemodynamic Staging. Circulation, 107 (2003) 1991-1997

[20]   J.S.N. Dutt, C. Livingstone, M.F. Cardosi, S.J. Wilkins and J. Davis, A clinical assessment of direct electrochemical urate measurements. Talanta, 68 (2006) 1463–1468

[21]   Y. Zhao, J. Bai, L.Wang et al, Simultaneous Electrochemical Determination of Uric Acid and Ascorbic Acid Using L-Cysteine Self-Assembled Gold Electrode. International Journal of Electrochemical Science, 1 (2006) 363-371

[22]   E. Popa, Y. Kubota, D.A. Tryk and A. Fujishima, Selective Voltammetric and Amperometric Detection of Uric Acid with Oxidized Diamond Film Electrodes. Analytical Chemistry, 72 (2000) 1724-1727

[23]   J.S.N. Dutt, M.F. Cardosi, C. Livingstone and J. Davis, Diagnostic Implications of Uric Acid in Electroanalytical Measurements. Electroanalysis, 17 (2005) 1233-1243

[24]   Diagnostic Services Handbook, Nottingham City Hospital NHS trust, UK, 2005.

[25]   D. Sharp and J. Davis, Integrated urate sensors for detecting wound infection. Electrochemistry Communications, 10 (2008) 709–713

[26]   H. BukolaEzekiel, D. Sharp, M. MartiVillalba and J.Davis, Laser-anodised carbon fibre: Coupled activation and patterning of sensor substrates. Journal of Physics and Chemistry of Solids, 69 (2008) 2932–2935

[27]   J. Lawrence, K.L. Robinson and N.S. Lawrence, Electrochemical Determination of Sulfide at Various Carbon Substrates: A Comparative Study. Analytical Science, 23 (2007) 673-676

[28]   C.A. Burtis, E.R. Ashwood and D.E. Burns, 2006. Tietz textbook of clinical chemistry and molecular diagnostics. 4th edition. Missouri:Elsevier Saunders

Chapter 10

Construction of a Disposable pH Sensor for Wound Management: A Generic Sensing Strategy?

Chapter 10

Construction of a Disposable pH Sensor for Wound Management: A Generic Sensing Strategy?

Abstract

The adaptation of the electrode assembly previously described in chapter 9, so that it could be used as a disposable pH sensor for integrated wound management, is described. It was found that by incorporating a fixed amount of potassium chloride as an internal reference, relative to the amount of chloride ions typically present within biological fluids, into the calibration standards, that the pre-printed silver/silver chloride paste reference electrode on the commercially available electrode assembly could be used to monitor the oxidation of uric acid. This allowed the pH of a sample to be determined accurately, on a disposable sensing strip, without the need for an external reference electrode. The performance characteristics of the uric acid based pH sensor were affected by the construction technique used during sensor fabrication. It was noted that cold sensor assembly was favourable over thermal construction methods giving a clearer voltammetric trace for uric acid. The applicability of using this fully disposable sensing assembly for measuring the pH of whole blood has been assessed and the possibility of adapting the sensor assembly for the analysis of reduced sulphydryl thiols is also explored.

10.1. Introduction

The sensor system developed in chapter 9 was used to explore the potential of utilising the characteristic shift in the position of the two electron, 2 proton oxidation of uric acid with pH to determine the latter within biological samples. The possibility of being able to determine the pH of biological fluids would clearly be a significant advantage in a number of clinical contexts given the problems that can occur when the pH of these fluids such as blood [1-2], wound exudates [3-5] and cerebrospinal fluids [6] deviate from the normal reference range. Although the system developed in chapter 9 displayed excellent performance characteristics for determining the pH of a sample, its use in a real life sensing scenario is limited due to the crude construction and complexity of the sensing platform. In this instance an external silver/silver chloride reference electrode was used alongside the screen printed carbon working and counter electrodes on a commercially available disposable electrode assembly. This places a significant size limitation on the assembly and severely impedes the possibility of using this sensor at the point of care. This chapter therefore describes the work carried out to develop an integrated sensing platform that could be used to determine the pH of biological samples, *in-situ*, at the point of care.

The plasma treated, screen printed electrode assemblies (PSPE) used in chapter 9 (**Figure 10.1**) have three electrodes available for use: a screen printed carbon

Figure 10.1 The electrode assembly – working electrode (WE), counter electrode (CE) and reference electrode (RE).

working electrode (WE) and counter electrode (CE) and a silver/silver chloride paste reference electrode (RE.) The fact that all of these electrodes are present opens up the possibility of using this electrode assembly as the full sensing unit as opposed to just using the WE and CE employed in the work detailed in chapter 9. The use of solid-state silver/silver chloride electrodes can however be problematic because of the need to have a fixed amount of internal electrolyte present at the electrode surface so that the reference potential can be produced [7]. Numerous routes have been developed so that these solid-state electrodes can be used as stable, accurate reference electrodes, which primarily involves coating the electrode surface with electrolyte doped

materials [7-10]. In this instance it was envisaged that a fixed amount of electrolyte, potassium chloride, could be incorporated into the uric acid pH calibration series, and the sample, therefore acting as the internal reference. This would allow the silver/silver chloride electrode on the sensing assembly to be used as the reference electrode, removing the need to have an external reference electrode present thereby making the assembly suitable for portable sensing applications. To make the electrode assembly suitable for use at the point of care it is necessary to develop a sensing format that would protect the electrode assembly from damage and, more importantly, allow the safe and controlled application of the sample. It was envisaged that the electrode assembly could therefore be incorporated within a laminate structure which would allow the aims to be met whilst enabling the electrodes to be connected to a portable potentiostat so that the sample could be processed and analysed .

The work detailed within this chapter looks at utilising the full PSPE assembly for determining the pH of biological fluids based on the position of the peak produced for the oxidation of uric acid. The last part of this chapter investigates whether the sensing platform can be modified to provide a generic device which, in this instance, could be used to detect the presence of reduced sulphydryl thiols and the applicability of this alternative sensing strategy has subsequently been assessed.
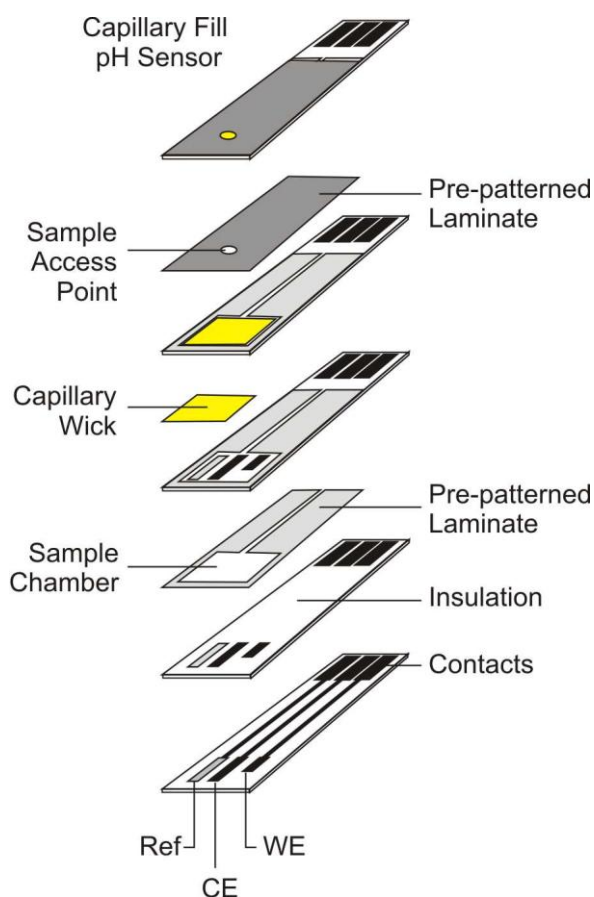
10.2. Experimental Details

10.2.1 Materials and Methods

All reagents were of the highest grade available, were used without further purification and unless stated otherwise were purchased from Sigma Aldrich (UK) or Alfa Aesar (UK). Stock solutions of uric acid (typically 10 mM) were prepared in 0.1 M sodium hydroxide, solutions of potassium chloride (typically 3M) were prepared in distilled water and glutathione solutions (typically 10mM) were prepared in pH7 Britton–Robinson buffer. The latter was also used as the electrolyte throughout and was adjusted to the appropriate pH through the addition of sodium hydroxide.

Electrochemical measurements were conducted using a µAutolab computer controlled potentiostat (Eco-Chemie, Utrecht, The Netherlands) using a plasma treated screen printed electrode assembly (PSPE) (Lifescan, UK) consisting of a plasma treated screen printed carbon working electrode, a screen printed carbon counter electrode and a silver/silver chloride paste reference electrode. The working electrode was modified by an anodic pre-treatment step prior to use by the application of a potential of +0.2V for 5 minutes in a solution of 0.1M sodium hydroxide. All measurements were conducted at $22^{o}C \pm 2^{o}C$.

10.2.2. Sensor Construction

Prototype sensors were prepared as illustrated in **Figure 10.2** using thermal or cold lamination methods. The sensor consisted of the electrode unit sandwiched between sleeves of a resin-polyester lamination pouch with a film thickness of 75 µm (Rexel, UK) which had been pre-patterned to give a capillary channel and sample application area (hole cut with a 2mm diameter). A piece of conventional cellulose filter paper ($25mm^{2}$, 200 micron) was placed within the sensor to act as the capillary wick, ensuring that the sample would have full contact with the electrodes, allowing effective analysis. Thermal lamination was achieved using a commercially available laminator and

Figure 10.2 Schematic showing the sensor assembly.

cold lamination was achieved by incorporating double sided adhesive tape with a thickness of 130 µm (3M, Berkshire, UK) between the laminate sheets. Electrical

connections to the electrodes were made *via* the addition of strips of copper shielding tape 100 μm thick, adhesive backed (RS Electronics, UK).
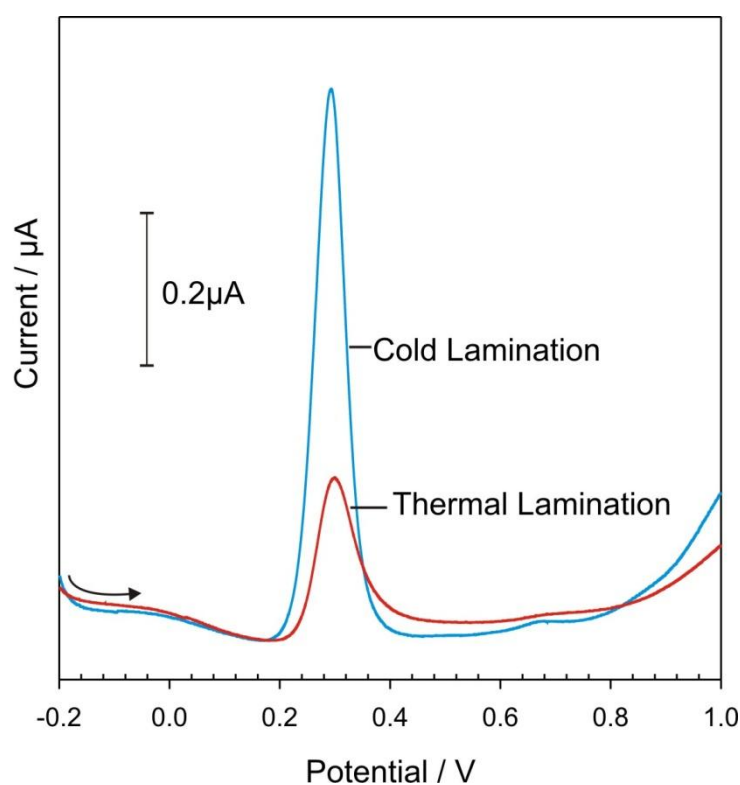
10.3. Results and Discussion

10.3.1. pH Sensor for Wound Management

Square-wave voltammograms showing the response of sensors constructed using thermal and cold lamination methods to uric acid (460μM, pH6.2, 97mM KCl) are shown in **Figure 10.3**. In both cases the two electron, two proton oxidation of uric acid, as described in chapter 9 (**Scheme 9.1**) can be seen at approximately +0.30V. It is apparent

Figure 10.3 Square-wave voltammograms detailing the response of the thermal and cold laminated anodised PSPE sensors to uric acid (460μM, pH6.2, 97mM KCl).

that the cold laminated sensor (**Figure 10.3 blue**) gives an improved electrode response to uric acid when compared to the thermally laminated sensor (**Figure 10.3 red**) with a larger, sharper oxidation peak observed. This can be attributed to the fact that the thermal lamination process has altered the structure of the screen printed carbon working electrode such that its electrochemical properties have been reduced, a possible explanation for this could be that the heat treatment of the sensor results in the re-dissolution of the particles within the ink therefore altering the electrodes

structure and for this reason the cold lamination fabrication technique was used to produce the rest of the sensors tested within this chapter.

In the previous experiment it can be noted that potassium chloride (97mM) is present within the sample to act as an internal reference electrolyte, providing a fixed concentration of chloride ions, and therefore ensuring that a stable reference potential is attained at the silver/silver chloride paste electrode. It is important to fix the concentration of chloride ions in this way as any variations will alter the reference potential produced, therefore rendering any results obtained inaccurate [7]. The performance of the fabricated sensor to detect uric acid when varying the chloride ion concentration was examined and the expected nernstian behaviour of a shift in the potential of the uric acid oxidation peak, on changing the chloride ion concentration, was observed. This is illustrated in the calibration graph displayed in **Figure 10.4** where the position of the uric acid oxidation peak is plotted against the logarithm (log) of the potassium chloride concentration.


The graph shows data with the equation:
$$E(V) = 0.0615 \, Log[Cl^-] + 0.3125$$
$$R^2 = 0.9766$$
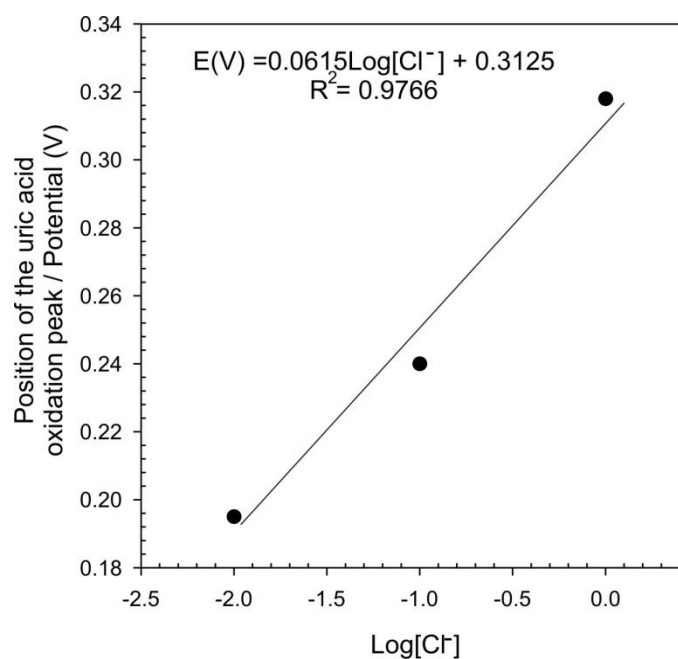
Figure 10.4 Variation in the position of the uric acid oxidation peak with the change in chloride ion concentration.

The oxidation position / chloride concentration relationship was linear, with the equation E(V) = 0.0615log[Cl-] + 0.315 having a correlation coefficient of R^2= 0.9766. This behaviour reinforces the need to have a fixed concentration of chloride

ions present for the unambigious determination of the pH ensuring that the latter is only thing that affects the position of the uric acid oxidation. For the purpose of this experiment the potassium chloride concentration was fixed at 97mM to match the chloride ion concentration typically present within whole blood [11]. It is noteworthy that the system can be easily adapted for use within other biological fluids by using the nominal chloride ion concentration within that fluid to calibrate the sensor.

In order to see if the new sensing assembly gave the same pH dependent oxidation of uric acid as described in chapter 9 an identical calibration procedure as to that previously used was carried out. In this instance, however, potassium chloride was present in the calibration standards to act as the internal reference electrolyte, allowing the inbuilt silver/silver chloride reference
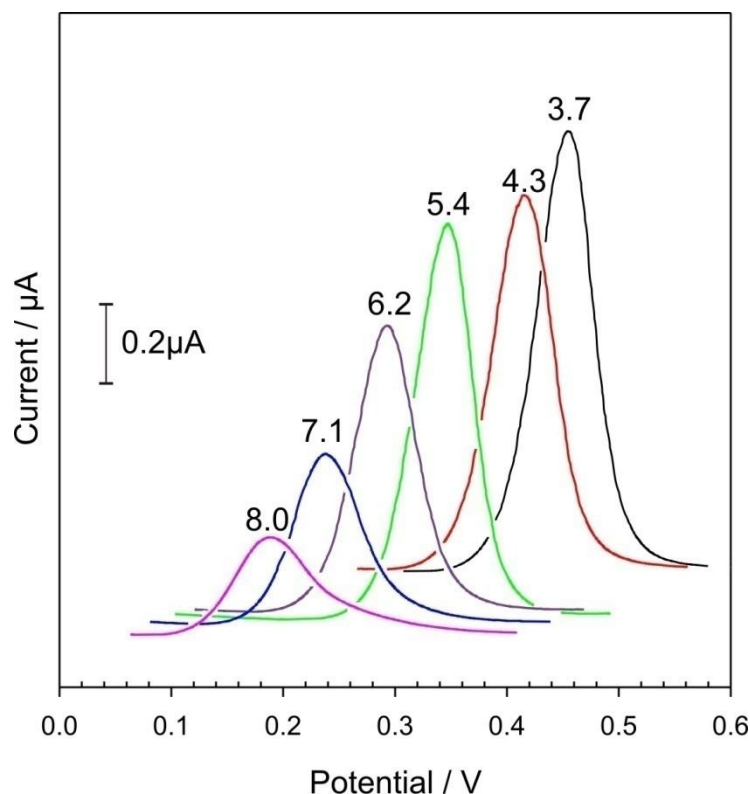
Figure 10.5 Square-wave voltammograms detailing the response of the sensor to uric acid (460µM) at various pH (KCl, 97mM).

electrode to be used as opposed to the external silver/silver chloride reference. Square-wave voltammograms detailing the response of the sensor to uric acid (460µM) in the presence of KCl (97mM) over a pH range of 3.7 to 8.0 are illustrated in **Figure 10.5**.

As observed in chapter 9, regardless of the pH, well defined peaks for the oxidation of the uric acid can be seen. The shift in peak position with changing pH gives the same linear response, with the oxidation shifting to more negative potentials as the pH increases, with the straight-line equation in this case being
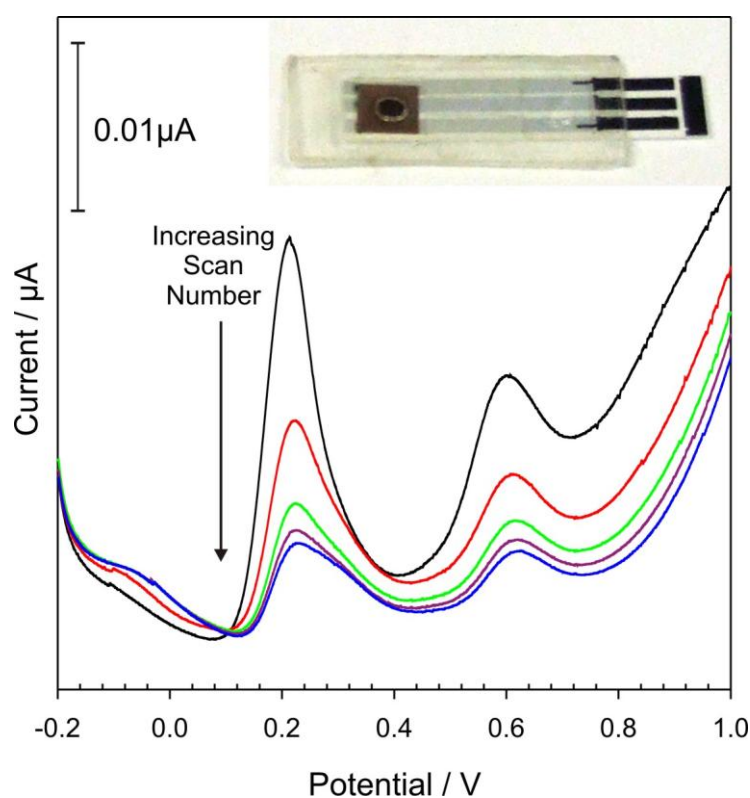
E(V)= -0.0635[pH] + 0.6918 having the correlation coefficient R^2=0.9969. The only difference in the voltammograms recorded in this chapter compared to those seen in chapter 9 is that all of the oxidation peaks are seen at more negative potentials which can however be explained by the fact that a different reference electrode has been used. The establishment of the same characteristic uric acid pH response highlights the applicability of using the sensing platform developed as a disposable sensor for making indirect pH measurements within biological fluids.

The viability of using the sensor within biofluids was subsequently assessed and whole blood samples were extracted from a volunteer *via* the fingerprick method and analysed directly without any sample pre-treatment. **Figure 10.6** shows the voltammetric response of the electrode assembly to a whole blood sample, with the repetitive scans showing the reproducibility of the approach and the

Figure 10.6 Square-wave voltammogram detailing the response of the sensor to a real sample. Insert: Photograph of complete sensing platform.

photographic insert showing the complete sensor assembly. As in chapter 9, the uric acid oxidation peak is visible as a sharp fully resolvable peak at +0.22V and once again provides an unambiguous signal from which the pH of the sample can be deduced. Other oxidation processes can also be seen on the voltammogram– a broad peak at +0.58V is observed and can be attributed to the direct oxidation of the other amino acids present within the sample.

Upon successive scanning it can be seen that the peak position for uric acid is stable for the duration of the experiment (five minutes) although it is apparent, due to peak broadening and the presence of a new oxidation process at -0.08V, that the electrode surface is being progressively fouled as the sample coagulates and oxidation products are deposited at the sensor surface. The height of the uric acid peak diminishes on successive scanning and, although irrelevant in this study, it is indicative of the depletion of the uric acid species at the electrode surface and the blocking of the electrochemical signal as the electrode becomes increasingly contaminated.

The position of the uric acid oxidation peak (+0.22V), and the previously determined calibration data, were used to determine the pH of the blood sample, ensuring the accuracy of the fabricated sensing assembly. The pH determined from the above oxidation potential was 7.392 (N=5, %RSD 0.910) and when the reproducibility between different sensing platforms was examined, the average pH was determined as being 7.39 (N=3, %RSD 0.822). The fact that these values fall well within the accepted pH range for venous blood (from 7.32 to 7.43) [11] and matches the values obtained in chapter 9 (same volunteer screened) shows the efficacy of the sensor for determining the pH of real samples, with the high inter reproducibility proving the accuracy of the system as a disposable sensing strategy.

10.3.2. A Generic Sensing Strategy – Thiol Analysis

It was envisaged that the uric acid pH sensor assembly used above could be adapted to facilitate the detection of other biologically relevant molecules including the reduced sulphydryl thiols cysteine, homocysteine and glutathione. Adaptation for detection of thiol species came in the form of having multiple layers to the capillary wick illustrated in **Figure 10.2**. Here the middle layer was loaded with the napthoquinone-adamantane derivative investigated within chapter 7 and it was envisaged that the presence of this derivative would facilitate thiol detection by exploiting the different hydrophobic/hydrophilic properties of the derivative and reaction product respectively (as previously discussed), with a voltammetric signal only being observed when the thiol species is present within the sample allowing the

label to be mobilised. The bottom and top layers of the capillary wick were left blank to ensure that unreacted quionone was not detected at the electrode assembly and also to protect the user from coming into contact with the reactive quinone.

To assess the applicability of this sensor for the analysis of sulphydryl thiols the performance of the sensor to detect glutathione was examined. **Figure 10.7** shows the voltammograms observed for the sensor in the absence and presence of glutathione (500μM, pH7, 97mM KCl) before and after a ten minute reaction period. The emergence of the quionone peak in the presence of the thiol is clearly visible at -0.67V after the ten minute period with no peak processes emerging for the blank. This response is enhanced when compared to the initial (0 minute) measurement suggesting that a time delay is required to allow the reaction, mobilisation and movement to the electrode surface to occur. Similar, less defined responses were seen for cysteine and homocysteine. These results confirm that the hydrophobic quinone is only mobilised within the sensor after it has been reacted with the thiol moiety, thus proving the possibility of using this approach for the analysis of thiol species.
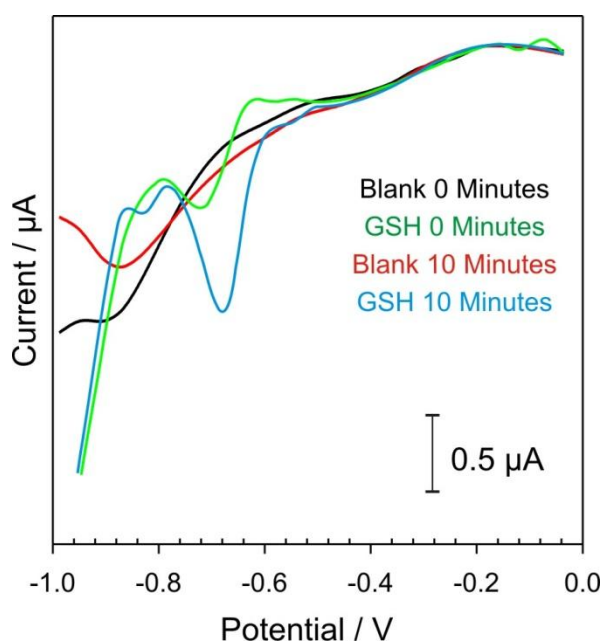
Figure 10.7 Square-wave voltammograms detailing the response of the adamantine-naphthoquinone sensor in the absence and presence of glutathione (500μM, pH7, 97mM KCl) before and after a ten minute reaction period.

The small current response obtained for these results, when a relatively large amount of thiol is analysed along with the time delay required to make a suitable

measurement, demonstrates that the efficacy of the approach for the detection of sulphydryl thiols is significantly limited, especially when attempting to transfer the approach to analysis within real biological fluids.

10.4. Conclusions

The fabricated sensor assembly has been shown capable of providing a robust and versatile sensing system for determining the pH of biological fluids. When comparing the possible fabrication routes available for sensor construction, it was found that thermal lamination routes appeared to alter the structure of the anodised working electrode resulting in a decrease in the performance characteristics and, as such, cold lamination techniques had to be used. The uric acid pH dependent response observed within this chapter was consistent with the data obtained in chapter 9, illustrating the effective transfer of the previous sensing strategy to a fully disposable sensing assembly and while more elaborate longevity or stability studies are necessary the primarily results are clearly promising, illustrating the development if of a sensor that can be used to determine the pH of biological fluids at the point of care, which could provide better wound care / management. The adaptation of the disposable sensing strip developed for the analysis of sulphydryl thiols has also been described and although the efficacy of the approach is limited for use for the analysis of these species over a clinically relevant range, it highlights the potential of the system as a universal sensing platform.

10.5. References

[1]   A. Smith and C. Taylor. Analysis of blood gases and acid-base balance. Surgery, 23 (2005) 194-198

[2]   V.J.J. Cardenas,J.B. Zwischenberger,W. Tao et al, Correction of blood pH attenuates changes in hemodynamics and organ blood flowing during permissive hypercapnia. Critical Care Medicine, 24 (1996) 827-834

[3]   L.A. Schneider, A. Korber, S. Grabbe and J. Dissemond, Influence of pH on wound-healing a new perspective for wound therapy. Archives of dermatological research, 298 (2007) 413-420

[4]   M.H. Pipelzadeh and I.L. Naylor,The in vitro enhancement of rat myofibroblast contractility by alterations to the pH of the physiological solution. European Journal of Pharmacology, 357 (1998) 257–259

[5]   G. Gethin, The significance of surface pH in chronic wounds. Wounds UK, 3 (2007) 52-56

[6]   B.K. Siesjo, The regulation of cerebrospinal fluid pH. Kidney International, 1 (1972) 360-374

[7]   R. Maminska, A. Dybko and W. Wroblewski, All-solid-state miniaturised planar reference electrodes based on ionic liquids. Sensors and Actuators B, 115 (2006) 552-227

[8]   D. Desmond, B. Lane, J. Alderman, J.D. Alderman, J.D. Glennon and D. Diamond, Evaluation of miniaturised solid state reference electrodes on a silicon based component. Sensors and Actuators B, 44 (1997) 389–396

[9]   A. Simonis, M. Dawgul, H. Luth and M.J. Schoning, Miniaturised reference electrodes for field-effect sensors compatible to silicon chip technology. Electrochimica Acta, 51 (2005) 930-937

[10]   J. Haa, S.M. Martin, Y. Jeon et al, A polymeric junction membrane for solid-state reference electrodes. Analytica Chimica Acta, 549 (2005) 59–66

[11]   C.A. Burtis, E.R. Ashwood and D.E. Burns, 2006. Tietz textbook of clinical chemistry and molecular diagnostics. 4th edition. Missouri:Elsevier Saunders

Chapter 11

Conclusions and Future Work

Chapter 11

Conclusions and Future Work

Chpater 1 of this thesis summarises the clinical significance and describes the current methods used for the detection of sulphydryl thiols. Throughout this chapter it is clear that the detection of suphydryl thiols is fraught with a number of analytical challenges and given the significance, that changes in their levels have in relation to the onset and/or progression of a number of clinical conditions, the development of methods that could facilitate their unambiguous detection would be a significant benefit within the medical community. The development of new, rapid, point of care diagnostics would provide the most advantageous approach for thiol analysis as this would negate some of the problems surrounding sample collection and storage providing a more accurate analysis. Numerous approaches to meet this aim have been investigated within this thesis. Electrochemical techniques, as discussed in chapter 2, have been exploited primarily as the thiol detection strategy because of their ease of use, versatility and low cost.

In Chapter 3, the experimental work described the investigation of silver-thiol interactions. These interactions were exploited as a possible route to improve sample processing, particularly interference removal and analyte pre-concentration, in an attempt to enhance thiol analysis. The work presented, section 3.3, highlights that two silver-thiol interaction routes are possible: the first being silver retention and thiol release and the second being silver release and thiol release, with the predominating route being dependent upon the chemical functionalities present on the thiol species involved. Both routes described have the potential to assist sample processing during thiol analysis *via* pre-concentration. The second route observed, has an additional application as it provides a route for the electrochemical controlled ejection of silver nanoparticles. The latter could be of benefit within smart sensors or bandages for preventing electrode fouling and the accumulation of bacteria within wound environments, with this hopefully providing an infection control route. The work carried out in this chapter provided a tentative assessment of the silver thiol

interactions studied. More work is needed to understand and explore these interactions further. This should, primarily be focused upon elucidating the mechanism of silver retention or release fully, but should also include an investigation into the possible exploitation of the silver release mechanism to provide antibacterial action.

Chapter 4 looked at the development of molecular imprinted polymers (MIPs) based on dimethylpyrrole analogues. It was envisaged that these would be able to facilitate the analysis of some simple amine compounds and, that the strategy developed could be adapted to provide a detection route for the sulphydryl thiols under study. The route employed allowed a range of potential MIP monomers to be synthesised, section 4.2.2, and subsequently polymerised at the electrode surface, section 4.3. However, when attempting to release the amine analyte template with hydroxylamine, opposed to having a complementary cavity left behind that would allow analyte reincorporation and detection, the polymer film was shown to degrade completely. So, instead of having a MIP, a sacrificial or protective type polymer had been developed. The possible application of which was subsequently investigated and the pontenial use highlighted. These systems could be investigated further by synthesising and studying dipyrrolic monomers with larger structures. Here, a longer polymer chain should be present and this may facilitate the patterening of the underlying electrode surface. This would be a useful film processing method where site specific spatial positioning on discrete electrode systems needs to be controlled.

Chapters 5 and 6 examined the possibility of using the natural product plumbagin as a material to facilitate the electrochemical detection of sulphydryl thiols. Chapter 5 illustrated how plumbagin interacted with a variety of different thiol derivatives giving a clearly resolved, selective voltammetric signature for cysteine, section 5.3. The nature of the voltammetric profile was assessed and the profile observed was elucidated. It was thought the selectivity seen was due to the fact that a cyclistaion reaction between the quinone and the amine functionality present on the thiol species is possible, creating a new conjugate with different electrochemical properties. The results of this work show that the new conjugate can be detected without any interference from the other species present within the sample. The detection strategy for cysteine was modified and an accurate, indirect route for the analysis of the cysteine disulphide cystine has been displayed and evaluated.

Interference studies and the applicability of the sensing technique for use within real biological samples should be investigated next to build upon the work carried out in this chapter.

Chapter 6 looked at developing the plumbagin thiol detection strategy further. It was envisaged that by polymerising the plumbagin that, a reactive polymer would be produced and that this would facilitate reagentless thiol analysis. In section 6.3.1, it was found that the polymer produced was unstable, degrading in the presence of the thiols species, thus limiting plumbagins use of to an *in-situ* electrochemical thiol label. It was however observed during this work that the polymer could catalyse the reduction of oxygen to produce reactive oxygen species (ROS). The ability of the plumbagin monomer and polymer to produce ROS was investigated fully, section 6.3.2 in an attempt to provide a route that could prevent electrode fouling. Further work is needed to identify the ROS species being produced, this would enable the potency of the system to be estimated and the potential applications tailored accordingly. Other, potentially polymerisable quinones could also be investigated to see if they generate ROS species, but more importantly, for the context of this project, to see if they could produce stable polymer films capable of sensing reduced thiol species.

The work presented in chapter 7 looked at using the quinone-thiol interactions, previously described in chapters 5 and 6, in an alternative way to facilitate the detection of sulphydyl thiols *via* colorimetric (ultraviolet-visible specrophotometric) methods. A range of structurally different benzoquinone and naphthoquinone derivatives, both commercially available and synthesised in house, were assessed. It was discovered that two derivatives, 2,6-dimethylbenzoquinone and 2-(adamantly-1-carboxylic acid-1,4-naphthoquinone ester, displayed superior reaction characteristics that could be exploited to selectively determine cysteine and homocysteine respectively *via* colorimetric means. The possible application of this route has been displayed. Its use is however limited, as upon evaluation it was found that the sensitivity of the technique was inadequate for realistic thiol analysis. This was hampered further given the low molar absorptivities of the derivatives, and the low reference concentrations of the sulphydryl thiols within biological samples. The

routes discussed within this chapter were also studied using electrochemical techniques to see if any improvement in the sensitivity could be achieved. It was demonstrated that the thiols could be detected *via* exploiting the different hydrophobic and hydrophilic properties of the naphthoquinone-adamantane derivative and its corresponding thiol conjugate. Even though this technique was subject to the same sensitivity problems previously described it highlights a new sensing approach that can be exploited further (chapter 10). Further work to try and develop a selective and sensitive colorimtric thiol label could be to:-

- investigate other commericially available quinones,
- to synthesise quinones that have stronger native chromophores present,
- to investgate quinone-complexes, where a displacement reaction could yield a colorimetric response.

Chapter 8 examined an alternative route to those described in chapters 4 and 6, which could potentially be used to facilitate the reagentless sensing of sulphydryl thiols. Electropolymerisable quinone/imine type materials were investigated and although the study displayed some interesting results in that the materials studied were reactive to sulphydryl thiols and polymerisable, the polymers produced did not provide a selective route for thiol analysis. Literature regarding the electrochemistry of these materials is limited and so it would be interesting to conduct a full, detailed electrochemical study on each of the compounds studied to clarify the reaction mechanism occuring. This would provide a vast amount of information allowing the potential applications of these molecules to be highlighted and exploited.

Chapter 9 looked at a different type of sensing strategy, the primary aim being to develop a route that could be used to determine the pH of a wound which should facilitate more effective wound management strategies. The work presented in section 9.3 shows that the pH of whole blood samples can be effectively determined by assessing the position of the voltammetric profile obtained for the oxidation of uric acid. The electrode response observed for the sensor could be enhanced by subjecting it to an anodic pre-treatment with the performance characteristics of a plasma treated and anodised screen printed carbon electrode providing a clear voltammetric trace that could be exploited. This work shows the potential of anodic pre-treatment for

enhancing the performance of screen printed electrodes and so this route could be applied to sensing platforms currently available for the analysis of other biologically relevant molecules. The work discussed in chapter 9, with regards to developing a wound pH sensor, was investigated further in chapter 10. Here a fully disposable sensing platform was constructed and evaluated. The sensor fabricated had excellent performance characteristics and could easily be used to determine the pH of biological fluids at the point of care. With regards to the pH sensor for monitoring wound status a large amount of future work needs to be conducted so that the production of a commercially viable sensing platform can be realised. This includes miniatuarising the device, conducting a more robust performance study, looking at a range of biologically fluids and potential sample interferents. Chapter 10 also tentatively assessed the adaptation of the sensing platform developed for pH analysis for the analysis of sulphydryl thiols by exploiting the different hydrophobic and hydrophilic properties of the naphthoquinone-adamantane derivative and its thiol conjugate as discussed in chapter 7. Although this route was found to be limited in terms of sensitivity it demonstrated the robust nature of the fabricated sensor and the possibility that a universal sensing platform had been developed.

The work presented in this thesis illustrates the drive to develop methods that are sensitive, selective and reproducible, that can be used to facilitate the detection of biologically relevant molecules. The move towards portable sensing formats is advantageous as it provides rapid on-site analysis. It is clear that some of the routes presented have been demonstrated as probable routes for use within this area, although further development and optimisation is required.

This project has laid the foundations of several sensing strategies and has highlighted the complexity of analysing biological fluids at the point of care. The work has also raised many questions as to how the techniques work and has indicated some new avenues that could be explored.

Appendix 1
Additional Data

Appendix 1
Additional Data

A1:C3. Appendix 1: Chapter 3 – Exploiting Silver-Thiol Interactions for Thiol Analysis

A1.C3.1 Inductively Coupled Plasma-Optical Emission Spectroscopy (ICP-OES) Experimental Details and Results

A1.C3.1.1. Introduction to ICP-OPES

ICP-OES is an accurate and versatile multi-element analytical technique. It can be used for the analysis of a range of major, minor and trace elements simultaneously, including silver [1], lead [2] and cadmium [3], in a variety of sample matrices and can therefore be used for a number of applications [4]. During ICP-OES analysis the sample is nebulised and introduced into the high temperature inductively coupled plasma. Once in the plasma the sample undergoes desolvation, vaporisation, atomisation and finally excitation and ionisation. In the latter stages, electrons within the atoms are promoted to higher energy levels and results in the atoms being present in an excited state. The excited atoms then return, from their excited state to there initial ground state. This process releases light (electromagnetic radiation) and gives rise to the analytical signal. The light emitted is spectrally resoved and the intensity of the light is measured at the detector. The wavelength of the light emitted is characteristic of the atom involved providing a qualitative measurement and the intensity of the light is proportional to the conecentration of the analyte present thus giving a quantitative measurement [4-5].

A1.C3.1.2. Experimental Details

Inductively coupled plasma-optical emission spectroscopy (ICP-OES) experiments were conducted on an ICP-OES 2100 DV instrument (Perkin Elmer, UK) equipped with a charge coupled device. All reagents were of the highest grade available, were used without further purification and unless stated otherwise were

purchased from Sigma Aldrich (UK) or Alfa Aesar (UK). A solution of 0.1M nitric acid was used to prepare the calibration standards and the sample solutions. The operating conditions for the ICP-OES were as follows:-

- Power
- Plasma gas flow rate
- Auxiliary gas flow rate
- Nebulizer gas flow rate
- Peristaltic pump speed
- Integration times
- Wash time
- Number of replicates – 3
- Carrier solution – 1% nitric acid
- Rinse solution – 1% nitric acid
- View Position – Axial
- Analytical wavelength for silver – 328.028nm

A1.C3.1.3. Results

Calibration Data

The calibration series consisted of one blank and 4 standard silver solutions (0.0ppm, 0.5ppm, 1.0ppm, 1.5ppm and 2.0ppm). These were analysed in triplicate to produce a linear calibration graph with the equation of the line being: Intensity = 109800[Concentration of silver (ppm)] + 954.5, having a correlation coefficient R^2 = 0.999841.

Sample Data

| Sample	Dilution Factor	Replicates	Average Corrected Intensity	Average Concentration of the analytical solution / mg/L	Average concentration of the sample solution / μg/ml	Standard deviation	Relative standard deviation / %
Interfacial solution (homocysteine)	125	3	110867.5	1.001	125.125	0.0016	0.16
Bulk solution (homocysteine)	N/A	3	34765.1	0.308	0.398	0.0051	1.64
Interfacial solution (3-mercaptopropane)	125	3	177.3	0.007	0.875	0.0004	5.19
Bulk solution (3-mercpatopropane)	N/A	3	62977.5	0.565	0.565	0.0054	0.95

Al.C3.2. Enlarged Figures

Figure 3.2 (A) EQCM profile and (B) corresponding explanatory schematic for the interaction of silver with homocysteine during the stages (1 to 7) of the experiment.
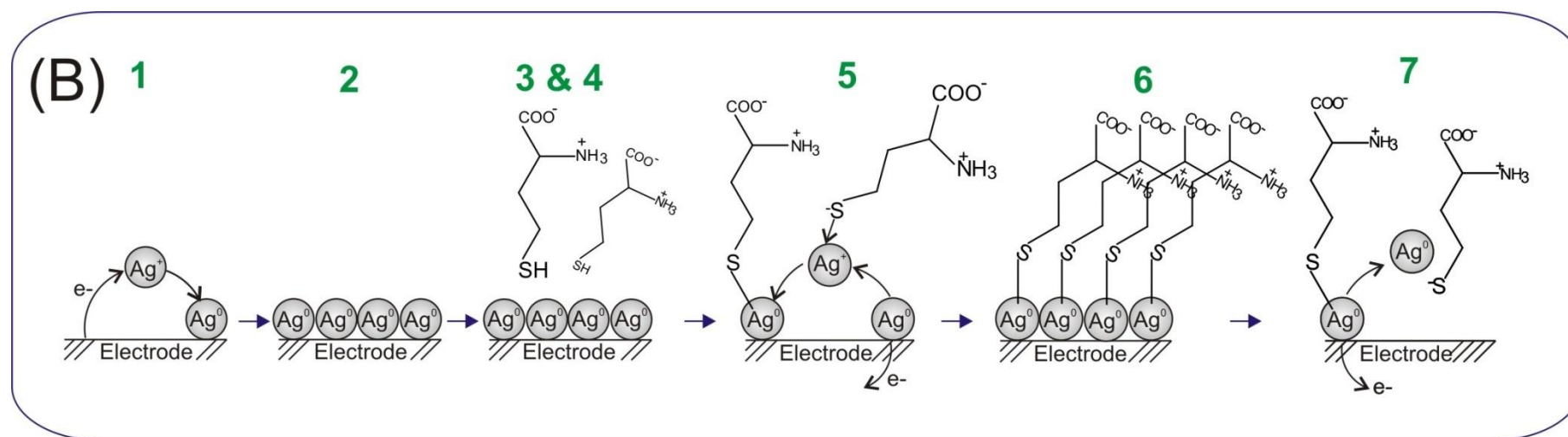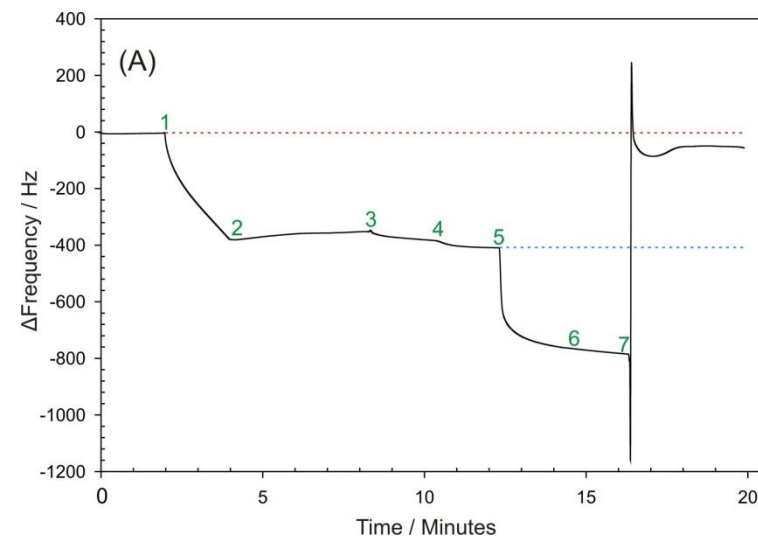
Figure 3.4 (A)The EQCM profile and (B) the corresponding explanatory schematic for the interaction of silver with methionine during the stages (1 to 7) of the experiment.
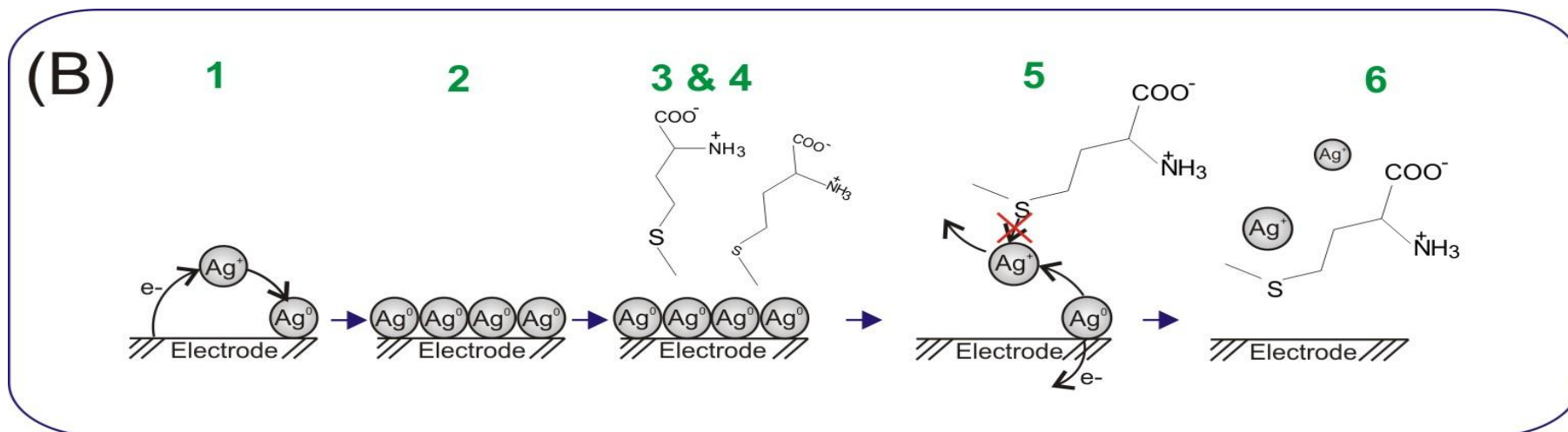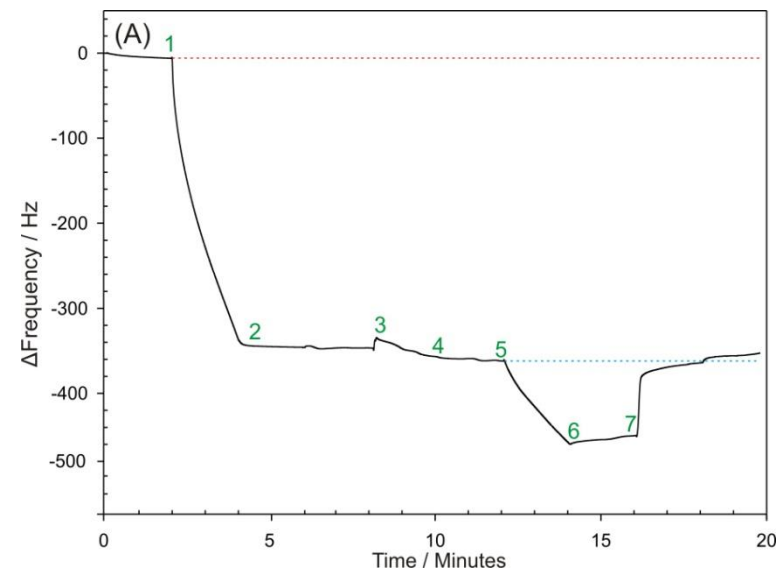
Figure 3.5 (A) The EQCM profile and (B) the corresponding explanatory schematic for the interaction of silver with 3-Mercaptopropane during the stages (1 to 7) of the experiment.
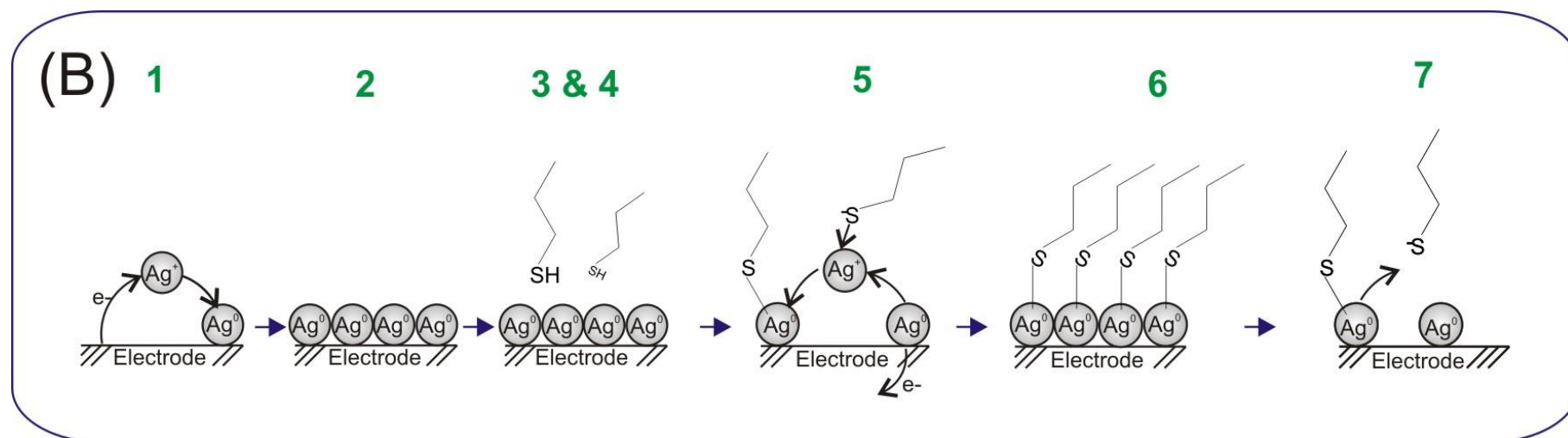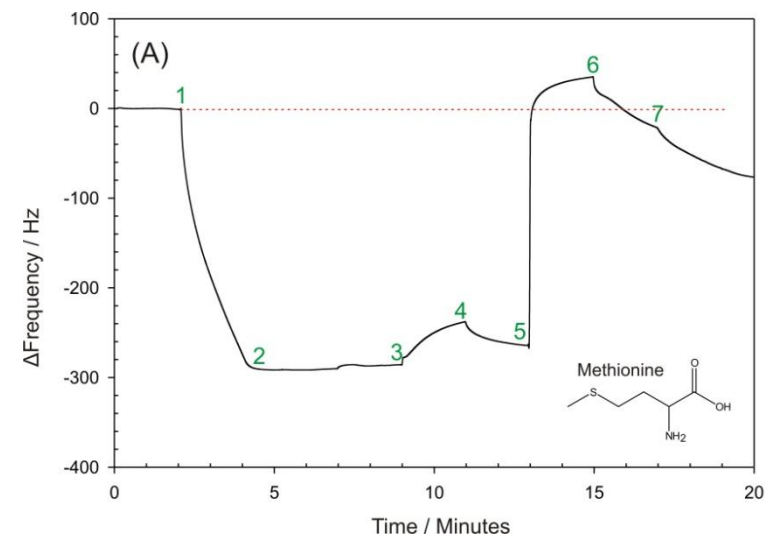
A1.C3.3. References

[1]   T.M. Ben and P. Westerhoff, Nanoparticle silver released into water from commercially available sock fabrics. Environmental Science and Technology, 42 (2008) 4133-4139

[2]   S. Cerutti, R.F. Orsi, J.A. Gasquez, R.A. Olsina and L.D. Martinez, Online preconcentration/determination of lead traces in bee honey by inductively coupled plasma optical emission spectrometry (ICP-OES) using a conical minicolumn pacted with activated carbon. Journal of Trace and Microprobe Techniques, 21 (2003) 421-423

[3]   S. Cerutti, M.F. Silva, J.A. Gasquez, R.A. Olsina and L.D. Martinez, On-line preconcentration of cadmium in drinking water on activated carbon using 8-hydroxyquinoline in a flow ijection system couples to an inductively coupled plasma optical emission spectrometer. Spectrochimica Acta Part B: Atomic Spectroscopy, 58 (2003) 43-50

[4]   C.B. Boss and K.J. Freden, 1997. Concepts, Instrumentation, and Techniques in Inductively Coupled Plasma Optical Emission Spectroscopy. 4th Edition, USA: The Perkin-Elmer Corporation.

Appendix 2
Publications and Conferences

Appendix 2

Publications

Laura A.A. Newton, Suh Sing U, Ray Leslie and James Davis. Dimethylsubstituted Pyrroles: A New Approach to Protective Polymers. Electrochemistry Communications, 11 (2009) 929-932

Himanshi Sahni, Laura A.A. Newton, Ray Leslie and James Davis. Electrochemically Modulated Film Permeability: A Functional Film for Controlled Reagent Release. Chemistry Letters, 38 (2009) 968-969

Laura A.A. Newton, Ray Leslie and James Davis. Countering COSHH Complacency in the Workplace: a Generic Toolkit. Journal of Chemical Health and Safety, 17 (2010) 16-20

Laura A.A. Newton, Emma Cowham, Duncan G. Sharp, Ray Leslie and James Davis. Plumbagin: A Natural Product for Smart Materials? New Journal of Chemistry, 34 (2010) 395-397

Laura A.A. Newton, Kiran Sandhu, Callum Livingstone, Ray Leslie and James Davis. Clinical Diagnostics for Homocysteine: A Rogue Amino Acid? Expert Review in Molecular Diagnostics, 10 (2010) 489-500

Madhura S. Damle, Laura A.A. Newton, Ray Leslie and James Davis. Plumbagin: A New Route to the Electroanalytical Determination of Cystine. Electroanalysis, 22 (2010) 2491-2495

Laura A.A. Newton, Ray Leslie and James Davis, Developing a Strategy for the Spatial Localisation and Autonomous Release of Silver Nanoparticles within Smart Implants. International Journal of Electrochemistry, 197936 (2011) 1-4

Jolene Phair, Laura Newton, Cliodhna McCormac, Marco F. Cardosi, Ray Leslie and James Davis, A disposable sensor for point of care wound pH montoring. Analyts, 136 (2011) 4692-4695

Conferences

- Rhine Meeting (2009), Hull, UK. Poster presentation - Designing Molecularly Imprinted Polymers for Drug Screening Applications.

- Nottingham Trent University School of Science and Technology Research Conference (2009), Nottingham, UK. Poster presentation - Developing Inks that Think.

- The 238th ACS National Meeting & Exposition (2009), Washington DC, USA. Poster presentation – Molecular parachutes for thiol detection at the point of care.

- The 238th ACS National Meeting & Exposition (2009), Washington DC, USA. Poster presentation – Origami: An interactive method of exploring the significance of molecular shape in everyday life.

- Eurovariety in Chemistry Education - University of Manchester (2009), Manchester, UK. Oral presentation - A novel approach to countering COSHH complacency in the lab or workplace.

- Nottingham Trent University School of Science and Technology Research Conference (2010), Nottingham, UK. Poster and Oral presentation - Novel methods for thiol detection at the point of care.

- Nanotech Conference and Expo (2010), Anaheim CA, USA. Oral presentation - Developing a Strategy for the Spatial Localisation and Autonomous Release of Silver Nanoparticles within Smart Implants.

- 61st Annual Meeting of the International Society of Electrochemistry (2010), Nice, France. Oral presentation - Combating Biofilm Formation with Superoxide Generating Smart Electro-Polymers.